Université de Montréal

Bcl-xL regulation and function in cell cycle checkpoints and progression

par
Jianfang Wang

Programme de Sciences biomédicales
Faculté de Médecine

Thèse présentée à la Faculté de Médecine
en vue de l'obtention du grade de doctorat en
Sciences biomédicales

Juin 2011

Université de Montréal

Faculté de Médecine

Cette thèse intitulée:

Bcl-xL regulation and function in cell cycle checkpoints and progression

Présentée par:
Jianfang Wang

a été évaluée par un jury composé des personnes suivantes:

Dr Alexander Parker, président-rapporteur
Dr Richard Bertrand, directeur de recherche
Dr Edward Bradley, membre du jury
Dr Moulay Alaoui-Jamali, examinateur externe
Dr Jean Vacher, représentant du doyen de la FESP

Abstract

Accumulating evidence suggest that Bcl-xL, an anti-apoptotic member of the Bcl-2 family, also functions in cell cycle progression and cell cycle checkpoints. To further understand Bcl-xL regulation and function in cell cycle progression, we first expressed a series of single-point Bcl-xL cDNA phospho-mutants, including Thr41Ala, Ser43Ala, Thr47Ala, Ser49Ala, Ser56Ala, Ser62Ala and Thr115Ala in human cancer cell lines and investigated their impact on cell cycle progression.

Analysis of this series of phosphorylation mutants reveals that cells expressing Bcl-xL(Ser62Ala) mutant are less stable at the G2 checkpoint and enter mitosis more rapidly than cells expressing wild type Bcl-xL or Bcl-xL phosphorylation mutants, including Thr41Ala, Ser43Ala, Thr47Ala, Ser56Ala and Thr115Ala. Dynamic phosphorylation and location studies on phospho-Bcl-xL(Ser62) in unperturbed, synchronized cells and during DNA damage-induced G2 arrest revealed that phospho-Bcl-xL(Ser62) translocates into nucleolar structures in VP16-exposed cells during G2 arrest. Using *in vitro* kinase assays, pharmacological inhibitors and specific siRNAs experiments, we found that Polo kinase 1 and MAPK9/JNK2 are major protein kinases involved in Bcl-xL(Ser62) phosphorylation and accumulation into nucleolar structures during the G2 checkpoint. In nucleoli, phospho-Bcl-xL(Ser62) binds to and co-localizes with CDK1(CDC2), the key cyclin-dependent kinase required for entry into mitosis. These data indicate that, during G2 checkpoint, phospho-Bcl-xL(Ser62) stabilizes G2 arrest by timely trapping CDK1(CDC2) in nucleolar structures to slow mitotic entry. It also highlights that DNA damage affects the dynamic composition of the nucleolus, which now emerges as a key event in the DNA damage response.

In a second study, we describe that cells expressing Bcl-xL(Ser62Ala) are also more stable at a sustained spindle-assembly checkpoint (SAC) after exposure to taxol than cells expressing wild-type Bcl-xL or other mutants, an effect that appears to be independent of its anti-apoptotic activity. Bcl-xL(Ser62) is strongly phosphorylated by PLK1 and MAPK14/SAPKp38α at prometaphase, metaphase and the anaphase boundary, while it is dephosphorylated at telophase and cytokinesis. Phospho-Bcl-xL(Ser62) localizes in centrosomes with γ-tubulin, along the mitotic spindle with dynein motor protein and in cytosol with SAC signaling components. In taxol-exposed cells, phospho-Bcl-xL(Ser62)

binds to the CDC20/MAD2/BUBR1/BUB3 complex, while Bcl-xL(Ser62Ala) does not. The data indicate that during SAC, Bcl-xL(Ser62) phosphorylation accelerates SAC resolution and cell entry into anaphase, even in the presence of unattached or misaligned chromosomes. Silencing Bcl-xL expression also leads nocodazole-exposed cells to tetraploidy and binucleation, consistent with a Bcl-xL function in SAC and genomic stability.

In the third study, the functional analysis of a Bcl-xL phosphorylation mutant series has revealed that cells expressing Bcl-xL(Ser49Ala) mutant are less stable at G2 checkpoint after DNA damage and enter cytokinesis much more slowly after microtubule poisoning than cells expressing wild-type Bcl-xL. These effects of Bcl-xL(Ser49Ala) mutant seem to be distinct from Bcl-xL function in apoptosis. Bcl-xL(Ser49) phosphorylation is cell cycle-dependent. In synchronized cells, phospho-Bcl-xL(Ser49) appears during the S phase and G2, whereas it disappears rapidly in early mitosis during prometaphase, metaphase and early anaphase, and re-appears during telophase and cytokinesis. During DNA damage-induced G2 arrest, an important pool of phospho-Bcl-xL(Ser49) accumulates in centrosomes which act as essential decision centers for progression from G2 to mitosis. During telophase/cytokinesis, phospho-Bcl-xL(Ser49) is found along microtubules and at midbody with dynein motor protein. In a series of *in vitro* kinase assays, specific small interfering RNA and pharmacological inhibition experiments, polo kinase 3 (PLK3) was implicated in Bcl-xL(Ser49) phosphorylation. These data indicate that during G2 checkpoint phospho-Bcl-xL(Ser49) is another downstream target of PLK3, acting to stabilize G2 arrest. Bcl-xL phosphorylation at Ser49 also correlates with essential PLK3 activity and function, enabling cytokinesis and mitotic exit.

Key words: Bcl-xL, phosphorylation, cell cycle, G2 checkpoint, spindle-assembly checkpoint.

Resumé

Quelques évidences suggèrent que Bcl-xL, un membre anti-apoptotique de la famille Bcl-2, possède également des fonctions au niveau du cycle cellulaire et de ses points-contrôle. Pour étudier la régulation et fonction de Bcl-xL au cours du cycle cellulaire, nous avons généré et exprimé dans des cellules humaines une série de mutants de phosphorylation incluant Thr41Ala, Ser43Ala, Thr47Ala, Ser49Ala, Ser56Ala, Ser62Ala et Thr115Ala.

L'analyse de cette série de mutants révèle que les cellules exprimant Bcl-xL(Ser62Ala) sont moins stables au point-contrôle G2 du cycle cellulaire comparées aux cellules exprimant le type sauvage ou les autres mutants de phosphorylation incluant Thr41Ala, Ser43Ala, Thr47Ala, Ser56Ala et Thr115Ala. Les études de cinétiques de phosphorylation et de localisation de phospho-Bcl-xL(Ser62) dans des cellules synchronisées et suite à l'activation du point-contrôle en G2 médié par l'étoposide (VP16), nous indiquent que phospho-Bcl-xL(Ser62) migre dans les corps nucléolaires durant l'arrêt en G2 dans les cellules exposées au VP16. Une série d'expériences incluant des essais kinase *in vitro*, l'utilisation d'inhibiteurs pharmacologiques et d'ARN interférant, nous révèlent que Polo kinase 1 (PLK1) et MAPK9/JNK2 sont les protéines kinase impliquées dans la phosphorylation de Bcl-xL(Ser62), et pour son accumulation dans les corps nucléolaires pendant le point-contrôle en G2. Nos résultats indiquent que durant le point-contrôle en G2, phospho-Bcl-xL(Ser62) se lie et se co-localise avec CDK1(CDC2), le complexe cycline-kinase qui contrôle l'entrée en mitose. Nos résultats suggèrent que dans les corps nucléolaires, phospho-Bcl-xL(Ser62) stabilise l'arrêt en G2 en séquestrant CDK1(CDC2) pour retarder l'entrée en mitose. Ces résultats soulignent également que les dommages à l'ADN influencent la composition des corps nucléolaires, structure nucléaire qui émerge maintenant comme une composante importante de la réponse aux dommages à l'ADN.

Dans une deuxième étude, nous décrivons que les cellules exprimant le mutant de phosphorylation Bcl-xL(Ser62Ala) sont également plus stables au point-contrôle de l'assemblage du fuseau de la chromatine (SAC) suite à une exposition au taxol, comparées aux cellules exprimant le type sauvage ou d'autres mutants de phosphorylation de Bcl-xL, incluant Thr41Ala, Ser43Ala, Thr47Ala, Ser56Ala. Cet effet est indépendent

de la fonction anti-apoptotique de Bcl-xL. Bcl-xL(Ser62) est fortement phosphorylé par PLK1 et MAPK14/SAPKp38α à la prométaphase, la métaphase et à la frontière de l'anaphase, et déphosphorylé à la télophase et la cytokinèse. Phospho-Bcl-xL(Ser62) se trouve dans les centrosomes avec γ-tubuline, le long du fuseau mitotique avec la protéine moteure dynéine et dans le cytosol mitotique avec des composantes du SAC. Dans des cellules exposées au taxol, phospho-Bcl-xL(Ser62) se lie au complexe inhibiteur CDC20/MAD2/BUBR1/BUB3, alors que le mutant Bcl-xL(Ser62Ala) ne se lie pas à ce complexe. Ces résultats indiquent que durant le SAC, la phosphorylation de Bcl-xL(Ser62) accélère la résolution du SAC et l'entrée des cellules en anaphase. Des expériences bloquant l'expression de Bcl-xL révèlent ègalement un taux très élevé de cellules tétraploïdes et binuclées après un traitement au nocodazole, consistant avec une fonction de Bcl-xL durant la mitose et dans la stabilité génomique.

Dans la troisième étude, l'analyse fonctionnelle de cette série de mutants de phosphorylation indique également que les cellules exprimant Bcl-xL(Ser49Ala) sont moins stables durant le point-contrôle G2 et entre en cytokinèse plus lentement dans des cellules exposées aux inhibiteurs de la polymérisation/dépolymérisation des tubulines, composantes des microtubules. Ces effets de Bcl-xL(Ser49Ala) sont indépendents de sa fonction anti-apoptotique. La phosphorylation de Bcl-xL(Ser49) est dynamique au cours du cycle cellulaire. Dans des cellules synchronisées, Bcl-xL(Ser49) est phosphorylé en phase S et G2, déphosphorylé à la prométaphase, la métaphase et à la frontière de l'anaphase, et re-phosphorylé durant la télophase et la cytokinèse. Au cours du point-contrôle G2 induit par les dommages à l'ADN, un pool important de phospho-Bcl-xL(Ser49) se trouve aux centrosomes, un site important pour la régulation de l'entrée en mitose. Durant la télophase et la cytokinèse, phospho-Bcl-xL(Ser49) se trouve le long des microtubules avec la protéine moteure dynéine et dans le cytosol mitotique. Finalement, nos résultats suggèrent que PLK3 est responsable de la phosphorylation de Bcl-xL(Ser49), une protéine kinase impliquée pour l'entrée des cellules en mitose et pour la progression de la mitose jusqu'à la division cellulaire.

Mots-clé: Bcl-xL, phosphorylation, cycle cellulaire, point-contrôle G2, mitose.

Contents

List of Figures

1. Introduction

3. Phospho-Bcl-xL(Ser62) plays a key role at the G2 checkpoint

Abbreviations

Ala, alanine;

APC/C, anaphase-promoting complex/cyclosome;

Asp, aspartic acid;

ATM, Ataxia telangiectasia mutated (kinase);

ATR, ataxia telangiectasia and rad-3-related (kinase);

Bax, Bcl-2-associated X protein;

Bak, Bcl-2 homologous antagonist-killer;

Bcl-2, B cell leukemia/lymphoma protein 2;

Bcl-xL, Bcl-2-related gene X, long isoform;

BH, Bcl-2 homology domain;

Bid, BH3 interacting death agonist;

Bim, Bcl-2-like protein 11;

BUB, budding uninhibited by benzimidazole protein;

CDC, cell division cycle (protein);

CDK, cyclin-dependent kinase;

CENP, centromere protein ;

CHK, checkpoint kinase ;

CLIP170, cytoplasmic linker protein 170;

CPT, camptothecin

DAPI, 4',6'-diamidino-2-phénylindole;

DNA, deoxyribonucleic acid;

GSK3, glycogen synthase kinase 3;

h, hour;

H1, histone 1;

H3, histone 3;

HA, influenza hemagglutinin epitope tag;

HEC1; highly expressed in cancer protein 1;

JNK, Jun N-terminal kinase;

MAD, mitotic arrest deficient protein;

MAPK, mitogen-activated protein kinase;

MAPKAPK2, mitogen-activated protein kinase-activated protein kinase 2;

Mcl-1, myeloid cell leukemia sequence 1;

min, minute;

ml, milliliter;

mM; millimolar;

MPS1, monopolar spindle 1 kinase;

nM, nanomolar;

PCNA, proliferating cell nuclear antigen;

PCR, polymerase chain reaction;

PI, propidium iodide;

PICH, polo-interacting checkpoint helicase;

PLK, polo kinase;

Puma, p53 upregulated modulator of apoptosis;

Rad-3, radiation gene 3;

RNA, Ribonucleic acid;

RNAi, RNA interference;

SAC, spindle-assembly checkpoint;

SAPK, stress-activated protein kinase;

Ser, serine;

siRNA, small interfering RNA;

Thr, threonine;

Tyr, tyrosine;

mg, milligram

μg, microgram

mM, micromolar

VP16, etoposide;

wt, wild-type.

Acknowledgements

I gratefully thank my supervisor, Dr. R Bertrand, for his support, help, advice and discussion during this research program. I also want to thank other members of the laboratory, Myriam, Nicolas and Sandra, and of Estelle Schmitt' laboratory for their helpful and resourceful discussion. The editorial work of Mr. Ovid Da Silva is much appreciated.

Special though to all my family - mother, father, sisters and brothers - and my friends.

I want to thank and mention studentship support from the China Scholarship Council, Faculté des études supérieures de l'Université de Montréal and the Fondation de l'Institut du cancer de Montréal. This project was funded by Canadian Institutes for Health Research.

1. Introduction

Over the last 15 years, close links between the cell cycle and apoptosis in cancer development and tumor reactions to cancer treatment have become eminently apparent [1-6]. In response to cancer chemotherapeutic drugs and radiotherapy, cells rapidly trigger the apoptotic program [7-9] or undergo cell cycle arrest [10-15], followed or not by premature senescence [16-20]. The Bcl-2 family of proteins stands out among the most crucial regulators of apoptosis and performs a vital function in controlling whether a cell will live or die after cancer chemotherapy and radiotherapy [21-30]. In addition, several studies have revealed that members of this family also interface with the cell cycle [20, 31-46] and DNA repair pathways [47-51], effects that are generally separable from their function in apoptosis.

Before I started my Ph.D., our laboratory reported that Bcl-xL, an anti-apoptotic Bcl-2 family member, in addition to counteracting BH3-only protein-mediated cell death signals after cancer chemotherapy, interfaces with the cell cycle checkpoint, stabilizes the G2 cell cycle checkpoint and favors the establishment of premature senescence in surviving cells after DNA topoisomerase I and II inhibitor treatments [20]. We also reported that Bcl-xL co-localizes with cyclin-dependent kinase 1 (cell division cycle 2) (CDK1(CDC2)) in nucleolar structures and binds to CDK1(CDC2) during the G2 checkpoint, whereas its overexpression stabilizes G2 arrest and premature senescence in surviving cells after DNA damage. Bcl-xL potently inhibits CDK1(CDC2) kinase activities. In *in vitro* kinase assays using recombinant Bcl-xL protein, this effect was reversed by a synthetic peptide between the 41st to 60th amino acids, a region rich in Ser- and Thr-phosphorylated residues within the flexible loop domain of Bcl-xL. A mutant deleted from the region (Bcl-xLΔP3) did not alter the anti-apoptotic function of Bcl-xL, but impeded its effect on CDK1(CDC2) activities and on the G2 checkpoint after DNA damage [20]. The fact that this Bcl-xL region (Figure 1) contains several putative phosphorylation sites strongly suggests that Bcl-xL phosphorylation level may govern Bcl-xL regulation and function in cell cycle checkpoints.

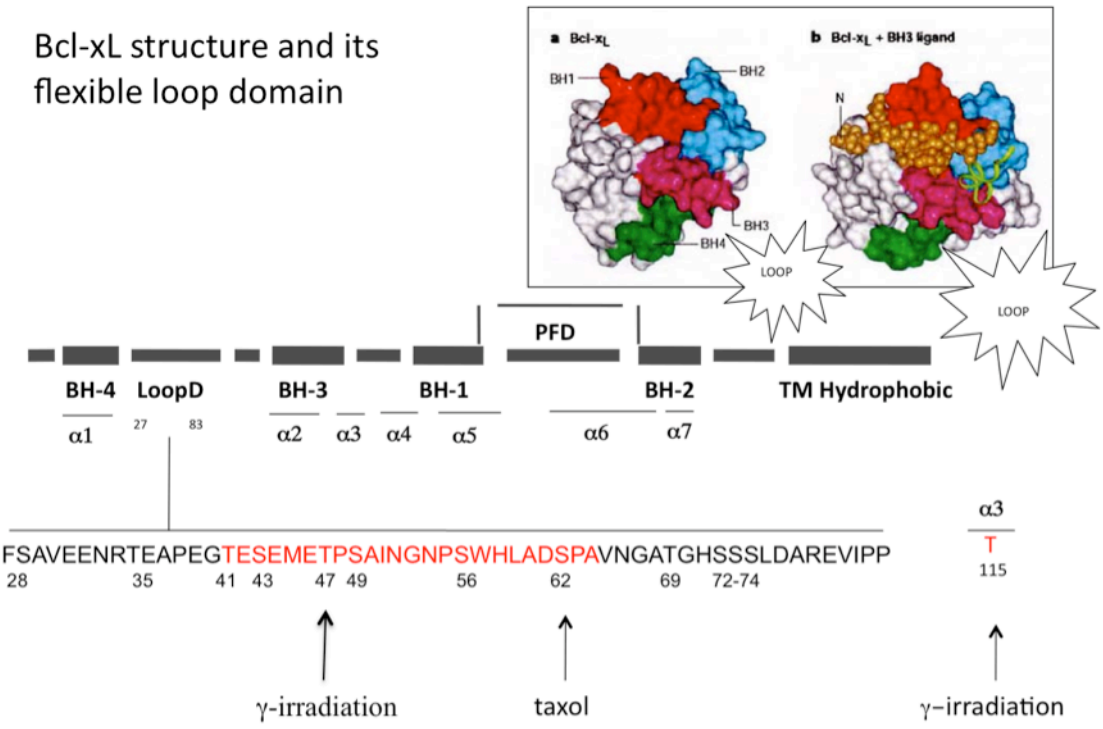

Figure 1. Bcl-xL structure and putative phosphorylation sites within the unstructured flexible loop domain. Upper right inset: schematic representation of the 3D structure of Bcl-xL (A) and Bcl-xL bound to a BH3 ligand (B) (From Youle and Strasser [52]). The unstructured flexible loop domain has been added to the illustration.

During my research program, we generated a series of single-point Bcl-xL cDNA phospho-mutants, including Thr41Ala, Ser43Ala, Thr47Ala, Ser49Ala, Ser56Ala, Ser62Ala and Thr115Ala, and expressed them in human cancer cell lines. We designed experimental assays to measure the stability of etoposide (VP16)-induced G2 arrest and microtubule poisoning-induced spindle-assembly checkpoint (SAC) as well as the kinetics of cytokinesis entry and mitotic exit. We developed specific anti-phospho-Bcl-xL antibodies directed against phospho-Bcl-xL sites of interest, phospho-Ser49 and phospho-Ser62. A combination of such original experiments allowed us to address the

roles of Bcl-xL phosphorylation events during cell cycle progression and checkpoints, and identify the specific protein kinases involved in Bcl-xL phosphorylation at Ser49 and Ser62.

1.1 Cell cycle and the cyclin/CDK complexes

In all living organisms, from the unicellular bacterium to multicellular mammals, the only way that new cells can be made is by duplication of their genetic materials and division into 2 daughter cells. This duplication and division are known as the cell cycle (reviewed in [53-56]). A schematic view of the cell cycle is presented in Figure 2.

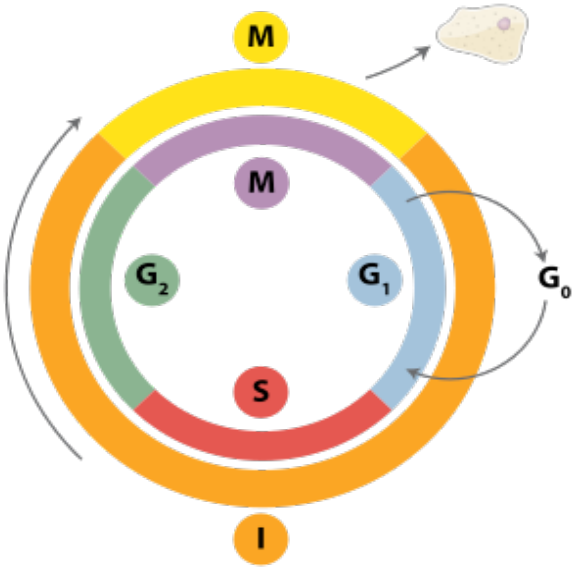

Figure 2. Illustration of the 4 phases of the cell cycle (From http://en.wikipedia.org/ wiki/File: Cell_Cycle_2.svg)

The eukaryotic cell cycle is divided into 4 phases: G1 phase (gap phase 1) following the M phase (M for mitosis) and before the S phase (S for DNA synthesis) in cycling cells or between the G0 phase (gap phase 0) and the S phase in temporarily quiescent cells; the G2 phase (gap phase 2) between the S phase and mitosis. G1, S, and

G2 together are called the interphase (I), occupying about 23 hours of a 24-hour cycle, with 1 hour for mitosis. In the G1 and G2 phases, cells take time to grow and, at the same time, monitor external and internal conditions and signals, then make decisions to either delay progress through G1 or allow commitment to the S phase, to either delay G2 or allow entry into mitosis. Chromosome duplication occurs during the S phase; in the M phase, chromosomes segregate and cells divide (reviewed in [53-56]).

The cell cycle control system is like a programmed clock that triggers essential processes of the cell cycle in a relatively fixed amount of time. The central components of the cell cycle control system are members of a family of protein kinases known as CDKs. The most important CDK regulators are proteins known as cyclins. CDKs are dependent on cyclins for their activity. Without cyclins, CDKs are inactive. Cyclins undergo a cycle of synthesis and degradation in each cell cycle. These changes in cyclin protein levels result in the cyclic assembly and activation of cyclin-CDK complexes, which trigger cell cycle events. Cyclin expressions along the cell cycle are shown in Figure 3A, and the major cyclins and CDKs in eukaryotic cells are illustrated in Figure 3B. At the G1 phase, cyclin D/CDK4 and cyclin D/CDK6 are the main cyclin-CDK complexes. During G1/S transition, cyclin E/CDK2 is the key regulator. During the S phase, cyclin A/CDK2 or cyclin A/CDK1 plays an essential role. During G2/M transition, cyclin B1/CDK1 controls the door to mitosis (reviewed in [53-56]). In addition to dynamic cyclin/CDK interactions, another level of control involves key phosphorylation and dephosphorylation events that are explained in sections below.

A)

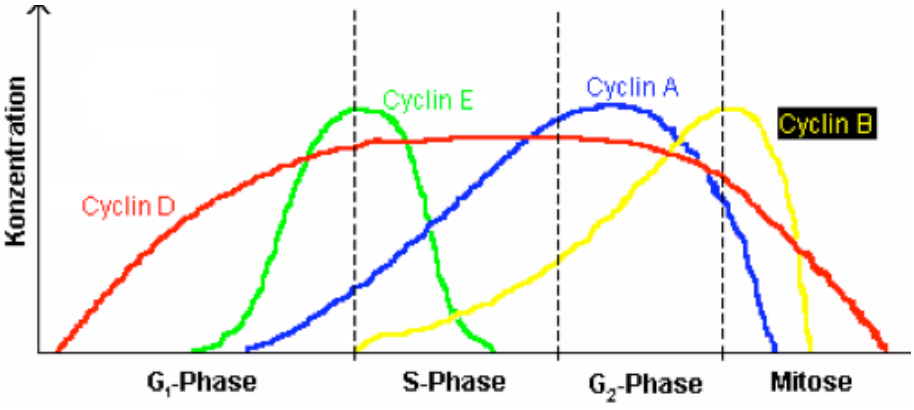

B)

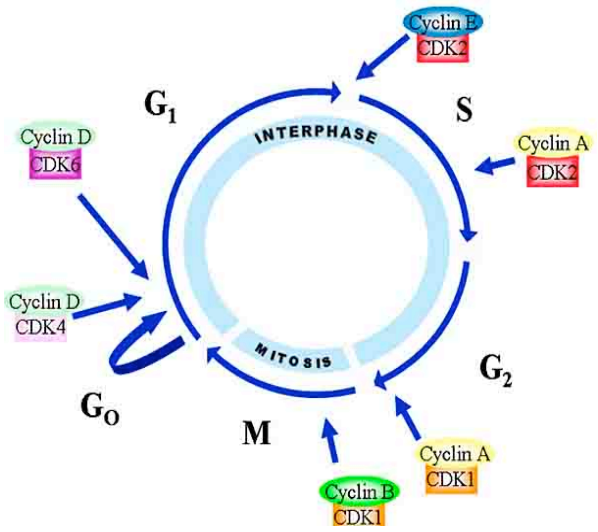

Figure 3. A) Expression of human cyclins through the cell cycle. Illustration from http://en.wikipedia.org/wiki/File:Cyclin_Expression.svg.

B) Major CDK/cyclin complexes during cell cycle progression. Illustration from Chin and D'Mello [57].

1.2 Cell cycle checkpoints

There are 6 major regulatory transitions or checkpoints in the cell-cycle control system of most eukaryotic cells: G1 restriction point, G1/S checkpoint, intra-S checkpoint, G2/M checkpoint, metaphase-to-anaphase transition or the SAC, and the mitotic exit network (MEN). When the cellular and tissue environments are not favorable to replicate, cells delay progress through G1 and enter or stay in G0. If the cellular and tissue environments are favorable, cells progress through the restriction point near the end of G1 and initiate their division cycles [58, 59]. The G1 checkpoint is a system that monitors DNA integrity before entering the S phase [11-13]. The intra-S checkpoint monitors replicative stress and DNA single- and double-strand breaks whereas the G2 checkpoint is a surveillance mechanism ensuring that proper DNA replication is achieved without mistakes or damage and/or production of DNA strand breaks [10, 11, 14, 15, 21, 60-64]. If DNA damage or replication errors are produced, the G2 checkpoint provides more time for DNA repair before entering mitosis. The SAC checks the alignment of chromosomes

at the equator of the spindle and senses the tension produced by attachment of kinetochores to microtubules; if errors occur, the SAC halts mitosis progression at metaphase, allowing more time to correct the mistakes [65-70]. Finally, the MEN controls cytokinesis and mitotic exit [71-75].

Depending on their genetic and environmental background, cells respond to DNA damage specifically, either by rapidly triggering cell death, primarily by apoptosis or, to a much lesser extent, by necrosis or other forms of atypical cell death, or by activating cell cycle checkpoints which arrest cell cycle progression at different phases of the cell cycle (Figure 4). It is generally believed that these checkpoints allow time to repair DNA damage or misaligned and mis-attached chromosomes at mitosis. If repair occurs in a satisfactory manner, the cells can resume cell cycle progression. If DNA damage is persistent and/or the checkpoint is not resolved, cells could then undergo cell death or enter into premature senescence. Cell cycle checkpoints are essential mechanisms that maintain genomic integrity, preventing mutations, chromosomal translocations, aberrations and aneuploidy, events intimately associated with tumorigenesis [15, 76-82].

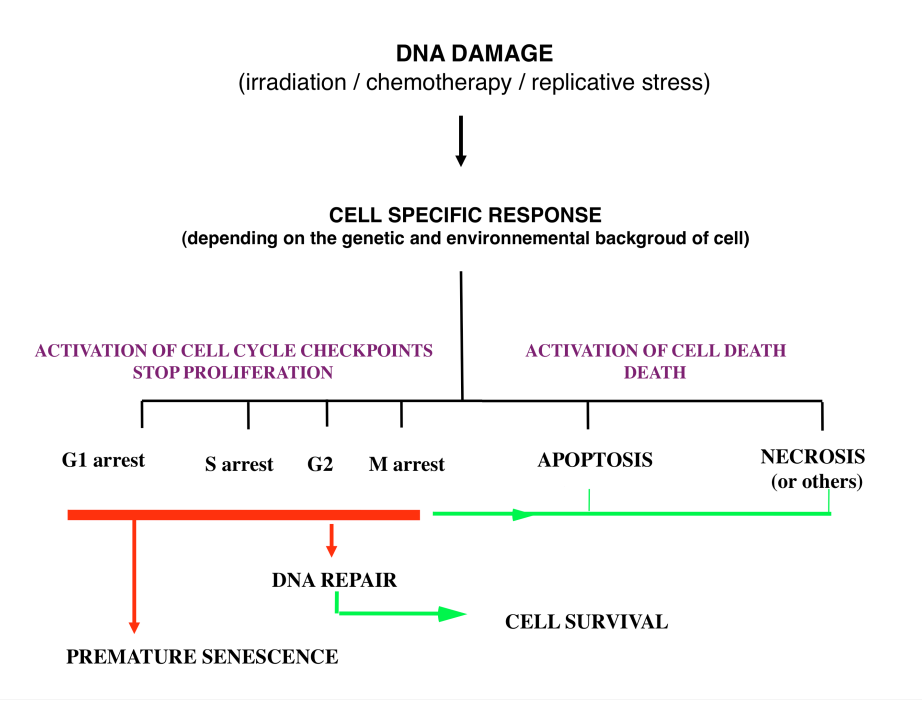

Figure 4. Schematic view of cell responses to DNA damage

Current anticancer drugs and radiotherapy can perturb the orderly progress of DNA replication and cell division [14, 15, 77]. In the laboratory, cancer chemotherapeutic drugs are deployed to induce cell cycle checkpoints and cell death in experimental models consisting of human cancer and variant, genetically-modified cell lines. DNA topoisomerase inhibitors, including camptothecin (a DNA topoisomerase I inhibitor) and VP16 (a DNA topoisomerase II inhibitor), induce DNA single- or double-strand breaks, leading to G2 arrest and/or apoptosis, depending on specific cellular responses and genetic background of the cells. Taxol and nocodazole, microtuble dynamic inhibitors, activate the mitotic SAC, followed or not by cell death or aberrant or avorted mitosis, resulting in aneuploidy, again depending on the specific cellular responses and genetic background of the cells. In the next sections, we will focus on molecular networks controlling the G2 checkpoint, the SAC and mitotic exit, within the contexts of our research program.

1.3 Regulatory networks controlling the G2 cell cycle checkpoint

To control the activity of cyclin B1/CDK1(CDC2) complexes [83-85], the G2 checkpoint is regulated by different pathways, including the classical ATM-CHK2 [86-88] and ATR-CHK1 pathways [89-93] as well as a third pathway initiated by MAPK14/SAPKp38α [94-99].

1.3.1 Cyclin B1/CDK1(CDC2) complex

By the end of the S phase, cyclin B1 starts to be synthesized due to cell cycle-regulated transcription in human cells [85, 100, 101]. During G2, mammalian cyclin B1/CDK1(CDC2) complexes are held in an inactive state by phosphorylation of CDK1(CDC2) at 2 negative regulatory sites, Thr14 and Tyr15, when it is bound to its cyclin partner, cyclin B1 [102-110]. Inhibitory phosphorylation is mediated by the kinases WEE1 and MYT1. WEE1 is a tyrosine kinase that phosphorylates Tyr15, and MYT1 is a

dual-specificity kinase that can phosphorylate both sites, with a tendency toward Thr14 [103-110]. CDK1(CDC2)-Tyr15-specific kinase WEE1 has been postulated to be a CHK1 target [111]. Indeed, WEE1 has been shown to be required for CHK1-mediated G2 arrest and retention of CDK1(CDC2)-Tyr15 phosphorylation [111].

For entry into mitosis, cells need to activate cyclin B1/CDK1(CDC2) complexes by dephosphorylating the 2 inhibitory sites. CDC25 phosphatases are responsible for these dephosphorylation events. Mammalian cells have 3 CDC25 protein phosphatases, CDC25A, B, and C, which appear to have some level of specificity for different cyclin/CDK complexes. Studies indicate that CDC25A regulates G1/S and G2/M transition, whereas CDC25B and CDC25C are involved in intra-S and G2/M regulation [112-119]. CDC25 phosphatases are responsible for triggering activation of cyclin B1/CDK1(CDC2) complexes by dephosphorylating the inhibitory CDK1(CDC2) sites Thr14 and Tyr15.

Entry into mitosis absolutely requires progressive accumulation of active cyclin B1/CDK1(CDC2) complexes in the nucleus. Cyclin B1/CDK1(CDC2) kinase activity is time-organized to coordinate and trigger different mitotic events, the initial activation of cyclin B1/CDK1(CDC2) complexes occurring about 20 to 25 minutes before nucleolar disassembly and nuclear envelope breakdown [120, 121]. After these events, cyclin B1/CDK1(CDC2) rapidly reaches its maximum activity to promote mitosis [120, 121].

1.3.2 ATR-CHK1 and ATM-CHK2 network pathways

In response to DNA damage, activation of ATM and/or ATR kinases elicits CHK1 and CHK2 phosphorylation and activation [86-93]. In turn, CHK1 and CHK2 are important intermediaries of cell cycle arrest and participate in the G2 checkpoint, in part by mediating CDK1(CDC2) inactivation through the inhibitory phosphorylation of CDC25A(Ser123), CDC25C(Ser216) and CDC25B(Ser230-Ser563) [112-119]. Phospho-rylation of CDC25 phosphatases by CHK1 and CHK2 creates a binding site for 14-3-3 proteins, which prevents CDC25 from dephosphorylating CDK1(CDC2). These phosphorylation events, which also impede the nuclear export of CDC25, then separate

CDC25 from cyclin B1/CDK1(CDC2). CDC25 phosphorylation also facilitates its association with SCF(β-TRCP) ubiquitin ligase complex, promoting their degradation [122-128].

PLK1 is inactivated in response to DNA damage by ATM/ATR-dependent phosphorylation [129, 130]. Because PLK1 can phosphorylate cyclin B1 to block its export from the nucleus, it is possible that PLK1 inactivation leaves cyclin B1 stranded in the cytoplasm, thus contributing to CDK1(CDC2) inactivation and G2 arrest [131-136]. However, PLK1 also mediates G2/M transition by phosphorylation/activation and evokes CDC25B and C translocation at centrosomes and nuclei to locally activate cyclin B1/CDK1(CDC2) [117, 137-139], indicating that PLK1 inhibition favors G2 arrest. Accordingly, PLK1 activation by Aurora A promotes checkpoint recovery and resolution after DNA damage [140-142]. In addition, PLK1-dependent activation of the transcription factor FoxM1 at G2 provides a positive-feedback loop associated with mitotic regulatory expression, including cyclin A, cyclin B1, CDC25c and PLK1 itself [143]. PLK3, another member of the Polo kinase family, negatively regulates CDC25C by phosphorylation on Ser216, thereby creating a binding site for 14-3-3 proteins, resulting in protein phosphatase sequestration in the cytoplasm, inhibition of CDC25C activity and G2 arrest [144, 145].

Although not essential for the G2 checkpoint, the tumor suppressor gene product p53, an ATM downstream target, could contribute to G2 arrest by regulating p21, GADD45, and 14-3-3 expression, which overall affects the activity of cyclin B1/CDK1(CDC2) [146-159]. The p53-dependent activation of p21 is, however, mostly linked to the G1 checkpoint and it is believed to have few effects, if any, on the G2 checkpoint [160-170].

1.3.3 The MAPK14/SAPKp38α signaling pathway

The third pathway involved in the G2 checkpoint is the MAPK14/SAPKp38α-initiated signaling pathway [94-99]. Several findings suggest that, after DNA damage, MAPK14/SAPKp38α could mediate the phosphorylation of key target proteins at Ser

residues, in a manner similar to those modified by CHK1 and CHK2. Indeed, MAPK14/SAPKp38α activates MAPKAPK2, which is directly responsible for CDC25B and C phosphorylation associated with 14-3-3 protein binding *in vitro* and in response to DNA damage in mammalian cells [94-98]. Thus, in addition to CHK1 and CHK2, MAPKAPK2 constitutes a third checkpoint kinase involved in coordinating and mediating the DNA damage response and G2 arrest of higher eukaryotic cells. A schematic representation of the molecular network involved in the G2 checkpoint is presented in Figure 5.

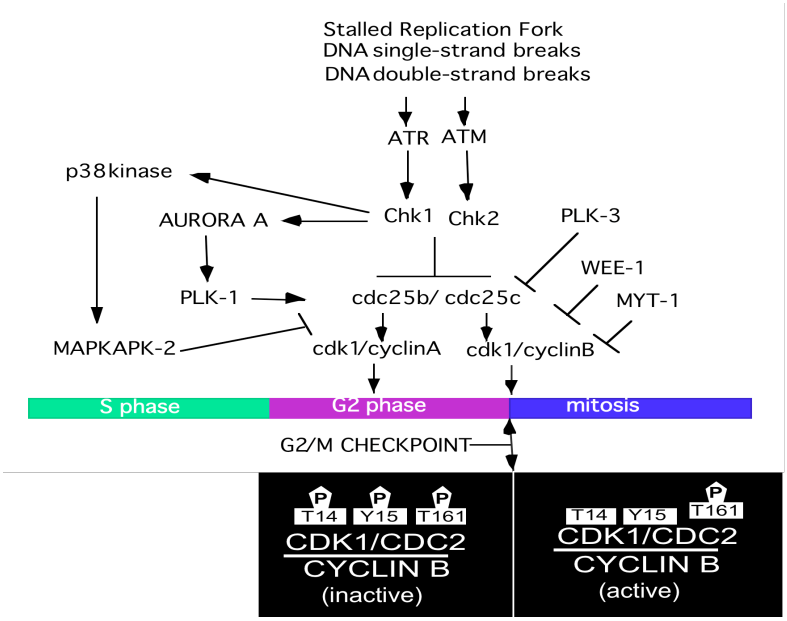

Figure 5. A simplified schematic view of the G2/M cell cycle checkpoint

1.4 The spindle-assembly checkpoint

The SAC is a surveillance mechanism employed by cells to detect the mis-attachment and mis-alignment of chromosomes and tension produced by chromosome capture at kinetochores by microtubules to prevent premature sister-chromatid separation, chromosome mis-segregation and aneuploidy [65-70]. The SAC is also active in response to cancer chemotherapeutic drugs that poison microtubule dynamics, including the clinically-used vinca alkaloids vinblastine and vincristine, tubulin polymerization inhibitors, and the taxane-ring molecule taxol, a tubulin depolymerization inhibitor [65, 66, 69].

1.4.1 The anaphase promoting complex/cyclosome and CDC20

The anaphase-promoting complex or cyclosome (APC/C), a multiprotein E3 ubiquitin ligase, is designed to signal the destruction of specific proteins by transferring multiple copies of the small protein ubiquitin, which target these proteins to proteasome-dependent proteolysis [171]. Vertebrate APC/C consists of at least 12 core subunits organized into 2 large domains, referred to as the "platform" and the "arc lamp", which are flexible relative to each other [67, 172]. The original work of Hartwell and coworkers first isolated multiple CDC mutants of *S. cerevisiae* [173]. Among the selection of mutants, they discovered that yeast harboring the CDC20 mutant arrested cell division in mitosis, and failed to initiate anaphase and chromosome segregation [174]. Human CDC20 contains WD40 repeats, C box, KEN box, MAD2-interacting motif, CRY box, IR motif, and *in vivo* phosphorylation sites. WD40 domains of CDC20 have been suggested to be involved in substrate binding. The C box and IR motif have been implicated in binding to APC/C [175, 176].

The elaborate ubiquitin-conjugating system marks proteins for destruction. E1, as an ATP-dependent, ubiquitin-activating enzyme, transfers ubiquitin to ubiquitin-conjugating enzyme E2, in a complex with E3. By means of the E3 component, E2-E3 complex recognizes a specific degradation signal on target proteins and covalently adds a chain of ubiquitin at the targeted substrate. Once a substrate is marked with the

polyubiquitin chain, its translocates into a proteasome core system that will digest it [177-179]. In concert with E1 and E2 components, the E3 ubiquitin ligase APC/C associated with CDC20 is the key regulator of metaphase-to-anaphase transition, which catalyzes the ubiquitinylation and destruction of 2 major substrate proteins, securin and cyclin B1, thus promoting the onset of anaphase and mitotic exit [180-190]. Indeed, at metaphase, sister-chromatid pairs are linked together by cohesin. Securin inhibits separase, a protease involved in cohesin proteolysis. APC/C-CDC20 degrades securin to relieve separase inhibition [191]. Then, active separase cleaves the SCC1 subunit of cohesin complexes and triggers sister-chromatid separation mediated by the action of microtubule force [67, 172]. By promoting the degradation of cyclin B1, APC/C-CDC20 lowers CDK1(CDC2) activity, an essential event that resumes mitosis and triggers mitotic exit [192-194].

1.4.2 MAD2- and BUBR1-bound APC/C-CDC20 inhibitory subcomplexes

Given the essential role of APC/C-CDC20 evoking entry into anaphase and initiating the segregation of chromosomes, APC/C-CDC20 is tightly regulated by the SAC, which negatively controls APC/C-CDC20 activity in a highly complex manner, mainly by regulating the ability of the limiting subunit CDC20 to activate APC/C, until all centromeric chromosomes have achieved bipolar kinetochore-microtubule attachment. SAC regulators and kinases are involved in an elaborate network that includes MPS1, PLK1, chromosome passenger complex (CPC) containing Aurora B, Survivin, Borealin, and INCEN-P as well as mitotic checkpoint complex containing MAD2, BUB1, BUB3 and BUBR1 (reviewed in [65-70]). The kinetochore localization of SAC components is a prerequisite for checkpoint signaling and amplification. By recruitment to kinetochores that are not, or improperly, captured by microtubules, SAC components are activated and generate "stop anaphase signals" that diffuse into the mitotic cytosol [195-201]. In these hierarchical signaling pathways, MPS1, Aurora B, BUB1 and PLK1 lie at the top, whereas BUB3, BUBR1, MAD1 and MAD2 are downstream. A schematic illustration of the ordered cascade is illustrated in Figure 6.

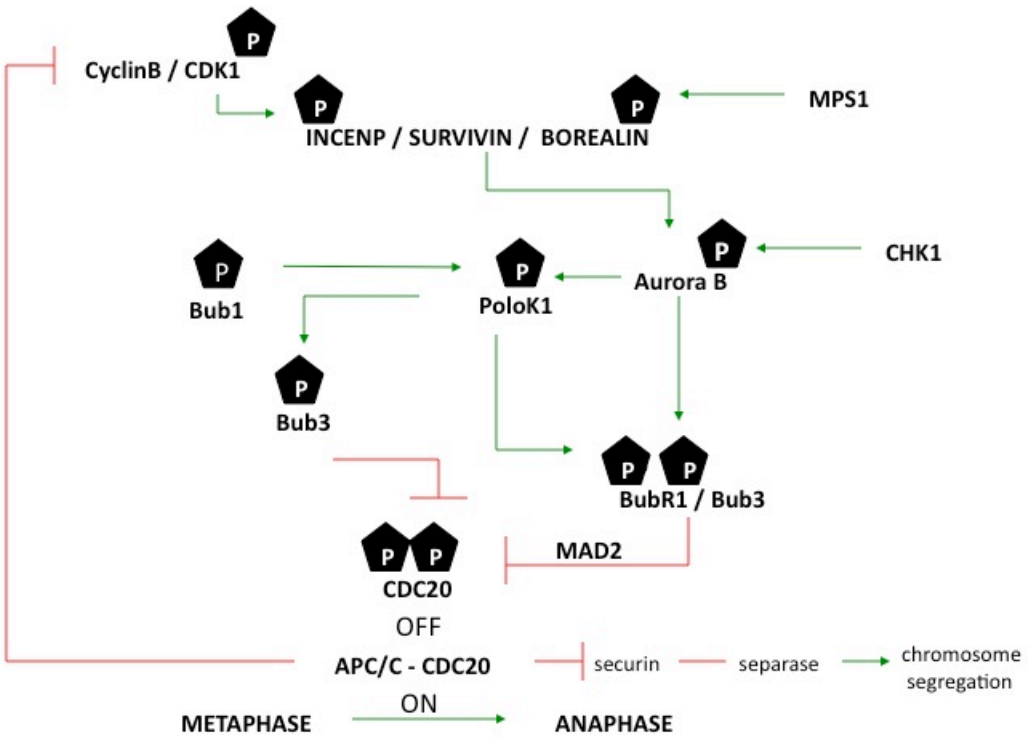

Figure 6. Signaling network during the SAC

MPS1, one the first kinases to be activated when chromosomes are mis-attached and mis-aligned to kinetochores and microtubules, participates in CPC and Aurora B activation [202-207]. On taxol but not nocodazole treatment, CHK1 also participates in Aurora B kinase activation [208, 209]. The importance of Aurora B, BUB1 and PLK1 in that network has been highlighted in several studies. CPC containing Aurora B with BUB1 collaborates to recruit and activate PLK1 at the unattached kinetochore [195, 198, 210-221]. Activated PLK1 then facilitates the kinetochore localization of PICH, MAD1-MAD2,

BUBR1-BUB3, and CDC20 [200, 222-226]. In early mitosis, CDK1 and PLK1 phosphorylate Emi1, a pseudo-substrate that inhibits APC/C-CDC20 activity, resulting in its ubiquitination and degradation [227-230]. PLK1 also phosphorylates and targets PICH to kinetochores, which is required for the kinetochore localization of MAD2 [231]. Other protein kinases, including NEK2A and TAO1, are also involved in the kinetochore localization of MAD2 [197, 232-236].

Several models explain how APC/C-CDC20 is inhibited during the SAC. Studies by Tang et al. and Vanoosthuyse and Hardwick have indicated that 6 residues of CDC20 are phosphorylated both *in vitro* and *in vivo* in a BUB1-dependent manner, providing a catalytic mechanism that negatively regulates APC/C-CDC20 activity [237, 238].

Dynamic subcomplexes have been shown to inhibit APC/C-CDC20 activity during the SAC. MAD2-CDC20 complex is one of the inhibitory forms of CDC20 complex [239, 240]. MAD2 is known to exist in 2 distinct structural conformations, termed "open" (O-MAD2) and "closed" (C-MAD2) [241, 242]. MAD2 can stably bind MAD1, which recruits MAD2 to kinetochores [243, 244]. A "template" model of kinetochore-dependent MAD2 activation, a modified version of the "2-state" model, has emerged from recent research on purified components of unattached chromosomes in cultured cells [245]. It has been observed that O-MAD2 can undergo conformational change to C-MAD2 in which its carboxyl-terminal "seatbelt" domain encloses either MAD1 or CDC20, thereby converting the initial O-MAD2 form to C-MAD2 conformation [245]. During SAC signaling, MAD2 dimerization status is also modified. Two distinct kinetic forms of MAD2 exist at kinetochores, one being the stably-associated MAD1-MAD2 template, and the other, rapidly exchanging MAD2. In these models, conformational change of MAD2, from O-MAD2 to C-MAD2, is required for its efficient binding to CDC20 [246-252].

Dynamic BUBR1-bound subcomplexes, including BUBR1-BUB3-MAD2-CDC20 and BUBR1-BUB3-CDC20, are major inhibitory subcomplexes of APC/C [196, 198, 253-262]. Several studies indicate that these BUBR1-bound subcomplexes are more stable in SAC-activated cells. The exact molecular mechanism by which they inhibit APC/C activity is, however, not completely resolved. Most studies suggest that these subcomplexes act as pseudo-substrates and thus interfere with the ability of APC/C-

CDC20 to interact with its physiological substrates, primarily securin and mitotic cyclins. BUBR1 also contains 2 conserved KEN boxes that appear to regulate CDC20 turnover [263], and BUBR1-bound CDC20 subcomplexes seem to favor CDC20 autoubiquitination and degradation [264-266]. Once CDC20 is autoubiquitinated, the reduced CDC20 level lowers its bioavailability, which, in turn, amplifies APC/C inhibition [266]. However, others have suggested the opposite. One consequence of CDC20 autoubiquitination is the dissociation of MAD2- and BUBR1-bound CDC20 inhibitory complexes, making APC/C available for free-bound CDC20, meaning APC/C-CDC20 activation and SAC resolution. Indeed, Reddy et al. showed that overexpression of UBCH10, the UBC that supports APC/C-catalyzed ubiquitination reactions, prevents cells from arresting at the SAC, even in the presence of nocodazole [265]. The addition of exogenous UBCH10 protein to extracts of nocodazole-arrested mitotic cells increases CDC20 autoubiquitination, disrupts MAD2- and BUBR1-bound CDC20 interactions, and activates APC/C [265]. p31-Comet is another conformation-specific MAD2-binding protein that plays a role in SAC inactivation and resolution [267, 268]. p31-Comet attaches to MAD1-bound MAD2, preventing active conformer generation of MAD2 as C-MAD2, and reducing the rate of MAD2-bound CDC20 inhibitory complexes. p31-Comet, along with UBCH10, stimulates the autoubiquitination of CDC20 and disassembly of MAD2-bound CDC20 complexes, leading to SAC inactivation and APC/C-CDC20 activation [265, 267, 268]. Meanwhile, USP44/protectin, a deubiquitinating enzyme, deubiquitinates CDC20 and maintains MAD2- and BUBR1-bound CDC20 interactions, contributing to SAC activation and APC/C-CDC20 inhibition [269]. Collectively, the activation of SAC kinases and components, cellular concentrations of MAD2- and BUBR1-bound CDC20 complexes as well as the expression level of UBCH10, p31-Comet and USP44/protectin all contribute to the delicate balance between 2 opposing dynamic processes that regulate the activation status of the SAC [265, 266, 269]. These processes are illustrated in Figure 7.

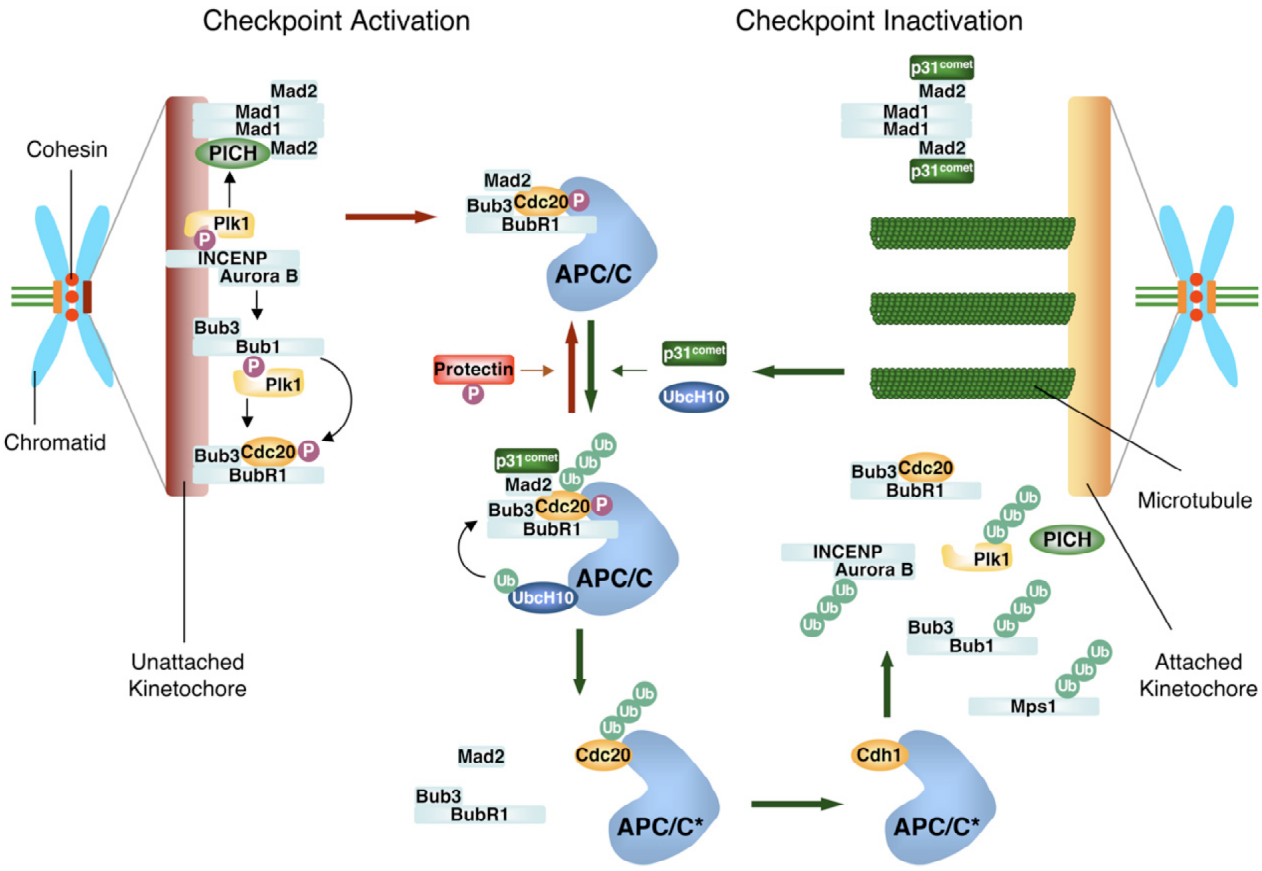

Figure 7. Model of APC/C-CDC20 regulation at the SAC (From Yu [68]).

1.4.3 Dismantling the SAC

SAC resolution and APC/C-CDC20 activation could be initiated by the loss of kinetochore localization of MAD1 and MAD2, and by the dissociation of MAD2- and BUBR1-bound CDC20 interactions. However, besides CDC20 autoubiquitination models and p31-Comet effects that inhibit the MAD2 conformation change described above, the exact mechanisms are poorly understood. A dynein motor protein-dependent 'stripping' mechanism has been proposed, where dynamic interaction between dynein motor protein along microtubules removes MAD2 as well as other outer kinetochore proteins from attached kinetochores and transports them to spindle poles, where they are released into

the mitotic cytosol [270-275]. More recently, another SAC silencing and resolution pathway dependent on PP1 activity has been identified in yeast. These studies propose that, upon successful chromosome bi-orientation, PP1 dephosphorylates BUBR1 at kinetochores, which relieves APC/C-CDC20 inhibition, promoting entry into anaphase and cytokinesis [276-278]. Even though several pathways have been identified for the dismantling of spindle checkpoint signaling, challenges remain to better understand which pathway is the major physiological mode of SAC silencing and resolution and/or whether different pathways could be employed by cells either alone or together, depending on SAC amplitude and/or length.

1.5 The mitotic exit signaling network

The final step of mitosis is cytokinesis, which controls the decision to physically divide a cell into 2 daughter cells that is often termed "mitotic exit". In most animal cells, cytokinesis begins in anaphase and ends shortly after telophase completion. There are 4 distinct stages of cytokinesis: initiation of the spindle midzone and cleavage furrow, contraction of the contractile ring, new membrane insertion, and completion by gap closure between the 2 daughter cells (reviewed in [279]).

The molecular orchestration and reorganization that occur during cytokinesis are far from being completely understood. Absolutely required, ubiquitin-mediated proteolysis controls the passage of cells through mitosis. Specific substrates are degraded as cells progress into, and through, mitosis, APC/C being the major ubiquitin ligase involved in the process. APC/C-CDC20 mediates the ubiquitination of mitotic cyclins leading to the rapid debit of mitotic CDK1(CDC2) activity, simultaneously targeting securin to lose chromosome cohesion and allowing sister-chromatid segregation to opposite poles of the anaphase spindle. These are the first events that contribute to mitosis exit [180, 280, 281]. Cytokinesis requires complete degradation of cyclin B1. By studying human cells engineered to express non-degradable cyclin B1, researchers have demonstrated that cyclin B1 level affects cytokinesis [192-194]. In cells expressing a non-degradable form of cyclinB1, a spindle midzone and cleavage furrow cannot be properly

formed [192-194] and chromosome passenger proteins remain at kinetochores, suggesting that cyclin B1 degradation is also required for translocation of various components from the kinetochores to the central spindle midzone [282]. In *Drosophila* embryos, high levels of non-degradable cyclin B1 prevent chromosome passenger proteins, including Aurora B kinase and its INCEN-P partner, from leaving the kinetochore and binding to the central spindle midzone [282]. Coupled to cyclin B1 destruction, CDK1(CDC2) activity declines at the onset of anaphase, and a series of CDK1(CDC2) substrates are rapidly dephosphorylated. Exit from mitosis is a complex transition, which converts proteins from a phosphorylated state to a dephosphorylated state, associated with cytoskeleton and microtubule remodeling. Figure 8 depicts the kinetics of CDK1(CDC2) kinase activity during mitosis and its progressive inhibition during cytokinesis [194].

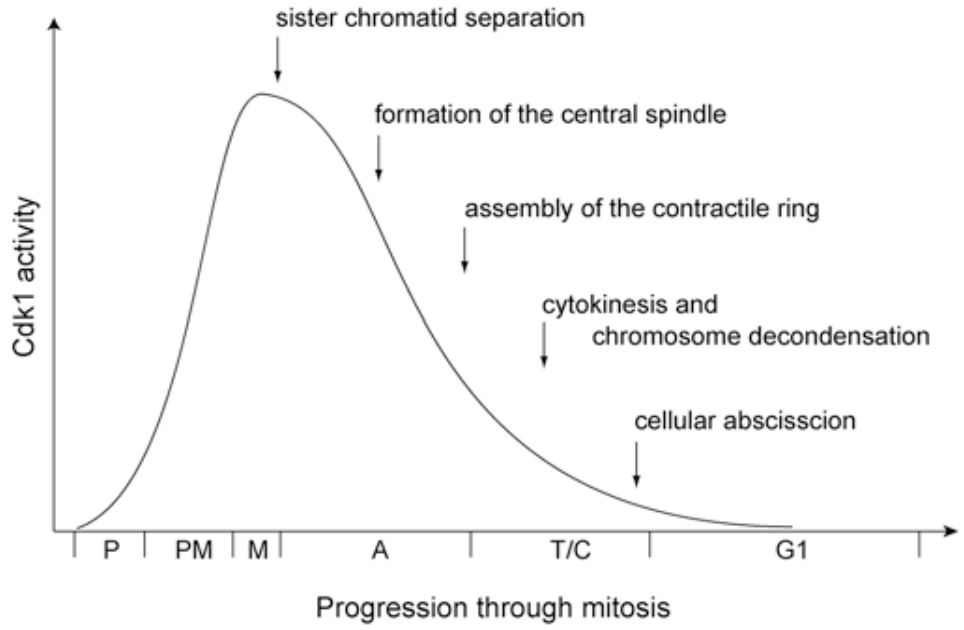

Figure 8. Kinetics of CDK1(CDC2) activity through mitotic progression (From Wolf et al. [194]).

After APC/C-CDC20 activation, CDC20 is replaced by the CDH1 subunit, expanding APC/C substrate specificity [283-289]. CDC20 and CDH1 confer certain substrate specificity to APC/C. The WD40-repeat domain of CDH1 recognizes short peptide motifs within APC/C substrates, of which the most common are D- and KEN-boxes [285, 288]. APC/C-CDH1 becomes active during anaphase and retains its activity during cytokinesis and in G1 cells. APC/C-CDH1 continues to degrade cyclin B1 [290] and is involved in the time control of cytokinesis [291]. By timely targeting of specific substrates, APC/C-CDH1 is required for cytoskeleton and microtubule reorganization and for the recruitment of proteins at the spindle midzone [291-293]. In a timely, regulated manner, APC/C-CDH1 commands the destruction of various kinases and components of the SAC, including Aurora A [294-297], MPS1 [298], NEK2A [299], Aurora B [300, 301], BUB1 [302], microtubule-associated proteins, such as NuSAP [303], SKAP2 [304], TPX2 [305] and, at the very end, PLK1 [306] – to resume mitotic exit.

Assembly of the cleavage furrow and contractile ring consisting of actin filaments and Myosin-II is far from being understood in mammals and involves more than 120 proteins in yeast (reviewed in [279]). In mammalian cells, PLK1 and presumably PLK3 activity, which is also found at the spindle midzone [307], is required for assembly of the cleavage furrow and contractile ring [308]. With Kinesin-6, PLK1 promotes the accumulation of active RhoA-GTP at the cleavage furrow, by phosphorylating RhoGAP that recruits RhoGEF which, in turn, activates RhoA-GTP [309]. In association with the scaffold protein anilin, RhoA-GTPase flux then contributes to Myosin-II activation at the contractile ring [310, 311]. Myosin-II is the driving force that constricts actin filaments at the contractile ring [279].

In addition to ubiquitin ligase activity, mitotic exit requires protein phosphatases. In budding yeast, the MEN controls post-anaphase CDK(CDC) activity to prevent premature cytokinesis. CDC14 is essential for timely, organized exit from mitosis in yeast [312-320]. In yeast, CDC14 is associated with 2 signaling networks, CDC14 early anaphase release (FEAR) and the MEN, that are pivotal for triggering CDK inactivation and localize chromosomal passenger proteins to the spindle midzone [71, 318-320]. Three CDC14 phosphatase homologs in human cells have been identified, CDC14A, B and C,

but whether they have a similar function in mitotic exit is still not known [321-323]. In addition to CDC14, phosphatases PP1 and PP2A have been shown to play roles in mitotic exit in Xenopus egg extracts, budding yeast and, more recently, in human cells [277, 324-329]. Indeed, Wu et al. demonstrated that PP1 activity is required to dephosphorylate CDK1(CDC2) substrates to allow mitotic exit [329].

1.6 Bcl-xL function in apoptosis

Bcl-xL [330], a Bcl-2 family member, has anti-apoptotic activities and has been studied extensively because of its importance in the regulation of apoptosis, during development, tumorigenesis and cellular responses to stress, including anticancer therapies [27, 28, 330-354]. A phenotype of mice deficient in the Bcl-x gene manifests abnormal development and death of fetal erythroid progenitors and neuronal cells, with the animals dying around embryonic day 14 displaying severe defects in erythropoiesis and neuronal development [332]. Bcl-xL usually resides in the cytosol, on the cytoplasmic face of the outer mitochondrial membrane (OMM), endoplasmic reticulum and nuclear envelope [355-357]. A schematic view of the Bcl-2 family members is presented in Figure 9.

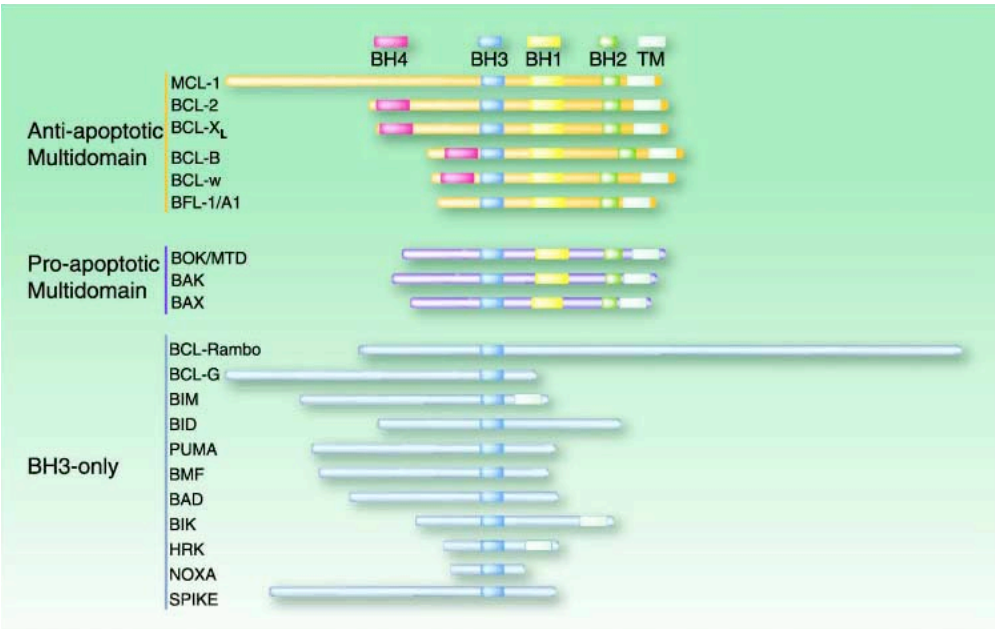

Figure 9. The Bcl-2 family members (From Danial [358])

Bcl-xL contains BH1, BH2, BH3 and BH4 domains, a COOH-terminus hydrophobic transmembrane domain, and an unstructured loop domain, between BH4 and BH3. The BH1, BH2 and BH3 domains create a hydrophobic pocket where the amphipathic α-helice of another BH3-containing protein can bind (Figure 1) [344, 359, 360]. The BH3 domain, particularly among BH3-only proteins, mediates interaction between BH3-only proteins and Bcl-xL protein, thereby promoting apoptosis [361-366]. The 3-dimensional organization of Bcl-xL identifies a 60 amino acid loop lacking a defined structure [359]. Compared to the full-length protein, Bcl-xL loop deletion mutant displays a similar or, in a few studies, an enhanced ability to inhibit apoptosis and does not present significant alterations in its ability to bind pro-apoptotic proteins, such as Bax, or prevent cytochrome c release and caspase activation [20, 367, 368].

Two classical pathways of apoptosis, intrinsic and extrinsic, converge to caspase activation. The extrinsic pathway is initiated by a series of death receptors upon ligand activation, while the intrinsic pathway is triggered by various developmental cues or cytotoxic insults, including viral infections, replication stress, DNA damage and growth factor deprivation, strictly controlled by the Bcl-2 family of proteins (reviewed in [52, 357, 369-371]). Activation and heterodimerization of the pro-apoptotic family members Bax and Bak are crucial for inducing permeabilization of the OMM and subsequent release of apoptogenic molecules, including cytochrome c, which leads, with Apaf-1 and dATP, to caspase-9 activation [372-383]. Anti-apoptotic proteins, such as Bcl-xL and Bcl-2, bind to and inhibit Bax and Bak activity. BH3-only proteins are potent mediators of cell death. BH3-only enabler or sensitizing proteins promote apoptosis by binding to, and inhibiting, pro-survival molecules, such as Bcl-2, Bcl-xL and Mcl-1, whereas BH3-only activator or activating proteins bind to and activate multidomain pro-apoptotic Bax and Bak proteins [363, 384]. Bax insertion and oligomerization into mitochondrial membranes require activation by a BH3-only activating protein, events that elicit OMM permeabilization; in contrast, the potency of anti-apoptotic proteins, such as Bcl-xL, to trap and inhibit these BH3-only activating proteins, prevents membrane permeabilization [366, 385-388]. A schematic view of these interplays is illustrated in Figure 10.

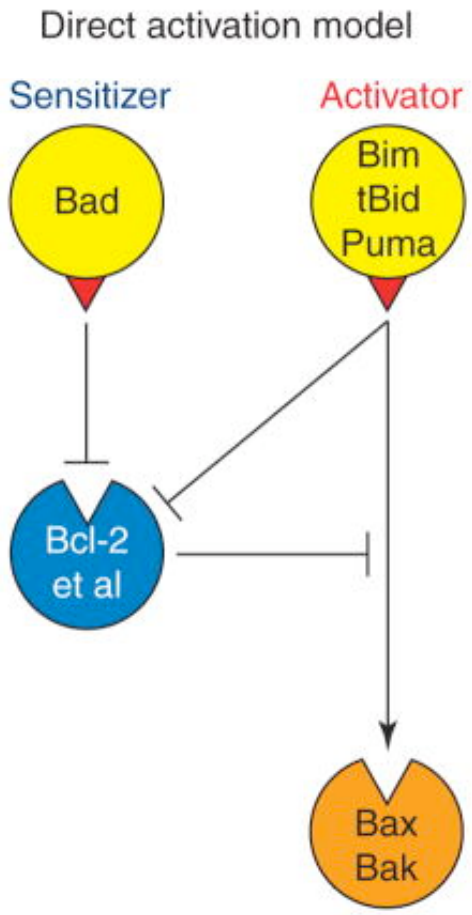

Figure 10. The mode of action of Bcl-2 family members. Anti-apoptotic proteins, such as Bcl-2 and Bcl-xL, maintain cell survival by inhibiting constitutively-expressed pro-apoptotic Bax and Bak proteins. Subsets of the BH3-only proteins like Bad, promote apoptosis by binding to and inhibiting pro-survival proteins, such as Bcl-2 and Bcl-xL, whereas BH3-only activator, like Bim, Bid and Puma proteins bind to and activate multidomain pro-apoptotic Bax and Bak proteins. (From Adams and Cory [371]).

The unexpected pore-forming ability of Bcl-xL protein has also emerged from its 3-dimensional structure. Structural similarities between Bcl-xL, particularly its α5- and α6-helices and the pore-forming domains of some toxins that act as channels, indicate that Bcl-2 members could also function by forming pores in intracellular organelles, including mitochondria (Figure 1) [340, 359, 385-388]. Whether these channel activities function by themselves, or in association with other megachannels, such as components of mitochondrial permeability transition pores, or others, is still not completely elucidated [387, 389-400].

1.6.1 p53-dependent and -independent activation

Activation of BH3-only proteins as a consequence of replicative stress or after exposure to DNA-damaging and microtubule-poisoning agents has been studied extensively. The transcriptional activity of p53 in response to genotoxic agents contributes to its apoptotic activity [401]. Bax itself was the first to be identified as a p53-dependent apoptotic target [402, 403] and the BH3-only proteins Bid, Noxa and Puma were also described as p53-dependent target genes involved in irradiation and anticancer drug-induced apoptosis [404-408]. In addition, direct activation of multidomain pro-apoptotic proteins, such as Bax and Bak, by p53, and direct neutralization of multidomain anti-apoptotic proteins, such as Bcl-2 and Bcl-xL by p53, were also reported [409-412].

Paradoxically, several observations have disclosed that cells lacking the ability to induce a cell cycle checkpoint, as a consequence of p53 disruption, could display hypersensitivity to DNA-damaging treatments and undergo apoptosis very rapidly, indicating the existence of p53-independent pathways of apoptosis [7, 9, 357, 413-424]. Indeed, many studies have now revealed that Bax and a multitude of BH3-only proteins, including Bim, Noxa, Puma, Bik and ITM2Bs, are activated in a p53-independent manner after DNA damage [357, 425-429]. Its appears that many transcription factors activate these genes independently of p53, including p63, p73, E2F1 and FOXO3A [430-442].

1.7 Bcl-2 family members and the cell cycle

Recent studies have revealed links between some Bcl-2-like family members, cell cycle progression and cell cycle checkpoint regulation (Figure 11). First, Bcl-2 has been shown to slow entry from the quiescent G0 into the G1 phase of the cell cycle in multiple cell lineages from transgenic mice. In contrast, Bcl-$2^{-/-}$ knockout cells enter the S phase more quickly [31, 32]. This effect of Bcl-2 on cell proliferation is genetically distinct from its function in apoptosis [31, 32]. More recently, phosphorylated forms of Bcl-2 also have been co-localized in nuclear structures and on mitotic chromosomes, disclosing the importance of phosphorylation events for Bcl-2 protein location [443]. Mcl-1, another Bcl-2 homologue known to function as an anti-apoptotic protein [444], inhibits cell cycle progression through the S phase of the cell cycle. The cell cycle regulatory function of Mcl-1 is partially mediated through its interaction with proliferating cell nuclear antigen, a cell cycle regulator that is crucial in DNA replication [40, 445]. More recently, some have reported that a proteolytic fragment of Mcl-1 regulates cell proliferation via interaction with CDK1(CDC2) [42] and that Mcl-1 is essential in ATR-mediated CHK1 phosphorylation [45]. Others have discerned the involvement of Bid, a BH3-only protein with pro-apoptotic activity, at the intra-S phase checkpoint under replicative stress and in response to DNA-damaging agents. This function of Bid is mediated through its phosphorylation at Ser78 and Ser61/64 by the DNA-damage signaling kinase ATM [43, 44].

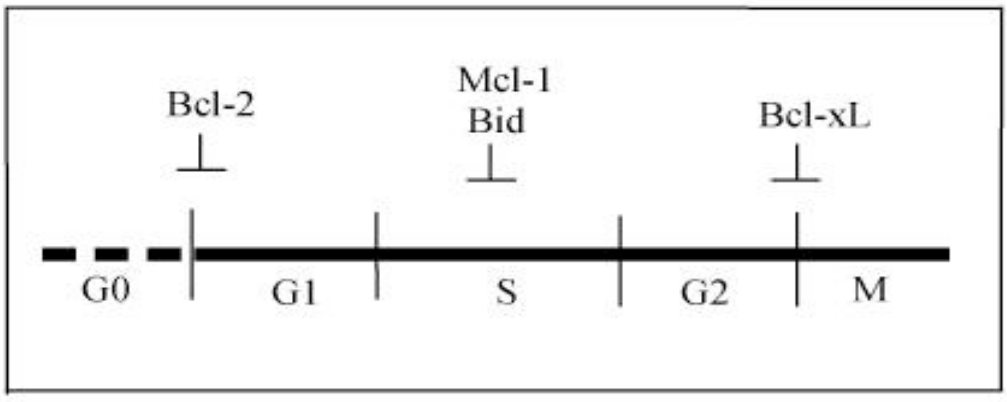

Figure 11. Schematic representation of the effects of Bcl-2, Mcl-1, Bid and Bcl-xL on cell cycle progression (From Schmitt et al. [159]).

Microtubule inhibitors widely used in cancer chemotherapy induce mitotic arrest and apoptosis linked to Bcl-2, Bcl-xL and Mcl-1 phosphorylation [446-453]. Kharbanda et al. have reported that Bcl-xL is phosphorylated within the unstructured loop domain at Thr47 and on Thr115, adjacent to the α3-helix of Bcl-xL, in response to ionizing radiation [454]. A few protein kinases have been proposed to phosphorylate Bcl-2 or Bcl-xL, including the Ask1/Jun-N-terminal protein kinase 1 pathway, normally activated at G2/M transition [454-461], and PLK1 that is also involved in G2/M transition and during mitosis [453]. The exact functions of these phosphorylation events are not yet understood.

2. Rationale of the thesis

2.1 Goal, hypothesis and specific objectives

A previous study in our laboratory showed that Bcl-xL stabilizes the G2 checkpoint, an activity that resides within the flexible loop domain of Bcl-xL, a region that is not essential for its anti-apoptotic function [20]. Our **goal** in this research program was to further understand the critical roles and molecular mechanisms by which Bcl-xL and its flexible loop domain interface with cell cycle progression and checkpoints. We **hypothesize** that Bcl-xL's functions in cell cycle progression and checkpoints are regulated by phosphorylation events within the Bcl-xL flexible loop domain that will influence: i) Bcl-xL location, ii) Bcl-xL protein/protein interactions with cell cycle checkpoint components, and iii) Bcl-xL activity in cell cycle progression and checkpoints. Toward this end, the **1st aim** of the research program was to generate a series of single-point Bcl-xL cDNA phosphorylation mutants, including Thr41Ala, Ser43Ala, Thr47Ala, Ser49Ala, Ser56Ala, Ser62Ala and Thr115Ala, and express them in human cancer cell lines. The **2nd aim** was to design experimental assays to measure the stability of DNA damage-induced G2 arrest and microtubule poisoning-induced SAC, and the kinetics of cytokinesis and mitotic exit, in cell lines expressing wild-type (wt) Bcl-xL, phosphorylation mutants and small interference RNA (siRNA) targeting Bcl-xL expression. The **3rd aim** was to develop specific anti-phospho-Bcl-xL antibodies directed against phospho-Bcl-xL sites of interest. The **4th aim** was to address the importance of these phosphorylation events for Bcl-xL location and function during cell cycle progression and checkpoints in wt synchronized cells or cells exposed to DNA-damaging and microtubule-poisoning agents. The **5th aim** was to identify the specific protein kinases involved in Bcl-xL phosphorylation at sites of interest. Finally, the **6th aim** was to initiate studies by dissecting the molecular mechanisms behind Bcl-xL function during cell cycle progression and checkpoints.

2.2 Presentation of the appended manuscripts

In this thesis, I present my data in 3 manuscripts that have been submitted recently. The functional screening assays deployed in our studies revealed that cells expressing the phosphorylation mutants Bcl-xL(Ser49Ala) and Bcl-xL(Ser62Ala) behave differently than cells expressing wt Bcl-xL, in response to VP16, a DNA topoisomerase II inhibitor, and taxol, a microtubule poison, not in terms of apoptosis protection, but in terms of checkpoint stability and resolution. These first observations were the basis to further develop strategies and experimental approaches to understand the function of phospho-BclxL(Ser62) and (Ser49) during cell cycle progression and checkpoints. The first manuscript described the effect of phospho-Bcl-xL(Ser62) on the G2 checkpoint. The second manuscript described the effects of phospho-Bcl-xL(Ser62) during mitosis. Finally, in the third manuscript, the data for phospho-Bcl-xl(Ser49) at the G2 checkpoint and during mitosis are presented.

2.3 Contribution of co-authors

Jianfang Wang (JW) performed more than 80-85% of all the works and experiments described in the 3 manuscripts. She designed, with the help of Richard Bertrand (RB), the experimental strategies and protocols, actively resolved technical problems that occured during these studies, and analysed the data. She wrote the first versions of the manuscripts and actively participated with RB in revision to the final versions. Myriam Beauchemin (MB), a technician in the laboratory, assisted JW for the generation and preparation of the constructs deployed in these studies, prepared and purified recombinant Bcl-xL protein and performed the *in vitro* kinase assays. MB was also involved in the validation of the specific phospho-antibodies produced in the course of these studies, and in the validation of siRNAs targeting Bcl-xL in the second manuscript. RB supervised the work, analysed the data with JW and MB and revised the manuscripts.

3. Phospho-Bcl-xL(Ser62) plays a key role at the G2 checkpoint

Authors: Jianfang Wang[1], Myriam Beauchemin[1] and Richard Bertrand[1,2,*]

Affiliations: [1]Centre de recherche, Centre hospitalier de l'Université of Montréal (CRCHUM) - Hôpital Notre-Dame and Institut du Cancer de Montréal, and [2]Département de médecine, Université de Montréal, Montréal (Québec) Canada

Running title: Bcl-xL and cell cycle checkpoint

Key words: Bcl-xL, CDK1(CDC2), cell cycle checkpoint, DNA damage, nucleolus.

Corresponding author*: CRCHUM - Hôpital Notre-Dame and Institut du Cancer de Montréal, 1560 Sherbrooke St. East (Room Y-5634),
Montréal (Québec) Canada H2L 4M1.

Abstract

Accumulating evidence suggest that Bcl-xL, an anti-apoptotic member of the Bcl-2 family, also functions in cell cycle progression and cell cycle checkpoints. Analysis of a series of phosphorylation mutants reveals that cells expressing Bcl-xL(Ser62Ala) mutant are less stable at the G2 checkpoint and enter mitosis more rapidly than cells expressing wild type Bcl-xL or Bcl-xL phosphorylation mutants, including Thr41Ala, Ser43Ala, Thr47Ala, Ser56Ala and Thr115Ala. Analysis of the dynamic phosphorylation and location of phospho-Bcl-xL(Ser62) in unperturbed, synchronized cells and during DNA damage-induced G2 arrest discloses that phospho-Bcl-xL(Ser62) translocates into nucleolar structures in VP16-exposed cells during G2 arrest. In a series of *in vitro* kinase assays, pharmacological inhibitors and specific siRNA experiments, we found that Polo kinase 1 and MAPK9/JNK2 are major protein kinases involved in Bcl-xL(Ser62) phosphorylation and accumulation into nucleolar structures during the G2 checkpoint. In nucleoli, phospho-Bcl-xL(Ser62) binds to and co-localizes with CDK1(CDC2), the key cyclin-dependent kinase required for entry into mitosis. These data indicate that, during G2 checkpoint, phospho-Bcl-xL(Ser62) stabilizes G2 arrest by timely trapping of CDK1(CDC2) in nucleolar structures to slow mitotic entry. It also highlights that DNA damage affects the dynamic composition of the nucleolus, which now emerges as a component of the DNA damage response.

Introduction

In mammals, development and tissue homeostasis require a carefully-orchestrated balance between cell proliferation, cell differentiation, cellular senescence and cell death. In recent years, several studies have reported that members of the Bcl-2 family, in addition to their central role in controlling apoptosis during development and cellular stress, also interface with the cell cycle, the DNA damage response, DNA repair pathways and premature senescence, effects that are generally distinct from their function in apoptosis (reviewed in [1, 2]).

Bcl-2 itself has been demonstrated to slow entry from the quiescent G0 to the G1 phase of the cell cycle prior to DNA replication in multiple cell lineages and transgenic mice [3]. In contrast, Bcl-$2^{-/-}$ knockout cells enter the S phase more quickly. This effect of Bcl-2 on cell proliferation is genetically distinct from its function in apoptosis [4]. Mcl-1, another Bcl-2 homologue known to function as an anti-apoptotic protein inhibits cell-cycle progression through the S phase of the cell cycle [5]. More recently, others have reported that a proteolytic fragment of Mcl-1 regulates cell growth via interaction with CDK1(CDC2) [6] and that Mcl-1 plays an essential part in ATR-mediated CHK1 phosphorylation [7]. Others have discerned the involvement of Bid, a BH3-only Bcl-2 family member with pro-apoptotic activity, at the intra-S phase checkpoint under replicative stress in response to DNA-damaging agents. This function of Bid is mediated through its phosphorylation by the DNA-damage signaling kinase ATM [8, 9].

Bcl-2 and/or Bcl-xL modulate the Rad51-dependent homologous recombination pathway as well as non-homologous end-joining and DNA damage mismatch repair activities, effects that are separable from their anti-apoptotic function [10-13]. Bcl-xL also fulfills specific functions distinct from its function in apoptosis during the cell cycle [14, 15]. Indeed, we previously reported that, in addition to its mitochondrial effect, which delays apoptosis, Bcl-xL co-localizes in nucleolar structures and binds CDK1(CDC2) during the G2 cell-cycle checkpoint, and its over-expression stabilizes G2 arrest in surviving cells after DNA damage [15]. Bcl-xL potently inhibits CDK1(CDC2) kinase activity, which is reversible by a synthetic peptide between the 41st to 61st amino acids within or near the described Thr47 and Ser62 phosphorylation sites within its flexible

loop domain. A mutant deleted of this region does not alter the anti-apoptotic function of Bcl-xL, but impedes its effect on CDK1(CDC2) activities and on G2 arrest after DNA damage [15].

To better understand the importance of the Bcl-xL flexible loop domain and putative phosphorylation events in regulating Bcl-xL location and function during the G2 checkpoint, we generated a series of single-point Bcl-xL cDNA phosphorylation mutants, including Thr41Ala, Ser43Ala, Thr47Ala, Ser56Ala, Ser62Ala and Thr115Ala. Stably-transfected cell populations were selected in human B lymphoma Namalwa and cervical carcinoma HeLa cells. In this study, we provide evidence that phospho-Bcl-xL(Ser62) is a key component in stabilizing DNA damage-induced cell cycle arrest.

Results

Effect of Bcl-xL and various Bcl-xL phosphorylation mutants on DNA damage-induced G2 arrest

To examine the G2 cell-cycle arrest function of Bcl-xL, we generated various Bcl-xL phosphorylation mutants, including Thr41Ala, Ser43Ala, Thr47Ala, Ser56Ala, Ser62Ala and Thr115Ala, then stably expressed them in Namalwa cells (Fig. 1A and Supplementary Fig. S1A). A well-established, simple experimental procedure, referred to as mitotic trap assay (Fig. 1B) [16], evaluated the kinetics of G2 arrest after DNA damage, the kinetics of mitotic entry after G2 arrest, and the kinetics of cell death. In the mitotic trap assay, cells entering mitosis after G2 arrest, a direct indicator of G2 checkpoint bypass or checkpoint recovery and adaptation, are trapped by adding nocadazole (0.35 μM) at 24-h intervals after VP16 treatment (10 μM/30 min in Namalwa cells) and monitored by flow cytometry with phospho-H3(Ser10) labeling and propidium iodide (PI) staining. Control Namalwa cells (Fig. 1C) or Namalwa cells stably transfected with empty vector (Fig. 1D) die rapidly after exposure to VP16. In contrast, cells stably expressing HA-Bcl-xL and all phosphorylation mutants show strong inhibition of apoptosis (Fig. 1E-F and Supplementary Fig. S1E-K; green bars). More than 70% of cells over-expressing wt HA-Bcl-xL are arrested in G2, 24 h after VP16 treatment (Figure 1E;

grey bars). However, some of them slowly escape from G2 and enter early mitosis, 48 to 72 h after VP16 treatment (Figure 1E; red bars). The phosphorylation mutants, including HA-Bcl-xL(Thr41Ala), (Ser43Ala), (Thr47Ala), (Ser56Ala) and (Thr115Ala), present a similar phenotype compared to wt HA-Bcl-xL, protecting cells from apoptosis and allowing G2 arrest, with some cells escaping G2 arrest 48 and 72 h post-VP16 treatment (Supplementary Fig. S1F-K). Strikingly, cells expressing the phosphorylation mutant HA-Bcl-xL(Ser62Ala) enter mitosis much more rapidly (Fig. 1F), revealing that Ser62 is important for Bcl-xL function at G2 arrest. In addition, expression of HA-Bcl-xL(Ser62Ala) has an effect similar to HA-Bcl-xL in protecting cells from apoptosis (Fig. 1E-F). Together, these observations suggest that Bcl-xL's function in cell cycle arrest is distinct from its function in apoptosis, with Ser62 as a key player.

HA-Bcl-xL(Ser62) phosphorylation and location during DNA damage-induced G2 arrest

HA-Bcl-xL(Ser62) phosphorylation occurs simultaneously to phosphorylation/activation of key components of the DNA damage response and G2 checkpoint, including ATM, ATR, CHK1, CHK2, Aurora A, Polo kinase 1 (PLK1), MAPKAPK2, MAPK14/SAPKp38α, MAPK9/JNK2 and MAPK8 /JNK1 as well as CDK1(CDC2) phosphorylation/inactivation of (Fig. 2A), pointing to a temporal and functional link between these events. A previous study from our laboratory indicated that Bcl-xL co-localized with CDK1(CDC2) in the nucleolus during the G2 checkpoint induced by camptothecin (CPT) and VP16 treatment in human cell lines [(15)]. The nucleolus acts on cell-cycle progression and genomic stability by phased sequestration and the release of regulatory proteins, including p19/ARF, MDM2, CDC14, PP1, p53, CDK1(CDC2), telomerase and the DNA helicases WRN and BLM (reviewed in [(17)]). Indirect *in cellular* immunofluorescence microscopy was undertaken to monitor the re-distribution of wt HA-Bcl-xL and phosphorylation mutant HA-Bcl-xL(Ser62Ala). We observed that a pool of wt HA-Bcl-xL and phospho-Bcl-xL(Ser62) co-localized strongly with nucleolin, a marker of the nucleolus, 48 h-post VP16 exposure (Fig. 2B). In contrast, the phosphorylation mutant HA-Bcl-xL(Ser62Ala) showed no co-location with nucleolin (Fig. 2C). Total phospho-Bcl-xL(Ser62) in Namalwa cells, expressing the

phosphorylation mutant HA-Bcl-xL(Ser62Ala), was also considerably reduced. The percentage of wt HA-Bcl-xL and phosphorylation mutant HA-Bcl-xL(Ser62Ala) that co-localized with nucleolin in Namalwa cells was quantified by image analysis (Fig. 2D). The percentages of total phospho-Bcl-xL(Ser62), including endogenous Bcl-xL and HA-tagged expressed protein, are illustrated in Fig. 2E. Altogether, these results indicate that Ser62 is required for Bcl-xL translocation to nucleoli 48 h-post VP16 treatment, and that accumulation of phospho-Bcl-xL(Ser62) into nucleoli coincides with the stabilization of G2 arrest. The specificity of phospho-Bcl-xL(Ser62) antibodies is depicted in Supplementary Fig. S2.

Endogenous Bcl-xL(Ser62) phosphorylation and location in unperturbed, synchronized cells and during DNA damage-induced G2 arrest

Because the above observations were made in HA-Bcl-xL-transfected and over-expressed cells, we next explored the role of endogenous Bcl-xL in the cell cycle. We performed these experiments in human wt HeLa cells. Indeed, wt HeLa cells are less prone to apoptosis after VP16 treatment, and undergo G2 arrest, with some cells escaping G2 arrest 48 and 72 h-post VP16 treatment (Fig. 3A, left panel). Bcl-xL(Ser62) phosphorylation is also seen in wt HeLa cells exposed to VP16 and accumulates in enriched nuclear fractions (Fig. 3B). In addition, HA-Bcl-xL transfection and over-expression in HeLa cells stabilizes G2 arrest (Fig. 3A, right panel). When wt HeLa cells are synchronized by double thymidine block and released upon progression from S to G2, endogenous Bcl-xL is progressively modified with accumulation of Ser62 phosphorylation (Fig. 3C). Phospho-Bcl-xL(Ser62) is found in cytosolic and nuclear extracts, with progressive accrual in nuclear extracts in late S and G2 (Fig. 3C), indicating that Bcl-xL phosphorylation on Ser62 occurs during normal cell cycle progression. We next investigated the subcellular location of endogenous phospho-Bcl-xL(Ser62) in wt HeLa cells by indirect immunofluorescence staining, in asynchronized control and VP16-exposed cells and, synchronized, untreated G2 cells (Fig. 3D-F). In wt HeLa cells exposed to VP16, phospho-Bcl-xL(Ser62) accumulated in nucleoli 24- and 48 h-post VP16 exposure. Accumulation in nucleoli was more marked after VP16 treatment in comparison to synchronized, untreated G2 cells (Fig. 3D). Phospho-Bcl-xL(Ser62)

was also found in Cajal bodies with coilin, a specific Cajal body marker, but the location remained unchanged under the conditions tested (Fig. 3E). Finally, phospho-Bcl-xL(Ser62) did not locate in centrosomes (Fig. 3F). Taken together, these results indicate that endogenous Bcl-xL is phosphorylated on Ser62 during normal cell cycle progression and that phospho-Bcl-xL(Ser62) accumulates much more strongly in nucleoli during DNA damage-induced G2 checkpoint in wt HeLa cells.

PLK1 and MAPK9/JNK2 are major protein kinases involved in Bcl-xL(Ser62) phosphorylation and accumulation in nucleoli during DNA damage-induced G2 arrest

Various protein kinases have been postulated to phosphorylate Bcl-xL on Ser62 under various experimental conditions including those driving activation of the mitotic spindle-assembly checkpoint [18-22]. No study has yet documented Bcl-xL phosphorylation on Ser62 at the G2 checkpoint. Based on an *in silico* consensus site prediction search (Supplementary Table S5), and on known protein kinases activated during the DNA damage response and G2 checkpoint (Fig. 2A), we first tested a panel of protein kinases by *in vitro* kinase assays with recombinant human Bcl-xL protein as substrate. Among all the kinases tested, PLK1, MAPK9/JNK2, GSK3α, GSK3β, MAPK8/JNK1, MAPKAPK2 and MAPK14/SAPKp38α were positive and able to phosphorylate recombinant Bcl-xL protein on Ser62 in *in vitro* kinase assays (Fig. 4A). The origin of the kinases, kinase assay description and enzyme-specific activities with control substrates are indicated in Supplementary Table S3 and Supplementary Fig. S3. Then, with specific pharmacological inhibitors and VP16-exposed cells, we observed that PLK, JNK and GSK3 inhibitors prevented Bcl-xL phosphorylation on Ser62 (Fig. 4B) in VP16-exposed cells. Deploying a series of specific siRNAs (Fig. 4C, and see supplementary Table S4 and supplemenatry Fig. S4 for additional information and controls), western blotting of enriched nuclear extracts revealed that the most important kinases involved in Bcl-xL(Ser62) phosphorylation in G2-arrested VP16-treated HeLa cells were PLK1, MAPK8/JNK1, MAPK9/JNK2 and, to a much lesser extent, GSK3β (Fig. 4D). Finally, to confirm these results and to monitor the effect of silencing the kinases on phospho-

Bcl-xL(Ser62) accumulation in nucleoli in VP16-exposed cells, indirect *in cellular* immunofluorescence microscopy was undertaken and quantified (Fig. 4E). The data indicate that PLK1 and MAPK9/JNK2 are major protein kinases associated with progressive phospho-Bcl-xL(Ser62) accumulation in nucleolar structures in VP16-exposed cells.

Phospho-Bcl-xL(Ser62) meets CDK1(CDC2) in nucleolar structures during DNA damage-induced G2 arrest

In a series of reciprocal co-immunoprecipitation experiments, we previously showed that nuclear Bcl-xL binds to CDK1(CDC2) during the G2 checkpoint [(15)]. Here, we repeated these experiments on enriched nuclear and enriched nucleolar extracts. In nuclear extracts, we observed that a pool of Bcl-xL protein co-immunoprecipitating with CDK1(CDC2) is phosphorylated on Ser62. The phosphorylation mutant Bcl-xL(Ser62Ala) in nuclear extracts also co-immunoprecipitated with CDK1(CDC2), but to an apparently lesser extent (Fig. 5A). When co-immunoprecipitation experiments were performed on nucleolar extracts (Fig. 5B), we noted that phospho-Bcl-xL(Ser62) co-immunoprecipitated with CDK1(CDC2), while the phosphorylation mutant Bcl-xL(Ser62Ala) was not present in nucleolar fractions. Reciprocal co-immunoprecipitation was also undertaken (Fig. 5B). CDK1(CDC2) protein co-localized with nucleolin in VP16-exposed cells (Fig. 5C) as well as with phospho-Bcl-xL(Ser62) in nucleolar structures (Fig. 5D). Together, the data suggest that during G2 checkpoint, Bcl-xL phosphorylation on Ser62 promotes Bcl-xL translocation to nucleoli where it will meet an important pool of CDK1(CDC2), contributing to its trapping in nucleolar structures to timely avoid entry into mitosis (Fig. 5E).

Discussion

Our study reveals Bcl-xL(Ser62) phosphorylation during the normal cell cycle and in DNA-damage-induced G2 arrest, and PLK1 and MAPK9/JNK2 are major protein

kinases responsible for Bcl-xL(Ser62) phosphorylation and progressive accumulation in nucleolar structures during the stabilization of DNA damage-induced G2 arrest. This function of phospho-Bcl-xL(Ser62) was clearly separable from Bcl-xL's known purpose in apoptosis, as the Bcl-xL(Ser62Ala) phosphorylation mutant retained its anti-apoptotic effect but lacked the G2-arrest stabilization function. This original role of phospho-Bcl-xL(Ser62) is associated with its translocation into the nucleolus after DNA damage, where it will meet CDK1(CDC2). The dynamic complex processes that occur in the nucleolus are emerging. Besides their traditional function in ribosome biogenesis, nucleolar structures are now appearing as key centers that either provide local concentration of activities essential for nuclear and cellular processes, or exclude and timely trap nuclear factors that would otherwise interfere with proper nuclear and cellular functions [17]. Indeed, the nucleolus acts on cell-cycle progression and genomic stability by phased sequestration and the release of regulatory proteins, including p19/ARF, MDM2, CDC14, PP1, p53, telomerase and the DNA helicases WRN and BLM [17]. CDK1(CDC2) as well as Bcl-xL or Bcl-2 have also been reported previously in nucleolar structures [15, 23, 24]. In the nucleolus, phospho-Bcl-xL(Ser62) binds to and co-localizes with CDK1(CDC2) in G2-arrested cells, indicating that its contributes to the temporal trapping of CDK1(CDC2), avoiding unwanted mitosis in the presence of DNA damage. It could also suggest that Bcl-xL(Ser62) protects nucleolar structures during DNA damage-induced G2 arrest to avoid rapid nucleolar disassembly associated with mitosis onset. Phospho-Bcl-xL(Ser62) was also located in Cajal bodies. Although not investigated further in this study, Cajal bodies are known to encompass dynamic trafficking and fusion with nucleolar structures [17, 25]. In the near future, it will certainly be of interest to further examine Cajal bodies/nucleoli interaction during the G2 checkpoint.

Entry into mitosis absolutely requires progressive accumulation of active cyclin B1/CDK1 (CDC2) complexes in the nucleus. Indeed, recent observations indicate that different levels of cyclin B1/CDK1(CDC2) kinase activity are timely organized to coordinate and trigger different mitotic events, the initial activation of cyclin B1/CDK1(CDC2) complexes occuring about 20 to 25 min before nucleolar disassembly and nuclear envelope breakdown [26]. When cyclin B1/CDK1(CDC2) activity reaches a specific threshold, it triggers both nucleolar disassembly and nuclear envelope

breakdown. After these events, cyclin B1/CDK1(CDC2) rapidly reaches maximum activity to resume mitosis [26]. Our data suggest that Bcl-xL(Ser62) phosphorylation is associated with its translocation to the nucleolus. In the nucleolus, phospho-Bcl-xL(Ser62) will meet CDK1(CDC2) during G2 checkpoint, playing a role in stabilizing G2 arrest by timely trapping of CDK1(CDC2) into nucleolar structures to avoid or slow down unwanted mitotic entry.

PLK1 activity is regulated both in time and space, and its many functions have been linked to cell entry into mitosis, centrosomes and microtubule-organizing centres, mitotic exit and cytokinesis (reviewed in [27]). Relatively little is known about its function during the S and G2 phases of the cell cycle. However, it has been reported recently that PLK1 accumulates in the nucleus during S and G2 phases revealing that PLK1 also has key functions during the S and G2 phases of the cell cycle [28]. Among them, it has been shown that PLK1 interacts with many chromatin-bound components including those of the replicative helicase, Mcm complexes, suggesting a possible role during replication and/or in monitoring replicative stress [29]. PLK1 also binds to and phosphorylates DNA topoisomerase IIα, promoting its activity [28]. Our observation that PLK1 is one of the key protein kinases associated with Bcl-xL(Ser62) phosphorylation during the G2 checkpoint illustrates additional functional roles for PLK1 along the cell cycle.

At G2/M transition, high PLK1 activation is promoted by BORA and Aurora A [30], and facilitates CDK1(CDC2)-cyclinB1 activation by promoting WEE1 downregulation and regulating CDC25 phosphatase activities [31]. PLK1 is an important target of the DNA damage response enabling cell-cycle arrest. In response to DNA damage, PLK1 ubiquitination, degradation and inactivation have been reported via a CDC14B/Cdh1 pathway. PLK1 also promotes checkpoint recovery after DNA damage (reviewed in [27]). However, mitotic entry in an unperturbed cell cycle can occur in the absence of PLK1, and PLK1 does not appear to act in an amplification loop with cyclin B1/CDK1 (CDC2) to trigger the early mitotic events [26].

Activation of various MAPK pathways during G2 and mitosis has also been documented. MAPK14/SAPKp38α directly activates MAPKAPK2, which is responsible for CDC25B/C phosphorylation and 14-3-3 protein binding *in vitro* in response to DNA

damage in mammalian cells [32]. Thus, MAPKAPK2, in addition to CHK1 and CHK2, is involved in coordinating the DNA damage response of higher eukaryotic cells. MAPK8/JNK1 and MAPK9/JNK2 are also strongly expressed during the G2 and early M-phase, accumulating in the nucleus during G2, and play a role in proper mitosis [33]. Inhibition or silencing of MAPK9/JNK2 only did not block entry of cells into mitosis but resulted in polyploidy, indicating that MAPK9/JNK2 also functions in maintaining genomic stability [34]. The MAPK9/JNK2 effect on Bcl-xL(Ser62) phosphorylation resulting in G2 checkpoint stabilization is consistent with a MAPK9/JNK2 - phospho-Bcl-xL(Ser62) function in genomic stability.

Phospho-Bcl-xL(Ser62) during the normal cell cycle and DNA damage-induced G2 checkpoint has not yet been documented. Phospho-Bcl-xL(Ser62) has been detected previously in cells treated with microtubule inhibitors, including nocodazole, paclitaxel, vinblastine and vincristine. Mitotic arrest induced by these compounds is associated with Bcl-2, Bcl-xL and Mcl-1 phosphorylation. Other studies have revealed that Bcl-2 and Mcl-1 phosphorylation is also tightly coupled with normal mitotic events [35, 36]. Bcl-2 phosphorylation multi-sites (Ser70, Ser87, Thr69) are located within the unstructured loop domain of the protein, a region generally not essential for its anti-apoptotic function. Multiple kinases have been proposed to phosphorylate Bcl-2 and/or Bcl-xL at Ser62 in microtubule inhibitor-exposed cells, but most studies have suggested that JNK, normally activated at G2/M, is the kinase responsible for Bcl-2 and Bcl-xL phosphorylation [19-22, 37, 38].

In summary, our study reveals Bcl-xL(Ser62) phosphorylation during the normal cell cycle and in DNA damage-induced G2 arrest and, PLK1 and MAPK9/JNK2 are major kinases responsible for Bcl-xL(Ser62) phosphorylation and progressive accumulation in nucleolar structures during stabilization of DNA damage-induced G2 arrest. It highlights that DNA damage also affects the dynamic composition of a subnuclear domain, the nucleolus, which now emerges as an important piece of the DNA damage cell response.

Materials and methods

Cell culture, cDNA construction and transfection.

Human Namalwa and HeLa cell lines were obtained from the American Type Culture Collection and grown at 37°C under 5% CO_2 in RPMI-1640 medium and DMEM medium supplemented with 10% heat-inactivated fetal bovine serum (FBS), 100 U/ml penicillin and 100 µg/ml streptomycin, respectively. The phosphorylation mutant pCEP4-HA-Bcl-xL and pCDNA3.1-HA-Bcl-xL vectors were generated by triple polymerase chain reactions (PCR) (15). All primers and details are provided in Supplementary Table S1. Transfected cells were grown under hygromycin B1 (pCEP4 vectors) or neomycin (pCDNA3.1 vectors) selection to obtain stable cell population prior to performing the experiments.

Mitotic trap assay and cell synchronisation

Mitotic trap assay has been described by Andreassen et al [(16)]. Briefly cells entering mitosis after G2 arrest were trapped by adding nocadazole (0.35 µM) at 24-h intervals after VP16 treatment. At the indicated times, the kinetics of G2 arrest, mitotic entry and cell death were monitored in Coulter EpicsXL flow cytometers with phospho-H3(Ser10) labeling and PI staining. HeLa cells were synchronized by double-thymidine block (2 mM) and release.

Protein extraction, subcellular fractionation, immunoblotting and co-immunoprecipitation

To prepare total protein extracts, the cells were extracted with lysis buffer containing 20 mM Hepes(KOH), pH 7.4, 120 mM NaCl, 1% Triton X-100, 2 mM phenylmethylsulfonyl fluoride (PMSF), a cocktail of protease inhibitors (Complete™, Roche Applied Science) and a cocktail of phosphatase inhibitors (PhosStop™ Roche Applied Science). Cytosolic and nuclear extracts were prepared with NE-PER Nuclear

and Cytoplasmic extraction reagents according to the manufacturer's protocol (ThermoScientific, Rockford IL). Nucleolar fractions were obtained from enriched nuclei according to a procedure adapted from published protocols [39]. Briefly, purified nuclei were re-suspended in 3 ml of 0.34 M sucrose containing 0.5 mM $MgCl_2$ and PhosStop™, and then sonicated on ice for 6 x 6-s bursts with 10-s intervals between each burst, with a XL-2000 Microson (Misonix Inc., Farmingdale NY) at power setting 5. Nucleoli were then purified by layering the sonicated solution on a 3-ml 0.88M sucrose cushion containing 0.5 mM $MgCl_2$ followed by centrifugation at 2,000 x *g* for 20 min. Nucleoli pellets were re-suspended in lysis buffer containing 20 mM Hepes(KOH), pH 7.4, 120 mM NaCl, 1% Triton X-100, 0.5% deoxycholate, 2 mM PMSF, a cocktail of protease and phosphatase inhibitors, incubated on ice for 30-min with insoluble materials discarded after centrifugation (10,000 x g; 20 min). For immunoprecipitation, samples were first pre-cleaned with a protein A- and G-Sepharose mixture and, after centrifugation, antibodies at 10 μg/ml concentration were incubated at 4°C for 4 h. All antibodies used in this study are listed in Supplementary Table S2.

Protein kinase assays and protein kinase chemical inhibitors

The kinases and kinase assays are described in Supplementary Table S3. Enzyme activities were tested on control substrates, and velocities were expressed as nmole/min/mg (data in Supplementary Fig. S3). Recombinant human Bcl-xL(ΔTM) protein was produced and purified, as described previously [15]. The protein kinase chemical inhibitors deployed in this study are listed in Supplementary Table S3.

siRNA-mediated protein kinase inhibition

HeLa cells were transfected with DharmaFECT-1 transfection reagent (ThermoScientific) according to the manufacturer's instructions, with 100 nM of either control siRNA or siRNA targeting different kinases (Supplementary Table S4). The cells were treated 10 h-post transfection with VP16 (10 μM) for 16 h, then washed twice with PBS, followed by

their incubation in drug-free medium for an additional 20 h prior to protein extraction and SDS-PAGE.

Immunofluorescence microscopy

Namalwa cells were spread by cytocentrifugation on glass slides and HeLa cells were seeded and grown directly on coverslips. Both cell types were fixed in methanol at -20°C for 30 min and rapidly immersed into ice-cold acetone for a few seconds. The slides were allowed to dry at room temperature and rehydrated in PBS. Nonspecific binding sites were blocked in PBS containing 5% FBS (blocking solution), then the slides were incubated sequentially with specific primary antibody (10 μg/ml in blocking solution), specific labeled-secondary antibody (10 μg/ml in blocking solution) followed by DAPI staining, also performed in blocking solution. All antibodies are listed in Supplementary Table S2. Images were generated with a Leica Microsystem mounted on a Leica DM6000B microscope and Leica DFC480 camera hooked up to a MacInctosh computer. All images were quantified with Clemex Vision software (Version 3.0.036, Clemex, Longueuil, QC, Canada), as described previously [(40)].

Supplementary information: Supplementary information for this article are available at the journal WEB site.

Disclosure of Conflicts of Interest

The authors declare no potential conflicts of interest.

Acknowledgements

This work was funded by grant MOP-97913 of the Canadian Institutes of Health Research to R.B. J.W. received scholarships from the China Scholarship Council

(Beijing, China), the Faculté des études supérieures (Université de Montréal, Canada) and the Fondation de l'Institut du cancer de Montréal (Canada).

References

1. Danial NN, Gimenez-Cassina A, Tondera D. Homeostatic functions of Bcl-2 proteins beyond apoptosis. Adv Exp Med Biol 2010; 687: 1-32.
2. Schmitt E, Paquet C, Beauchemin M, Bertrand R. DNA-damage response network at the crossroads of cell-cycle checkpoints, cellular senescence and apoptosis. J Zhejiang Univ Sci B 2007; 8: 377-97.
3. Borner C. Diminished cell proliferation associated with the death-protective activity of Bcl-2. J Biol Chem 1996; 271: 12695-8.
4. Huang DCS, Oreilly LA, Strasser A, Cory S. The anti-apoptosis function of Bcl-2 can be genetically separated from its inhibitory effect on cell cycle entry. EMBO J 1997; 16: 4628-38.
5. Fujise K, Zhang D, Liu J, Yeh ET. Regulation of apoptosis and cell cycle progression by MCL1. Differential role of proliferating cell nuclear antigen. J Biol Chem 2000; 275: 39458-65.
6. Jamil S, Sobouti R, Hojabrpour P, Raj M, Kast J, Duronio V. A proteolytic fragment of Mcl-1 exhibits nuclear localization and regulates cell growth via interaction with Cdk1. Biochem J 2005; 387: 659-67.
7. Jamil S, Mojtabavi S, Hojabrpour P, Cheah S, Duronio V. An essential role for MCL-1 in ATR-mediated CHK1 phosphorylation. Mol Biol Cell 2008; 19: 3212-20.
8. Zinkel SS, Hurov KE, Ong C, Abtahi FM, Gross A, Korsmeyer SJ. A role for proapoptotic BID in the DNA-damage response. Cell 2005; 122: 579-91.
9. Kamer I, Sarig R, Zaltsman Y, et al. Proapoptotic Bid is an ATM effector in the DNA-damage response. Cell 2005; 122: 593-603.
10. Saintigny Y, Dumay A, Lambert S, Lopez BS. A novel role for the Bcl-2 protein family: specific suppression of the RAD51 recombination pathway. EMBO J 2001; 20: 2596-607.
11. Wiese C, Pierce AJ, Gauny SS, Jasin M, Kronenberg A. Gene conversion is strongly induced in human cells by double-strand breaks and is modulated by the expression of Bcl-x(L). Cancer Res 2002; 62: 1279-83.
12. Youn CK, Cho HJ, Kim SH, et al. Bcl-2 expression suppresses mismatch repair activity through inhibition of E2F transcriptional activity. Nat Cell Biol 2005; 7: 137-47.
13. Wang Q, Gao F, May WS, Zhang Y, Flagg T, Deng X. Bcl-2 negatively regulates DNA double-strand-break repair through a nonhomologous end-joining pathway. Mol Cell 2008; 29: 488-98.

14. Janumyan YM, Sansam CG, Chattopadhyay A, et al. Bcl-xL/Bcl-2 coordinately regulates apoptosis, cell cycle arrest and cell cycle entry. EMBO J 2003; 22: 5459-70.

15. Schmitt E, Beauchemin M, Bertrand R. Nuclear co-localization and interaction between Bcl-xL and Cdk1(cdc2) during G2/M cell cycle checkpoint. Oncogene 2007; 26: 5851-65.

16. Andreassen PR, Skoufias DA, Margolis RL. Analysis of the spindle-assembly checkpoint in HeLa cells. Methods Mol Biol 2004; 281: 213-25.

17. Boulon S, Westman BJ, Hutten S, Boisvert FM, Lamond AI. The Nucleolus under Stress. Mol Cell 2010; 40: 216-27.

18. Poruchynsky MS, Wang EE, Rudin CM, Blagosklonny MV, Fojo T. Bcl-X(L) is phosphorylated in malignant cells following microtubule disruption. Cancer Res 1998; 58: 3331-8.

19. Fan M, Goodwin M, Vu T, Brantley-Finley C, Gaarde WA, Chambers TC. Vinblastine-induced phosphorylation of Bcl-2 and Bcl-XL is mediated by JNK and occurs in parallel with inactivation of the Raf-1/MEK/ERK cascade. J Biol Chem 2000; 275: 29980-5.

20. Kharbanda S, Saxena S, Yoshida K, et al. Translocation of SAPK/JNK to mitochondria and interaction with Bcl-x(L) in response to DNA damage. J Biol Chem 2000; 275: 322-7.

21. Basu A, Haldar S. Identification of a novel Bcl-xL phosphorylation site regulating the sensitivity of taxol- or 2-methoxyestradiol-induced apoptosis. FEBS Lett 2003; 538: 41-7.

22. Terrano DT, Upreti M, Chambers TC. Cyclin-dependent kinase 1-mediated Bcl-xL/Bcl-2 phosphorylation acts as a functional link coupling mitotic arrest and apoptosis. Mol Cell Biol 2010; 30: 640-56.

23. Barboule N, Truchet I, Valette A. Localization of phosphorylated forms of Bcl-2 in mitosis: co-localization with Ki-67 and nucleolin in nuclear structures and on mitotic chromosomes. Cell Cycle 2005; 4: 590-6.

24. Migone F, Deinnocentes P, Smith BF, Bird RC. Alterations in CDK1 expression and nuclear/nucleolar localization following induction in a spontaneous canine mammary cancer model. J Cell Biochem 2006; 98: 504-18.

25. Dellaire G, Bazett-Jones DP. Beyond repair foci: subnuclear domains and the cellular response to DNA damage. Cell Cycle 2007; 6: 1864-72.

26. Gavet O, Pines J. Progressive activation of CyclinB1-Cdk1 coordinates entry to mitosis. Dev Cell 2010; 18: 533-43.

27. Takaki T, Trenz K, Costanzo V, Petronczki M. Polo-like kinase 1 reaches beyond mitosis-cytokinesis, DNA damage response, and development. Curr Opin Cell Biol 2008; 20: 650-60.

28. Li H, Wang Y, Liu X. Plk1-dependent phosphorylation regulates functions of DNA topoisomerase II alpha in cell cycle progression. J Biol Chem 2008; 283: 6209-21.

29. Tsvetkov L, Stern DF. Interaction of chromatin-associated Plk1 and Mcm7. J Biol Chem 2005; 280: 11943-7.

30. Seki A, Coppinger JA, Jang CY, Yates JR, Fang G. Bora and the kinase Aurora a cooperatively activate the kinase Plk1 and control mitotic entry. Science 2008; 320: 1655-8.

31. Lobjois V, Jullien D, Bouche JP, Ducommun B. The polo-like kinase 1 regulates CDC25B-dependent mitosis entry. Biochim Biophys Acta 2009; 1793: 462-8.

32. Manke IA, Nguyen A, Lim D, Stewart MQ, Elia AE, Yaffe MB. MAPKAP kinase-2 is a cell cycle checkpoint kinase that regulates the G2/M transition and S phase progression in response to UV irradiation. Mol Cell 2005; 17: 37-48.

33. Oktay K, Buyuk E, Oktem O, Oktay M, Giancotti FG. The c-Jun N-terminal kinase JNK functions upstream of Aurora B to promote entry into mitosis. Cell Cycle 2008; 7: 533-41.

34. MacCorkle RA, Tan TH. Inhibition of JNK2 disrupts anaphase and produces aneuploidy in mammalian cells. J Biol Chem 2004; 279: 40112-21.

35. Ling YH, Tornos C, Perez-Soler R. Phosphorylation of Bcl-2 is a marker of M phase events and not a determinant of apoptosis. J Biol Chem 1998; 273: 18984-91.

36. Scatena CD, Stewart ZA, Mays D, et al. Mitotic phosphorylation of Bcl-2 during normal cell cycle progression and Taxol-induced growth arrest. J Biol Chem 1998; 273: 30777-84.

37. Maundrell K, Antonsson B, Magnenat E, et al. Bcl-2 undergoes phosphorylation by C-Jun N-terminal kinase stress-activated protein kinases in the presence of the constitutively active GTP-binding protein Rac1. J Biol Chem 1997; 272: 25238-42.

38. Yamamoto K, Ichijo H, Korsmeyer SJ. Bcl-2 is phosphorylated and inactivated by an ASK1/Jun N-terminal protein kinase pathway normally activated at G(2)/M. Mol Cell Biol 1999; 19: 8469-78.

39. Ochs RL. Methods used to study structure and function of the nucleolus. Methods Cell Biol 1998; 53: 303-21.

40. Parent N, Winstall E, Beauchemin M, Paquet C, Poirier GG, Bertrand R. Proteomic analysis of enriched lysosomes at early phase of camptothecin-induced apoptosis in human U-937 cells J Proteomics 2009; 72: 960-73.

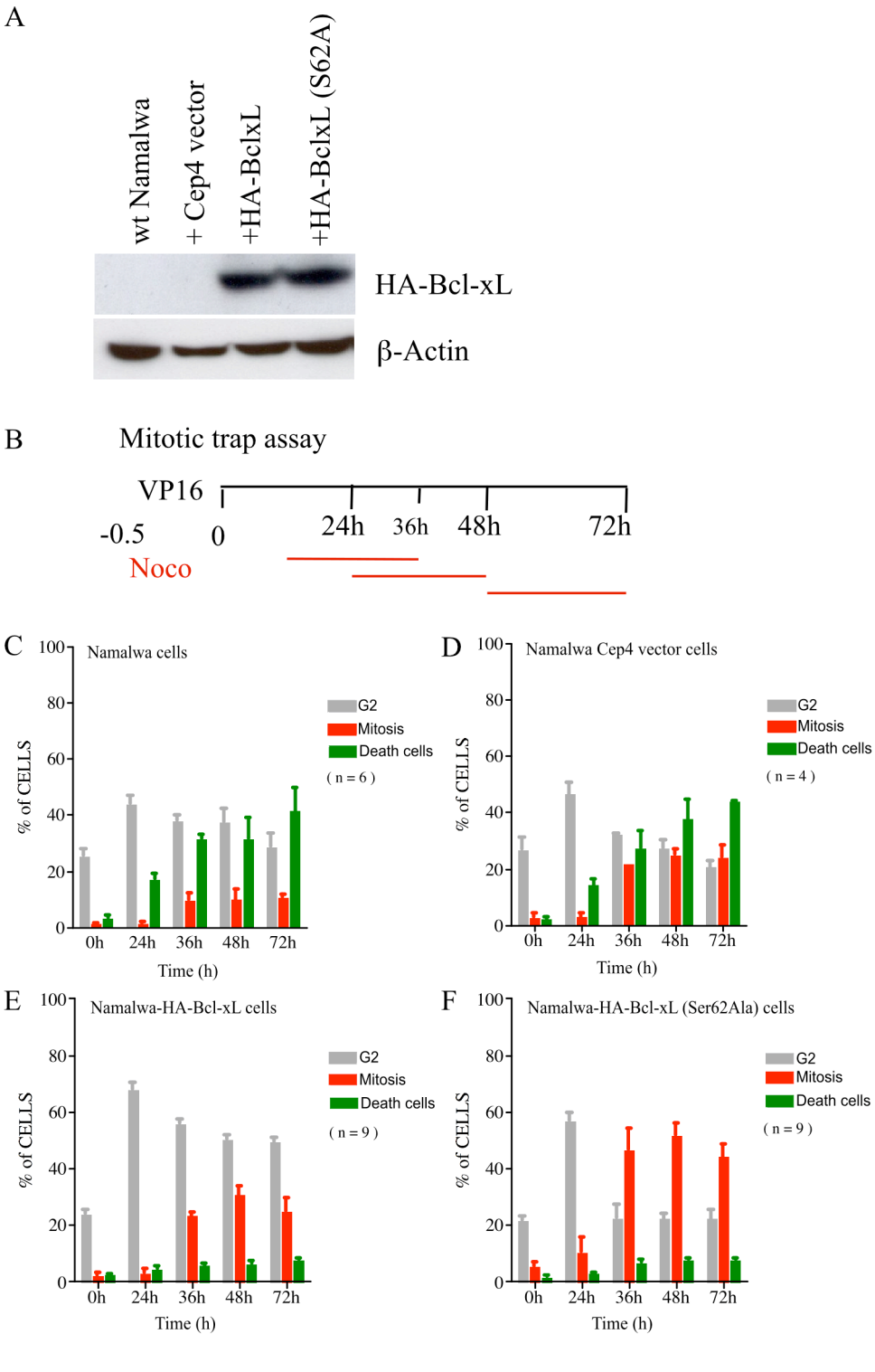
A
wt Namalwa
+ Cep4 vector
+HA-BclxL
+HA-BclxL (S62A)
HA-Bcl-xL
β-Actin
B
Mitotic trap assay
VP16
-0.5
0
24h
36h
48h
72h
Noco
C
Namalwa cells
% of CELLS
Time (h)
G2
Mitosis
Death cells
(n = 6)
D
Namalwa Cep4 vector cells
(n = 4)
E
Namalwa-HA-Bcl-xL cells
(n = 9)
F
Namalwa-HA-Bcl-xL (Ser62Ala) cells
(n = 9)

Figure 1

Figure 1 Effect of Bcl-xL and Bcl-xL(Ser62Ala) phosphorylation mutant on DNA damage-induced G2 arrest. (**A**) Expression level of HA-Bcl-xL and Bcl-xL(Ser62Ala) phosphorylation mutant in stably-transfected Namalwa cell populations. β-actin expression is shown as control. (**B**) Schematic view of the mitotic trap assay; VP16 was administered at 10 μM for 30 min; nocodazole treatments (0.35 μM) at the indicated intervals trapped cells entering mitosis. (**C-F**) Kinetics of G2 arrest (grey bars), mitotic slippage (red bars) and cell death (green bars) in wt Namalwa cells and Namalwa cells expressing HA-Bcl-xL and Bcl-xL(Ser62Ala) phosphorylation mutant. Bars represent the means ± s.e.m. of *n* independent experiments. Data with additional HA-Bcl-xL phosphorylation mutants are in Supplementary Fig. S1.

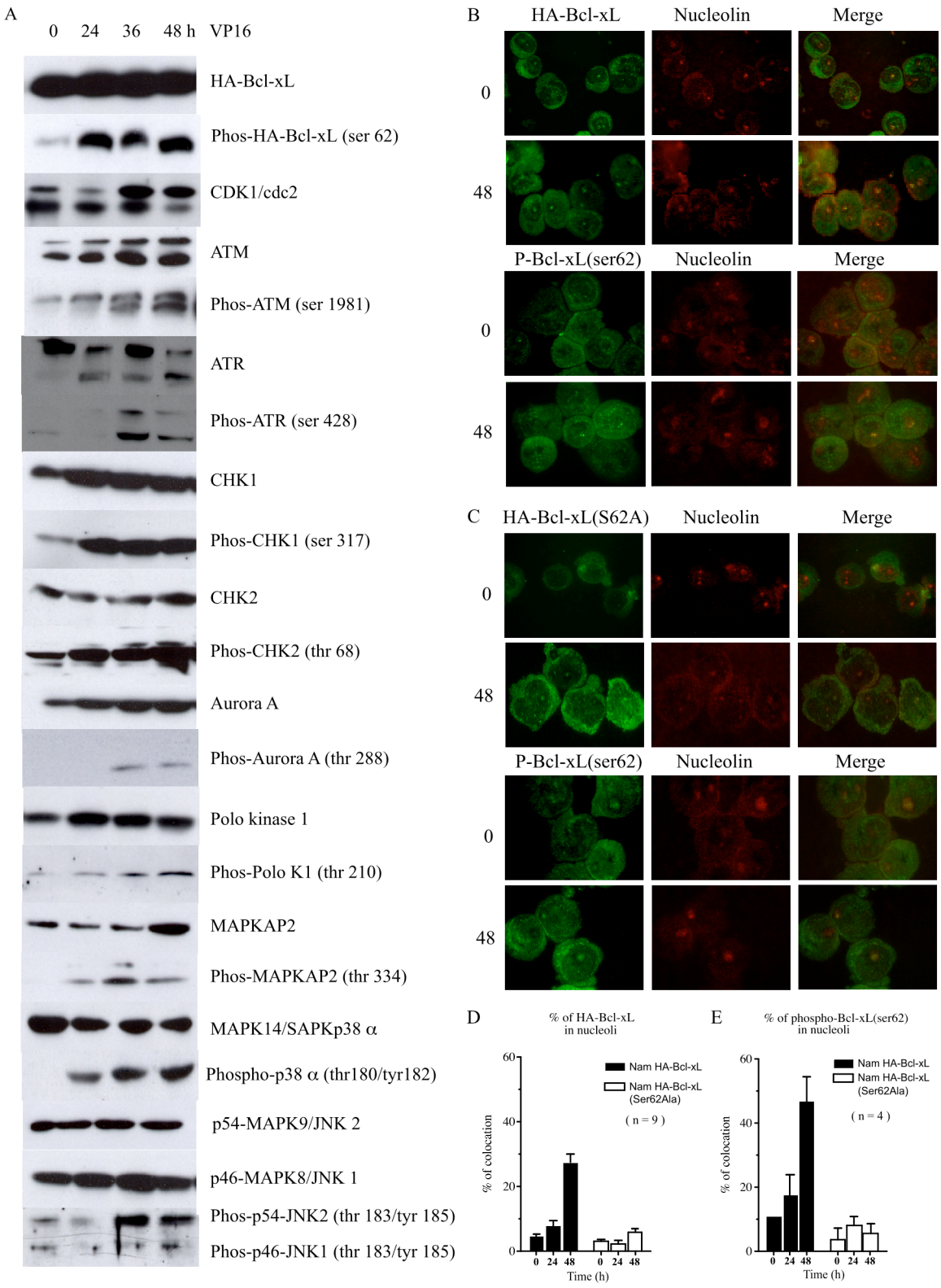
A
0 24 36 48 h VP16
HA-Bcl-xL
Phos-HA-Bcl-xL (ser 62)
CDK1/cdc2
ATM
Phos-ATM (ser 1981)
ATR
Phos-ATR (ser 428)
CHK1
Phos-CHK1 (ser 317)
CHK2
Phos-CHK2 (thr 68)
Aurora A
Phos-Aurora A (thr 288)
Polo kinase 1
Phos-Polo K1 (thr 210)
MAPKAP2
Phos-MAPKAP2 (thr 334)
MAPK14/SAPKp38 α
Phospho-p38 α (thr180/tyr182)
p54-MAPK9/JNK 2
p46-MAPK8/JNK 1
Phos-p54-JNK2 (thr 183/tyr 185)
Phos-p46-JNK1 (thr 183/tyr 185)
B
HA-Bcl-xL
Nucleolin
Merge
0
48
P-Bcl-xL(ser62)
Nucleolin
Merge
0
48
C
HA-Bcl-xL(S62A)
Nucleolin
Merge
0
48
P-Bcl-xL(ser62)
Nucleolin
Merge
0
48
D
% of HA-Bcl-xL in nucleoli
Nam HA-Bcl-xL
Nam HA-Bcl-xL (Ser62Ala)
(n = 9)
% of colocation
Time (h)
E
% of phospho-Bcl-xL(ser62) in nucleoli
Nam HA-Bcl-xL
Nam HA-Bcl-xL (Ser62Ala)
(n = 4)
% of colocation
Time (h)

Figure 2

Figure 2 HA-Bcl-xL(Ser62) phosphorylation and location during DNA damage-induced G2 arrest. (**A**) Expression and phosphorylation kinetics of HA-Bcl-xL and key components of DNA damage responses after VP16 treatment (10 μM for 30 min). (**B**) Co-location kinetics of HA-Bcl-xL and phospho-Bcl-xL(Ser62) with nucleolin in Namalwa cells expressing HA-Bcl-xL exposed to VP16 (10 μM for 30 min). (**C**) Co-location kinetics of HA-Bcl-xL(Ser62Ala) and phospho-Bcl-xL(Ser62) with nucleolin in Namalwa cells expressing the phosphorylation mutant HA-Bcl-xL(Ser62Ala) exposed to VP16 (10 μM for 30 min). (**D**) Percentage of HA-Bcl-xL and **(E)** phospho-Bcl-xL(Ser62) located in nucleoli in Namalwa cells expressing HA-Bcl-xL and HA-Bcl-xL(Ser62Ala) mutant exposed to VP16 (10 μM for 30 min). Bars represent the means ± s.e.m. from micrographs obtained in *n* independent experiments.

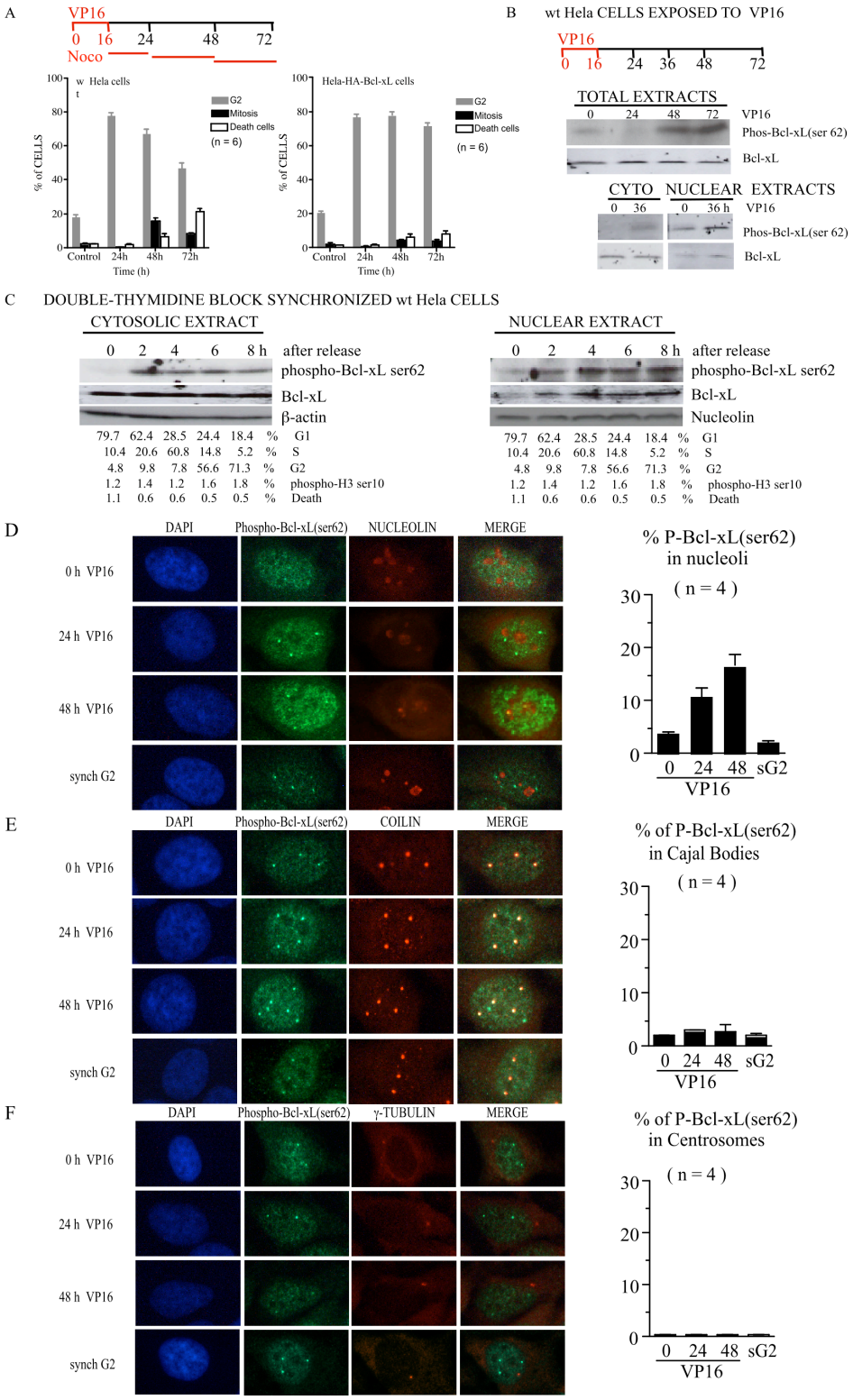
A
VP16
0 16 24 48 72
Noco
w t Hela cells
Hela-HA-Bcl-xL cells
G2
Mitosis
Death cells
(n = 6)
% of CELLS
Control 24h 48h 72h
Time (h)
B
wt Hela CELLS EXPOSED TO VP16
VP16
0 16 24 36 48 72
TOTAL EXTRACTS
0 24 48 72
VP16
Phos-Bcl-xL(ser 62)
Bcl-xL
CYTO NUCLEAR EXTRACTS
0 36 0 36 h
VP16
Phos-Bcl-xL(ser 62)
Bcl-xL
C
DOUBLE-THYMIDINE BLOCK SYNCHRONIZED wt Hela CELLS
CYTOSOLIC EXTRACT
0 2 4 6 8 h after release
phospho-Bcl-xL ser62
Bcl-xL
β-actin
79.7 62.4 28.5 24.4 18.4 % G1
10.4 20.6 60.8 14.8 5.2 % S
4.8 9.8 7.8 56.6 71.3 % G2
1.2 1.4 1.2 1.6 1.8 % phospho-H3 ser10
1.1 0.6 0.6 0.5 0.5 % Death
NUCLEAR EXTRACT
0 2 4 6 8 h after release
phospho-Bcl-xL ser62
Bcl-xL
Nucleolin
79.7 62.4 28.5 24.4 18.4 % G1
10.4 20.6 60.8 14.8 5.2 % S
4.8 9.8 7.8 56.6 71.3 % G2
1.2 1.4 1.2 1.6 1.8 % phospho-H3 ser10
1.1 0.6 0.6 0.5 0.5 % Death
D
DAPI
Phospho-Bcl-xL(ser62)
NUCLEOLIN
MERGE
0 h VP16
24 h VP16
48 h VP16
synch G2
% P-Bcl-xL(ser62) in nucleoli
(n = 4)
0 24 48 sG2
VP16
E
DAPI
Phospho-Bcl-xL(ser62)
COILIN
MERGE
0 h VP16
24 h VP16
48 h VP16
synch G2
% of P-Bcl-xL(ser62) in Cajal Bodies
(n = 4)
0 24 48 sG2
VP16
F
DAPI
Phospho-Bcl-xL(ser62)
γ-TUBULIN
MERGE
0 h VP16
24 h VP16
48 h VP16
synch G2
% of P-Bcl-xL(ser62) in Centrosomes
(n = 4)
0 24 48 sG2
VP16

Figure 3

Figure 3 Endogenous Bcl-xL(Ser62) phosphorylation and location in unperturbed synchronized cells and during DNA damage-induced G2 arrest. (**A**) wt HeLa cells and HeLa cells expressing HA-Bcl-xL were exposed to VP16 (10 μM, 16 h), and the kinetics of G2 arrest (grey bars), mitotic slippage (black bars) and cell death (white bars) were monitored by mitotic trap assay. Bars represent the means ± s.e.m. of 6 independent experiments. (**B**) Expression kinetics of endogenous Bcl-xL and phospho-Bcl-xL(Ser62) in wt Hela cells exposed to VP16 (10 μM, 16 h). Total protein extracts and proteins obtained from cytosolic and nuclear extracts are shown. Western blots are representative of 3 independent experiments. (**C**) Kinetics of expression of endogenous Bcl-xL and phospho-Bcl-xL(Ser62) in synchronized wt Hela cells after double-thymidine block release. Expression levels in cytosolic and nuclear extracts are represented. β-actin and nucleolin expression is presented as control. Phase distributions analyzed by flow cytometry with phospho-H3(Ser10) labeling and PI staining are indicated. Western blots are representative of 2 independent experiments. (**D**) Co-location kinetics of endogenous phospho-Bcl-xL(Ser62) with nucleolin (nucleolus marker), (**E**) coilin (Cajal body marker) and (**F**) γ-tubulin (centrosome marker) in wt Hela cells exposed to VP16 (10 μM, 16 h). Percentage of phospho-Bcl-xL(Ser62) in nucleoli, Cajal bodies and centrosomes during VP16-induced G2 checkpoint and during normal G2 phase of the cell cycle in synchronized wt Hela cells (sG2) are indicated in the right panels. Bars represent the means ± s.e.m. from 12 micrographs obtained in 4 independent experiments.

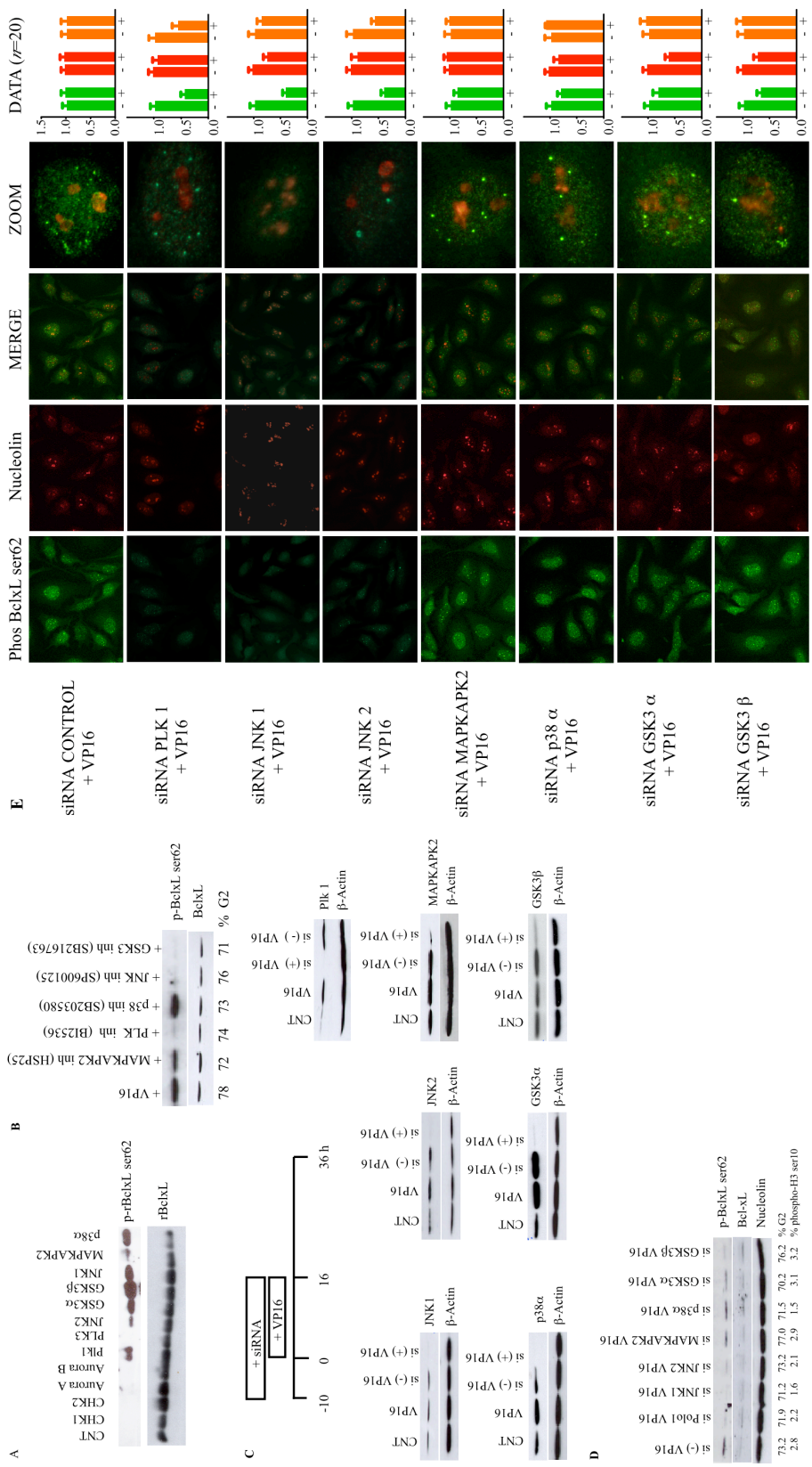
A
CNT
CHK1
CHK2
Aurora A
Aurora B
Plk1
PLK3
JNK2
GSK3α
GSK3β
JNK1
MAPKAPK2
p38α
p-rBclxL ser62
rBclxL
B
+ VP16
+ MAPKAPK2 inh (HSP25)
+ PLK inh (BI2536)
+ p38 inh (SB203580)
+ JNK inh (SP600125)
+ GSK3 inh (SB216763)
p-BclxL ser62
BclxL
% G2
78 72 74 73 76 71
C
+ siRNA
+ VP16
-10 0 16 36 h
CNT
VP16
si (+) VP16
si (-) VP16
Plk 1
β-Actin
MAPKAPK2
JNK2
GSK3β
GSK3α
JNK1
p38α
D
si (-) VP16
si polo1 VP16
si JNK1 VP16
si JNK2 VP16
si MAPKAPK2 VP16
si p38α VP16
si GSK3α VP16
si GSK3β VP16
p-BclxL ser62
Bcl-xL
Nucleolin
% G2
% phospho-H3 ser10
73.2 71.9 71.2 73.2 77.0 71.5 70.2 76.2
2.8 2.2 1.6 2.1 2.9 1.5 3.1 3.2
E
siRNA CONTROL + VP16
siRNA PLK 1 + VP16
siRNA JNK 1 + VP16
siRNA JNK 2 + VP16
siRNA MAPKAPK2 + VP16
siRNA p38 α + VP16
siRNA GSK3 α + VP16
siRNA GSK3 β + VP16
Phos BclxL ser62
Nucleolin
MERGE
ZOOM
DATA (n=20)

Figure 4

Figure 4 PLK1 and MAPK9/JNK2 are major protein kinases involved in Bcl-xL(Ser62) phosphorylation and accumulation in nucleoli during DNA damage-induced G2 arrest. (**A**) *In vitro* kinase assays of a panel of purified and active protein kinases with recombinant human Bcl-xL(ΔTM) protein as substrate. All enzyme activities were tested on control substrates (Supplemental Figure 2). Western blots are representative of 4 independent experiments. (**B**) Effects of specific protein kinase inhibitors on Bcl-xL phosphorylation on Ser62 in Namalwa cells exposed to VP16. Cells were first exposed to VP16 (10 μM, 30 min) and, 12 h-post treatment, kinase inhibitors were added for an additional 12 h: MAPKAPK2 inhibitor (KKALNRQLGVAA, 10 μM); PLK inhibitor (BI2536, 0.1 μM), p38 inhibitor (SB203580, 2.0 μM), JNK inhibitor (SP600125, 5.0 μM), GSK3 inhibitor (SB216763, 10 μM). Western blots are representative of 4 independent experiments. (**C**) Effects of specific siRNAs on silencing PLK1, MAPK8/JNK1, MAPK9/JNK2, MAPKAPK2, MAPK14/SAPKp38α, GSK3α and GSK3β expression in wt Hela cells. Schematic view of these experiments **(C-E)** is showed. Additional controls are illustrated in Supplementary Fig. S4. (**D**) Effects of silencing PLK1, MAPK8/JNK1, MAPK9/JNK2, MAPKAP2, MAPK14/SAPKp38α, GSK3α and GSK3β expression in wt HeLa cells on the phosphorylation level of endogenous Bcl-xL(Ser62) after VP16 treatment. Representative western blotting of nuclear extracts of 3 independent experiments. (**E**) Co-location of endogenous phospho-Bcl-xL(Ser62) with nucleolin (nucleolus marker) in wt Hela cells exposed to VP16 where various protein kinases are silenced. Quantitation of micrographs is shown in the right panels. Green bars are total phospho-Bcl-xL(Ser62) staining in cells; red bars are total nucleoli staining in cells; orange bars are the phospho-Bcl-xL(ser62)/nucleoli staining ratio. Data are presented relative to wt HeLa cells exposed to VP16, and symbols are: (-) cells treated with siRNA control and VP16, (+) cells treated with specific siRNA targeting the given protein kinase and VP16. Bars represent the means ± s.e.m. from 20 micrographs obtained in 3 independent experiments.

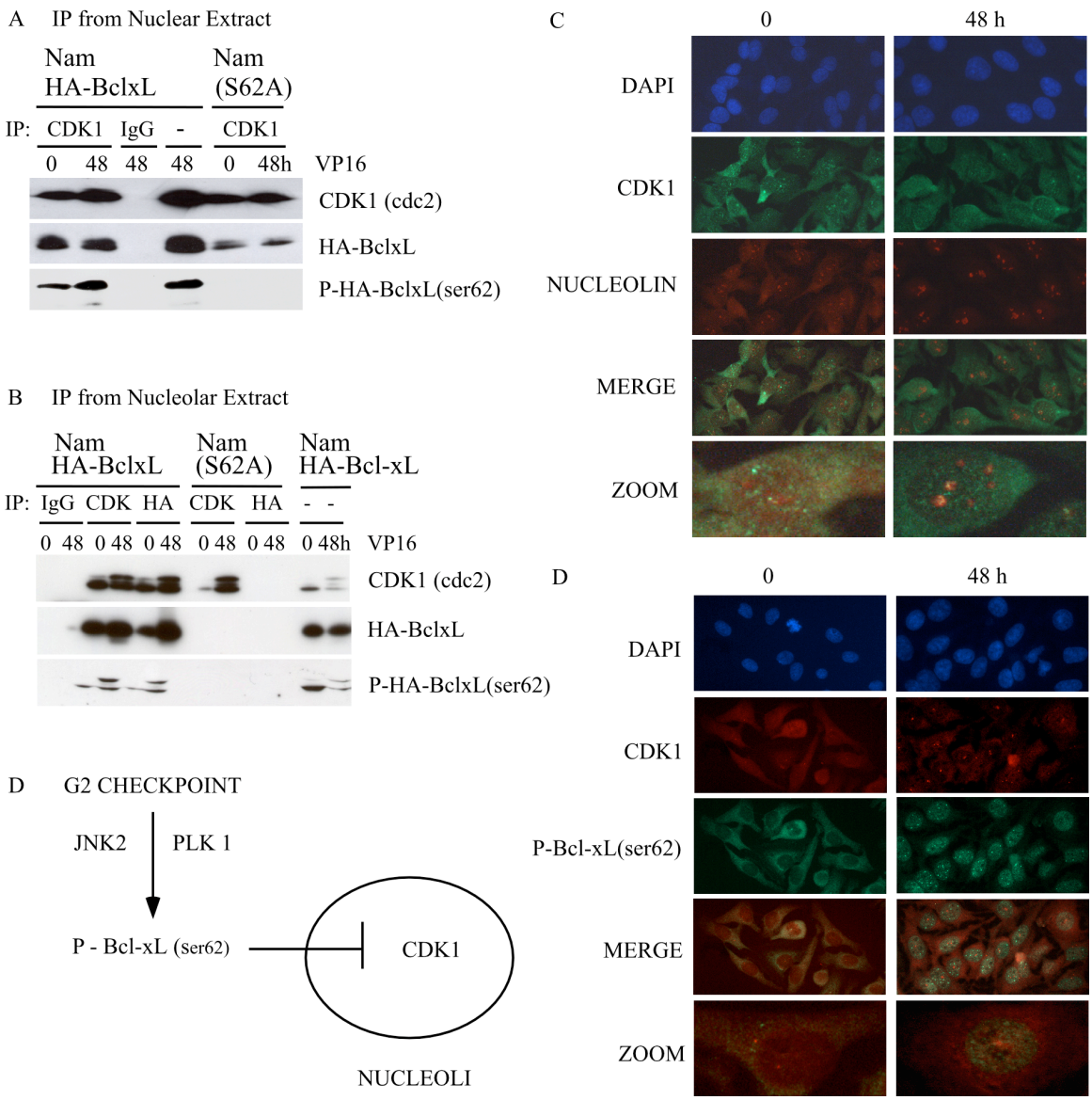
A
IP from Nuclear Extract
Nam HA-BclxL
Nam (S62A)
IP: CDK1 IgG - CDK1
0 48 48 48 0 48h
VP16
CDK1 (cdc2)
HA-BclxL
P-HA-BclxL(ser62)
B
IP from Nucleolar Extract
Nam HA-BclxL
Nam (S62A)
Nam HA-Bcl-xL
IP: IgG CDK HA CDK HA - -
0 48 0 48 0 48 0 48 0 48 0 48h
VP16
CDK1 (cdc2)
HA-BclxL
P-HA-BclxL(ser62)
C
0
48 h
DAPI
CDK1
NUCLEOLIN
MERGE
ZOOM
D
0
48 h
DAPI
CDK1
P-Bcl-xL(ser62)
MERGE
ZOOM
D
G2 CHECKPOINT
JNK2
PLK 1
P - Bcl-xL (ser62)
CDK1
NUCLEOLI

Figure 5

Figure 5 Phospho-Bcl-xL(Ser62) meets CDK1(CDC2) in nucleolar structures during DNA damage-induced G2 arrest. (**A**) Co-immunoprecipitation of HA-Bcl-xL, HA-Bcl-xL(Ser62Ala) and phospho-HA-Bcl-xL(Ser62) with CDK1(CDC2) from enriched nuclear extracts obtained from Namalwa cells expressing HA-Bcl-xL or HA-Bcl-xL(Ser62Ala) mutant exposed to VP16 (10 μM for 30 min). IgG represents co-immunoprecipitation experiments with control immunoglobulins and (-) indicates a nuclear extract obtained from Namalwa cells expressing HA-Bcl-xL 48 h-post VP16 treatment loaded as a western blot control. Representative of 2 independent experiments. (**B**) Reciprocal co-immunoprecipitation of HA-Bcl-xL, HA-Bcl-xL(Ser62Ala) and phospho-Bcl-xL(Ser62) with CDK1(CDC2) from enriched nucleolar extracts purified from Namalwa cells expressing HA-Bcl-xL and HA-Bcl-xL(Ser62Ala) mutant exposed to VP16 (10 μM for 30 min). IgG, CDK and HA represent co-immunoprecipitation experiments with control immunoglobulins, CDK1(CDC2) and HA-epitope tag antibodies, respectively. (-) indicates nucleolar extracts obtained from Namalwa cells expressing HA-Bcl-xL before and after VP16 treatment loaded as western blot controls. (**C**) Co-location of CDK1(CDC2) with nucleolin and (**D**) CDK1(CDC2) with phospho-Bcl-xL(Ser62) 36 h after the beginning of VP16 treatment (10 μM, 16 h) in wt HeLa cells. Micrographs are representative of 2 independent experiments. (**E**) Schematic view of a proposed model.

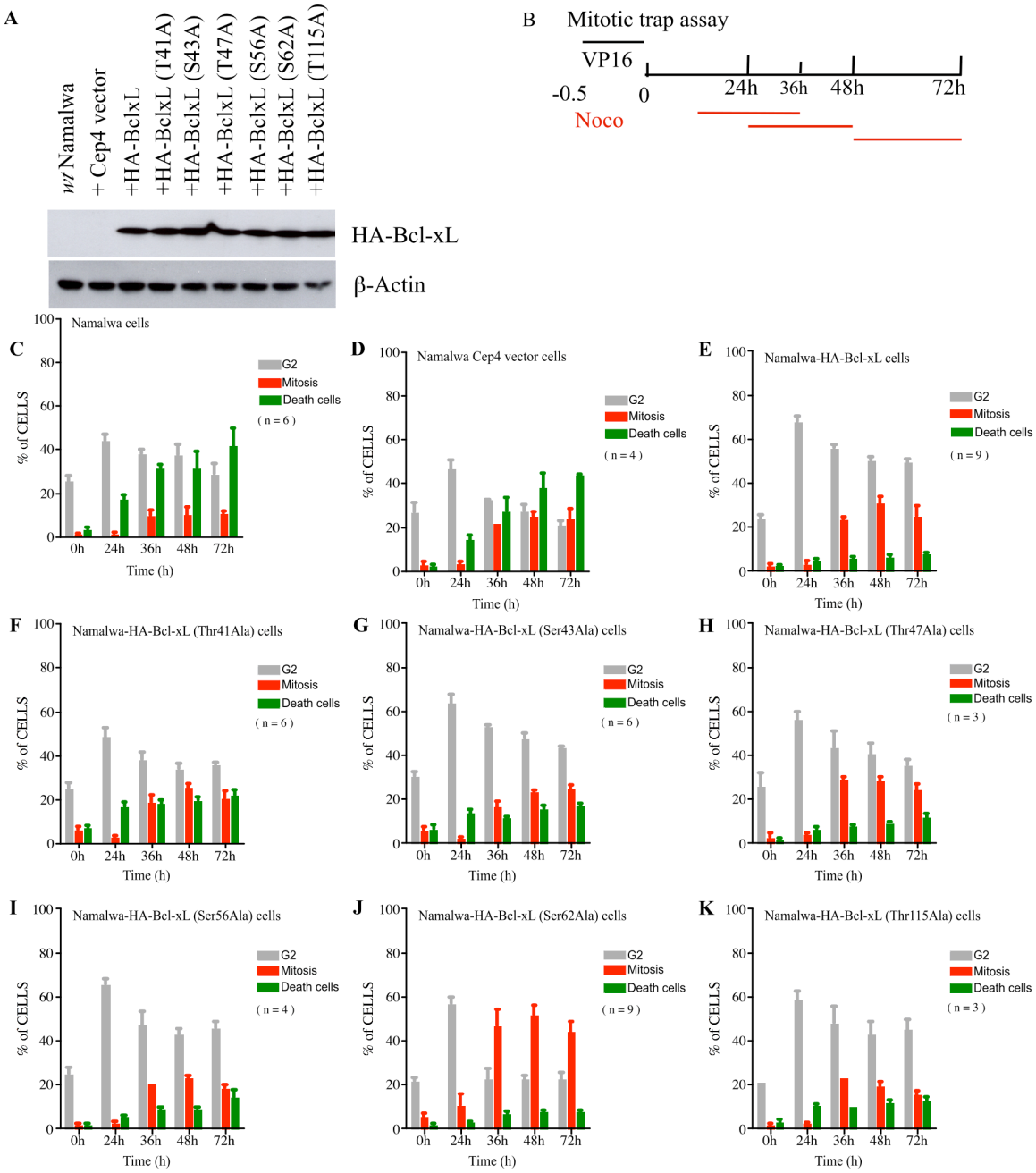

Supplemental Figure S1

Supplementary Figure S1 Effect of Bcl-xL and various Bcl-xL phosphorylation mutants on DNA damage-induced G2 arrest. (**A**) Expression level of HA-Bcl-xL and various phosphorylation mutants in stably-transfected Namalwa cell populations. β-actin expression is shown as control. (**B**) Schematic view of the mitotic trap assay; VP16 was administered at 10 μM for 30 min; nocodazole treatments (0.35 μM) at the indicated intervals trapped cells entering mitosis. (**C-K**) Kinetics of G2 arrest (grey bars), mitotic slippage (red bars) and cell death (green bars) in Namalwa cells expressing HA-Bcl-xL and various phosphorylation mutants. Bars represent the means ± s.e.m. of *n* independent experiments.

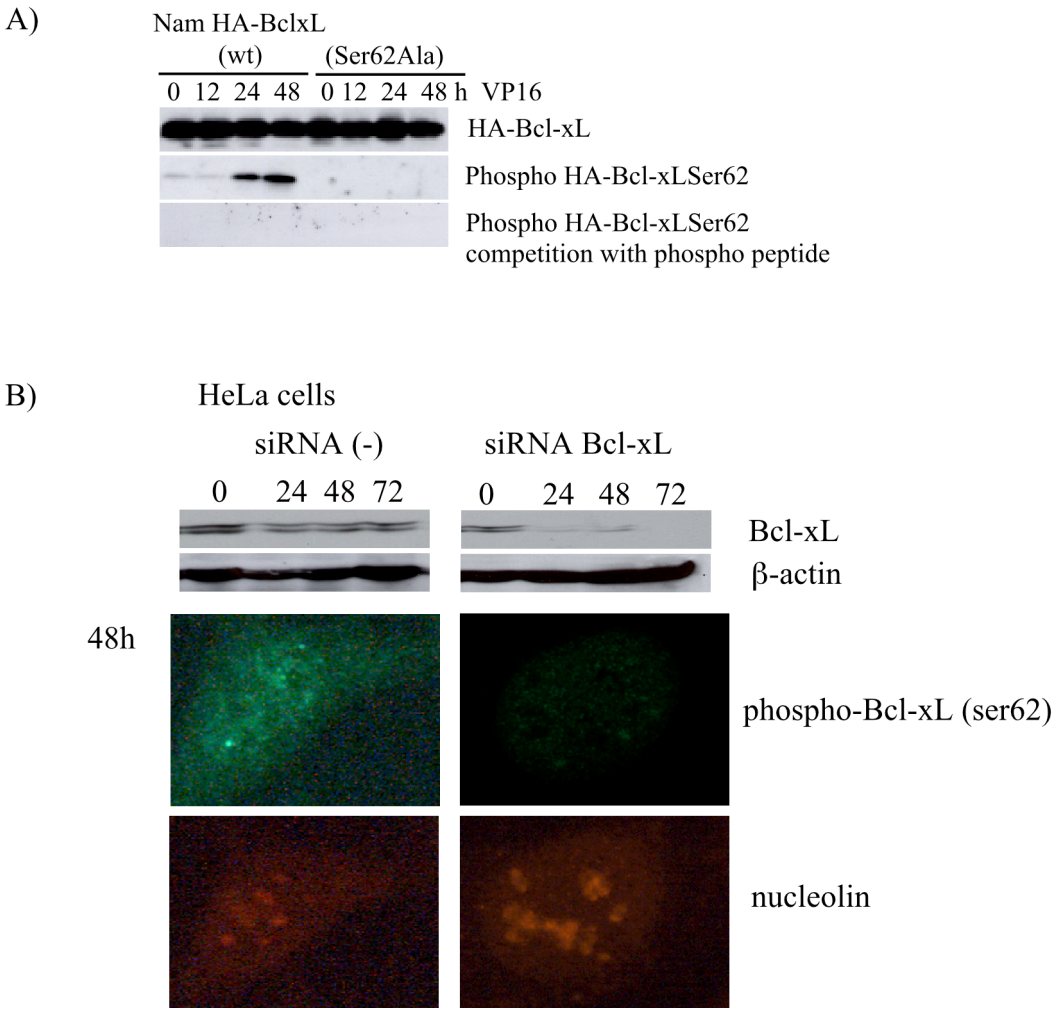

Supplemental Figure S2

Supplementary Figure S2 Specificity of the phospho-Bcl-xL(ser62) antibodies**. (A)** Expression of phospho-HA-Bcl-xL(Ser62) in Namalwa cells expressing expressing HA-Bcl-xL and HA-Bcl-xL(Ser62Ala) mutant exposed to VP16 (10 μM for 30 min). HA-Bcl-xL expression is shown as control. **(B)** Staining of phospho-Bcl-xL(Ser62) in wt HeLa cells exposed to control siRNA or siRNA targeting the expression of Bcl-xL. Nucleolin staining and Western blottings are shown as control.

A) Recombinant Enzyme

	Specific activity Assay #1	Assay #2
CHK1	7.7 nmole/min/mg	7.9 nmole/min/mg
CHK2	176 nmole/min/mg	268 nmole/min/mg
p38α /MAPK14	76 nmole/min/mg	129 nmole/min/mg
JNK1/MAPK8	39 nmole/min/mg	48 nmole/min/mg
JNK2/MAPK9	138 nmole/min/mg	263 nmole/min/mg
MAPKAPK2	541 nmole/min/mg	778 nmole/min/mg
PLK1	8.4 nmole/min/mg	14.3 nmole/min/mg
PLK3	13.9 nmole/min/mg	17.5 nmole/min/mg
Aurora A	14.5 nmole/min/mg	18 nmole/min/mg
Aurora B	508 nmole/min/mg	420 nmole/min/mg
NEK2	398 nmole/min/mg	530 nmole/min/mg
GSK3β	5.0 nmole/min/mg	8.6 nmole/min/mg

B) Immunoprecipitated enzyme

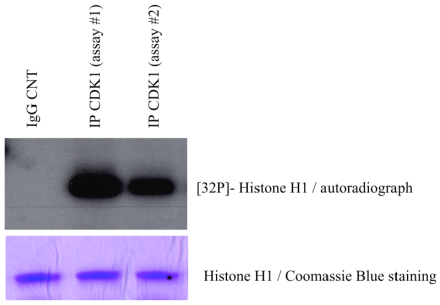

assay #1 IP from 1.0 x 10^6 cells
assay #2 IP from 0.5 x 10^6 cells

C) In vitro kinase assay with [^{32}P] γATP and recombinant Bcl-xL as substrate

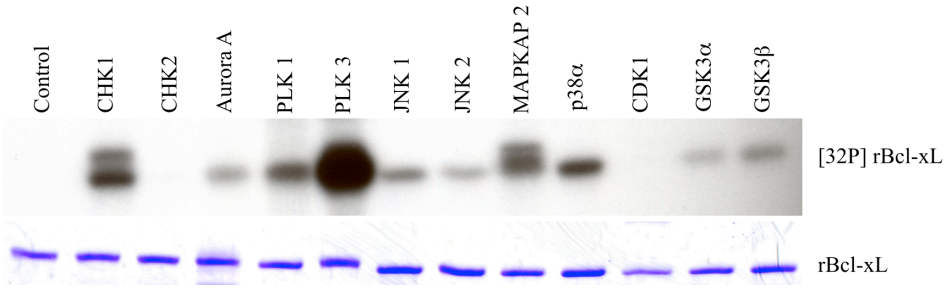

Supplemental Figure S3

Supplementary Figure S3 *In vitro* kinase assays. **(A)** Enzyme activities were tested on control substrates with recombinant purified kinases. Velocities are expressed as nmole/min/mg. Two independent experiments are shown. **(B)** Cdk1(cdc2) enzyme activities tested on histone H1 control substrate with cdk1(cdc2) kinase purified by immunoprecipitation. Two independent immunoprecipitation assays are shown. **(C)** In vitro kinase essay with [^{32}P]-γATP and recombinant Bcl-xL as substrate. Autoradiography and Coomassie staining are shown.

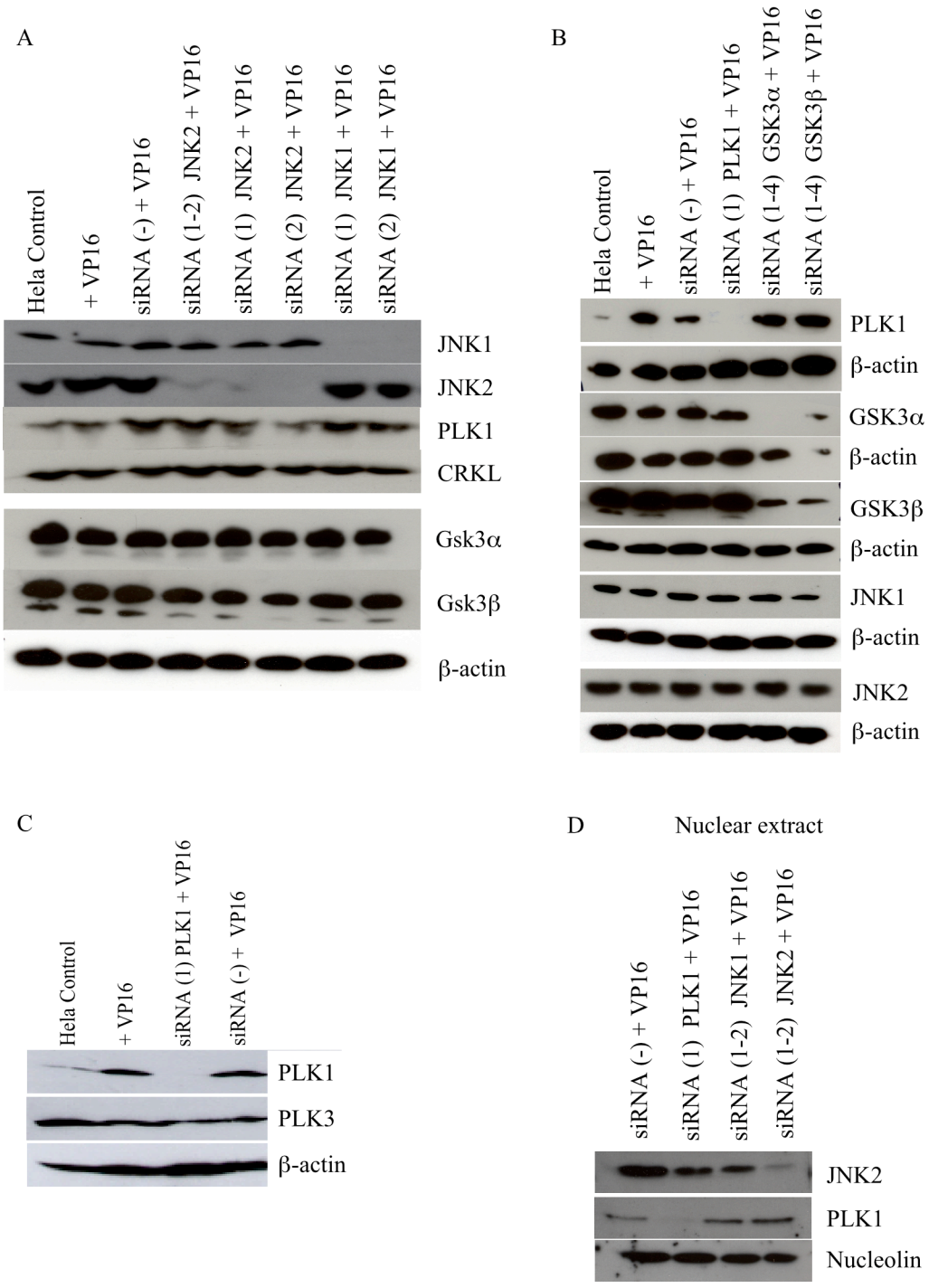

Supplemental Figure S4

Supplementary Figure S4 Specificity of the SiRNAs. **(A)** Effects of silencing MAPK8/JNK1 and MAPK9/JNK2 with different targeted sequences on the expression of PLK1, MAPK8/JNK1, MAPK9/JNK2, GSK3α and GSK3β expression in wt HeLa cells (HeLa control) and HeLa cells exposed to VP16 (+VP16). CRKL or β−actin expression is shown as control. **(B)** Effects of silencing PLK1, GSK3α and GSK3β on the expression of PLK1, MAPK8/JNK1, MAPK9/JNK2, GSK3α and GSK3β expression in wt HeLa cells (HeLa control) and HeLa cells exposed to VP16 (+VP16). β−actin expression is shown as control. **(C)** Effects of silencing PLK1 on the expression of PLK1 and PLK3 in wt HeLa cells (HeLa control) and HeLa cells exposed to VP16 (+VP16). β−actin expression is shown as control. **(D)** Effects of silencing PLK1, MAPK8/JNK1 and MAPK9/JNK2, on the expression of PLK1, MAPK8/JNK1 and MAPK9/JNK2 in nuclear extracts obtained from HeLa cells exposed to VP16 (+VP16). Nucleolin expression is shown as control.

Supplemental TABLE S1 cDNA constructs

HA-Bcl-xL (T41A)

5'-end oligonucleotide (+) with *Nhe1* + START ATG codon:	5'- gctagcccacc **atg** ggc cgc atc ttt ta
3'-end oligonucleotide (-) with STOP TGA codon:	5'- ctcgag **tca** ttt ccg act gaa gag tga
Overlapping oligonucleotide (+) containing T41A substitution:	5'- gcc cca gaa ggg **g**ct gaa tcg gag atg
Overlapping oligonucleotide (-) containing T41A substitution:	5- cat ctc cga ttc ag**c** ccc ttc tgg ggc
(from *wt* HA-Bcl-xL as template / subcloned *Nhe1/ Xho1* in Cep4 vector)	

HA-Bcl-xL (S43A)

5'-end oligonucleotide (+) with *Nhe1* + START ATG codon:	5'- gctagcccacc **atg** ggc cgc atc ttt ta
3'-end oligonucleotide (-) with STOP TGA codon and *XhoI:*	5'- ctcgag **tca** tttc cga ctg aag agt ga
Overlapping oligonucleotide (+) containing S43A substitution:	5'-gaa ggg act gaa **g**cg gag atg gag acc
Overlapping oligonucleotide (-) containing S43A substitution:	5'-ggt ctc cat ctc cg**c** ttc agt ccc ttc
(from *wt* HA-Bcl-xL as template / subcloned *Nhe1/ Xho1* in Cep4 vector)	

HA-Bcl-xL (T47A)

5'-end oligonucleotide (+) with *Not1* + START ATG codon:	5'- gcggccgc **atg** tct cag agc aac cgg ga
3'-end oligonucleotide (-) with STOP TGA codon and *XhoI:*	5'- ctcgag **tca** tttc cga ctg aag agt ga
Overlapping oligonucleotide (+) containing T47A substitution:	5'-tcg gag atg gag **g**cc ccc agt gcc atc
Overlapping oligonucleotide (-) containing T47A substitution:	5'-gat ggc act ggg gg**c** ctc cat ctc cga
(from *wt* Bcl-xL as templat / subcloned *Not1/ XhoI* in Cep4-HA vector)	

HA-Bcl-xL (S56A)

5'-end oligonucleotide (+) with *Not1* + START ATG codon:	5'- gcggccgc**atg** tct cag agc aac cgg gag
3'-end oligonucleotide (-) with STOP TGA codon and *XhoI:*	5'- ctcgag **tca** tttc cga ctg aag agt ga
Overlapping oligonucleotide (+) containing S56A substitution:	5'- aat ggc aac cca **g**cc tgg cac ctg gca
Overlapping oligonucleotide (-) containing S56A substitution:	5'- tgc cag gtg cca gg**c** tgg gtt gcc att
(from *wt* Bcl-xL as template / subcloned *Not1/ XhoI* in Cep4-HA vector)	

HA-Bcl-xL (S62A)

5'-end oligonulcleotide (+) with *Not1* + START ATG codon:	5'- gcggccgc**atg** tct cag agc aac cgg gag
3'-end oligonucleotide (-) with STOP TGA codon and *XhoI:*	5'- ctcgag **tca** ttt ccg act gaa gag tga
Overlapping oligonucleotide (+) containing S62A substitution:	5- cac ctg gca gac **gcc** ccc gcg gtg aat
Overlapping oligonucleotide (-) containing S62A substitution:	5- att cac cgc ggg **ggc** gtc tgc cag gtg
(from *wt* Bcl-xL as template / subcloned *Not1/ XhoI* in Cep4-HA vector)	

HA-Bcl-xL (T115A)

5'-end oligonulcleotide (+) with *Not1* + START ATG codon:	5'- gcggccgc**atg** tct cag agc aac cgg gag
3'-end oligonucleotide (-) with STOP TGA codon and *XhoI:*	5'- ctcgag **tca** ttt ccg act gaa gag tga
Overlapping oligonucleotide (+) containing T115A substitution:	5- cag ctc cac atc **g**cc cca ggg aca gca
Overlapping oligonucleotide (-) containing T115A substitution:	5- tgc tgt ccc tgg gg**c** gat gtg gag ctg
(from *wt* Bcl-xL as template / subcloned *Not1/ XhoI* in Cep4-HA vector)	

Supplemental TABLE S1 cDNA constructs. The phosphorylation mutant pCEP4-HA-Bcl-xL and pCDNA3.1-HA-Bcl-xL vectors were generated by triple polymerase chain reactions (PCR) with wt pCEP4-HA-Bcl-xL vector as DNA template. The first fragments were amplified by *Vent* polymerase, with specific adapter primers containing restriction site sequences at the ATG start codon and anti-sense junction primers corresponding to the flanking sequences at each mutation site, as listed in Table S1. The second fragments were amplified by *Vent* polymerase, with sense junction primers corresponding to flanking sequences at each mutation site and adapter anti-sense primers containing restriction site sequences at the TGA stop codon. The 2 amplified fragments were gel-purified, heat-denaturated, and slowly annealed on ice. After elongation by *Taq* polymerase for 10 min, the third PCR, with specific adapter primers containing sequences at the ATG start codon and TGA stop codon, was amplified. The amplified fragment was first cloned in pCR2.1Topo vector (Invitrogen Corporation), sequenced, and then sub-cloned in the eukaryotic expression vectors pCEP4 and pCDNA3.1 (Invitrogen Corporation). For some constructs, the HA-tag sequences were not amplified by PCR; these amplified fragments were than sub-cloned in-frame into the pCEP4-HA vector. All primers are listed in Supplemental Table 1. Purified constructs were transfected in Namalwa cells by electroporation at 0.27 kV (Gene Pulser, BioRad, Hercules, CA) and in HeLa cells by Lipofectamine2000 transfection according to the manufacturer's protocol (Invitrogen Corporation).

Supplemental TABLE S2

ANTIBODIES	ID	Species	Source
Cyclin B1	clone GNS-1	mouse mAb	BD Biosciences
Phospho-cdc2 Thr161	# 9114	rabbit pAb	Cell Signaling
Phospho-cdc2 Tyr15	# 4539	rabbit pAb	Cell Signaling
Cdc2/CDK1	# PC25	rabbit pAb	Calbiochem
Cdc2/CDK1	clone 1/cdk1	mouse mAb	BD Biosciences
ATM	clone D2E2	rabbit mAb	Cell Signaling
Phospho ATM Ser1981	clone 10H11.E12	mouse mAb	Cell Signaling
ATR	# 2790	rabbit pAb	Cell Signaling
Phospho ATR Ser428	# 2853	rabbit pAb	Cell Signaling
Chk1	# 2345	rabbit pAb	Cell Signaling
Phospho Chk1 Ser317	# 2344	rabbit pAb	Cell Signaling
Chk2	# 2662	rabbit pAb	Cell Signaling
Phospho Chk2 Thr68	# 2661	rabbit pAb	Cell Signaling
Plk1	clone 208G4	rabbit mAb	Cell Signaling
Phospho Plk1 Thr210	clone K50483	mouse mAb	BD Biosciences
Plk3	clone B37-2	mouse mAb	BD Biosciences
Aurora A	clone 1G4	rabbit mAb	Cell Signaling
Phospho Aurora A Thr288	clone C39D8	rabbit mAb	Cell Signaling
MAPKAPK2	# 3042	rabbit pAB	Cell Signaling
Phospho-MAPKAPK2 Thr334	clone 27B7	rabbit mAb	Cell Signaling
p38α / MAPK14	clone L53F8	mouse mAb	Cell Signaling
Phospho p38α Thr180/Tyr182	clone 28B10	mouse mAb	Cell Signaling
JNK1/MAPK8	clone G151-333	mouse mAb	BD Biosciences
JNK2/MAPK9	# 4672	rabbit pAb	Cell Signaling
Phospho JNK Thr183/Tyr185	# 9251	rabbit pAb	Cell Signaling
GSK3α	# 9338	rabbit pAb	Cell Signaling
GSK3β	clone 27C10	rabbit mAb	Cell Signaling
Bcl-xL	clone 2H12	mouse mAb	BD Biosciences
Phospho-BclxL Ser62	custom	rabbit pAb	GenScript
Phospho-BclxL Ser62	# 4428G	rabbit pAb	InVitrogen
HA tag	clone 12CA5	mouse mAb	Roche Applied
HA tag	# A00168	goat pAb	GenScript
Coilin	Ab11822	mouse mAb	Abcam
Nucleolin	clone 4E2	mouse mAb	GeneTex
Actin	clone 4C40	mouse mAb	Sigma
Phospho H3 (ser10) Alexa 488	# 9708	rabbit pAb	Cell Signaling
Anti-Mouse IgG Alexa 488	# A11001	goat pAb	InVitroGen
Anti-Rabbit IgG Alexa 488	# A11008	goat pAb	InVitroGen
Anti-Mouse IgG Alexa 594	# A11005	goat pAb	InVitroGen
Anti-Rabbit IgG Alexa 594	# A11012	goat pAb	InVitroGen
Anti-Mouse IgG HP-linked	# NA931V	sheep pAb	GE Healthcare
Anti-Rabbit IgG HP-linked	# NA934V	donkey pAb	GE Healthcare
Normal Rabbit IgG	# sc-2027	rabbit IgG	Santa Cruz
Normal Mouse IgG	# sc-2025	mouse IgG	Santa Cruz
ProteinG Plus/ProteinA Agarose	# IP05	----------	Calbiochem

Supplemental TABLE S3

Recombinant Enzyme	Source	Control Substrate	Source	Buffer
CHK1	Sigma-Aldrich	RXRX(L/A)S((R/F)	Cell Signaling	A
CHK2	Sigma-Aldrich	AMRLERQDSIFYPK	AnaSpec	A
p38α /MAPK14	Cell Signaling	ATF-2 (19-96)	Cell Signaling	B
JNK1/MAPK8	Cell Signaling	c-Jun (1-89)	Cell Signaling	B+
JNK2/MAPK9	Cell Sciences	c-Jun (1-89)	Cell Signaling	A
MAPKAPK2	Cell Signaling	KKKLNRTLSVA	AnaSpec	A+
PLK1	Cell Signaling	RISDELMDATFADQEAK	AnaSpec	A
PLK3	Cell Signaling	RISDELMDATFADQEAK	AnaSpec	A
Aurora A	Cell Signaling	RRSLLE	Cell Signaling	A
Aurora B	Cell Signaling	LRRLSLGLRRLSLGLR		
		RLSLGLRRLSLG	AnaSpec	A
NEK2	Cell Signaling	RFRRSRRMI	AnaSpec	A
GSK3α	Cell Signaling	RRAAEELDSRAGSPQL	AnaSpec	A
GSK3β	Sigma-Aldrich	GPHRSTPESRAAV	AnaSpec	A+
Immunoprecipitated Enzyme				
CDC2/CDK1	Namalwa cells	Histone H1	Sigma-Aldrich	B+

Buffer A (5x):	25 mM MOPS pH 7.2
	25 mM $MgCl_2$
	12.5 mM β-glycerol-2-phosphate
	0.5 mM Na_3VO_4
	5 mm EGTA
	2 mM EDTA
	0.25 mM dithiothreitol
	500 μM ATP*
	* 0.05 μCi/μl [^{32}P]-γATP
Buffer A+ (5x):	buffer A + 50 μg/ ml BSA

Buffer B (5x):	125 mM TRIS pH 7.2
	50 mM $MgCl_2$
	25 mM β-glycerol-2-phosphate
	0.5 mM Na_3VO_4
	10 mM dithiothreitol
	500 μM ATP*
	* 0.05 μCi/μl [^{32}P]-γATP
Buffer B+ (5x):	buffer B + 50 μg/ ml BSA

Target	INHIBITOR	Source	Concentration
p38	SB 203580	Calbiochem	2 μM
JNK	SP 600125	Sigma-Aldrich	5 μM
MAPKAPK2	H-KKALNRQLGVAA-OH	Calbiochem	10 μM
PLK	BI 2536	Axon MedChem	0.1 μM
Aurora	ZM 447439	Tocris BioScience	0.1 μM
GSK3	SB 216763	Sigma-Aldrich	10 μM

Supplemental Table S3. Listing of the protein kinase assays and protein kinase inhibitors. Source, control substrates and reaction buffers are indicated.

Supplemental Table S3

Supplemental TABLE S4

Target		siRNA Target sequence	Source
PLK 1	(1)	5' -AGAUUGUGCCUAAGUCUCU-3'	Mol Biol Cell 15:5623, 2004
MAPK8/JNK1	(1)	5'-GCCCAGUAAUAUAGUAGUA-3'	Cell Cycle 7: 533, 2008
	(2)	5'-GGCAUGGGCUACAAGGAAA-3'	Cell Cycle 7: 533, 2008
MAPK9/JNK2	(1)	5'-AGCCAACUGUGAGGAAUUA-3'	Cell Cycle 7: 533, 2008
	(2)	5'-UCGUGAACUUGUCCUCUUA-3'	Cell Cycle 7: 533, 2008
MAPK14/ p38α	(1)	5'-GGAAUUCAAUGAUGUGUAU-3'	On-Target plus sequence /Dharmacon
	(2)	5'-UCUCCGAGGUCUAAAGUAU-3'	On-Target plus sequence/ Dharmacon
	(3)	5'-GUAAUCUAGCUGUGAAUGA-3'	On-Target plus sequence /Dharmacon
	(4)	5'-GUCCAUCAUUCAUGCGAAA-3'	On-Target plus sequence /Dharmacon
MAPKAPK2	(1)	5'-CGAAUGGGCCAGUAUGAAU-3'	On-Target plus sequence /Dharmacon
	(2)	5'-GUUAUACACCGUACUAUGU-3'	On-Target plus sequence /Dharmacon
	(3)	5'-GGCAUCAACGGCAAAGUUU-3'	On-Target plus sequence /Dharmacon
	(4)	5'-CCACCAGCCACAACUCUUU-3'	On-Target plus sequence /Dharmacom
GSK3α	(1)	5'-CAUCAAAGUGAUUGGCAAU-3'	SMART POOL /Dharmacon
	(2)	5'-AGUUGACCAUCCCUAUCCU-3'	SMART POOL //Dharmacon
	(3)	5'-CUGAUUACACCUCAUCCAU-3'	SMART POOL /Dharmacon
	(4)	5'-UUCUCAUCCCUCCUCACUU-3'	SMART POOL /Dharmacom
GSK3β	(1)	5'-GAUCAUUUGGUGUGGUAUA-3'	SMART POOL /Dharmacon
	(2)	5'-GCUAGAUCACUGUAACAUA'-3	SMART POOL /Dharmacon
	(3)	5'-GUUCCGAAGUUUAGCCUAU-3'	SMART POOL /Dharmacon
	(4)	5'-GCACCAGAGUUGAUCUUUG-3'	SMART POOL /Dharmacon
NON-TARGETING			SMART POOL / Dharmacom

Supplemental Table S4. Listing of the SiRNA targeted sequence deployed in this study.

Supplemental TABLE S5

Bcl-xL	W-H-L-A-D-(pS$_{62}$)-P-A-V-N

Protein Kinase	Consensus motif
CHK1	Φ-X-β-X-X-(pS/T)
CHK2	R/F-R/Φ-L/I-L/R-R-X-X-(pS/T)-F/I-F/I/R
Aurora A	R/K/N-R-X-(pS/T)- Φ
MAPK8/JNK1	(pS/T)-P
MAPK9/JNK2	(pS/T)-P
MAPK14/SAPKp38α	(pS/T)-P
Cdk1(cdc2)	(pS/T)-P-X-K/R
GSK3	(pS/T)-X-X-X-S
PLK-1	D/EX(pS/T)-Φ-X-D/E
Nek-2	R/K-X-X-A/I-(pS/T)-R/K
MAPKAPK2	Φ-X-R-X-X-(pS/T)- Φ

Supplemental Table S5. These protein kinases were identified as putative protein kinase involved with Bcl-xL(Ser62) phosphorylation by *in silico* consensus site prediction search using either GPS2.0, NetPhosK, NetworKIN, or PhosphoELM softwares.

4. Phospho-Bcl-xL(Ser62) in spindle-assembly checkpoint and mitosis progression

Authors: Jianfang Wang[1], Myriam Beauchemin[1] and Richard Bertrand[1,2*]

Affiliations: [1]Centre de recherche, Centre hospitalier de l'Université de Montréal (CRCHUM) – Hôpital Notre-Dame and Institut du Cancer de Montréal, and [2]Département de médecine, Université de Montréal, Montréal (Québec) Canada

Running title: Bcl-xL and the spindle-assembly checkpoint

Key words*:* Bcl-xL, spindle-assembly checkpoint, PLK1, MAPK14/SAPKp38α, APC/C-CDC20

****Corresponding author****:* CRCHUM – Hôpital Notre-Dame and Institut du Cancer de Montréal, 1560 Sherbrooke St. East (Room Y-5634),
Montréal (Québec) Canada H2L 4M1.

Abstract

Analysis of a series of phosphorylation mutants reveals that cells expressing Bcl-xL(Ser62Ala) are more stable at a sustained spindle-assembly checkpoint (SAC) after exposure to taxol than cells expressing wild-type Bcl-xL or other phosphorylation mutants, an effect that appears to be independent of its anti-apoptotic activity. Bcl-xL(Ser62) is strongly phosphorylated by PLK1 and MAPK14/SAPKp38α at prometaphase, metaphase and the anaphase boundary, while it is dephosphorylated at telophase and cytokinesis. Phospho-Bcl-xL(Ser62) localizes in centrosomes with γ-tubulin, along the mitotic spindle with dynein motor protein and in cytosol with SAC signaling components. In taxol-exposed cells, phospho-Bcl-xL(Ser62) binds to the CDC20/MAD2/BUBR1/BUB3 complex, while Bcl-xL(Ser62Ala) does not. These data indicate that during SAC, Bcl-xL(Ser62) phosphorylation accelerates SAC resolution and cell entry into anaphase, even in the presence of unattached or misaligned chromosomes. Silencing Bcl-xL expression also leads nocodazole-exposed cells to tetraploidy and binucleation, consistent with a Bcl-xL function in SAC and genomic stability.

Introduction

Mitosis involves proper alignment and accurate segregation of sister chromatids into two daughter cells to ensure precise inheritance of the genome. Failure of the process can lead to cell death or genetic instability, aneuploidy and diseases, including cancer (reviewed in [1-3)]. After DNA replication and centrosome duplication, entry into mitosis absolutely requires progressive accumulation of active cyclin B1/CDK1 complexes in the nucleus that will initiate chromosome condensation, nuclear envelope breakdown, disassembly of the nuclear lamina and many forms of nuclear bodies, including Cajal bodies and nucleoli [4-7]. Centrosomes become separated by the end of prophase, and, during prometaphase, highly dynamic mitotic microtubules form a bipolar spindle to which chromosomes must be bi-oriented and perfectly aligned by the end of metaphase. The spindle-assembly checkpoint (SAC) is the safety program that ensures the fidelity of chromosome bi-orientation and alignment, controlling entry into anaphase. It is constitutively active until proper microtubule attachment to and tension on kinetochores and individual sister chromatids at centromeric chromosomes (reviewed in [1-3]). Functionally, the SAC negatively regulates the ability of the limiting subunit CDC20 to activate the anaphase-promoting complex or cyclosome (APC/C), as APC/C^{CDC20}, a large multiprotein E3 ubiquitin ligase consisting of at least 11 core subunits, that targets key mitotic substrates, including cyclin B and securin, provoking entry into anaphase and mitosis conclusion [8, 9].

The ability of CDC20 to activate APC/C, evoking entry into anaphase, is tightly regulated by several mechanisms, until all centromeric chromosomes have achieved bipolar kinetochore-microtubule attachment. During prometaphase/metaphase, when CDC20 is concentrated at kinetochores, the established view is that various mitotic checkpoint proteins, including BUB1, BUBR1, BUB3, MAD1 and MAD2, bind to kinetochores that lack attachment/tension, and generate a "stop anaphase signal" that diffuses into the mitotic cytosol [1-3, 8-11]. This "stop anaphase signal" consists of a BUB3/BUBR1/MAD2 complex which diffuses into the mitotic cytosol, binds to CDC20 and inhibits APC/C [12-19]. Direct phosphorylation of CDC20 by BUB1 and cyclin B1/CDK1 has also been reported, providing a direct catalytic mechanism that prevents CDC20 binding to APC/C during the SAC [20-22].

In recent years, several studies have reported that members of the Bcl-2 family, in addition to their central role in controlling apoptosis during development and cellular stress, also play a part in the cell cycle and DNA repair pathways, effects that are generally distinct from their function in apoptosis and that influence genomic stability (reviewed in [23, 24]). Bcl-xL phosphorylation at Ser62 has been detected previously in a variety of cell lines treated with microtubule inhibitors, including nocodazole, paclitaxel, vinblastine, vincristine, colchicine and pironetin [25-33], but the exact function of Bcl-xL(Ser62) phosphorylation during mitosis remains elusive. Bcl-xL(Ser62) is located within the unstructured loop domain of the protein, a region generally not essential for its anti-apoptotic function [34-36]. However, studies have indicated that a deletion mutant of the loop domain displays an enhanced ability to inhibit apoptosis with no significant alterations in its ability to bind pro-apoptotic Bax [34]. Some have suggested that Bcl-xL phosphorylation maintains its anti-apoptotic function [30], while others have reported that phosphorylation causes Bcl-xL to release bound Bax and promote apoptosis [31]. No study has investigated other possible Bcl-xL functions acting directly on mitosis regulation and progression.

To better understand the importance of Bcl-xL phosphorylation events within its flexible loop domain in regulating Bcl-xL location and function during mitosis, we generated a series of single-point Bcl-xL cDNA phosphorylation mutants, including Thr41Ala, Ser43Ala, Thr47Ala, Ser56Ala, Ser62Ala and Thr115Ala and selected stably-transfected human cell populations. We also investigated Bcl-xL phosphorylation and location kinetics during mitosis and deployed siRNAs targeting Bcl-xL expression. In this study, we provide evidence that phospho-Bcl-xL(Ser62) is a key component of mitosis progression at the SAC, which appears to be separate from its anti-apoptotic function.

Results

Effect of Bcl-xL and various Bcl-xL phosphorylation mutants on SAC stability and mitosis progression

To examine the mitotic functions of Bcl-xL, we first generated various HA-tagged Bcl-xL phosphorylation mutants, including Thr41Ala, Ser43Ala, Thr47Ala, Ser56Ala,

Ser62Ala and Thr115Ala, then stably expressed them in Namalwa cells (Figure 1A and Supplemental Figure S1A). Simple experimental monitoring by flow cytometry with phospho-H3(Ser10) labeling and propidium iodide (PI) staining were used to evaluate the kinetics of early mitotic entry and stability (N4 DNA content, phospho-H3(Ser10)-positive), mitotic exit (N4 DNA content, phospho-H3(Ser10)-negative), G1 entry (N2 DNA content, phospho-H3(Ser10)-negative), and the kinetics of cell death (sub-G1 DNA content) in taxol-exposed cells. Control Namalwa cells (Figure 1B) or Namalwa cells stably transfected with empty vector (Figure 1C) died rapidly after taxol treatment (green bars). In contrast, cells stably expressing HA-Bcl-xL and HA-Bcl-xL(Ser62Ala) mutant showed similar strong inhibition of apoptosis (Figure 1D-E; green bars). Up to 80% of cells over-expressing wild type (wt) HA-Bcl-xL and HA-Bcl-xL(Ser62Ala) mutants accumulated in early mitosis (N4 DNA/phospho-H3(Ser10)-positive; red bars) from 12- to 24-h taxol exposure. Interestingly, HA-Bcl-xL-expressing cells started to lose the phospho-H3(Ser10) marker by 36 h, whereas HA-Bcl-xL(Ser62Ala) mutant cells were still stable in early mitosis by 36 h (N4 DNA/phospho-H3(Ser10)-positive; red bars), gradually losing the phospho-H3(Ser10) marker only at 48 to 60 h after taxol treatment. The phosphorylation mutants, including HA-Bcl-xL(Thr41Ala), (Ser43Ala), (Thr47Ala), (Ser56Ala) and (Thr115Ala), did not present a phenotype similar to HA-Bcl-xL(Ser62Ala) (Supplemental Figure S1B-I), revealing the specificity of the HA-Bcl-xL(Ser62Ala) effect on mitosis regulation and progression. Co-commitly, phosphorylation of HA-Bcl-xL(Ser62) appeared rapidly in taxol-exposed cells in parallel with phospho-histone H3(Ser10), but not on HA-Bcl-xL(Ser62Ala) mutant (Figure 1F). Together, these results indicated that Bcl-xL(Ser62) phosphorylation occurred at a SAC in taxol-exposed cells. Phospho-Bcl-xL(Ser62) also appeared to accelerate SAC resolution and cell entry into anaphase. Indeed, failure of this phosphorylation in cells expressing the HA-Bcl-xL(Ser62Ala) mutant maintained taxol-exposed cells at the SAC for a longer time period with no striking difference in apoptosis level.

Endogenous Bcl-xL(Ser62) phosphorylation and location in synchronized cells and in taxol-sustained SAC in wt HeLa cells

Because the above observations were made in HA-Bcl-xL-transfected and over-expressed cells, we next monitored and explored the role of endogenous phospho-Bcl-xL(Ser62) during mitosis. First, wt HeLa cells were synchronized by double thymidine block and released upon progression to G2. The cells were then treated with nocodazole (0.35 μM, 4-h), and prometaphase/metaphase cells were collected by mitotic shake-off. A portion of these cells was released from nocodazole and by growth in the presence of MG-132 (25 μM), a proteasome inhibitor that prevents cyclinB1 and securin destruction, to obtain a cell population at the anaphase boundary. A second set was also released from nocodazole and by growth in the presence of blebbistatin (10 μM), a selective non-muscle contractile motor myosin II inhibitor that prevents furrow ingression, to attain a cell population at telophase/cytokinesis. A schematic view of these experiments appears in Figure 2A. Western blotting disclosed that Bcl-xL was highly phosphorylated on Ser62 at prometaphase, metaphase and the anaphase boundary, while it was rapidly dephosphorylated at telophase/cytokinesis (Figure 2A). Bcl-xL level remained stable along mitosis, and cyclinB1 and phospho-H3(Ser10) expression was also shown to be a specific early mitotic phase marker (Figure 2A). We next looked for the location of phospho-Bcl-xL(Ser62) in unperturbed, synchronized wt HeLa cells. In these experiments, wt HeLa cells were synchronized by double thymidine block and release upon progression to G2 and entry into mitosis. The cells were collected at 30-min intervals from 9 to 12 h after double thymidine block and release to acquire mitotic cells at all steps of mitosis. Phospho-Bcl-xL(Ser62) did not co-localize with kinetochore structural proteins, including CENPA and HEC1, the microtubule plus-end tracking-associated protein CLIP170, but localized in centrosomes with γ-tubulin, in mitotic cytosol with the SAC signaling kinase PLK1, and in cytosol as well as along the microtubule spindle with the motor protein dynein (Figure 2B). Controls with Bcl-xL antibodies are illustrated in Supplemental Figure S2. Similar observations were made in taxol-exposed wt HeLa cells. More than 50 to 60% of wt HeLa cells harbored N4 DNA content and phospho-H3(Ser10) positivity 24-h post-taxol exposure (Figure 3A) with

Bcl-xL phosphorylation on Ser62 (Figure 3B). The cells gradually lost Bcl-xL(Ser62) phosphorylation with the early mitotic and SAC phospho-H3(Ser10) marker. In these cells 24 h post-taxol treatment, phospho-Bcl-xL(Ser62) had a similar location compared to the normal mitosis step at prometaphase and metaphase, with no co-location with kinetochore structural proteins, including CENPA and HEC1, and co-location in centrosomes with γ-tubulin, in mitotic cytosol with SAC signaling components, including PLK1, BUBR1 and MAD2, and the motor protein dynein (Figure 3C). A summary of microscopy analysis is presented in Tables 1A and 1B.

The importance of Bcl-xL in SAC resolution and cell fate

Because the above observations reveal a role of Bcl-xL in SAC and mitosis progression, we hypothesized that silencing Bcl-xL expression would have an impact on SAC stability and resolution. To perform these experiments, we used nocodazole which has less toxicity than taxol in wt HeLa cells. Two types of experiments were conducted. First, we monitored SAC resolution/adaptation under continuous nocodazole treatment in cells transfected with control siRNAs or siRNAs targetting Bcl-xL expression. A schematic illustration of these experiments appears in the upper left panel of Figure 4A, with Bcl-xL expression shown in the upper right panel (Figure 4A). When Bcl-xL expression was suppressed, the cells lost phospho-H3(Ser10) labeling more rapidly than cells expressing Bcl-xL (Figure 4A, red bars). Moreover, these cells did not enter into G1 (Figure 4A, blue bars) and remained with N4 DNA content (Figure 4A, grey bars), indicating tetraploidy. Second, we monitored SAC resolution/recovery under conditions where cells were released from nocodazole treatment, and in cells transfected with control siRNA or siRNA targeting Bcl-xL expression. A schematic view of these experiments is shown in the upper left panel of Figure 4B, with Bcl-xL expression illustrated in the upper right panel (Figure 4B). When Bcl-xL expression was suppressed, the cells rapidly lost phospho-H3(Ser10) labeling compared to cells expressing Bcl-xL (Figure 4A, red bars). In addition, these cells did not enter into G1 as fast as cells expressing Bcl-xL (Figure 4B, blue bars), and more cells retained N4 DNA content (Figure 4B, grey bars) or died (Figure 4B, green bars). Finally, further observation of

tetraploid cells under the microscope revealed that they were binucleated (Figure 4C).

PLK1 and MAPK14/SAPKp38α are major protein kinases involved in Bcl-xL(Ser62) phosphorylation during mitosis

Based on an *in silico* consensus site prediction search and on known protein kinases activated during mitosis, we first tested a panel of protein kinases by *in vitro* kinase assays with recombinant human Bcl-xL protein as substrate (Figure 5A). Among all the kinases tested, PLK1, MAPK8/JNK1, MAPK9/JNK2, MAPKAP2, MAPK14/SAPKp38α, GSK3α and GSK3β were positive and able to phosphorylate recombinant Bcl-xL protein on Ser62 in *in vitro* kinase assays (Figure 5A), while CHK1, PLK3, AuroraB, MPS1, CDK1(CDC2), BUB1, BUB3 and BUBR1 failed to phosphorylate recombinant Bcl-xL protein on Ser62 (Figure 5A). Enzyme-specific activities with control substrates are indicated in Supplemental Figure S3, and details of the kinase assays are given in Supplemental Table S1A. Then, with specific pharmacological inhibitors and nocodazole-exposed cells, we observed that PLK and MAPK14/SAPKp38α inhibitors prevented Bcl-xL phosphorylation on Ser62 in nocodazole-exposed cells (Figure 5B). A schematic illustration of these experiments, and Bcl-xL and phospho-H3(Ser10) expression appear in Figure 5B. Deploying a series of specific siRNAs, Western blotting of cell extracts from cells collected by mitotic shake-off revealed again that the most important kinases involved in Bcl-xL(Ser62) phosphorylation of wt HeLa cells were PLK1 and MAPK14/SAPKp38α (Figure 5C). These experiments and the expression level of phospho-Bcl-xL(Ser62), Bcl-xL, phospho-H3(Ser10), PLK1, MAPK14/SAPKp38α, , MAPKAP2, MAPK8/JNK1, MAPK9/JNK2 and β-actin are schematically illustrated in Figure 5C. Additional controls and siRNA experiments are reported in Supplemental Figure S4, with details in Supplemental Table S1B. The data indicate that PLK1 and MAPK14/SAPKp38α are major protein kinases associated with Bcl-xL(Ser62) phosphorylation during mitosis.

Interaction between phospho-Bcl-xL(Ser62) and the CDC20/MAD2/BUBR1/BUB3 complex

During SAC, a "stop anaphase signal" consisting of MAD2, BUBR1 and BUB3 complex bound to CDC20 in mitotic cytosol negatively controls APC/C activity. In co-immunoprecipitation experiments performed in transfected Namalwa cells, we observed that HA-Bcl-xL protein co-immunoprecipitated with MAD2, BUBR1, BUB3 and CDC20, but not BUB1, in unperturbed and taxol-exposed cells (24 h), while HA-Bcl-xL(Ser62Ala) mutant was only bound to MAD2 and, to a much lesser extent, BUB3 (Figure 6A). These interactions were lost as the cells gradually progressed into the later stage of mitosis 48 h post-taxol exposure (Figure 1D, red bars). A series of reciprocal co-immunoprecipitations confirmed that MAD2, BUBR1 and CDC20 interact with phospho-HA-Bcl-xL(Ser62) (Figure 6B). CDC27 (APC-3), a subunit of APC, did not co-immunoprecipitate in these experiments.

Discussion

Our study indicates that during SAC, PLK1 and MAPK14/p38α mediated Bcl-xL(Ser62) phosphorylation, binding it to the inhibitory CDC20/MAD2/BUBR1/BUB3 complex in a way that accelerates SAC resolution and leading cells to enter anaphase more rapidly, even in the presence of unattached or misaligned chromosomes. Silencing Bcl-xL expression also leads nocodazole-exposed cells to tetraploidy and binucleation, consistent with Bcl-xL function in genomic stability. Phospho-Bcl-xL(Ser62) also localizes in centrosomes with γ-tubulin and along the microtubule spindle with dynein motor protein, but its functions at these locations were not further addressed in this study. Importantly, phospho-Bcl-xL(Ser62) function in mitosis appears to be separable from Bcl-xL's known role in apoptosis, as Bcl-xL(Ser62Ala) phosphorylation mutant keeps its anti-apoptotic effect but clearly shows different behavior during SAC resolution and mitotic progression. Figure 6C provides a schematic view of the proposed model.

Bcl-xL phosphorylation has been detected previously in mitotic cells treated with microtubule inhibitors and binders, including nocodazole, paclitaxel, vinblastine, vincristine, colchicine and pironetin, and a few protein kinases have been proposed to phosphorylate Bcl-xL at Ser62 in microtubule inhibitor-exposed cells. Most studies have

suggested that JNK, normally activated at G2/M, is the kinase responsible for Bcl-2 and Bcl-xL phosphorylation [25-33, 37]. Unlike other studies which investigated single protein kinases, in this work we simultaneously probed more than 14 protein kinases in a combination of assays, including *in vitro* kinase assays, pharmacological inhibitors and siRNAs. Most importantly, siRNA analysis was performed in a highly-enriched mitotic cell population collected by mitotic shake-off, to eliminate and avoid contamination or unwanted effects of these protein kinases in the G2 cell population. Our systemic approach may explain difference between our study and others [25-33, 37]. In our experiment, two major protein kinases, PLK1 and MAPK14/SAPKp38α, involved in Bcl-xL(Ser62) phosphorylation during mitosis, have been identified. PLK1 activity is known to be highly regulated in both time and space, and has key functions for cell entry into mitosis, SAC regulation, mitotic exit and cytokinesis (reviewed in [38, 39]). MAPK14/SAPKp38α is another major protein kinase activated during mitosis [40], that plays key roles during SAC, at metaphase/anaphase transition [40-47].

The current model of SAC regulation, supported by many studies indicates that unattached kinetochores generate the formation of a "stop anaphase signal" containing the proteins MAD2, BUBR1 and BUB3 that diffuse into mitotic cytosol and sequester CDC20 to interfere with APC/C activity [1-3, 8-19]. However, subsequent entry into anaphase required SAC resolution and APC/C activation by a mechanism that remains poorly understood. SAC resolution or mitotic slippage in the presence of unattached or misaligned chromosomes has often been observed with microtubule poisons [48-54], and SAC silencing or resolution at least required ubiquitination, deubiquitination and proteolysis [55-59]. Several findings in our study support a role of Bcl-xL in SAC resolution, even in the presence of unattached or misaligned chromosomes. First, cells overexpressing wt Bcl-xL or the phosphorylation mutant Bcl-xL(Ser62Ala) show differences in phospho-H3(Ser10) dephosphorylation kinetics while retaining N4 DNA content, a measure of SAC resolution in taxol-exposed cells. Second, phospho-Bcl-xL(Ser62) phosphorylation and de-phosphorylation kinetics correlate with SAC/On and SAC/Off kinetics. Third, phospho-Bcl-xL(Ser62) binds to the CDC20/MAD2/BUBR1/ BUB3 inhibitory complex, while Bcl-xL(Ser62Ala) does not. Finally, silencing Bcl-xL expression also accelerates SAC resolution. Our data do not exclude that, in addition to

Bcl-xL phosphorylation on Ser62, other events may also occur to regulate Bcl-xL function during mitosis. The formation of SAC inhibitory complex consisting of CDC20/MAD2/BUBR1/BUB3 is highly dynamic, and several intermediates have been resolved in a reconstituted cell-free system [19]. In the near future, it will be of interest to use the reconstituted cell-free system with recombinant Bcl-xL protein and the combination of phosphorylation mutant and phosphorylation mimetic recombinant Bcl-xL proteins to resolve their actions on the formation, stability and diassembly of the CDC20/MAD2/BUBR1/BUB3 inhibitory complex.

These data indicate that during SAC, Bcl-xL(Ser62) phosphorylation accelerates SAC resolution and cell entry into anaphase, even in the presence of unattached or misaligned chromosomes. Such Bcl-xL action will raise the occurrence of tetraploidy and binucleation, with a direct consequence on genomic stability. The association between anti-apoptotic Bcl-2 or Bcl-xL and genomic stability has previously been suggested in the context of DNA damage and DNA repair. Indeed, they have been shown to influence nucleotide excision repair [60], base excision repair [61], DNA mismatch repair [62], the Rad51-dependent homologous recombination pathway [63, 64], gene conversion [65] and the non-homologous end-joining pathway [66], providing significant effects on genomic stability. Bcl-xL also showed specific functions during the G2 checkpoint mediated by DNA damage, effects that are independent of its anti-apoptotic role, but which influence genomic stability [36]. Similarly, mice bearing a Bcl-xL transgene incur malignant conversion of benign tumors [67]. To the best of our knowledge, this is the first observation to reveal that phospho-Bcl-xL(Ser62) is associated with genomic stability, influencing tetraploidy and binucleation as a consequence of its direct function on SAC resolution and mitosis progression. Our finding is in harmony with those observations of others which reveal that dysfunctional SAC has a dramatic effect on aneuploidy and tumorigenesis in mice [68].

Materials and methods

Cell culture, cDNA construction and cell analysis

Human Namalwa and HeLa cell lines were obtained from the American Type Culture Collection and grown at 37°C under 5% CO_2 in RPMI-1640 medium and DMEM supplemented with 10% heat-inactivated fetal bovine serum (FBS), 100 U/ml penicillin and 100 μg/ml streptomycin, respectively. The phosphorylation mutant pCEP4-HA-Bcl-xL and pCDNA3.1-HA-Bcl-xL vector were generated by triple polymerase chain reactions. All primers and details are provided in Supplemental Table S1C. Transfected cells were grown under hygromycin B1 (pCEP4 vectors) or neomycin (pCDNA3.1 vectors) selection to attain a stable cell population prior to performing the experiments. The kinetics of mitotic entry, cell cycle phase distribution and cell death were monitored in Coulter EpicsXL flow cytometers with phospho-H3(Ser10) labeling and PI staining. HeLa cells were synchronized by double-thymidine block (2 mM) and release.

Protein extraction and immunoblotting

To prepare total protein extracts, cells were extracted with lysis buffer containing 20 mM Hepes(KOH), pH 7.4, 120 mM NaCl, 1% Triton X-100, 2 mM phenylmethylsulfonyl fluoride, a cocktail of protease inhibitors (Complete™, Roche Applied Science) and a cocktail of phosphatase inhibitors (PhosStop™ Roche Applied Science). For immunoprecipitation, the samples were first pre-cleaned with a protein A- and G-Sepharose mixture and, after centrifugation, antibodies at 10 μg/ml concentration were incubated at 4°C for 4 h. All antibodies used in this study are listed in Supplemental Table S1D.

Immunofluorescence microscopy

HeLa cells were seeded and grown directly on coverslips. The cells were fixed in methanol at -20°C for 30 min and rapidly immersed in ice-cold acetone for a few seconds. The slides were allowed to dry at room temperature and rehydrated in PBS. Nonspecific binding sites were blocked in PBS containing 5% FBS (blocking solution); then, the slides were incubated sequentially with specific primary antibody (10 μg/ml in blocking solution), specific labeled secondary antibody (10 μg/ml in blocking solution), followed by DAPI staining, also performed in blocking solution. All antibodies are listed in Supplemental Table S1E. Images were generated with a Leica Microsystem mounted

on a Leica DM6000B microscope and Leica DFC480 camera hooked up to a Macintosh computer.

Protein kinase assays and protein kinase chemical inhibitors

The kinases and kinase assays are described in Supplemental Table S1A. Enzyme activities were tested on control substrates, and velocities were expressed as nmole/min/mg (data in Supplemental Figure S3). Recombinant human Bcl-xL(ΔTM) protein was produced and purified, as described previously [36]. The protein kinase chemical inhibitors deployed in this study are listed in Supplemental Table S1A.

siRNA-mediated protein kinase inhibition

HeLa cells were transfected with DharmaFECT-1 transfection reagent (ThermoScientific) according to the manufacturer's instructions, with 100 nM of either control siRNA or siRNA targeting different kinases (Supplemental Table S1C). The cells were treated 48 h post-transfection with taxol (0.1 μm) or nocodazole (0.35 μm), as indicated prior to protein extraction and SDS-PAGE.

Online supplemental materials: Supplemental materials for this article, including supplemental figures and tables, are available at the Journal website.

Disclosure of conflicts of interest

The authors declare no potential conflicts of interest.

Acknowledgements

This work was funded by grant MOP-97913 from the Canadian Institutes of Health Research to R.B. J.W. received scholarships from the China Scholarship Council (Beijing, China), the Faculté des études supérieures (Université de Montréal, Canada) and the Fondation de l'Institut du cancer de Montréal (Canada).

Abbreviations list:

APC/C, anaphase-promoting complex/cyclosome; Bcl, B cell leukemia/lymphoma

protein; BUB, budding uninhibited by benzimidazole protein; CDC, cell division cycle protein; CDK, cyclin-dependent kinase; CENPA, centromere protein A; CHK1, checkpoint kinase 1; CLIP170, cytoplasmic linker protein 170; GSK3, glycogen synthase kinase 3; HEC1; highly expressed in cancer protein 1; H3, histone 3; JNK, Jun N-terminal kinase; MAD, mitotic arrest deficient protein; MAPK, mitogen-activated protein kinase; MAPKAPK2, mitogen-activated protein kinase-activated protein kinase 2; MPS1, monopolar spindle 1 kinase; PLK, polo kinase; SAC, spindle-assembly checkpoint; SAPK, stress-activated protein kinase; siRNA, silencing RNA; wt, wild type.

References

1. Musacchio A, Salmon ED. The spindle-assembly checkpoint in space and time. Nature Rev Mol Cell Biol 2007; 8: 379-93.
2. Sullivan M, Morgan DO. Finishing mitosis, one step at a time. Nat Rev Mol Cell Biol 2007; 8: 894-903.
3. Bolanos-Garcia VM, Blundell TL. BUB1 and BUBR1: multifaceted kinases of the cell cycle. Trends Biochem Sci 2011; 36:141-150
4. Lohka MJ, Hayes MK, Maller JL. Purification of maturation-promoting factor, an intracellular regulator of early mitotic events. Proc Natl Acad Sci USA 1988; 85: 3009-13.
5. Labbe JC, Picard A, Peaucellier G, Cavadore JC, Nurse P, Doree M. Purification of MPF from starfish: identification as the H1 histone kinase p34cdc2 and a possible mechanism for its periodic activation. Cell 1989; 57: 253-63.
6. Gautier J, Minshull J, Lohka M, Glotzer M, Hunt T, Maller JL. Cyclin is a component of maturation-promoting factor from Xenopus. Cell 1990; 60: 487-94.
7. Gavet O, Pines J. Progressive activation of CyclinB1-Cdk1 coordinates entry to mitosis. Dev Cell 2010; 18: 533-43.
8. Taylor SS, Scott MI, Holland AJ. The spindle checkpoint: a quality control mechanism which ensures accurate chromosome segregation. Chromosome Res 2004; 12: 599-616.
9. Baker DJ, Dawlaty MM, Galardy P, van Deursen JM. Mitotic regulation of the anaphase-promoting complex. Cell Mol Life Sci 2007; 64: 589-600.
10. Chan GK, Liu ST, Yen TJ. Kinetochore structure and function. Trends Cell Biol 2005; 15: 589-98.
11. Cheeseman IM, Desai A. Molecular architecture of the kinetochore-microtubule interface. Nature Rev Mol Cell Biol 2008; 9: 33-46.

12. Fang G, Yu H, Kirschner MW. The checkpoint protein MAD2 and the mitotic regulator CDC20 form a ternary complex with the anaphase-promoting complex to control anaphase initiation. Genes Dev 1998; 12: 1871-83.

13. Sudakin V, Chan GK, Yen TJ. Checkpoint inhibition of the APC/C in HeLa cells is mediated by a complex of BUBR1, BUB3, CDC20, and MAD2. J Cell Biol 2001; 154: 925-36.

14. Tang Z, Bharadwaj R, Li B, Yu H. Mad2-independent inhibition of APCCdc20 by the mitotic checkpoint protein BubR1. Dev Cell 2001; 1: 227-37.

15. Fang G. Checkpoint protein BubR1 acts synergistically with Mad2 to inhibit anaphase-promoting complex. Mol Biol Cell 2002; 13: 755-66.

16. Dai W, Wang Q, Liu T, et al. Slippage of mitotic arrest and enhanced tumor development in mice with BubR1 haploinsufficiency. Cancer Res 2004; 64: 440-5.

17. Sudakin V, Yen TJ. Purification of the mitotic checkpoint complex, an inhibitor of the APC/C from HeLa cells. Methods Mol Biol 2004; 281: 199-212.

18. Peters JM. The anaphase promoting complex/cyclosome: a machine designed to destroy. Nat Rev Mol Cell Biol 2006; 7: 644-56.

19. Kulukian A, Han JS, Cleveland DW. Unattached kinetochores catalyze production of an anaphase inhibitor that requires a Mad2 template to prime Cdc20 for BubR1 binding. Dev Cell 2009; 16: 105-17.

20. D'Angiolella V, Mari C, Nocera D, Rametti L, Grieco D. The spindle checkpoint requires cyclin-dependent kinase activity. Genes Dev 2003; 17: 2520-5.

21. Chung E, Chen RH. Phosphorylation of Cdc20 is required for its inhibition by the spindle checkpoint. Nat Cell Biol 2003; 5: 748-53.

22. Tang Z, Shu H, Oncel D, Chen S, Yu H. Phosphorylation of Cdc20 by Bub1 provides a catalytic mechanism for APC/C inhibition by the spindle checkpoint. Mol Cell 2004; 16: 387-97.

23. Schmitt E, Paquet C, Beauchemin M, Bertrand R. DNA-damage response network at the crossroads of cell-cycle checkpoints, cellular senescence and apoptosis. J Zhejiang Univ Sci B 2007; 8: 377-97.

24. Danial NN, Gimenez-Cassina A, Tondera D. Homeostatic functions of Bcl-2 proteins beyond apoptosis. Adv Exp Med Biol 2010; 687: 1-32.

25. Poruchynsky MS, Wang EE, Rudin CM, Blagosklonny MV, Fojo T. Bcl-X(L) is phosphorylated in malignant cells following microtubule disruption. Cancer Res 1998; 58: 3331-8.

26. Fang GF, Chang BS, Kim CN, Perkins C, Thompson CB, Bhalla KN. Loop domain is necessary for taxol-induced mobility shift and phosphorylation of Bcl-2 as well as for inhibiting taxol-induced cytosolic accumulation of cytochrome c and apoptosis. Cancer Res 1998; 58: 3202-8.

27. Johnson AL, Bridgham JT, Jensen T. Bcl-x(Long) protein expression and phosphorylation in granulosa cells. Endocrinology 1999; 140: 4521-9.

28. Fan M, Du C, Stone AA, Gilbert KM, Chambers TC. Modulation of mitogen-activated protein kinases and phosphorylation of Bcl-2 by vinblastine represent persistent forms of normal fluctuations at G2-M. Cancer Res 2000; 60: 6403-7.

29. Basu A, Haldar S. Identification of a novel Bcl-xL phosphorylation site regulating the sensitivity of taxol- or 2-methoxyestradiol-induced apoptosis. FEBS Lett 2003; 538: 41-7.

30. Du L, Lyle CS, Chambers TC. Characterization of vinblastine-induced Bcl-xL and Bcl-2 phosphorylation: evidence for a novel protein kinase and a coordinated phosphorylation/dephosphorylation cycle associated with apoptosis induction. Oncogene 2005; 24: 107-17.

31. Upreti M, Galitovskaya EN, Chu R, et al. Identification of the major phosphorylation site in Bcl-xL induced by microtubule inhibitors and analysis of its functional significance. J Biol Chem 2008; 283: 35517-25.

32. Tamura Y, Simizu S, Muroi M, et al. Polo-like kinase 1 phosphorylates and regulates Bcl-x(L) during pironetin-induced apoptosis. Oncogene 2009; 28: 107-16.

33. Terrano DT, Upreti M, Chambers TC. Cyclin-dependent kinase 1-mediated Bcl-xL/Bcl-2 phosphorylation acts as a functional link coupling mitotic arrest and apoptosis. Mol Cell Biol 2010; 30: 640-56.

34. Chang BS, Minn AJ, Muchmore SW, Fesik SW, Thompson CB. Identification of a novel regulatory domain in Bcl-X(L) and Bcl-2. EMBO J 1997; 16: 968-77.

35. Burri SH, Kim CN, Fang GF, et al. 'Loop' domain deletional mutant of Bcl-xL is as effective as p29Bcl-xL in inhibiting radiation-induced cytosolic accumulation of cytochrome C (cyt c), caspase-3 activity, and apoptosis. Int J Radiat Oncol Biol Phys 1999; 43: 423-30.

36. Schmitt E, Beauchemin M, Bertrand R. Nuclear co-localization and interaction between Bcl-xL and Cdk1(cdc2) during G2/M cell cycle checkpoint. Oncogene 2007; 26: 5851-65.

37. Fan M, Goodwin M, Vu T, Brantley-Finley C, Gaarde WA, Chambers TC. Vinblastine-induced phosphorylation of Bcl-2 and Bcl-XL is mediated by JNK and occurs in parallel with inactivation of the Raf-1/MEK/ERK cascade. J Biol Chem 2000; 275: 29980-5.

38. Takaki T, Trenz K, Costanzo V, Petronczki M. Polo-like kinase 1 reaches beyond mitosis-cytokinesis, DNA damage response, and development. Curr Opin Cell Biol 2008; 20: 650-60.

39. Archambault V, Glover DM. Polo-like kinases: conservation and divergence in their functions and regulation. Nat Rev Mol Cell Biol 2009; 10: 265-75.

40. Takenaka K, Moriguchi T, Nishida E. Activation of the protein kinase p38 in the spindle assembly checkpoint and mitotic arrest. Science 1998; 280: 599-602.

41. Kurata S. Selective activation of p38 MAPK cascade and mitotic arrest caused by low level oxidative stress. J Biol Chem 2000; 275: 23413-6.

42. Chao JI, Yang JL. Opposite roles of ERK and p38 mitogen-activated protein kinases in cadmium-induced genotoxicity and mitotic arrest. Chem Res Toxicol 2001; 14: 1193-202.

43. Campos CB, Bedard PA, Linden R. Activation of p38 mitogen-activated protein kinase during normal mitosis in the developing retina. Neuroscience 2002; 112: 583-91.

44. Fan L, Yang X, Du J, Marshall M, Blanchard K, Ye X. A novel role of p38 alpha MAPK in mitotic progression independent of its kinase activity. Cell Cycle 2005; 4: 1616-24.

45. Cha H, Wang X, Li H, Fornace AJ, Jr. A functional role for p38 MAPK in modulating mitotic transit in the absence of stress. J Biol Chem 2007; 282: 22984-92.

46. Yen AH, Yang JL. Cdc20 proteolysis requires p38 MAPK signaling and Cdh1-independent APC/C ubiquitination during spindle assembly checkpoint activation by cadmium. J Cell Physiol 2010; 223: 327-34.

47. Yuan J, Xu BZ, Qi ST, et al. MAPK-activated protein kinase 2 is required for mouse meiotic spindle assembly and kinetochore-microtubule attachment. PLoS ONE 2010; 5: e11247.

48. Ikui AE, Yang CP, Matsumoto T, Horwitz SB. Low concentrations of taxol cause mitotic delay followed by premature dissociation of p55CDC from Mad2 and BubR1 and abrogation of the spindle checkpoint, leading to aneuploidy. Cell Cycle 2005; 4: 1385-8.

49. Brito DA, Rieder CL. Mitotic checkpoint slippage in humans occurs via cyclin B destruction in the presence of an active checkpoint. Curr Biol 2006; 16: 1194-200.

50. Gascoigne KE, Taylor SS. Cancer cells display profound intra- and interline variation following prolonged exposure to antimitotic drugs. Cancer Cell 2008; 14: 111-22.

51. Orth JD, Tang Y, Shi J, et al. Quantitative live imaging of cancer and normal cells treated with Kinesin-5 inhibitors indicates significant differences in phenotypic responses and cell fate. Mol Cancer Ther 2008; 7: 3480-9.

52. Bekier ME, Fischbach R, Lee J, Taylor WR. Length of mitotic arrest induced by microtubule-stabilizing drugs determines cell death after mitotic exit. Mol Cancer Ther 2009; 8: 1646-54.

53. Yang Z, Kenny AE, Brito DA, Rieder CL. Cells satisfy the mitotic checkpoint in Taxol, and do so faster in concentrations that stabilize syntelic attachments. J Cell Biol 2009; 186: 675-84.

54. Huang HC, Shi J, Orth JD, Mitchison TJ. Evidence that mitotic exit is a better cancer therapeutic target than spindle assembly. Cancer Cell 2009; 16: 347-58.

55. Reddy SK, Rape M, Margansky WA, Kirschner MW. Ubiquitination by the anaphase-promoting complex drives spindle checkpoint inactivation. Nature 2007; 446: 921-5.

56. Stegmeier F, Rape M, Draviam VM, et al. Anaphase initiation is regulated by antagonistic ubiquitination and deubiquitination activities. Nature 2007; 446: 876-81.

57. Nilsson J, Yekezare M, Minshull J, Pines J. The APC/C maintains the spindle assembly checkpoint by targeting Cdc20 for destruction. Nat Cell Biol 2008; 10: 1411-20.

58. Visconti R, Palazzo L, Grieco D. Requirement for proteolysis in spindle assembly checkpoint silencing. Cell Cycle 2010; 9: 564-9.

59. Zeng X, Sigoillot F, Gaur S, et al. Pharmacologic inhibition of the anaphase-promoting complex induces a spindle checkpoint-dependent mitotic arrest in the absence of spindle damage. Cancer Cell 2010; 18: 382-95.

60. Liu YF, Naumovski L, Hanawalt P. Nucleotide excision repair capacity is attenuated in human promyelocytic Hl60 cells that overexpress Bcl-2. Cancer Res 1997; 57: 1650-3.

61. Kuo ML, Shiah SG, Wang CJ, Chuang SE. Suppression of apoptosis by Bcl-2 to enhance benzene metabolites-induced oxidative DNA damage and mutagenesis: a possible mechanism of carcinogenesis. Mol Pharmacol 1999; 55: 894-901.

62. Youn CK, Cho HJ, Kim SH, et al. Bcl-2 expression suppresses mismatch repair activity through inhibition of E2F transcriptional activity. Nat Cell Biol 2005; 7: 137-47.

63. Saintigny Y, Dumay A, Lambert S, Lopez BS. A novel role for the Bcl-2 protein family: specific suppression of the RAD51 recombination pathway. EMBO J 2001; 20: 2596-607.

64. Dumay A, Laulier C, Bertrand P, et al. Bax and Bid, two proapoptotic Bcl-2 family members, inhibit homologous recombination, independently of apoptosis regulation. Oncogene 2006; 25: 3196-205.

65. Wiese C, Pierce AJ, Gauny SS, Jasin M, Kronenberg A. Gene conversion is strongly induced in human cells by double-strand breaks and is modulated by the expression of Bcl-x(L). Cancer Res 2002; 62: 1279-83.

66. Wang Q, Gao F, May WS, Zhang Y, Flagg T, Deng X. Bcl-2 negatively regulates DNA double-strand-break repair through a nonhomologous end-joining pathway. Mol Cell 2008; 29: 488-98.

67. Pena JC, Rudin CM, Thompson CB. A Bcl-x(L) transgene promotes malignant conversion of chemically initiated skin papillomas. Cancer Res 1998; 58: 2111-6.

68. Li M, Fang X, Wei Z, York JP, Zhang P. Loss of spindle assembly checkpoint-mediated inhibition of Cdc20 promotes tumorigenesis in mice. J Cell Biol 2009; 185: 983-94.

TABLE 1A Phase distribution *versus* labeling (number of cells) in synchronized human wt HeLa cells collected from 9 to 12 h after double thymidine block-release

P-Bcl-xL(S62)	**PROMETAPHASE**	**METAPHASE**	**ANAPHASE**	**TELOPHASE**	**CYOKINESIS**	**TOTAL**
+ CENPA	17/22 (-)	17/17 (-)	11/11 (-)	10/10 (-)	16/16 (-)	76
+ PLK1	45/45 (+)	46/46 (+)	21/21 (+)	12/19 (-)	14/14 (-)	145
+ γ-Tubulin	21/21 (+)	19/19 (+)	15/15 (+)	08/10 (-)	15/15 (-)	80
+ Clip-170	36/36 (-)	30/30 (-)	23/23 (-)	10/14 (-)	09/13 (-)	116
+ Dynein	24/24 (+)	20/20 (+)	10/10 (+)	07/10 (-)	14/14 (-)	78
+ HEC1	36/36 (-)	26/26 (-)	11/11 (-)	9/9 (-)	17/17 (-)	99
Bcl-xL	**PROMETAPHASE**	**METAPHASE**	**ANAPHASE**	**TELOPHASE**	**CYOKINESIS**	**TOTAL**
+ CENPA	32/32 (-)	19/19 (-)	10/10 (-)	09/09 (-)	12/12 (-)	82
+ PLK1	55/55 (+)	28/29 (+)	21/21 (+)	08/12 (+)	14/14 (-)	131
+ γ-Tubulin	28/28 (+)	22/22 (+)	11/11 (+)	12/12 (+)	14/18 (+)	91
+ Clip-170	27/27 (-)	12/20 (-)	10/19 (-)	10/16 (-)	10/13 (-)	95
+ Dynein	36/36 (+)	23/23 (+)	11/11 (+)	08/08 (+)	08/08 (+)	86
+ HEC1	27/27 (-)	22/22 (-)	12/12 (-)	11/11 (-)	13/13 (-)	85
TOTAL	389	293	175	140	167	1,164

TABLE 1B Phase distribution *versus* labeling (number of cells) in human wt HeLa cells collected after taxol treatment (0.1 μm, 24 h)

	Bcl-xL	**P-Bcl-xL(S62)**	**TOTAL**
+ CENPA	94/94 (-)	91/102 (-)	196
+HEC1	171/171 (-)	90/98 (-)	269
+ Dynein	30/30 (+)	24/24 (+)	54
+ γ-Tubulin	84/90 (+)	85/92 (+)	182
+ PLK1	143/143 (+)	81/81 (+)	224
+ BubRI	50/55 (+)	58/61 (+)	116
+ MAD2	40/46 (+)	32/41 (+)	87
TOTAL	629	499	1128

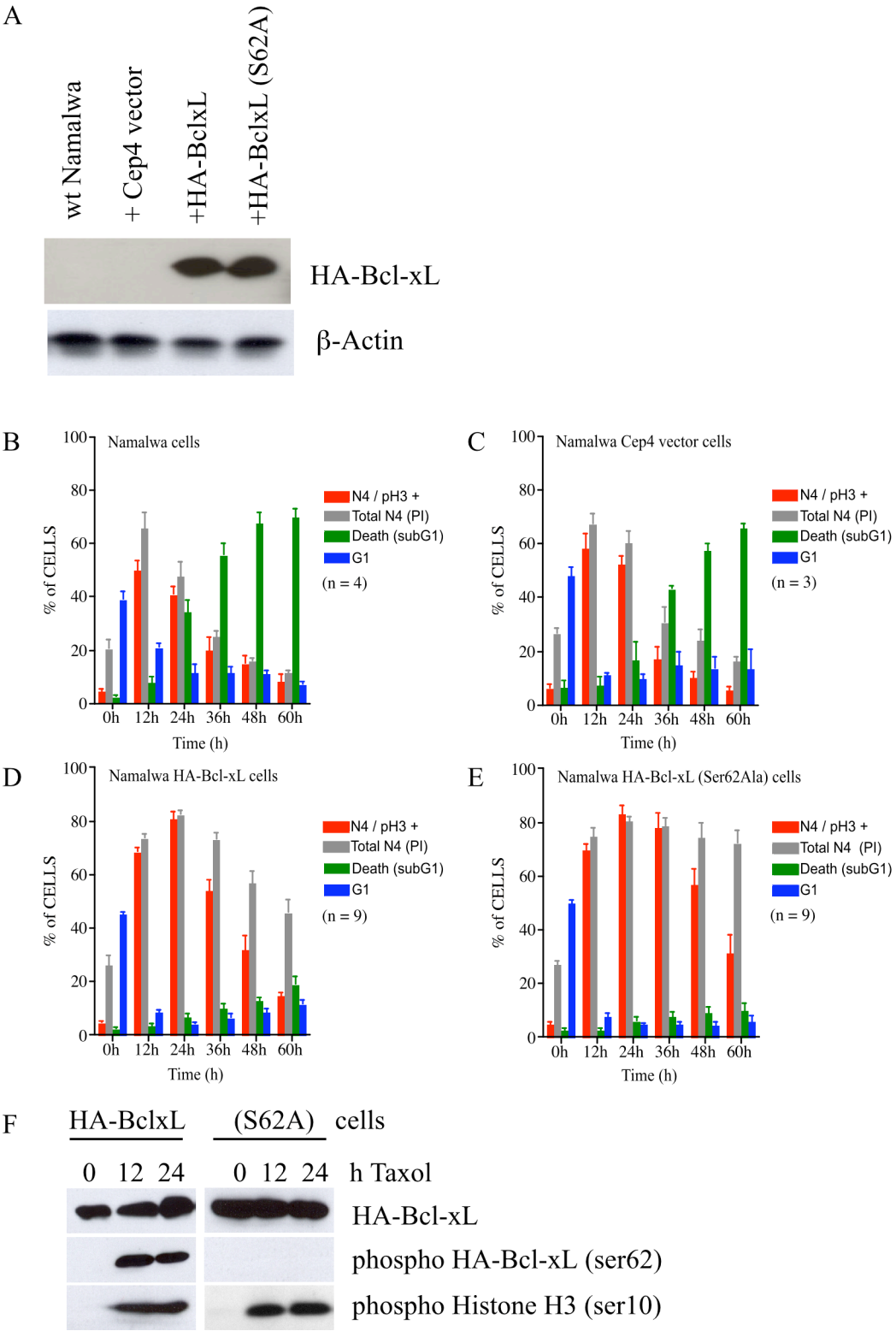
A
wt Namalwa
+ Cep4 vector
+HA-BclxL
+HA-BclxL (S62A)
HA-Bcl-xL
β-Actin
B
Namalwa cells
% of CELLS
Time (h)
N4 / pH3 +
Total N4 (PI)
Death (subG1)
G1
(n = 4)
C
Namalwa Cep4 vector cells
(n = 3)
D
Namalwa HA-Bcl-xL cells
(n = 9)
E
Namalwa HA-Bcl-xL (Ser62Ala) cells
(n = 9)
0h 12h 24h 36h 48h 60h
F
HA-BclxL
(S62A)
cells
0 12 24 0 12 24 h Taxol
HA-Bcl-xL
phospho HA-Bcl-xL (ser62)
phospho Histone H3 (ser10)

Figure 1

Figure 1 Effect of Bcl-xL and Bcl-xL(Ser62Ala) phosphorylation mutant on the stability of the SAC. (**A**) Expression level of HA-Bcl-xL and Bcl-xL(Ser62Ala) phosphorylation mutant in stably-transfected Namalwa cell populations. β-actin expression is shown as control. (**B-E**) Kinetics of G2/M cells (PI staining; grey bars), early mitotic cells (phospho-H3(Ser10) staining; red bars), dead cells (PI staining; green bars) and G1 cells (PI staining; blue bars) in wt Namalwa cells and Namalwa cells expressing empty vector, HA-Bcl-xL and HA-Bcl-xL(Ser62Ala) phosphorylation mutant during taxol treatment (0.1 μM). Bars represent the means ± s.e.m. of *n* independent experiments. (**F**) Expression and phosphorylation kinetics of HA-Bcl-xL(Ser62) and phospho-histone H3(Ser10) after taxol treatment (0.1 μM) in Namalwa cells expressing HA-Bcl-xL and Bcl-xL(Ser62Ala) phosphorylation mutant. Data on additional HA-Bcl-xL phosphorylation mutants are reported in Supplemental Figure S1A-I, and additional controls for the specificity of phospho-Bcl-xL(Ser62) Ab are shown in Supplemental Figure S1J-K.

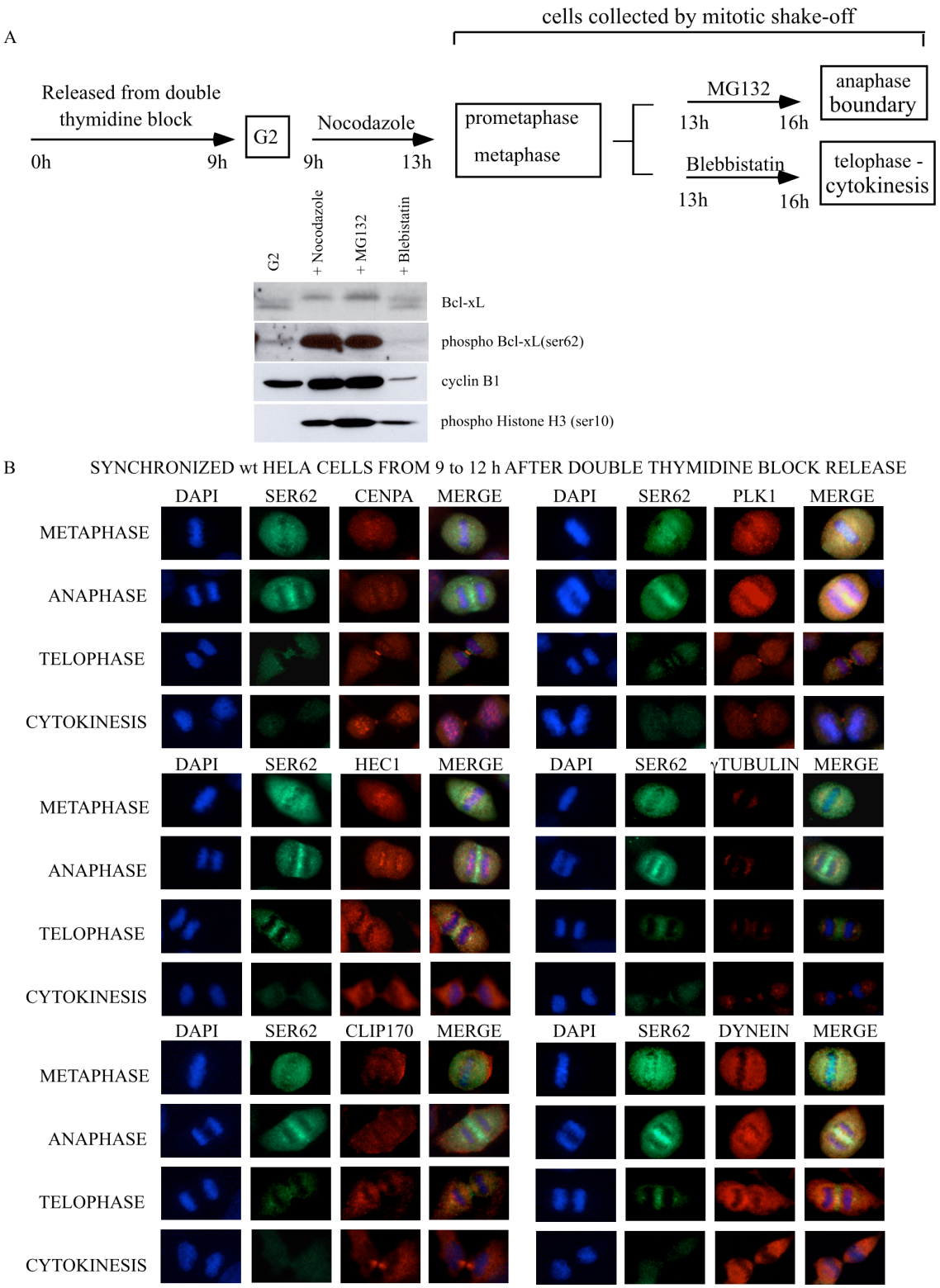
A
cells collected by mitotic shake-off
Released from double thymidine block
0h
9h
G2
Nocodazole
9h
13h
prometaphase
metaphase
MG132
13h
16h
anaphase boundary
Blebbistatin
13h
16h
telophase - cytokinesis
G2
+ Nocodazole
+ MG132
+ Blebistatin
Bcl-xL
phospho Bcl-xL(ser62)
cyclin B1
phospho Histone H3 (ser10)
B
SYNCHRONIZED wt HELA CELLS FROM 9 to 12 h AFTER DOUBLE THYMIDINE BLOCK RELEASE
DAPI
SER62
CENPA
MERGE
DAPI
SER62
PLK1
MERGE
METAPHASE
ANAPHASE
TELOPHASE
CYTOKINESIS
DAPI
SER62
HEC1
MERGE
DAPI
SER62
γTUBULIN
MERGE
METAPHASE
ANAPHASE
TELOPHASE
CYTOKINESIS
DAPI
SER62
CLIP170
MERGE
DAPI
SER62
DYNEIN
MERGE
METAPHASE
ANAPHASE
TELOPHASE
CYTOKINESIS

Figure 2

Figure 2 Bcl-xL(Ser62) phosphorylation and location in synchronized wt HeLa cells at mitosis. (**A**) Expression kinetics of Bcl-xL, phospho-Bcl-xL(Ser62), cyclin B1 and phospho-H3(Ser10) in wt HeLa cells obtained at different steps of mitosis. A schematic view of these experiments is illustrated on top. (**B**) Co-location of phospho-Bcl-xL(Ser62) with CENPA, HEC1, CLIP170, PLK1, γ-tubulin and dynein motor protein at different steps of mitosis. Micrographs with Bcl-xL Ab labeling are shown in Supplemental Figure S2. Representative of a total of 1,164 mitotic cells (3 experiments). Summary in Table 1A.

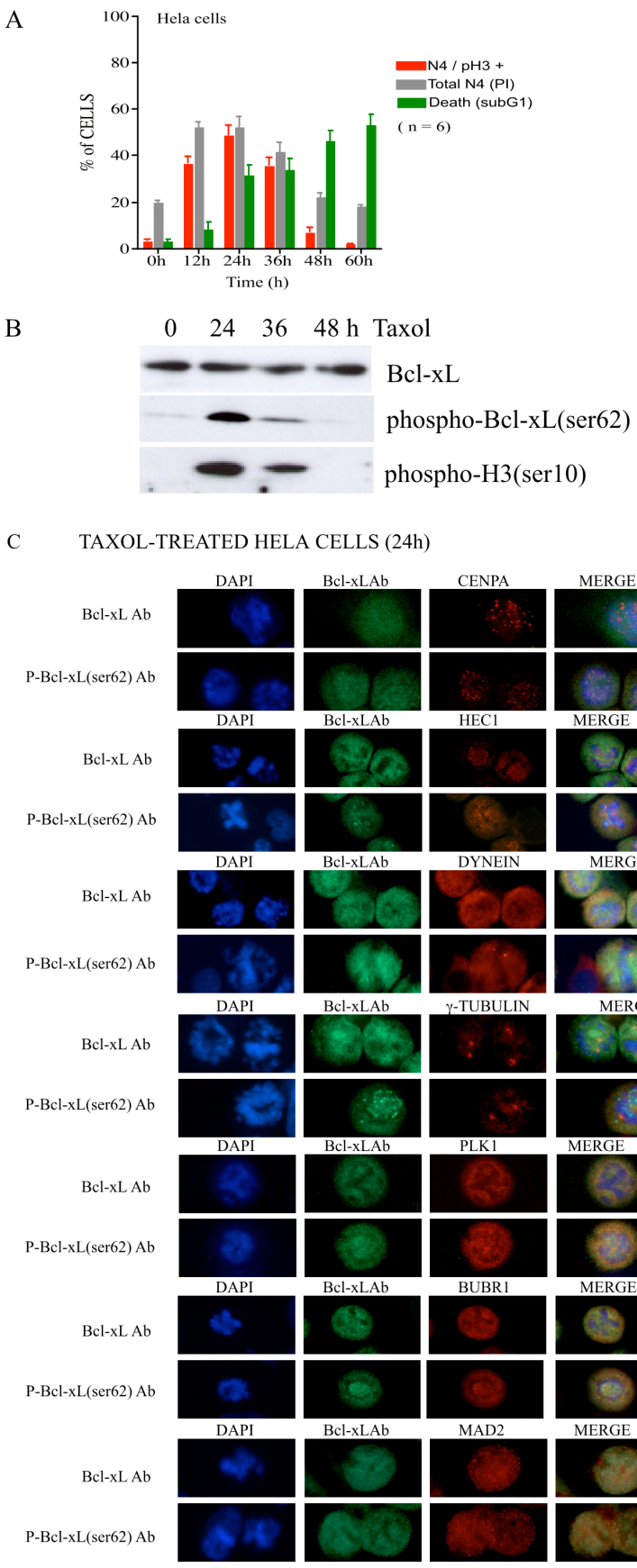
A
Hela cells
% of CELLS
100
80
60
40
20
0
0h
12h
24h
36h
48h
60h
Time (h)
N4 / pH3 +
Total N4 (PI)
Death (subG1)
(n = 6)
B
0
24
36
48 h
Taxol
Bcl-xL
phospho-Bcl-xL(ser62)
phospho-H3(ser10)
C
TAXOL-TREATED HELA CELLS (24h)
DAPI
Bcl-xLAb
CENPA
MERGE
Bcl-xL Ab
P-Bcl-xL(ser62) Ab
HEC1
DYNEIN
γ-TUBULIN
PLK1
BUBR1
MAD2

Figure 3

Figure 3 Bcl-xL(Ser62) phosphorylation and location in taxol-exposed wt HeLa cells. (**A**) Kinetics of G2/M cells (PI staining; grey bars), early mitotic cells (phospho-H3(Ser10) labeling; red bars), dead cells (PI staining; green bars) and G1 cells (PI staining; blue bars) of wt HeLa cells during taxol treatment. Bars represent the means ± s.e.m. of *n* independent experiments. (**B**) Expression kinetics of Bcl-xL, phospho-Bcl-xL(Ser62) and phospho-H3(Ser10), in wt HeLa cells exposed to taxol. (**C**) Co-location of phospho-Bcl-xL(Ser62) with CENPA, HEC1, dynein motor protein, γ-tubulin, PLK1, BubR1 and Mad2 in wt HeLa cells exposed to taxol (0.1 μM; 24 h). Representative of a total of 1,128 cells (3 experiments). Summary in Table 1B.

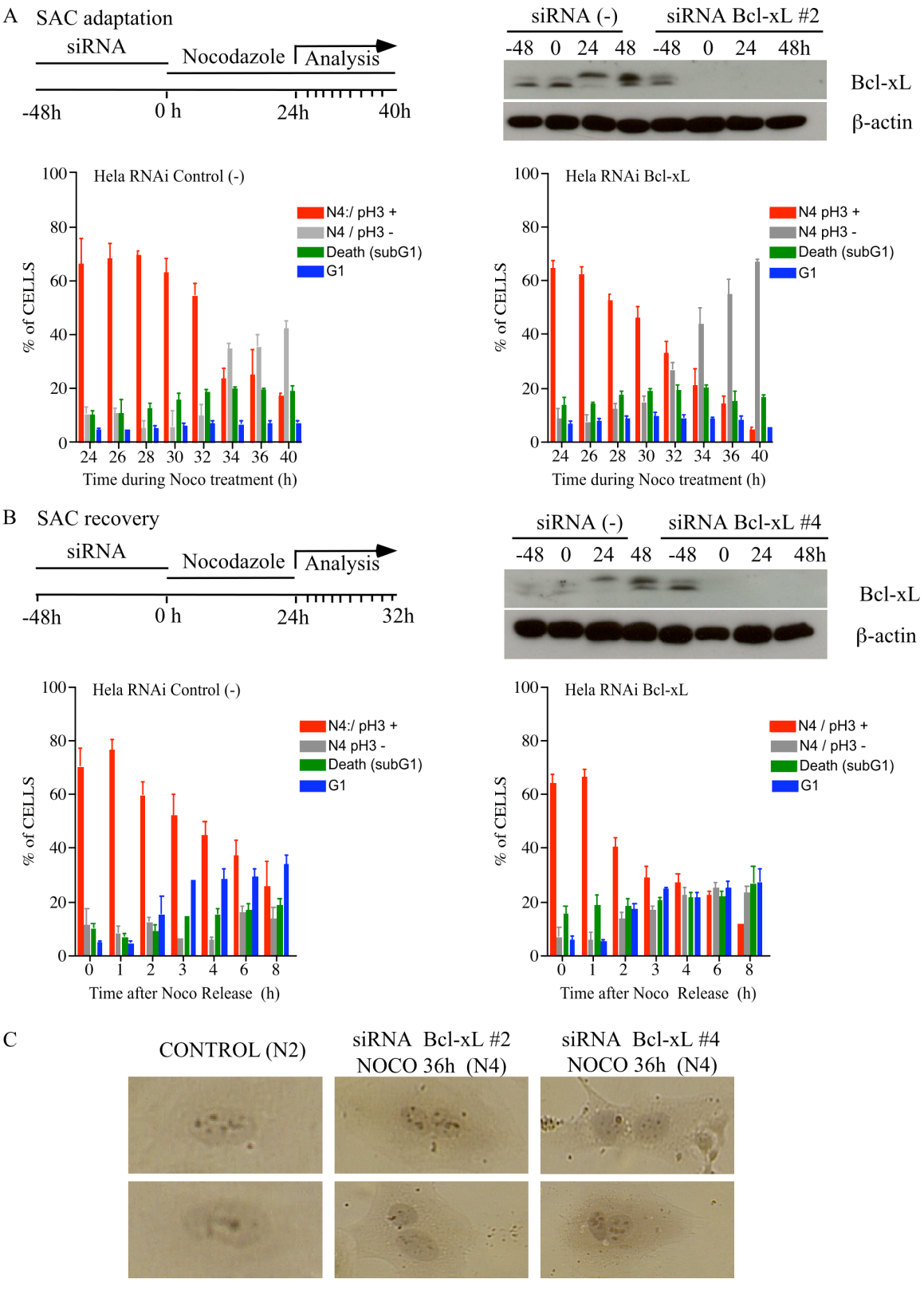
A
SAC adaptation
siRNA
Nocodazole
Analysis
-48h
0 h
24h
40h
siRNA (-)
siRNA Bcl-xL #2
-48 0 24 48 -48 0 24 48h
Bcl-xL
β-actin
Hela RNAi Control (-)
N4:/ pH3 +
N4 / pH3 -
Death (subG1)
G1
% of CELLS
Time during Noco treatment (h)
Hela RNAi Bcl-xL
N4 pH3 +
N4 pH3 -
B
SAC recovery
32h
siRNA Bcl-xL #4
Time after Noco Release (h)
C
CONTROL (N2)
siRNA Bcl-xL #2
NOCO 36h (N4)
siRNA Bcl-xL #4
NOCO 36h (N4)

Figure 4

Figure 4 Effect of silencing Bcl-xL expression on the stability and resolution of the SAC. wt HeLa cells were transfected with control siRNAs or siRNAs targeting Bcl-xL 48 h prior to (**A**) continuous nocodazole treatment (SAC resolution/adaptation experiments), and (**B**) 24-h nocodazole treatment, followed by drug release (SAC resolution/recovery experiments). Schematic views of these experiments appear in the upper left panels, and Bcl-xL expression kinetics are reported in the upper right panels (**A** and **B**). β-actin expression is shown as control. The lower panels (**A** and **B)** present the kinetics of G2/M cells (PI staining; grey bars), early mitotic cells (phospho-H3(Ser10) labeling; red bars), dead cells (PI staining; green bars) and G1 cells (PI staining; blue bars) of HeLa cells transfected with control siRNAs or siRNAs targeting Bcl-xL, at the indicated times after nododazole treatment (0.35 μM). Bars represent the means ± s.e.m. of 4 independent experiments. (**C**) Light microscopy of HeLa cells 36 h post-nocodazole treatment.

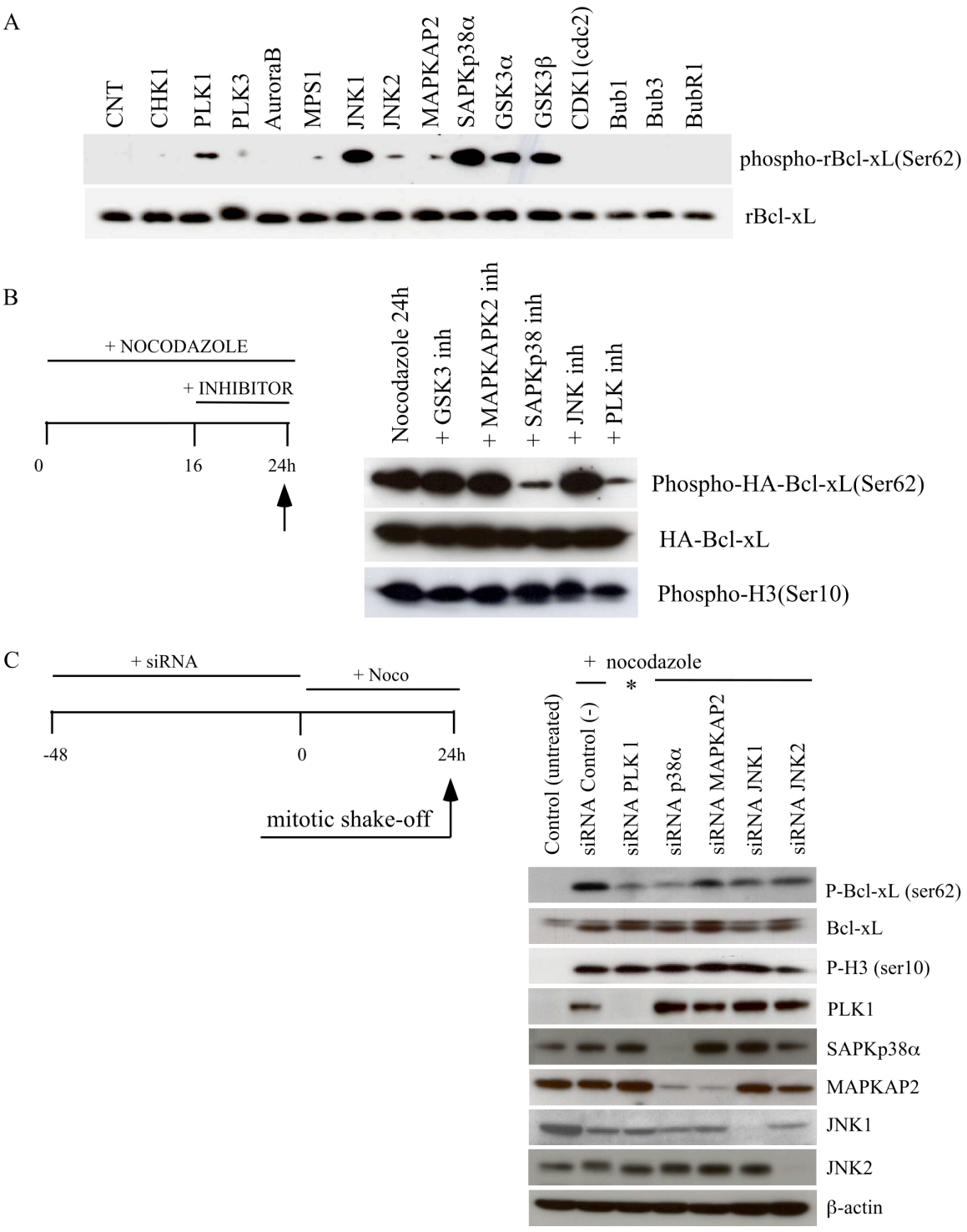
A
CNT
CHK1
PLK1
PLK3
AuroraB
MPS1
JNK1
JNK2
MAPKAP2
SAPKp38α
GSK3α
GSK3β
CDK1(cdc2)
Bub1
Bub3
BubR1
phospho-rBcl-xL(Ser62)
rBcl-xL
B
+ NOCODAZOLE
+ INHIBITOR
0
16
24h
Nocodazole 24h
+ GSK3 inh
+ MAPKAPK2 inh
+ SAPKp38 inh
+ JNK inh
+ PLK inh
Phospho-HA-Bcl-xL(Ser62)
HA-Bcl-xL
Phospho-H3(Ser10)
C
+ siRNA
+ Noco
-48
0
24h
mitotic shake-off
+ nocodazole
*
Control (untreated)
siRNA Control (-)
siRNA PLK 1
siRNA p38α
siRNA MAPKAP2
siRNA JNK1
siRNA JNK2
P-Bcl-xL (ser62)
Bcl-xL
P-H3 (ser10)
PLK1
SAPKp38α
MAPKAP2
JNK1
JNK2
β-actin

Figure 5

Figure 5 PLK1 and MAPK14/SAPKp38α are major protein kinases involved in Bcl-xL(Ser62) phosphorylation at mitosis. (**A**) *In vitro* assays of a panel of purified and active protein kinases with recombinant human Bcl-xL(ΔTM) protein as substrate. All enzyme activities were tested on control substrates (Supplemental Figure S3). Western blots are representative of 2 independent experiments. (**B**) Effects of specific protein kinase inhibitors on Bcl-xL phosphorylation on Ser62 in Namalwa cells exposed to taxol. The cells were first exposed to nocodazole (0.35 μM) and, 16 h post-treatment, kinase inhibitors were added for an additional 8 h: GSK3 inhibitor (SB216763, 10 μM); MAPKAPK2 inhibitor (KKALNRQLGVAA, 10 μM); SAPK/p38 inhibitor (SB203580, 2.0 μM), JNK inhibitor (SP600125, 5.0 μM); PLK inhibitor (BI2536, 0.1 μM). Western blots representative of 3 independent experiments with either taxol or nocodazole. (**C**) Effects of specific siRNAs targeting PLK1, MAPKAPK2, MAPK14/SAPKp38α, MAPK8/JNK1 and MAPK9/JNK2 expression on Bcl-xL(Ser62) phosphorylation in nocodazole-exposed HeLa cells. A schematic view of these experiments is presented. Representative Western blotting of 3 independent experiments. *Nocodazole treatment was avoided in these cells.

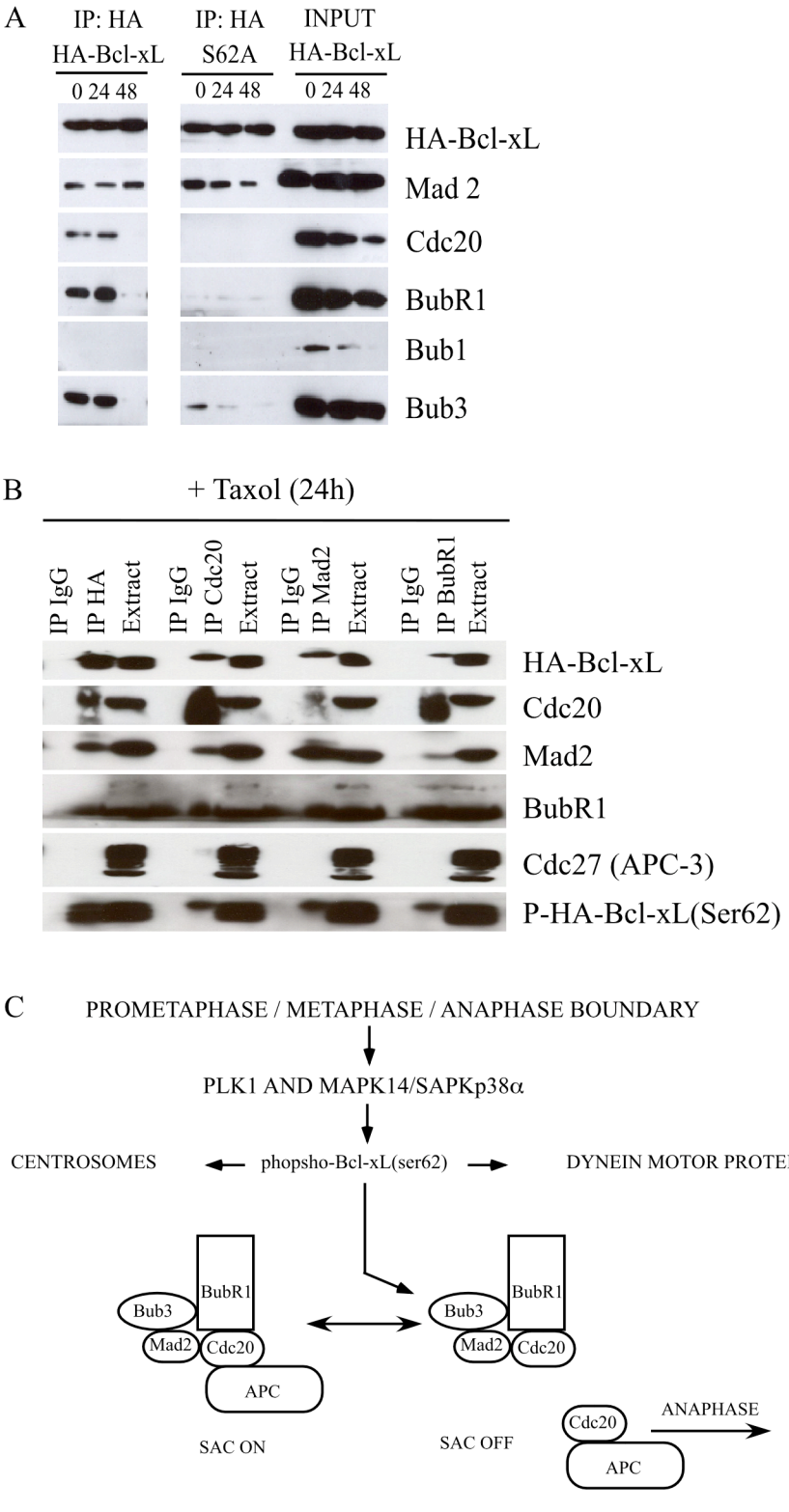
A
IP: HA
HA-Bcl-xL
0 24 48
IP: HA
S62A
0 24 48
INPUT
HA-Bcl-xL
0 24 48
HA-Bcl-xL
Mad 2
Cdc20
BubR1
Bub1
Bub3
B
+ Taxol (24h)
IP IgG
IP HA
Extract
IP IgG
IP Cdc20
Extract
IP IgG
IP Mad2
Extract
IP IgG
IP BubR1
Extract
HA-Bcl-xL
Cdc20
Mad2
BubR1
Cdc27 (APC-3)
P-HA-Bcl-xL(Ser62)
C
PROMETAPHASE / METAPHASE / ANAPHASE BOUNDARY
PLK1 AND MAPK14/SAPKp38α
CENTROSOMES
phopsho-Bcl-xL(ser62)
DYNEIN MOTOR PROTEIN
Bub3
BubR1
Mad2
Cdc20
APC
SAC ON
Bub3
BubR1
Mad2
Cdc20
SAC OFF
Cdc20
APC
ANAPHASE

Figure 6

Figure 6 Phospho-Bcl-xL(Ser62) interacts with SAC components. (**A**) Co-immunoprecipitation of HA-Bcl-xL and HA-Bcl-xL(Ser62Ala) mutant protein with Mad2, Cdc20, BubR1, and Bub3 but not Bub1 in taxol-exposed (0.1 μM) Namalwa cells expressing either HA-Bcl-xL or HA-Bcl-xL(Ser62Ala) mutant protein. (**B**) Reciprocal co-immunoprecipitation of HA-Bcl-xL and phospho-Bcl-xL(Ser62) with Mad2, Cdc20, and BubR1, but not Cdc27 (APC-3) in taxol-exposed Namalwa cells (0.1 μM, 24 h). IgG represents co-immunoprecipitation experiments with control immunoglobulins. Extract means a mitotic protein extract obtained from Namalwa cells expressing HA-Bcl-xL after taxol treatment (0.1 μM, 24 h). Representative of 4 independent experiments. (**C**) Schematic view of a proposed model.

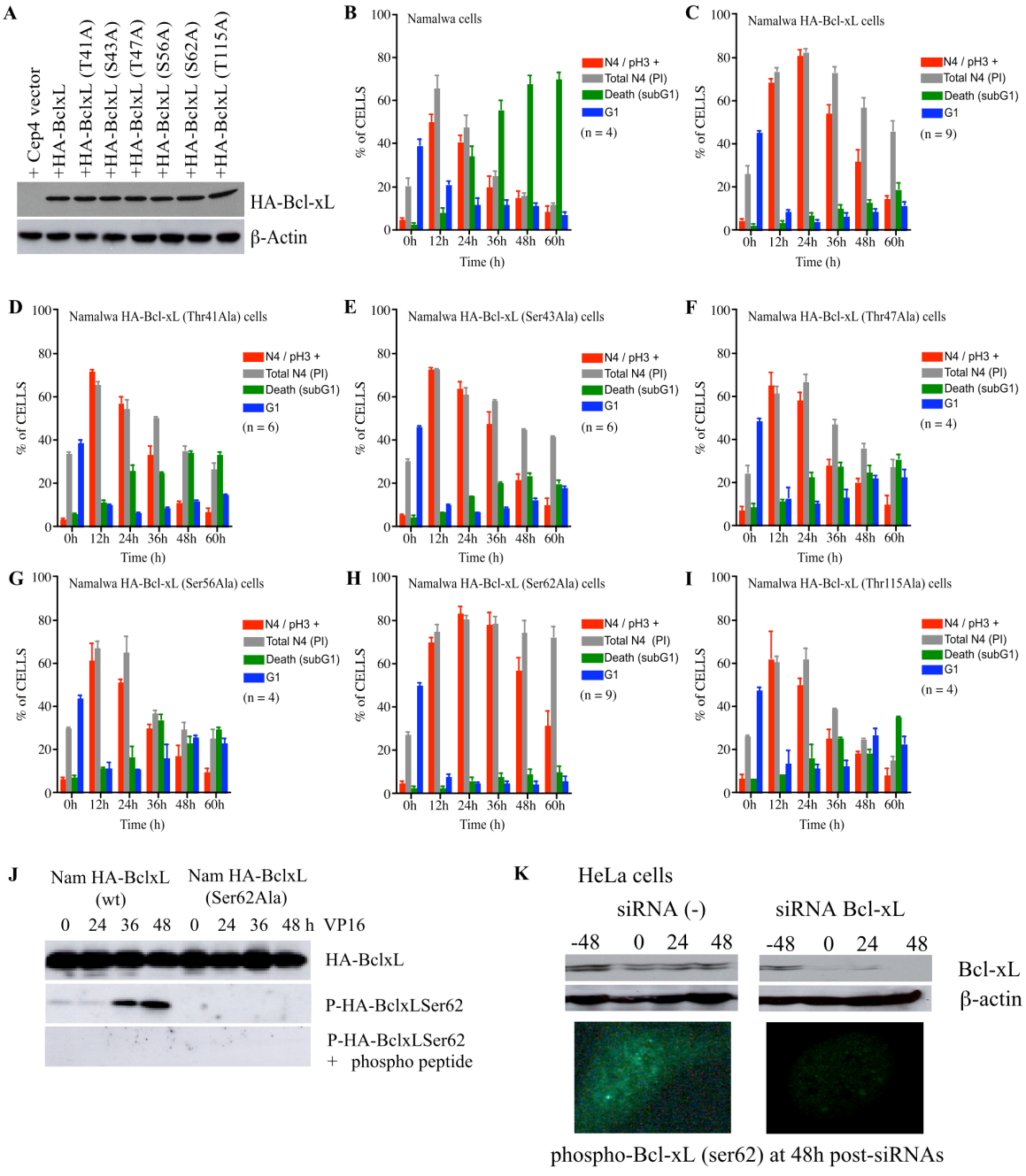

Supplemental Figure S1

Supplemental Figure S1 Effect of Bcl-xL and various phosphorylation mutants on the stability of the SAC. (**A**) Expression level of HA-Bcl-xL, HA-Bcl-xL(Th41Ala), Bcl-xL(Ser43Ala), HA-Bcl-xL(Th47Ala), Bcl-xL(Ser56Ala), Bcl-xL(Ser62Ala) and HA-Bcl-xL(Th115Ala) phosphorylation mutants in stably-transfected Namalwa cell populations. β-actin expression is shown as control. (**B-I**) Kinetics of G2/M cells (PI staining; grey bars), early mitotic cells (phospho-H3(Ser10) staining; red bars), dead cells (PI staining; green bars) and G1 cells (PI staining; blue bars) in wt Namalwa cells and Namalwa cells expressing HA-Bcl-xL, HA-Bcl-xL(Th41Ala), Bcl-xL(Ser43Ala), HA-Bcl-xL(Th47Ala), Bcl-xL(Ser56Ala), Bcl-xL(Ser62Ala) and HA-Bcl-xL(Th115Ala) phosphorylation mutants during taxol treatment (0.1 μM). Bars represent the means ± s.e.m. of *n* independent experiments. (**J-K**) Specificity of phospho-Bcl-xL(ser62) antibodies**.** (**J**) Phospho-HA-Bcl-xL(Ser62) in Namalwa cells expressing HA-Bcl-xL and HA-Bcl-xL(Ser62Ala) mutant exposed to VP16 (10 μM for 30 min). HA-Bcl-xL expression is shown as control. **(K)** Staining of phospho-Bcl-xL(Ser62) in wt HeLa cells exposed to control siRNA or siRNA targeting Bcl-xL expression. Western blottings are shown as control.

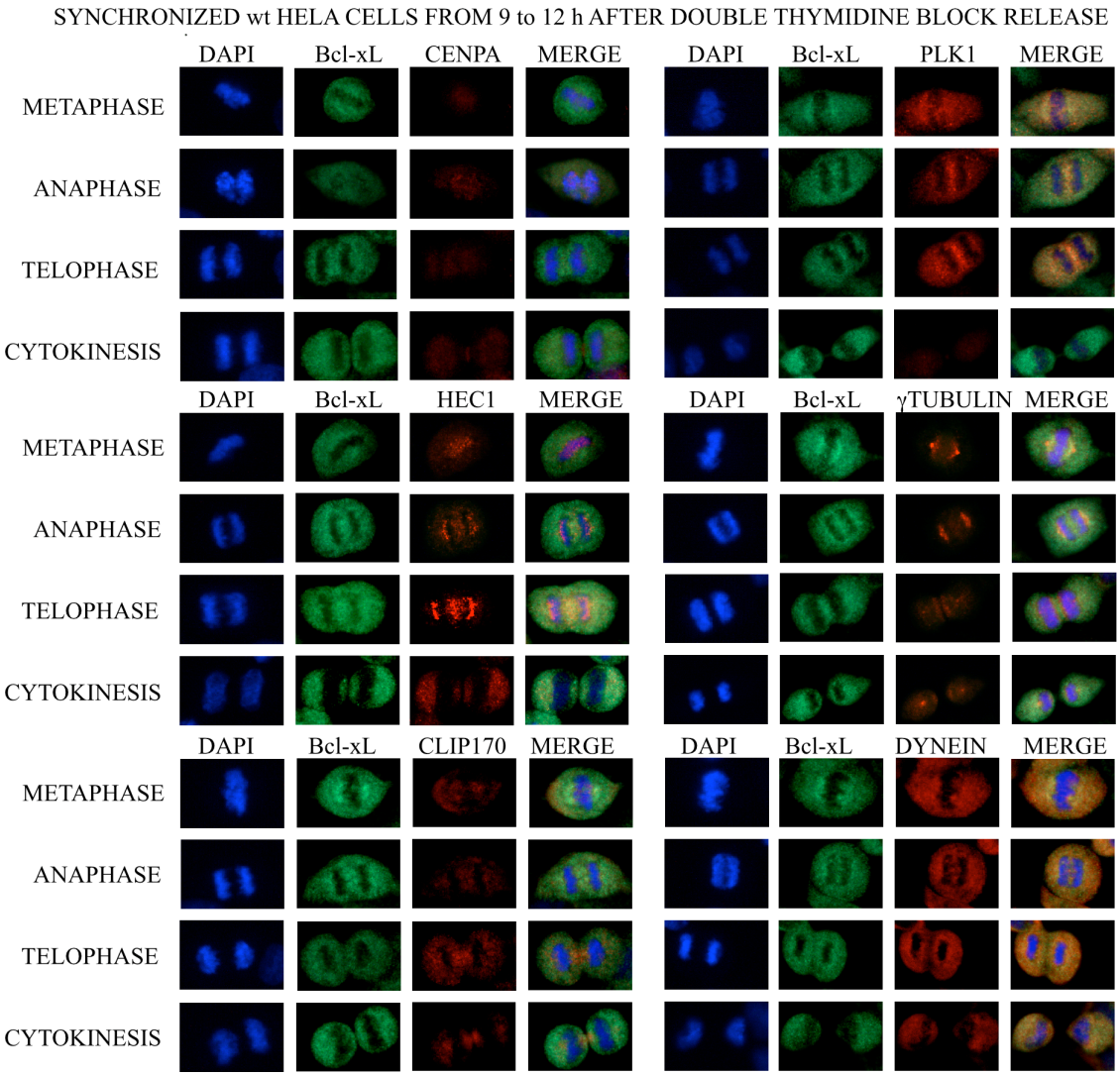

Supplemental Figure S2

Supplemental Figure S2 Bcl-xL location in synchronized wt HeLa cells at mitosis. Co-location of Bcl-xL with CENPA, HEC1, CLIP170, PLK1, γ-tubulin and dynein motor protein at different steps of mitosis. Micrographs with phospho-Bcl-xL(Ser62) Ab labeling are shown in Figure 2. Representative of a total of 1,164 mitotic cells (3 experiments). Summary in Table 1A.

A) Recombinant Enzyme

	Specific activity	
	Assay #1	Assay #2
CHK1	7.7 nmole/min/mg	7.9 nmole/min/mg
CHK2	176 nmole/min/mg	268 nmole/min/mg
p38α /MAPK14	76 nmole/min/mg	129 nmole/min/mg
JNK1/MAPK8	39 nmole/min/mg	48 nmole/min/mg
JNK2/MAPK9	138 nmole/min/mg	263 nmole/min/mg
MAPKAPK2	541 nmole/min/mg	778 nmole/min/mg
PLK1	8.4 nmole/min/mg	14.3 nmole/min/mg
PLK3	13.9 nmole/min/mg	17.5 nmole/min/mg
Aurora A	14.5 nmole/min/mg	18 nmole/min/mg
Aurora B	508 nmole/min/mg	420 nmole/min/mg
NEK2	398 nmole/min/mg	530 nmole/min/mg
GSK3β	5.0 nmole/min/mg	8.6 nmole/min/mg

B) Immunoprecipitated enzyme

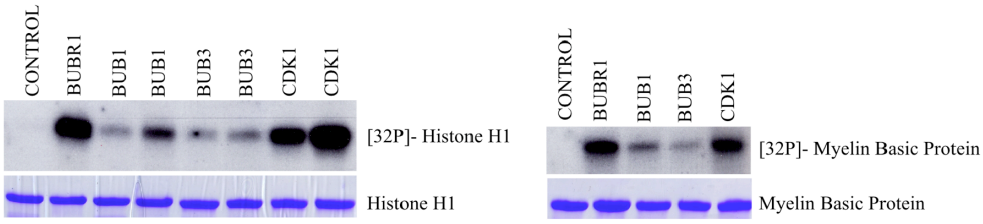

C) In vitro kinase assay with [^{32}P] γATP and recombinant Bcl-xL as substrate

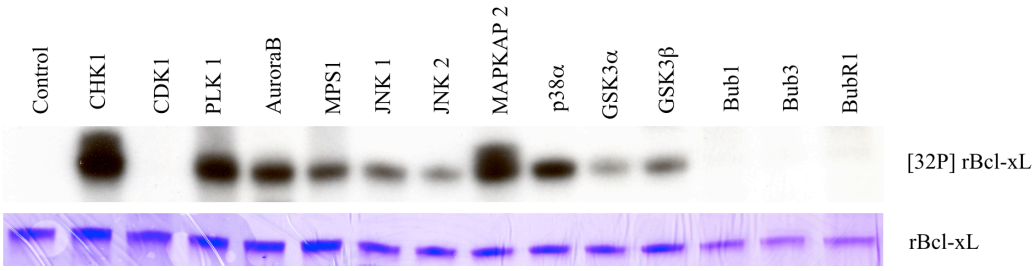

Supplemental Figure S3

Supplemental Figure S3 *In vitro* kinase assays. **(A)** Enzyme activities were tested on control substrates with recombinant purified kinases. Velocities are expressed as nmole/min/mg. 2 independent experiments are reported. **(B)** BubR1, Bub1, Bub3 and Cdk1(cdc2) enzyme activities tested on histone H1 and myelin basic protein control substrates with kinases purified by immunoprecipitation. 2 independent immunoprecipitation assays are reported. **(C)** In vitro kinase assays with [^{32}P]-γATP and recombinant Bcl-xL as substrates. Autoradiography and Coomassie staining are shown.

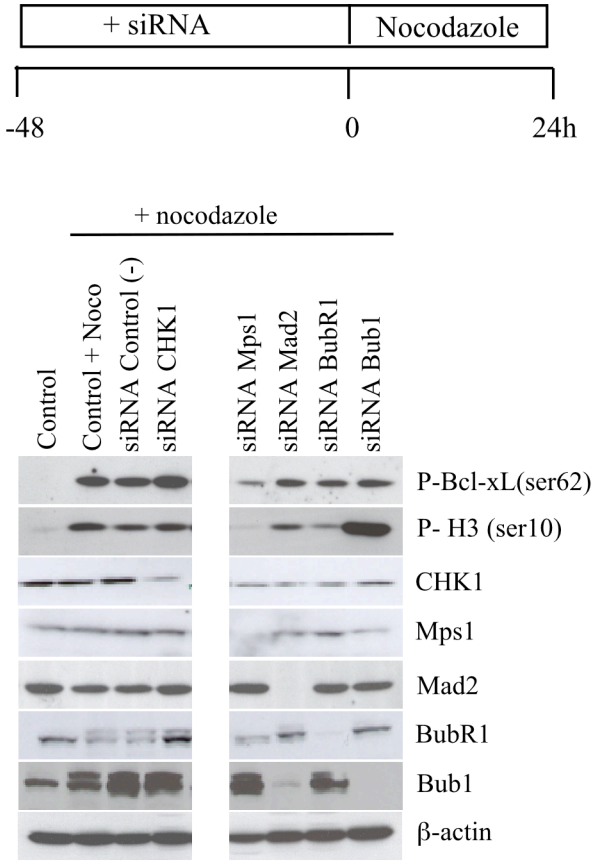

Supplemental Figure S4

Supplemental Figure S4 Effects of specific siRNAs targeting CHK1, MPS1, Mad2, BubR1 and Bub1 expression on Bcl-xL(Ser62) phosphorylation in nocodazole-exposed HeLa cells. Silencing efficiency was monitored by Western blottings with corresponding antibodies. Representative Western blottings of 2 to 3 independent experiments.

Note: HeLa cells treated with siRNA targeting MPS1 fail to enter into mitosis (phospho-H3(ser10) negative).

Supplemental TABLE S1-A

Recombinant Enzyme	Source	Control Substrate	Source	Buffer
CHK1	Sigma-Aldrich	RXRX(L/A)S((R/F)	Cell Signaling	A
MAPK14/SAPK p38α	Cell Signaling	ATF-2 (19-96)	Cell Signaling	B
MAPK8/ JNK1	Cell Signaling	c-Jun (1-89)	Cell Signaling	B+
MAPK9/ JNK2	Cell Sciences	c-Jun (1-89)	Cell Signaling	A
MAPKAPK2	Cell Signaling	KKKLNRTLSVA	AnaSpec	A+
PLK1	Cell Signaling	RISDELMDATFADQEAK	AnaSpec	A
PLK3	Cell Signaling	RISDELMDATFADQEAK	AnaSpec	A
Aurora A	Cell Signaling	RRSLLE	Cell Signaling	A
Aurora B	Cell Signaling	LRRLSLGLRRLSLGLRRL SLGLRRLSLG	AnaSpec	A
NEK2	Cell Signaling	RFRRSRRMI	AnaSpec	A
GSK3α	Cell Signaling	RRAAEELDSRAGSPQL	AnaSpec	A
GSK3β	Sigma-Aldrich	GPHRSTPESRAAV	AnaSpec	A+
Mps1	Cell Signaling	Myelin basic protein	Sigma-Aldrich	B
Immunprecipitated Enzyme				
CDC2/CDK1	Namalwa cells	Histone H1/ MBP	Sigma-Aldrich	B+
Bub1	Namalwa cells	Histone H1/MBP	Sigma-Aldrich	B+
BubR1	Namalwa cells	Histone H1/MBP	Sigma-Aldrich	B+
Bub3	Namalwa cells	Histone H1/ MBP	Sigma-Aldrich	B+

Buffer A (5x):	25 mM MOPS pH 7.2 25 mM $MgCl_2$ 12.5 mM β-glycerol-2-phosphate 0.5 mM Na_3VO_4 5 mm EGTA 2 mM EDTA 0.25 mM dithiothreitol 500 μM ATP* * 0.05 μCi/μl [^{32}P]-γATP
Buffer A+ (5x):	buffer A + 50 μg/ ml BSA

Buffer B (5x):	125 mM TRIS pH 7.2 50 mM $MgCl_2$ 25 mM β-glycerol-2-phosphate 0.5 mM Na_3VO_4 10 mM dithiothreitol 500 μM ATP* * 0.05 μCi/μl [^{32}P]-γATP
Buffer B+ (5x):	buffer B + 50 μg/ ml BSA

Target	INHIBITOR	Source	Concentration
SAPKp38α	SB 203580	Calbiochem	2 μM
JNK	SP 600125	Sigma-Aldrich	5 μM
MAPKAPK2	H-KKALNRQLGVAA-OH	Calbiochem	10 μM
PLK	BI 2536	Axon MedChem	0.1 μM
Aurora	ZM 447439	Tocris BioScience	0.1 μM
GSK3	SB 216763	Sigma-Aldrich	10 μM

Supplemental Table S1-A. Listing of the protein kinase assays and protein kinase inhibitors. Source, control substrates and reaction buffers are indicated.

Supplemental TABLE S1-B

Target		siRNA Target sequence	REFERENCE
Bcl-xL	(2)	5'-GAAAUGACCAGACACUGAC-3'	On-Target plus sequence/ Dharmacom
	(4)	5'-UUAGUGAUGUGGAAGAGAA-3'	On-Target plus sequence/ Dharmacom
PLK 1	(1)	5' -AGAUUGUGCCUAAGUCUCU-3'	Mol Biol Cell 15:5623, 2004
CHK1	(1)	5'-UCGUGAGCGUUUGUUGAAC-3'	J Biol Chem 278:14806, 2004
Aurora A	(1)	5'-GGCAACCAGTGTACCTCAT-3'	Nature 455:119, 2008
Aurora B	(1)	5'-AACGCGGCACUUCACAAUUGA-3'	Nat Cell Biol 7:93, 2004
	(2)	5'-GGAAAGAAGGGAUCCCUAA-3'	Mol Biol Cell 17:2547, 2006
Bub1	(1)	5'-GAGUGAUCACGAUUUCUAA-3'	J Cell Biol 185:5841, 2004
	(2)	5'-GCCUGCCAACCCCUGGGAA-3'	J Cell Biol 178;283, 2007
BubR1	(1)	5'-AACGGGCAUUUGAAUAUGAA-3'	Nat Cell Biol 7:93, 2004
Mad2	(1)	5'-GGAAGAGUCGGGACCACAG-3'	Nat Cell Biol 7:93, 2004
	(2)	5'-AAGUGGUGAGGUCCUGGAAAG-3'	Mol Cancer Res 7:371, 2009
Mps1	(1)	5'-GACAGAUGAUUCAGUUGUA-3'	Cell 132:233, 2008
MAPK8/ JNK1	(1)	5'-GCCCAGUAAUAUAGUAGUA-3'	Cell Cycle 7: 533, 2008
	(2)	5'-GGCAUGGGCUACAAGGAAA-3'	Cell Cycle 7: 533, 2008
MAPK9/ JNK2	(1)	5'-AGCCAACUGUGAGGAAUUA-3'	Cell Cycle 7: 533, 2008
	(2)	5'-UCGUGAACUUGUCCUCUUA-3'	Cell Cycle 7: 533, 2008
MAPK14 / p38α	(1)	5'-GGAAUUCAAUGAUGUGUAU-3'	On-Target plus sequence/ Dharmacom
	(2)	5'-UCUCCGAGGUCUAAAGUAU-3'	On-Target plus sequence/ Dharmacom
	(3)	5'-GUAAUCUAGCUGUGAAUGA-3'	On-Target plus sequence/ Dharmacom
	(4)	5'-GUCCAUCAUUCAUGCGAAA-3'	On-Target plus sequence/ Dharmacom
MAPKAPK2	(1)	5'-CGAAUGGGCCAGUAUGAAU-3'	On-Target plus sequence/ Dharmacom
	(2)	5'-GUUAUACACCGUACUAUGU-3'	On-Target plus sequence/ Dharmacom
	(3)	5'-GGCAUCAACGGCAAAGUUU-3'	On-Target plus sequence/ Dharmacom
	(4)	5'-CCACCAGCCACAACUCUUU-3'	On-Target plus sequence/ Dharmacom
GSK3α	(1)	5'-CAUCAAAGUGAUUGGCAAU-3'	SMART POOL/ Dharmacom
	(2)	5'-AGUUGACCAUCCCUAUCCU-3'	SMART POOL / Dharmacom
	(3)	5'-CUGAUUACACCUCAUCCAU-3'	SMART POOL / Dharmacom
	(4)	5'-UUCUCAUCCCUCCUCACUU-3'	SMART POOL/ Dharmacom
GSK3β	(1)	5'-GAUCAUUUGGUGUGGUAUA-3'	SMART POOL / Dharmacom
	(2)	5'-GCUAGAUCACUGUAACAUA'-3	SMART POOL / Dharmacom
	(3)	5'-GUUCCGAAGUUUAGCCUAU-3'	SMART POOL / Dharmacom
	(4)	5'-GCACCAGAGUUGAUCUUUG-3'	SMART POOL / Dharmacom
NON-TARGETING			SMART POOL / Dharmacom

Supplemental Table S1-B. Listing of the siRNA targeted sequences deployed in this study.

Supplemental TABLE S1-C Oligonucleotides for cDNA constructs

HA-Bcl-xL (T41A)

5'-end oligonucleotide (+) with *Nhe1* + START ATG codon:	5'- gctagcccacc**atg**ggccgcatctttta
3'-end oligonucleotide (-) with STOP TGA codon:	5'- ctcgag**tca**tttccgactgaagagtga
oligonucleotide (+) containing T41A substitution:	5'- gccccagaaggg**gc**tgaatcggagatg
oligonucleotide (-) containing T41A substitution:	5- catctccgattc**agc**cccttctggggc

(from *wt* HA-Bcl-xL as template / subcloned *Nhe1/ Xho1* in Cep4 vector)

HA-Bcl-xL (S43A)

5'-end oligonucleotide (+) with *Nhe1* + START ATG codon:	5'- gctagcccacc**atg**ggccgcatctttta
3'-end oligonucleotide (-) with STOP TGA codon and *XhoI:*	5'- ctcgag**tca**tttcgactgaagagtga
Overlapping oligonucleotide (+) containing S43A substitution:	5'-gaagggactgaa**gcg**gagatgagacc
Overlapping oligonucleotide (-) containing S43A substitution:	5'-ggtctccatctc**cgc**ttcagtcccttc

(from *wt* HA-Bcl-xL as template / subcloned *Nhe1/ Xho1* in Cep4 vector)

HA-Bcl-xL (T47A)

5'-end oligonucleotide (+) with *Not1* + START ATG codon:	5'- gcggccgc**atg**tctcagagcaaccgggag
3'-end oligonucleotide (-) with STOP TGA codon and *XhoI:*	5'- ctcgag**tca**tttccgactgaagagtga
Overlapping oligonucleotide (+) containing T47A substitution:	5'-tcggagatggag**gcc**cccagtgccatc
Overlapping oligonucleotide (-) containing T47A substitution:	5'-gatggcactggg**ggc**ctccatctccga

(from *wt* Bcl-xL as templat / subcloned *Not1/ XhoI* in Cep4-HA vector)

HA-Bcl-xL (S56A)

5'-end oligonucleotide (+) with *Not1* + START ATG codon:	5'- gcggccgc**atg**tctcagagcaaccgg gag
3'-end oligonucleotide (-) with STOP TGA codon and *XhoI:*	5'- ctcgag**tca**tttccgactgaagagtga
Overlapping oligonucleotide (+) containing S56A substitution:	5'- aatggcaaccca**gcc**tggcacctggca
Overlapping oligonucleotide (-) containing S56A substitution:	5'- tgccaggtgcca**ggc**tgggttgccatt

(from *wt* Bcl-xL as template / subcloned *Not1/ XhoI* in Cep4-HA vector)

HA-Bcl-xL (S62A)

5'-end oligonulcleotide (+) with *Not1* + START ATG codon:	5'- gcggccgc**atg**tctcagagcaaccgggag
3'-end oligonucleotide (-) with STOP TGA codon and *XhoI:*	5'- ctcgag**tca**tttccgactgaagagtga
Overlapping oligonucleotide (+) containing S62A substitution:	5'- cacctggcagac**gcc**cccgcggtgaat
Overlapping oligonucleotide (-) containing S62A substitution:	5- attcaccgcggg**ggc**gtctgccaggtg

(from *wt* Bcl-xL as template / subcloned *Not1/ XhoI* in Cep4-HA vector)

HA-Bcl-xL (T115A)

5'-end oligonulcleotide (+) with *Not1* + START ATG codon:	5'- gcggccgc**atg**tctcagagcaaccgggag
3'-end oligonucleotide (-) with STOP TGA codon and *XhoI:*	5'- ctcgag**tca**tttccgactgaagagtga
Overlapping oligonucleotide (+) containing T115A substitution:	5- cagctccacatc**gcc**ccagggacagca
Overlapping oligonucleotide (-) containing T115A substitution:	5- tgctgtccctgg**ggc**gatgtggagctg

(from *wt* Bcl-xL as template / subcloned *Not1/ XhoI* in Cep4-HA vector)

Supplemental TABLE S1-C cDNA constructs. The phosphorylation mutant pCEP4-HA-Bcl-xL and pCDNA3.1-HA-Bcl-xL vectors were generated by triple polymerase chain reactions (PCR) with wt pCEP4-HA-Bcl-xL vector as DNA template. The first fragments were amplified by *Vent* polymerase, with specific adapter primers containing restriction site sequences at the ATG start codon and anti-sense junction primers corresponding to the flanking sequences at each mutation site, as listed in Table S1. The second fragments were amplified by *Vent* polymerase, with sense junction primers corresponding to flanking sequences at each mutation site and adapter anti-sense primers containing restriction site sequences at the TGA stop codon. The 2 amplified fragments were gel-purified, heat-denaturated, and slowly annealed on ice. After elongation by *Taq* polymerase for 10 min, the third PCR, with specific adapter primers containing sequences at the ATG start codon and TGA stop codon, was amplified. The amplified fragment was first cloned in pCR2.1Topo vector (Invitrogen Corporation), sequenced, and then sub-cloned in the eukaryotic expression vectors pCEP4 and pCDNA3.1 (Invitrogen Corporation). For some constructs, the HA-tag sequences were not amplified by PCR; these amplified fragments were than sub-cloned in-frame into the pCEP4-HA vector. All primers are listed in Supplemental Table 1. Purified constructs were transfected in Namalwa cells by electroporation at 0.27 kV (Gene Pulser, BioRad, Hercules, CA) and in HeLa cells by Lipofectamine2000 transfection according to the manufacturer's protocol (Invitrogen Corporation).

Supplemental TABLE S1-D

ANTIBODIES	ID	Species	Source
Cyclin B1	clone GNS-1	mouse mAb	BD Biosciences
Cdc2/CDK1	# PC25	rabbit pAb	Calbiochem
Cdc2/CDK1	clone 1/cdk1	mouse mAb	BD Biosciences
Plk1	clone 208G4	rabbit mAb	Cell Signaling
Plk3	clone B37-2	mouse mAb	BD Biosciences
Aurora A	clone 1G4	rabbit mAb	Cell Signaling
Aurora B	# 3094	rabbit mAb	Cell Signaling
MAPKAPK2	# 3042	rabbit pAB	Cell Signaling
MAPK14/SAPK p38α	clone L53F8	mouse mAb	Cell Signaling
MAPK8/ JNK1	clone G151-333	mouse mAb	BD Biosciences
MAPK9/ JNK2	# 4672	rabbit pAb	Cell Signaling
GSK3α	# 9338	rabbit pAb	Cell Signaling
GSK3β	clone 27C10	rabbit mAb	Cell Signaling
MPS1/TKK	# 3255	rabbit pAb	Cell Signaling
MPS1/TKK	clone BC032858	mouse mAb	Abcam
Bub1	clone 14H5	mouse mAb	Upstate/ Millipore
BubR1	# A300-386A	rabbit pAb	Bethyl
BubR1	# 4116	rabbit pAb	Cell Signaling
BubR1	clone9/BubR1	mouse mAb	BD Transduction
Bub3	clone31/Bub3	mouse mAb	BD Transduction
Bub3	# 3049	rabbit pAb	Cell Signaling
Mad2	# A300-300A	rabbit pAb	Bethyl Lab
Mad2	clone 48/Mad2	mouse mAb	BD Transduction
cdc20	clone 41/p55cdc	mouse mAb	BD Transduction
cdc20	# A301-179A	rabbit pAb	Bethyl Lab
cdc20	# A301-180A	rabbit pAb	Bethyl Lab
CENP-A	# 07-574	rabbit pAb	Upstate/Millipore
CENP-A	clone 3-19	mouse mAb	Assay Designs
Dynein	clone 74.1	mouse mAb	Millipore
HEC1	clone 9G3	mouse mAb	Abcam
EB1	clone 5/ EB1	mouse mAb	BD Transduction
Clip-170	custom	from Niels Galjart,	Rotterdam
Bcl-xL	clone 2H12	mouse mAb	BD Biosciences
Phospho-BclxL Ser62	custom	rabbit pAb	GenScript
HA tag	clone 12CA5	mouse mAb	Roche Applied Sci
HA tag	# A00168	goat pAb	GenScript
γ-tubulin	clone GTU88	mouse mAb	Abcam
α-tubulin	clone DM1A	mouse mAb	Sigma-Aldrich
β-tubulin	clone DM1B	mouse mAb	Calbiochem
β-Actin	clone 4C40	mouse mAb	Sigma
Phospho H3(ser10)	# 06-570	rabbit pAb	Upstate/Millipore
Phospho H3 ser10 Alexa 488	# 9708	rabbit pAb	Cell Signaling
Anti-Mouse IgG Alexa 488	# A11001	goat pAb	InVitroGen
Anti-Rabbit IgG Alexa 488	# A11008	goat pAb	InVitroGen
Anti-Mouse IgG Alexa 594	# A11005	goat pAb	InVitroGen
Anti-Rabbit IgG Alexa 594	#A11012	goat pAb	InVitroGen
Anti-Mouse IgG HP-linked	# NA931V	sheep pAb	GE Healthcare
Anti-Rabbit IgG HP-linked	# NA934V	donkey pAb	GE Healthcare
Normal Rabbit IgG	# sc-2027	rabbit IgG	Santa Cruz Biotech
Normal Mouse IgG	# sc-2025	mouse IgG	Santa Cruz Biotech

5. Bcl-xL phosphorylation at Ser49 by polo kinase 3 during cell cycle progression and checkpoints

Authors: Jianfang Wang[1], Myriam Beauchemin[1] and Richard Bertrand[1,2*]

Affiliations: [1]Centre de recherche, Centre hospitalier de l'Université de Montréal (CRCHUM) – Hôpital Notre-Dame and Institut du cancer de Montréal, and [2]Département de médecine, Université de Montréal, Montréal (Québec) Canada

Running title: Bcl-xL phosphorylation and cell cycle

Key words*:* Bcl-xL, PLK3, cell cycle, G2 arrest, cytokinesis, mitotic exit

****Corresponding author****:* CRCHUM – Hôpital Notre-Dame and Institut du cancer de Montréal, 1560 Sherbrooke St. East (Room Y-5634), Montréal (Québec) Canada H2L 4M1.

Abstract

Functional analysis of a Bcl-xL phosphorylation mutant series has revealed that cells expressing Bcl-xL(Ser49Ala) mutant are less stable at G2 checkpoint after DNA damage and enter cytokinesis more slowly after microtubule poisoning than cells expressing wild-type Bcl-xL. These effects of Bcl-xL(Ser49Ala) mutant seem to be separable from Bcl-xL function in apoptosis. Bcl-xL(Ser49) phosphorylation is cell cycle-dependent. In synchronized cells, phospho-Bcl-xL(Ser49) appears during the S phase and G2, whereas it disappears rapidly in early mitosis during prometaphase, metaphase and early anaphase, and re-appears during telophase and cytokinesis. During DNA damage-induced G2 arrest, an important pool of phospho-Bcl-xL(Ser49) accumulates in centrosomes which act as essential decision centers for progression from G2 to mitosis. During telophase/cytokinesis, phospho-Bcl-xL(Ser49) is found with dynein motor protein. In a series of *in vitro* kinase assays, specific small interfering RNA and pharmacological inhibition experiments, polo kinase 3 (PLK3) was implicated in Bcl-xL(Ser49) phosphorylation. These data indicate that, during G2 checkpoint, phospho-Bcl-xL(Ser49) is another downstream target of PLK3, acting to stabilize G2 arrest. Bcl-xL phosphorylation at Ser49 also correlates with essential PLK3 activity and function, enabling cytokinesis and mitotic exit.

Introduction

Bcl-xL (Bcl-2-related gene x, long isoform), a Bcl-2 (B cell leukemia/lymphoma protein-2) family member, is well-characterized for its function in apoptosis [1]. Regulation of outer mitochondrial membrane permeabilization is the major way in which Bcl-xL protein exerts its anti-apoptosis regulatory and survival effect, which means preserving mitochondrial membrane integrity, mitochondrial transmembrane potential as well as ATP production, and preventing the release of apoptogenic factors in cytosol (reviewed in [2-4]). Elucidation of Bcl-xL's 3-dimensional structure has provided a first structural model in which α-helices located in BH1 (a Bcl-2 homology domain), BH2 and BH3 domains create an elongated hydrophobic pocket domain where a BH3 amphipathic α-helix of another Bcl-2-like protein can bind [5-7]. Bcl-xL binds to pro-apoptotic family members through protein-protein interactions, forming a complex dynamic network of hetero-oligomers, depending on the cellular environment, stress condition and their subcellular localization [8-13]. Heterodimerization between pro- and anti-apoptotic molecules controls cell fate, indicating that the relative concentration of one faction versus the other greatly influences the susceptibility of cells to death signals (reviewed in [14, 15]). BH3-only proteins are potent mediators of cell death. A subset, referred to as BH3-only enabler or sensitizing proteins, promotes apoptosis by binding to and inhibiting pro-survival molecules, such as Bcl-2, Bcl-xL and Mcl-1, whereas BH3-only activator or activating proteins bind to and activate multidomain pro-apoptotic Bax and Bak proteins [10, 16]. Bax insertion and oligomerization into membranes require activation, i.e. structural reorganization by a BH3-only activating protein, events that lead to outer mitochondrial membrane permeabilization; in contrast, the ability of anti-apoptotic proteins, such as Bcl-xL, to trap and inhibit these BH3-only activating proteins, prevents membrane permeabilization [17-20].

The unexpected pore-forming ability of Bcl-xL protein has emerged from unfolding of its 3-dimensional structure. Structural similarities between Bcl-xL, particularly its α5- and α6-helices and the pore-forming domains of some bacterial toxins that act as channels for either ions or proteins, suggest that Bcl-2 members could function

by constituting pores in intracellular organelles, including mitochondria [5, 17-21]. Whether these channel activities function by themselves, or in association with other megachannels, such as components of mitochondrial permeability transition pores, or others, is still not completely elucidated [3, 4, 19, 22-31].

Several studies have revealed that, in addition to their key role in controlling apoptosis, some Bcl-2 family members interface with the cell cycle, DNA damage responses and repair pathways, functions that are distinct from their role in apoptosis (reviewed in [32, 33]). Indeed, Bcl-xL and/or Bcl-2 modulate the homologous recombination pathway as well as non-homologous end-joining and DNA damage mismatch repair activities, effects that are separable from their anti-apoptotic task [34-37]. Bcl-xL also fulfills functions during the cell cycle [38-40]. Bcl-xL phosphorylation at Ser62, within the unstructured loop domain of the protein, has been detected most often in cells treated with microtubule poisons, including nocodazole, paclitaxel, vinblastine, vincristine, colchicine and pironetin [41-49], and coupled, more recently, with specific G2 and mitotic events (Wang et al., 2011; manuscripts submitted). Similarly, Bcl-xL phosphorylation at Thr47 and Thr115 has been documented in response to genotoxic stress induced by ionizing radiation [50].

To search for potentially important phosphorylation site(s) regulating Bcl-xL's function during the cell cycle, we generated and monitored the effects of a series of single-point Bcl-xL phosphorylation mutants within its unstructured loop domain, a region generally not essential for its anti-apoptotic function [42, 51, 52]. Taking a variety of experimental approaches with stably-transfected human cell populations and non-transfected wild-type (wt) cells, we now provide evidence that Bcl-xL(Ser49) phosphorylation is a key element regulating Bcl-xL's functions at the G2 cell cycle checkpoint and entry into cytokinesis, influencing mitotic exit.

Results

Effect of HA-Bcl-xL and HA-Bcl-xL(Ser49Ala) phosphorylation mutant on G2 checkpoint stability and mitosis progression

First, human B lymphoma Namalwa cells were transfected with expression vectors encoding wt HA-Bcl-xL and HA-Bcl-xL(Ser49Ala) mutant, and stably-transfected cell populations were selected. The protein expression levels are illustrated in Fig 1A (top right panel). A well-established experimental procedure, referred to as mitotic trap assay [53], evaluated the kinetics of G2 arrest after DNA damage, the kinetics of mitotic entry after G2 arrest, and the kinetics of cell death. In this assay, cells entering mitosis after G2 arrest are trapped by adding nocodazole (0.35 μM) at 24-h intervals after etoposide (VP16) treatment (10 μM/30 min in Namalwa cells) and monitored by flow cytometry with phospho-H3(Ser10) labeling as well as propidium iodide (PI) staining (Fig. 1A; top left panel). Control Namalwa cells or Namalwa cells stably transfected with empty vector die rapidly after exposure to VP16 (Fig 1A; green bars). In contrast, cell populations stably expressing wt HA-Bcl-xL and the phosphorylation mutant HA-Bcl-xL(Ser49Ala) show strong inhibition of apoptosis (Fig. 1A; green bars). More than 70% of cells over-expressing wt HA-Bcl-xL are arrested in G2, 24 h after VP16 treatment (Fig 1A, grey bars), while some cells slowly escape from G2 and enter early mitosis, 36 to 72 h after VP16 (Fig. 1A; red bars). In contrast, cells expressing the phosphorylation mutant HA-Bcl-xL(Ser49Ala) enter mitosis much more rapidly, 36 to 72 h after VP16 (Fig. 1A; red bars), revealing that Ser49 is essential for Bcl-xL's function in G2 arrest. These observations also suggest that Bcl-xL's role in G2 arrest is distinct from its function in apoptosis.

Similar experimental monitoring by flow cytometry with phospho-H3(Ser10) labeling and PI staining was undertaken to evaluate the kinetics of early mitotic entry and stability of the spindle-assembly checkpoint (N4 DNA content, phospho-H3(Ser10)-positive), mitosis progression into cytokinesis (N4 DNA content, phospho-H3(Ser10)-negative, after taxol treatment), G1 entry (N2 DNA content, phospho-H3(Ser10)-negative), and cell death kinetics (sub-G1 DNA content) in taxol-exposed cells (Fig. 1B). Both Namalwa cells and Namalwa cells stably transfected with empty vector die rapidly

after taxol treatment, while cells stably expressing wt HA-Bcl-xL and the phosphorylation mutant HA-Bcl-xL(Ser49Ala) show strong inhibition of apoptosis (Fig. 1B; green bars). Up to 80-85% of cells over-expressing wt HA-Bcl-xL and HA-Bcl-xL(Ser49Ala) mutants accumulate in early mitosis (Fig. 1B; red bars) from 12- to 24-h taxol exposure. Interestingly, HA-Bcl-xL-expressing cells gradually start to lose the phospho-H3(Ser10) marker by 36 h, whereas most HA-Bcl-xL(Ser49Ala) mutant cells are still stable in early mitosis at 36 h, slowly losing the phospho-H3(Ser10) marker only at 48 to 60 h after taxol treatment (Fig. 1B; red bars). These results indicate that Bcl-xL(Ser49) is required for spindle-assembly checkpoint resolution and/or entry into cytokinesis. Again, this effect of Bcl-xL(Ser49Ala) on mitosis progression in taxol-exposed cells appears separable from its anti-apoptotic function.

Bcl-xL(Ser49) phosphorylation and location during DNA damage-induced G2 arrest and in unpertubed, synchronized wt Hela cells

First, antibodies were produced to monitor Bcl-xL(Ser49) phosphorylation. The specificity of phospho-Bcl-xL(Ser49) antibodies is depicted in Supplementary Figure S1-A. Experiments were then performed in human non-transfected wt HeLa cells, which undergo G2 arrest after VP16 treatment (10 μm; 16 h), with some cells escaping G2 arrest 48 to 72 h post-VP16 treatment (Fig. 2A, right panel). Bcl-xL(Ser49) phosphorylation is observed in wt HeLa cells exposed to VP16 (Fig. 2A, left panel). When wt HeLa cells are synchronized by double thymidine block and released upon progression from S to G2, Bcl-xL is progressively phosphorylated on Ser49 (Fig. 2B, left panel), suggesting that Bcl-xL(Ser49) phosphorylation also occurs during normal cell cycle progression. Cell cycle phase distribution during these experiments is indicated in Fig. 2B, right panel. We next investigated the subcellular location of phospho-Bcl-xL(Ser49) in wt HeLa cells by indirect immunofluorescence staining, in synchronized G2 control and VP16-induced G2 arrest (Fig. 2C). In HeLa cells exposed to VP16, a pool of phospho-Bcl-xL(Ser49) accumulated in centrosomes with γ-tubulin 24 and 48 h post-VP16 exposure (Fig. 2C). In contrast, no significant accumulation of phospho-Bcl-xL(Ser49) in centrosomes was detected in synchronized, untreated G2 cells (Fig. 2C).

Phospho-Bcl-xL(Ser49) was not found in nuclear structures with colin, a specific Cajal body marker, and nucleolin, a specific nucleolus marker (Fig. 2C). Taken together, these results suggest that Bcl-xL is phosphorylated on Ser49 during normal cell cycle progression and that phospho-Bcl-xL(Ser49) accumulates much more strongly in centrosomes during DNA damage-induced G2 checkpoint in HeLa cells.

Bcl-xL(Ser49) phosphorylation and location during mitosis progression

We next monitored phospho-Bcl-xL(Ser49) during mitosis. First, wt HeLa cells were synchronized by double thymidine block and released upon progression to G2. They were then treated with nocodazole (0.35 μM, 4 h), and prometaphase/metaphase cells were collected by mitotic shake-off. A portion of these cells was released from nocodazole and growth in the presence of MG-132 (25 μM), a proteasome inhibitor that prevents cyclinB1 and securin destruction, to obtain a cell population at the anaphase boundary. A second set was also released from nocodazole and by growth in the presence of blebbistatin (10 μM), a selective non-muscle contractile motor myosin II inhibitor that averts furrow ingression, to attain a cell population at telophase/cytokinesis. A schematic view of these experiments appears in Fig. 3A (top panel). Western blotting revealed that Bcl-xL is timely dephosphorylated at Ser49 at prometaphase, metaphase and the anaphase boundary, while it is rapidly phosphorylated at telophase/cytokinesis (Fig. 3A). Total Bcl-xL level remained stable along mitosis. Interestingly, the Bcl-xL(Ser49) phosphorylation pattern was exactly opposite that of Bcl-xL(Ser62) (Fig. 3A), indicating differential function. CyclinB1 and phospho-H3(Ser10) expression is shown as a specific early mitotic phase marker (Fig. 3A). The location of phospho-Bcl-xL(Ser49) in telophase/cytokinesis was then investigated. In these experiments, HeLa cells were synchronized by double thymidine block and release upon progression to G2 and entry into mitosis. They were collected at 30-min intervals from 9 to 12 h after double thymidine block and release to acquire mitotic cells at all steps of mitosis. In telophase/cytokinesis, phospho-Bcl-xL(Ser49) co-localizes strongly with the microtubule associated dynein motor protein (Fig. 3B). Phospho-Bcl-xL(Ser49) does not localize in centrosomes with γ-tubulin in telophase/cytokinesis (Fig. 3B). A summary of microscopy

analysis is presented in Supplemental Table S1.

Polo kinase 3 (PLK3) is involved in Bcl-xL(Ser49) phosphorylation

To identify the putative protein kinase involved in Bcl-xL(Ser49) phosphorylation, a panel of protein kinases was first tested in *in vitro* kinase assays with recombinant human Bcl-xL protein as substrate. Among all the kinases tested, PLK3 was the only one able to phosphorylate recombinant Bcl-xL protein on Ser49 in *in vitro* kinase assays (Fig. 4A). Enzyme-specific activities with control substrates were carried on (not show) . The specificity of Ser49 phosphorylation by PLK3 was validated by mass spectrometry (Supplemental Figure S1-B). PLK3 participation in Bcl-xl(Ser49) phosphorylation during DNA damage-induced G2 arrest was validated by using 2 specific small interfering RNAs (siRNAs) targeting PLK3 mRNA. A schematic illustration of these experiments appears in Fig. 4B.

With siRNAs targeting PLK3 mRNA, several attempts were made to confirm its involvement in Bcl-xL(Ser49) phosphorylation at telophase/cytokinesis (data not reported). Interfering with PLK3 expression does not allow cells to enter cytokinesis, an effect reported previously [54-57]. Trying to circumvent it, we adopted a protocol similar to that described in Fig. 3, where synchronized cells at G2 are first allowed to accumulate at metaphase with nocodazole, then released in the presence of blebbistatin to enrich the cell population at telophase/cytokinesis. A fraction of the cells were released from nocodazole by blebbistatin and BI-2536, a PLK inhibitor. The experiments are illustrated schematically in Fig. 4B. Inhibiting PLK activities in these cells prevented Bcl-xL(Ser49) phosphorylation. However, they failed to enter telophase/cytokinesis as cyclin B1 and phospho-H3(Ser10) expression remained significantly high. Together, these experiments confirmed that cytokinesis requires PLK3 activity. Quenching its expression with siRNAs or suppressing its activity in a timely manner in synchronized cells after nocodazole release causes cytokinesis defects, which also correlate with failure to phosphorylate Bcl-xL(Ser49).

Discussion

This study reveals a new phosphorylation site within Bcl-xL – Bcl-xL(Ser49) – that undergoes dynamic phosphorylation/dephosphorylation events during cell cycle progression. Phospho-Bcl-xL(Ser49) is essential in at least 2 key events of the cell cycle, G2 checkpoint and progression to telophase/cytokinesis during mitosis. A pool of phospho-Bcl-xL(Ser49) strongly localizes at centrosomes with γ-tubulin during the G2 checkpoint induced by DNA damage and with the microtubule associated dynein motor protein during telophase/cytokinesis. PLK3, which has known essential functions during cell cycle progression, is a key kinase involved in Bcl-xL(Ser49) phosphorylation. Importantly, phospho-Bcl-xL(Ser49) functions during G2 checkpoint and, in mitosis, it appears to be separable from Bcl-xL's known role in apoptosis, as Bcl-xL(Ser49Ala) phosphorylation mutant retains its anti-apoptotic effect but clearly shows different cell cycle behavior in DNA damage-induced G2 arrest and taxol-mediated mitotic actions.

Bcl-xL phosphorylation at Ser62 is well-documented and generally associated with microtubule poisoning [41-49]. Phospho-Bcl-xL(Ser62) functions have remained elusive until recently. We have recently observed that it undergoes differential location during G2 and spindle-assembly checkpoints (Wang et al., 2011; manuscripts submitted). A pool of phospho-Bcl-xL(Ser 62) is located in Cajal bodies in interphase and a pool accumulates with CDK1(CDC2) in nucleoli during G2 checkpoint, whereas its interacts with the inhibitory CDC20/MAD2/BUBR1/BUB3 complex during spindle-assembly checkpoints (Wang et al., 2011; manuscripts submitted). Interestingly, in this study, we noted a differential pattern of expression and location for phospho-Bcl-xL(Ser49) compared to phospho-Bcl-xL(Ser62). Phospho-Bcl-xL(Ser49) accumulates in centrosomes during G2 checkpoint, is rapidly dephosphorylated at early mitotic phases and is re-phosphorylated during telophase/cytokinesis. These dynamic changes of location and phosphorylation/dephosphorylation events strongly indicate differential functions. Although the exact molecular mechanisms were not fully addressed here, functional changes in cell cycle progression and cell behavior in response to VP16 and taxol treatment are documented, with cells expressing the Bcl-xL(Ser49Ala) phosphorylation mutant.

PLK3 activity and function have been reviewed recently [58]. Observed in centrosomes and nucleoli during interphase [56, 59], PLK3 is found at spindle poles and midbody during cytokinesis [55, 56]. PLK3 activity increases rapidly after DNA damage in an ATM-dependent manner, and is involved in G2 arrest by phosphorylating and inhibiting CDC25C phosphatase [60-63]. Its exact functions during mitosis remain unclear, but overexpression of PLK3's polo box domain, but not the kinase domain, causes mitotic arrest and cytokinesis defects [54-56]. Similarly, cells harbouring PLK3 knockdown by small hairpin RNA presented incomplete cytokinesis, which produced multinucleated cells [57]. PLK3 strongly phosphorylated Bcl-xL(Ser49) in *in vitro* kinase assays. RNA interference experiments conducted during G2 arrest confirmed that PLK3 is the key enzyme in Bcl-xL(Ser49) phosphorylation. During cytokinesis, our results are strongly indicative of PLK3's involvement, having demonstrated correlations between PLK3 expression and activity, failure to enter cytokinesis and to phosphorylate Bcl-xL at Ser49. The functional outcome of phospho-Bcl-xL(Ser49) on the stability of G2 checkpoint and kinetics of cytokinesis also correlates with PLK3 functions during G2 arrest and cytokinesis, suggesting that Bcl-xL is a downstream target of PLK3 and part of the network mediating PLK3's effect.

In summary, our data disclose a yet uncharacterized phosphorylation site within Bcl-xL. Bcl-xL(Ser49) is phosphorylated during normal cell cycle progression and checkpoints. Interfering with Bcl-xL(Ser49) phosphorylation destabilizes DNA damage-induced G2 arrest and slows entry into cytokinesis, but has no effect on the kinetics of VP16- and taxol-induced apoptosis. Our data also indicate that PLK3 is involved in Bcl-xL(Ser49) phosphorylation at G2 checkpoint and cytokinesis. Additional work is underway to dissect the molecular mechanisms of phospho-Bcl-xL(Ser49) action.

Materials and methods

Cell culture, cDNA construction and cell analysis

Human Namalwa and HeLa cell lines were obtained from the American Type Culture Collection and grown at 37°C under 5% CO_2 in RPMI-1640 medium and DMEM supplemented with 10% heat-inactivated fetal bovine serum (FBS), 100 U/ml penicillin and 100 µg/ml streptomycin, respectively. The phosphorylation mutant pCEP4-HA-Bcl-xL(Ser49Ala) was generated by triple polymerase chain reactions (PCR) with wt pCEP4-HA-Bcl-xL vector as DNA template. Briefly, the first fragments were amplified by *Vent* polymerase, with specific adapter primers containing restriction site sequences at the ATG start codon and anti-sense junction primers circumscribing the mutated codon with flanking sequences. The second fragments were amplified by *Vent* polymerase, with sense junction primers containing the mutated codon, with flanking sequences and adapter anti-sense primers comprising restriction site sequences at the TGA stop codon. The 2 amplified fragments were gel-purified, heat-denaturated, and slowly annealed on ice. After elongation by *Taq* polymerase for 10 min, a third PCR, with specific adapter primers containing sequences at the ATG start codon and TGA stop codon, was amplified. The amplified fragment was first cloned in pCR2.1Topo vector (Invitrogen Corporation), sequenced, and then sub-cloned in the eukaryotic expression vector pCEP4 (Invitrogen Corporation). Purified constructs were transfected in Namalwa cells by electroporation at 0.27 kV (Gene Pulser, BioRad, Hercules, CA), and cells were grown under hygromycin B1 selection to attain a stable cell population prior to performing the experiments. The kinetics of mitotic entry, cell cycle phase distribution and cell death were monitored in Coulter EpicsXL flow cytometers with phospho-H3(Ser10) labeling and PI staining. HeLa cells were synchronized by double-thymidine block (2 mM) and release.

Protein extraction and immunoblotting

To prepare protein extracts, cells were lysed in buffer containing 20 mM Hepes(KOH), pH 7.4, 120 mM NaCl, 1% Triton X-100, 2 mM phenylmethylsulfonyl

fluoride, a cocktail of protease inhibitors (Complete™, Roche Applied Science) and a cocktail of phosphatase inhibitors (PhosStop™, Roche Applied Science). The antibodies tested in this study are listed in Supplemental Table S2. Bcl-xL(Ser49) antibodies were prepared and purified by GeneScript, using the phosphopeptide-KLH conjugate CTESEMETP(pS)AING as immunogen. The affinity and specificity of the preparations were first analyzed with ELISA, deploying coated phosphopeptide and non-phosphopeptide as antigens.

Immunofluorescence microscopy

HeLa cells, seeded and grown directly on coverslips, were fixed in methanol at -20°C for 30 min and rapidly immersed in ice-cold acetone for a few seconds. The slides were allowed to dry at room temperature and rehydrated in PBS. Nonspecific binding sites were blocked in PBS containing 5% FBS (blocking solution); then, the slides were incubated sequentially with specific primary antibody (10 µg/ml in blocking solution), specific labeled secondary antibody (10 µg/ml in blocking solution), followed by DAPI staining, also performed in blocking solution. Images were generated with a Leica Microsystem mounted on a Leica DM6000B microscope and Leica DFC480 camera hooked up to a Macintosh computer.

Protein kinase assays and protein kinase chemical inhibitors

The kinases and kinase assays are described in Supplemental Table S3. Enzyme activities were tested on control substrates, and velocities were expressed as nmole/min/mg (data not showed). Recombinant human Bcl-xL(ΔTM) protein was produced and purified, as described previously [40]. BI-2536 was obtained from Axon MedChem Corp.

siRNA-mediated protein kinase inhibition

HeLa cells were transfected with DharmaFECT-1 transfection reagent (ThermoScientific) according to the manufacturer's instructions, with 100 nM of either control siRNA (non-targeting Smart Pool) or siRNA #3 and #4 targeting PLK3 mRNA obtained from Dharmacon,ThermoScientific.

Online supplemental materials: Supplemental materials for this article, including supplemental figures and tables, are available on the journal website.

Acknowledgements: This work was supported by Grant MOP-97913 from the Canadian Institutes of Health Research to R.B. J.W. received scholarships from the China Scholarship Council (Beijing, China), the Faculté des études supérieures (Université de Montréal, Canada) and the Fondation de l'Institut du cancer de Montréal (Canada). The authors thank Dr. Estelle Schmitt (CRCHUM, Canada) for her valuable suggestions and the preparation of Bcl-xL mutant cDNAs. The editorial work of Mr. Ovid Da Silva is appreciated.

Abbreviations: Bcl, B cell leukemia/lymphoma protein; Bcl-xL, Bcl-2-related gene x, long isoform; BH, Bcl-2 homology domain; CENPA: CENPA, centromere protein A; CLIP170, cytoplasmic linker protein 170; HA, influenza hemagglutinin epitope tag; HEC1; highly expressed in cancer protein 1; PCR, polymerase chain reaction; PI, propidium iodide; PLK, polo kinase; siRNA, small interfering RNA; VP16, etoposide; wt, wild-type

Disclosure of conflicts of interest: The authors declare no potential conflicts of interest.

References

1. Boise LH, Gonzalez-Garcia M, Postema CE, Ding L, Lindsten T, Turka LA, et al. Bcl-x, a bcl-2-related gene that functions as a dominant regulator of apoptotic cell death. Cell 1993; 74:597-608.
2. Paquet C, Bertrand R. Unique and multi-domain Bcl-2 family members: post-translation modification and apoptosis regulation. In: Gayathri A, Ed. Recent Research Developments in Biophysics and Biochemistry. Trivandrum: Research Signpost Publisher, 2003:291-325.
3. Kroemer G, Galluzzi L, Brenner C. Mitochondrial membrane permeabilization in cell death. Physiol Rev 2007; 87:99-163.
4. Tait SW, Green DR. Mitochondria and cell death: outer membrane permeabilization and beyond. Nat Rev Mol Cell Biol 2010; 11:621-32.
5. Muchmore SW, Sattler M, Liang H, Meadows RP, Harlan JE, Yoon HS, et al. X-ray and NMR structure of human Bcl-xL, an inhibitor of programmed cell death. Nature 1996; 381:335-41.
6. Sattler M, Liang H, Nettesheim D, Meadows RP, Harlan JE, Eberstadt M, et al. Structure of Bcl-x(L)-Bak peptide complex: recognition between regulators of apoptosis. Science 1997; 275:983-6.
7. Diaz JL, Oltersdorf T, Horne W, McConnell M, Wilson G, Weeks S, et al. A common binding site mediates heterodimerization and homodimerization of Bcl-2 family members. J Biol Chem 1997; 272:11350-5.
8. Sedlak TW, Oltvai ZN, Yang E, Wang K, Boise LH, Thompson CB, et al. Multiple Bcl-2 family members demonstrate selective dimerizations with Bax. Proc Natl Acad Sci USA 1995; 92:7834-8.
9. Cheng EH, Wei MC, Weiler S, Flavell RA, Mak TW, Lindsten T, et al. BCL-2, BCL-X(L) sequester BH3 domain-only molecules preventing BAX- and BAK-mediated mitochondrial apoptosis. Mol Cell 2001; 8:705-11.
10. Letai A, Bassik M, Walensky L, Sorcinelli M, Weiler S, Korsmeyer S. Distinct BH3 domains either sensitize or activate mitochondrial apoptosis, serving as prototype cancer therapeutics. Cancer Cell 2002; 2:183-92.
11. Kuwana T, Bouchier-Hayes L, Chipuk JE, Bonzon C, Sullivan BA, Green DR, et al. BH3 domains of BH3-only proteins differentially regulate Bax-mediated mitochondrial membrane permeabilization both directly and indirectly. Mol Cell 2005; 17:525-35.
12. Certo M, Del Gaizo Moore V, Nishino M, Wei G, Korsmeyer S, Armstrong SA, et al. Mitochondria primed by death signals determine cellular addiction to antiapoptotic BCL-2 family members. Cancer Cell 2006; 9:351-65.
13. Willis SN, Fletcher JI, Kaufmann T, van Delft MF, Chen L, Czabotar PE, et al. Apoptosis initiated when BH3 ligands engage multiple Bcl-2 homologs, not Bax or Bak. Science 2007; 315:856-9.

14. Adams JM, Cory S. Bcl-2-regulated apoptosis: mechanism and therapeutic potential. Curr Opin Immunol 2007; 19:488-96.

15. Youle RJ, Strasser A. The Bcl-2 protein family: opposing activities that mediate cell death. Nat Rev Mol Cell Biol 2008; 9:47-59.

16. Chittenden T. BH3 domains: intracellular death-ligands critical for initiating apoptosis. Cancer Cell 2002; 2:165-6.

17. Lovell JF, Billen LP, Bindner S, Shamas-Din A, Fradin C, Leber B, et al. Membrane binding by tBid initiates an ordered series of events culminating in membrane permeabilization by Bax. Cell 2008; 135:1074-84.

18. Kim H, Tu H-C, Ren D, Takeuchi O, Jeffers JR, Zambetti GP, et al. Stepwise activation of Bax and Bak by tBid, Bim and Puma initiates mitochondrial apoptosis. Mol Cell 2009; 36:487-99.

19. Dewson G, Kluck RM. Mechanisms by which Bak and Bax permeabilise mitochondria during apoptosis. J Cell Sci 2009; 122:2801-8.

20. Gavathiotis E, Reyna DE, Davis ML, Bird GH, Walensky LD. BH3-triggered structural reorganization drives the activation of proapoptotic Bax. Mol Cell 2010; 40:481-92.

21. Minn AJ, Velez P, Schendel SL, Liang H, Muchmore SW, Fesik SW, et al. Bcl-xL forms an ion channel in synthetic lipid membranes. Nature 1997; 385:353-7.

22. Zoratti M, Szabo I. The mitochondrial permeability transition. Biochim Biophys Acta 1995; 1241:139-76.

23. Shimizu S, Narita M, Tsujimoto Y. Bcl-2 family proteins regulate the release of apoptogenic cytochrome c by the mitochondrial channel VDAC. Nature 1999; 399:483-7.

24. Harris MH, Thompson CB. The role of the Bcl-2 family in the regulation of outer mitochondrial membrane permeability. Cell Death Differ 2000; 7:1182-91.

25. Shimizu S, Konishi A, Kodama T, Tsujimoto Y. BH4 domain of antiapoptotic bcl-2 family members closes voltage-dependent anion channel and inhibits apoptotic mitochondrial changes and cell death. Proc Natl Acad Sci USA 2000; 97:3100-5.

26. Shimizu S, Shinohara Y, Tsujimoto Y. Bax and bcl-xL independently regulate apoptotic changes of yeast mitochondria that require VDAC but not adenine nucleotide translocator. Oncogene 2000; 19:4309-18.

27. Kroemer G, Reed JC. Mitochondrial control of cell death. Nature Med 2000; 6:513-9.

28. Zamzami N, Kroemer G. The mitochondrion in apoptosis: how Pandora's box opens. Nat Rev Mol Cell Biol 2001; 2:67-71.

29. Pavlov EV, Priault M, Pietkiewicz D, Cheng EH, Antonsson B, Manon S, et al. A novel, high conductance channel of mitochondria linked to apoptosis in mammalian cells and Bax expression in yeast. J Cell Biol 2001; 155:725-32.

30. Qian S, Wang W, Yang L, Huang HW. Structure of transmembrane pore induced by Bax-derived peptide: evidence for lipidic pores. Proc Natl Acad Sci USA 2008; 105:17379-83.

31. Yamaguchi R, Lartigue L, Perkins G, Scott RT, Dixit A, Kushnareva Y, et al. Opa1-mediated cristae opening is Bax/Bak and BH3 dependent, required for apoptosis, and independent of Bak oligomerization. Mol Cell 2008; 31:557-69.

32. Schmitt E, Paquet C, Beauchemin M, Bertrand R. DNA-damage response network at the crossroads of cell-cycle checkpoints, cellular senescence and apoptosis. J Zhejiang Univ Sci B 2007; 8:377-97.

33. Danial NN, Gimenez-Cassina A, Tondera D. Homeostatic functions of Bcl-2 proteins beyond apoptosis. Adv Exp Med Biol 2010; 687:1-32.

34. Saintigny Y, Dumay A, Lambert S, Lopez BS. A novel role for the Bcl-2 protein family: specific suppression of the RAD51 recombination pathway. EMBO J 2001; 20:2596-607.

35. Wang Q, Gao F, May WS, Zhang Y, Flagg T, Deng X. Bcl-2 negatively regulates DNA double-strand-break repair through a nonhomologous end-joining pathway. Mol Cell 2008; 29:488-98.

36. Wiese C, Pierce AJ, Gauny SS, Jasin M, Kronenberg A. Gene conversion is strongly induced in human cells by double-strand breaks and is modulated by the expression of Bcl-x(L). Cancer Res 2002; 62:1279-83.

37. Youn CK, Cho HJ, Kim SH, Kim HB, Kim MH, Chang IY, et al. Bcl-2 expression suppresses mismatch repair activity through inhibition of E2F transcriptional activity. Nat Cell Biol 2005; 7:137-47.

38. Janumyan YM, Sansam CG, Chattopadhyay A, Cheng N, Soucie EL, Penn LZ, et al. Bcl-xL/Bcl-2 coordinately regulates apoptosis, cell cycle arrest and cell cycle entry. EMBO J 2003; 22:5459-70.

39. Janumyan Y, Cui Q, Yan L, Sansam CG, Vanlentin M, Yang E. G0 function of Bcl-2 and Bcl-xL requires Bax, Bak, and p27 phosphorylation by Mirk, revealing a novel role of Bax and Bak in quiescence regulation. J Biol Chem 2008; 283:34108-20.

40. Schmitt E, Beauchemin M, Bertrand R. Nuclear co-localization and interaction between Bcl-xL and Cdk1(cdc2) during G2/M cell cycle checkpoint. Oncogene 2007; 26:5851-65.

41. Poruchynsky MS, Wang EE, Rudin CM, Blagosklonny MV, Fojo T. Bcl-X(L) is phosphorylated in malignant cells following microtubule disruption. Cancer Res 1998; 58:3331-8.

42. Fang GF, Chang BS, Kim CN, Perkins C, Thompson CB, Bhalla KN. Loop domain is necessary for taxol-induced mobility shift and phosphorylation of Bcl-2 as well as for inhibiting taxol-induced cytosolic accumulation of cytochrome c and apoptosis. Cancer Res 1998; 58:3202-8.

43. Johnson AL, Bridgham JT, Jensen T. Bcl-x(Long) protein expression and phosphorylation in granulosa cells. Endocrinology 1999; 140:4521-9.

44. Fan M, Du C, Stone AA, Gilbert KM, Chambers TC. Modulation of mitogen-activated protein kinases and phosphorylation of Bcl-2 by vinblastine represent persistent forms of normal fluctuations at G2-M. Cancer Res 2000; 60:6403-7.

45. Basu A, Haldar S. Identification of a novel Bcl-xL phosphorylation site regulating the sensitivity of taxol- or 2-methoxyestradiol-induced apoptosis. FEBS Lett 2003; 538:41-7.

46. Du L, Lyle CS, Chambers TC. Characterization of vinblastine-induced Bcl-xL and Bcl-2 phosphorylation: evidence for a novel protein kinase and a coordinated phosphorylation/dephosphorylation cycle associated with apoptosis induction. Oncogene 2005; 24:107-17.

47. Upreti M, Galitovskaya EN, Chu R, Tackett AJ, Terrano DT, Granell S, et al. Identification of the major phosphorylation site in Bcl-xL induced by microtubule inhibitors and analysis of its functional significance. J Biol Chem 2008; 283:35517-25.

48. Tamura Y, Simizu S, Muroi M, Takagi S, Kawatani M, Watanabe N, et al. Polo-like kinase 1 phosphorylates and regulates Bcl-x(L) during pironetin-induced apoptosis. Oncogene 2009; 28:107-16.

49. Terrano DT, Upreti M, Chambers TC. Cyclin-dependent kinase 1-mediated Bcl-xL/Bcl-2 phosphorylation acts as a functional link coupling mitotic arrest and apoptosis. Mol Cell Biol 2010; 30:640-56.

50. Kharbanda S, Saxena S, Yoshida K, Pandey P, Kaneki M, Wang Q, et al. Translocation of SAPK/JNK to mitochondria and interaction with Bcl-x(L) in response to DNA damage. J Biol Chem 2000; 275:322-7.

51. Chang BS, Minn AJ, Muchmore SW, Fesik SW, Thompson CB. Identification of a novel regulatory domain in Bcl-X(L) and Bcl-2. EMBO J 1997; 16:968-77.

52. Srivastava RK, Mi QS, Hardwick JM, Longo DL. Deletion of the loop region of Bcl-2 completely blocks paclitaxel-induced apoptosis. Proc Natl Acad Sci USA 1999; 96:3775-80.

53. Andreassen PR, Skoufias DA, Margolis RL. Analysis of the spindle-assembly checkpoint in HeLa cells. Methods Mol Biol 2004; 281:213-25.

54. Conn CW, Hennigan RF, Dai W, Sanchez Y, Stambrook PJ. Incomplete cytokinesis and induction of apoptosis by overexpression of the mammalian polo-like kinase, Plk3. Cancer Res 2000; 60:6826-31.

55. Wang Q, Xie S, Chen J, Fukasawa K, Naik U, Traganos F, et al. Cell cycle arrest and apoptosis induced by human Polo-like kinase 3 is mediated through perturbation of microtubule integrity. Mol Cell Biol 2002; 22:3450-9.

56. Jiang N, Wang X, Jhanwar-Uniyal M, Darzynkiewicz Z, Dai W. Polo box domain of Plk3 functions as a centrosome localization signal, overexpression of which causes mitotic arrest, cytokinesis defects, and apoptosis. J Biol Chem 2006; 281:10577-82.

57. Naik MU, Naik UP. Calcium- and integrin-binding protein 1 regulates microtubule organization and centrosome segregation through polo like kinase 3 during cell cycle progression. Int J Biochem Cell Biol 2011; 43:120-9.

58. Strebhardt K. Multifaceted polo-like kinases: drug targets and antitargets for cancer therapy. Nat Rev Drug Discov 2010; 9:643-60.

59. Zimmerman WC, Erikson RL. Polo-like kinase 3 is required for entry into S phase. Proc Natl Acad Sci USA 2007; 104:1847-52.

60. Xie S, Wu H, Wang Q, Cogswell JP, Husain I, Conn C, et al. Plk3 functionally links DNA damage to cell cycle arrest and apoptosis at least in part via the p53 pathway. J Biol Chem 2001; 276:43305-12.

61. Bahassi EM, Conn CW, Myer DL, Hennigan RF, McGowan CH, Sanchez Y, et al. Mammalian Polo-like kinase 3 (Plk3) is a multifunctional protein involved in stress response pathways. Oncogene 2002; 21:6633-40.

62. Myer DL, Bahassi el M, Stambrook PJ. The Plk3-Cdc25 circuit. Oncogene 2005; 24:299-305.

63. Bahassi EM, Myer DL, McKenney RJ, Hennigan RF, Stambrook PJ. Priming phosphorylation of Chk2 by polo-like kinase 3 (Plk3) mediates its full activation by ATM and a downstream checkpoint in response to DNA damage. Mutat Res 2006; 596:166-76.

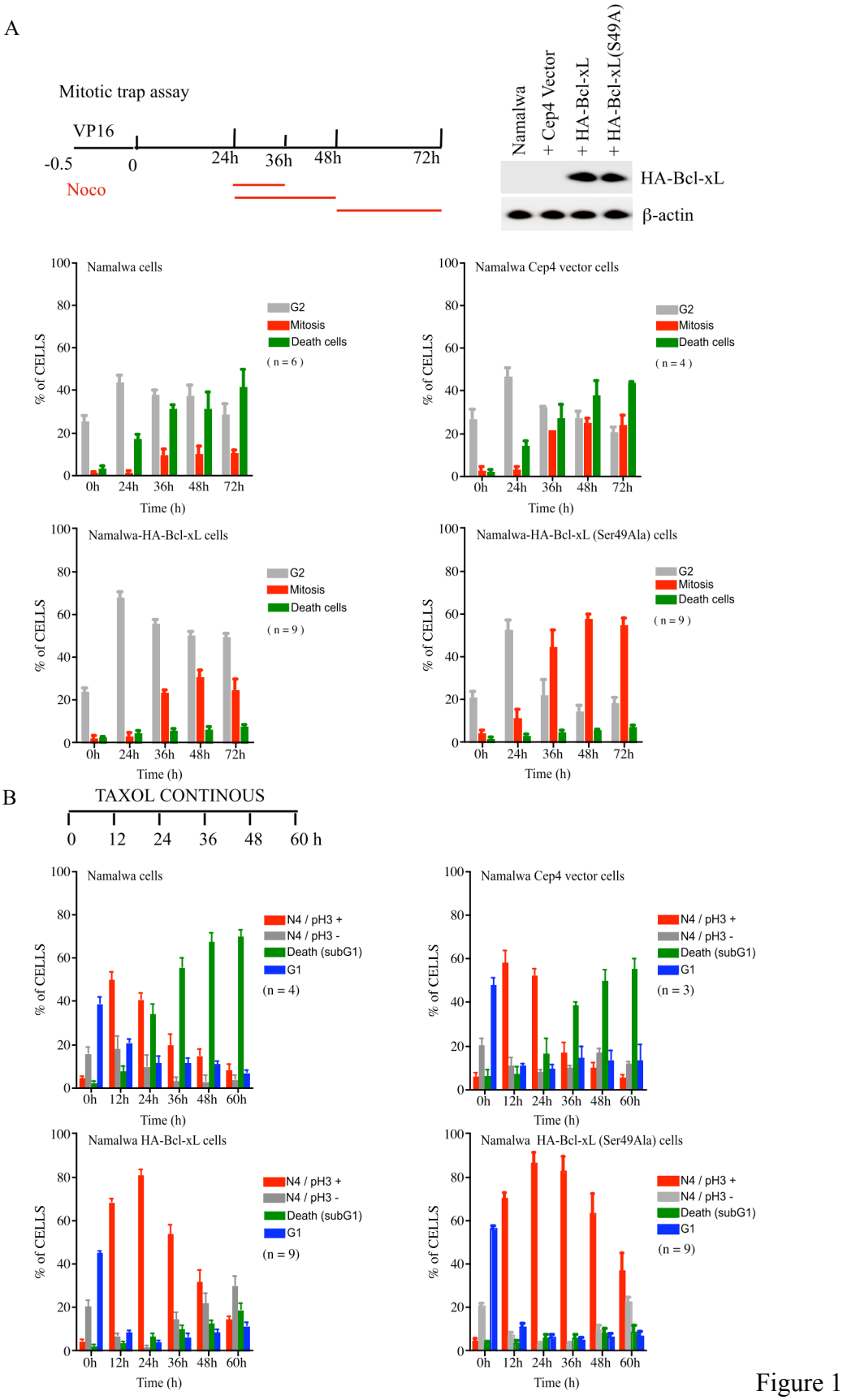
A
Mitotic trap assay
VP16
-0.5
0
24h
36h
48h
72h
Noco
Namalwa
+ Cep4 Vector
+ HA-Bcl-xL
+ HA-Bcl-xL(S49A)
HA-Bcl-xL
β-actin
Namalwa cells
Namalwa Cep4 vector cells
Namalwa-HA-Bcl-xL cells
Namalwa-HA-Bcl-xL (Ser49Ala) cells
% of CELLS
Time (h)
G2
Mitosis
Death cells
(n = 6)
(n = 4)
(n = 9)
B
TAXOL CONTINOUS
0 12 24 36 48 60 h
Namalwa cells
Namalwa Cep4 vector cells
Namalwa HA-Bcl-xL cells
Namalwa HA-Bcl-xL (Ser49Ala) cells
N4 / pH3 +
N4 / pH3 -
Death (subG1)
G1
(n = 4)
(n = 3)
(n = 9)

Figure 1

Figure 1 Effect of Bcl-xL and Bcl-xL(Ser49Ala) phosphorylation mutant on G2 checkpoint resolution and entry into cytokinesis. **A**) G2 checkpoint experiments are illustrated schematically in the top left panel. The expression levels of HA-Bcl-xL, HA-Bcl-xL(Ser49Ala) phosphorylation mutant and β-actin in stably-transfected Namalwa cell populations are shown in the top right panel. Kinetics of G2 cells (N4 DNA content, phospho-H3(Ser10)-negative; grey bars), early mitotic cells (N4 DNA content, phospho-H3(Ser10)-positive) and dead cells (sub-G1 cells; green bars) in wt Namalwa cells and Namalwa cells expressing empty vector, HA-Bcl-xL and HA-Bcl-xL(Ser49Ala) phosphorylation mutant after VP16 treatment. Bars represent the means ± s.e.m. of *n* independent experiments. **B)** Taxol experiments are illustrated schematically in the top left. Kinetics of early mitotic cells (N4 DNA content, phospho-H3(Ser10)-positive), late mitotic cells (or G2 at time 0) (N4 DNA content, phospho-H3(Ser10)-negative), dead cells (sub-G1 cells; green bars) and G1 cells (N2 DNA content; blue bars) in wt Namalwa cells and Namalwa cells expressing empty vector, HA-Bcl-xL and HA-Bcl-xL(Ser49Ala) phosphorylation mutant during taxol treatment (0.1 μM). Bars represent the means ± s.e.m. of *n* independent experiments.

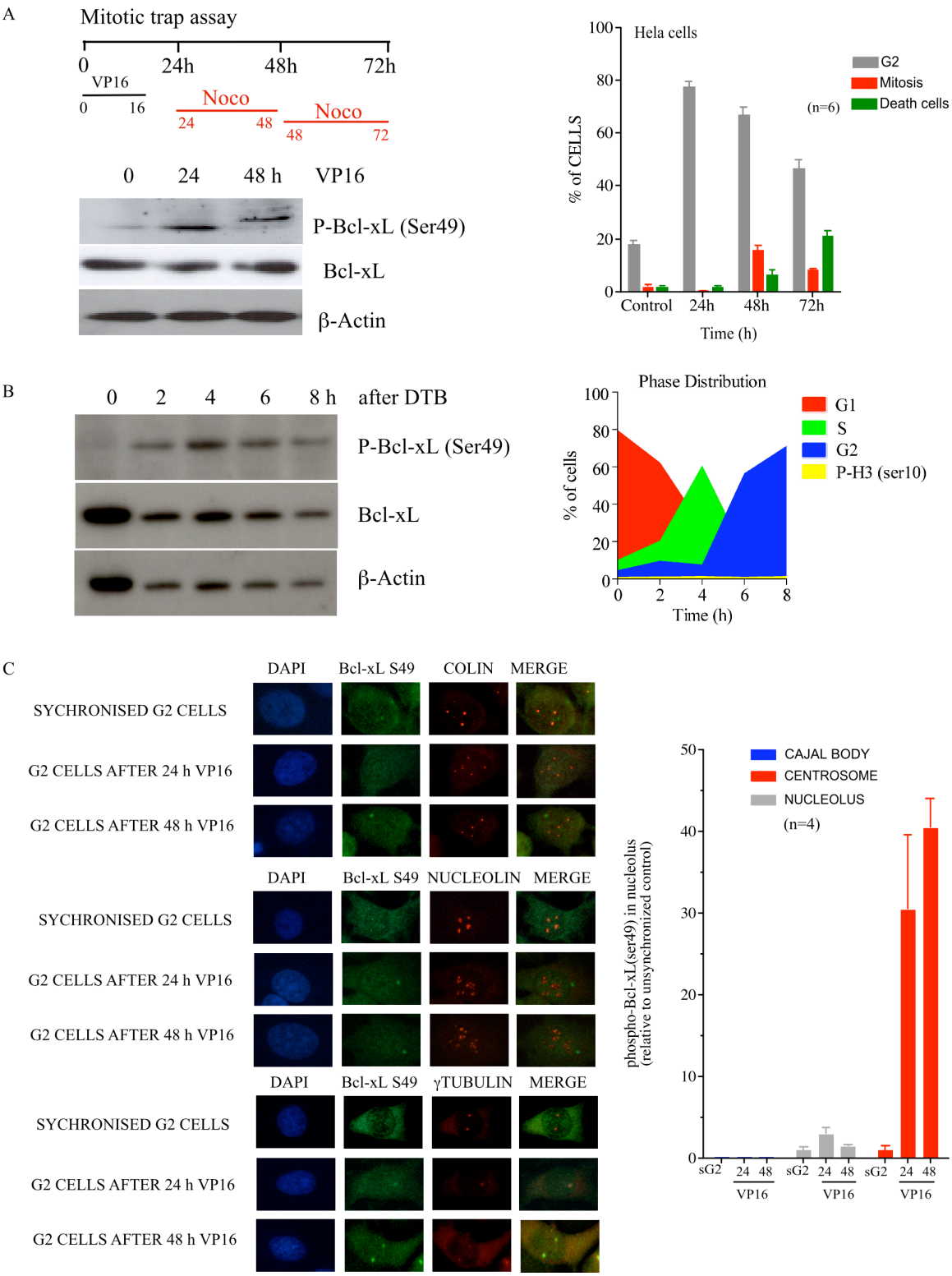
A
Mitotic trap assay
0
24h
48h
72h
VP16
0 16
Noco
24 48
Noco
48 72
0 24 48 h VP16
P-Bcl-xL (Ser49)
Bcl-xL
β-Actin
Hela cells
G2
Mitosis
Death cells
(n=6)
% of CELLS
Control 24h 48h 72h
Time (h)
B
0 2 4 6 8 h after DTB
P-Bcl-xL (Ser49)
Bcl-xL
β-Actin
Phase Distribution
G1
S
G2
P-H3 (ser10)
% of cells
Time (h)
C
DAPI Bcl-xL S49 COLIN MERGE
SYCHRONISED G2 CELLS
G2 CELLS AFTER 24 h VP16
G2 CELLS AFTER 48 h VP16
DAPI Bcl-xL S49 NUCLEOLIN MERGE
SYCHRONISED G2 CELLS
G2 CELLS AFTER 24 h VP16
G2 CELLS AFTER 48 h VP16
DAPI Bcl-xL S49 γTUBULIN MERGE
SYCHRONISED G2 CELLS
G2 CELLS AFTER 24 h VP16
G2 CELLS AFTER 48 h VP16
CAJAL BODY
CENTROSOME
NUCLEOLUS
(n=4)
phospho-Bcl-xL(ser49) in nucleolus
(relative to unsynchronized control)
sG2 24 48 sG2 24 48 sG2 24 48
VP16 VP16 VP16

Figure 2

Figure 2 Bcl-xL(Ser49) phosphorylation and location during DNA damage-induced G2 arrest and in unpertubed, synchronized wt Hela cells at interphase. **A**) Expression kinetics of phospho-Bcl-xL(Ser49), Bcl-xL and β-actin in wt HeLa cells treated with VP16. These experiments are illustrated schematically at the top. Kinetics of G2 cells (N4 DNA content, phospho-H3(Ser10)-negative; grey bars), early mitotic cells (N4 DNA content, phospho-H3(Ser10)-positive; red bars) and dead cells (sub-G1 cells; green bars) in wt HeLa cells treated with VP16 appear on the right histogram. Bars represent the means ± s.e.m. of *n* independent experiments. **B**) Expression kinetics of phospho-Bcl-xL(Ser49), Bcl-xL and β-actin in synchronized HeLa cells after double-thymidine block release. Cell cycle phase distribution during these experiments is illustrated in the right histogram. **C**) Co-location of phospho-Bcl-xL(Ser49) with colin (Cajal body markers), nucleolin (nucleolus marker) and γ-tubulin (centrosome marker) in synchronized G2 cells and during VP16-induced DNA damage and G2 arrest. The percentages of phospho-Bcl-xL(Ser49) in nucleoli, Cajal bodies and centrosomes during VP16-induced G2 checkpoint and during normal G2 phase of the cell cycle in synchronized wt Hela cells (sG2) are indicated in the right histogram. Bars represent the means ± s.e.m. from micrographs obtained in 4 independent experiments.

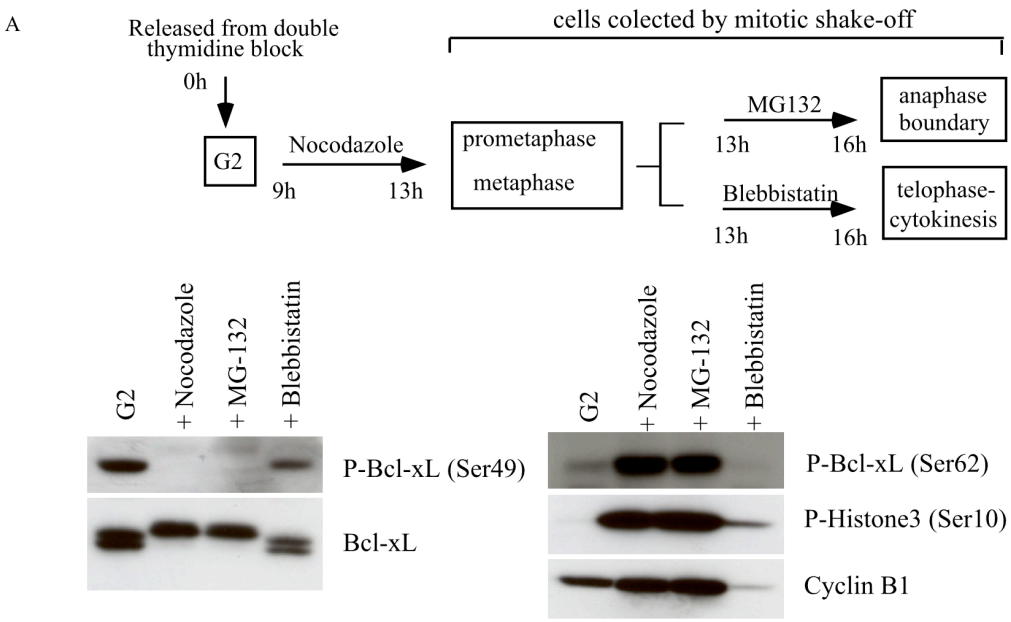
A
Released from double thymidine block
0h
G2
Nocodazole
9h
13h
cells colected by mitotic shake-off
prometaphase
metaphase
MG132
13h
16h
anaphase boundary
Blebbistatin
13h
16h
telophase-cytokinesis
G2
+ Nocodazole
+ MG-132
+ Blebbistatin
P-Bcl-xL (Ser49)
Bcl-xL
P-Bcl-xL (Ser62)
P-Histone3 (Ser10)
Cyclin B1

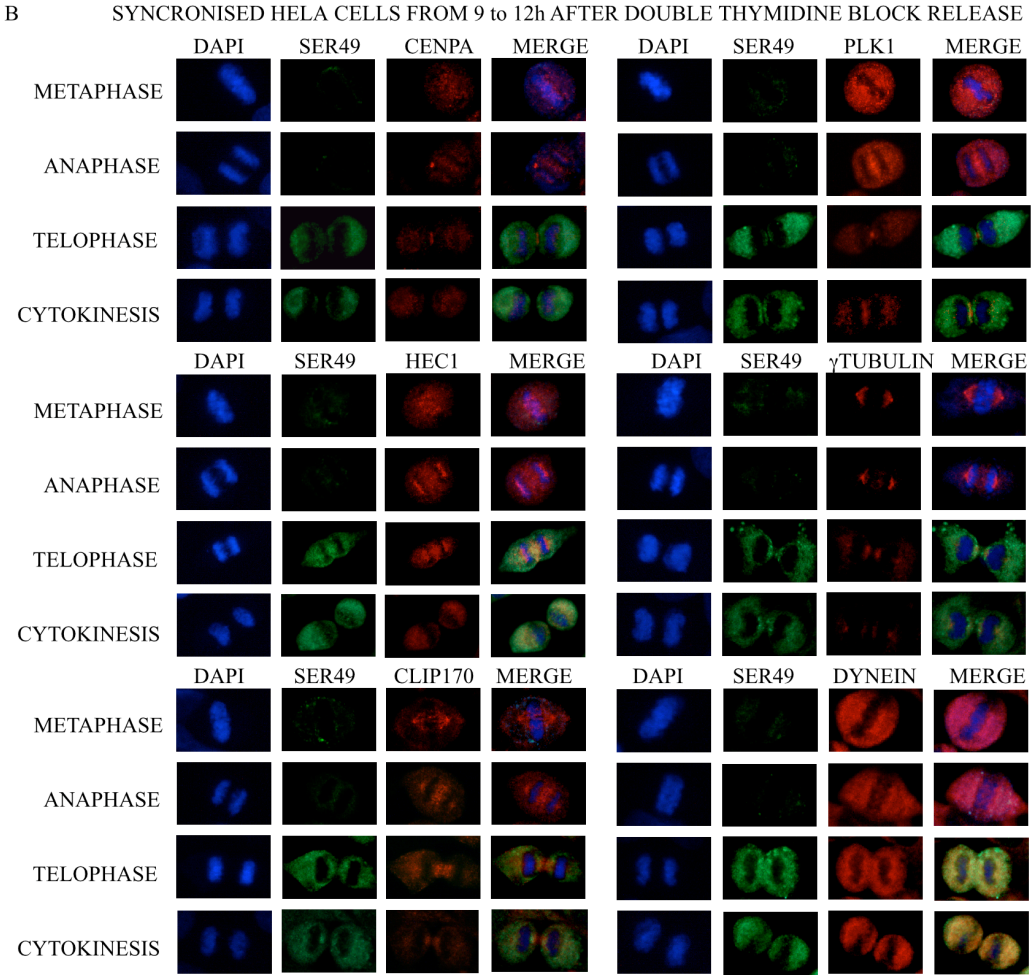
B
SYNCRONISED HELA CELLS FROM 9 to 12h AFTER DOUBLE THYMIDINE BLOCK RELEASE
DAPI
SER49
CENPA
MERGE
PLK1
METAPHASE
ANAPHASE
TELOPHASE
CYTOKINESIS
HEC1
γTUBULIN
CLIP170
DYNEIN

Figure 3

Figure 3 Bcl-xL(Ser49) phosphorylation and location during mitosis progression. **A**) Expression kinetics of phospho-Bcl-xL(Ser49), phospho-Bcl-xL(Ser62), Bcl-xL, phospho-H3(Ser10) and cyclin B1 in wt HeLa cells obtained at different steps of mitosis. The design of these experiments is illustrated at the top. **B**) Co-location of phospho-Bcl-xL(Ser49) only with dynein motor protein in telophase/cytokinesis. Representative of a total of 624 cells obtained from 3 experiments. Details in Supplemental Table S1.

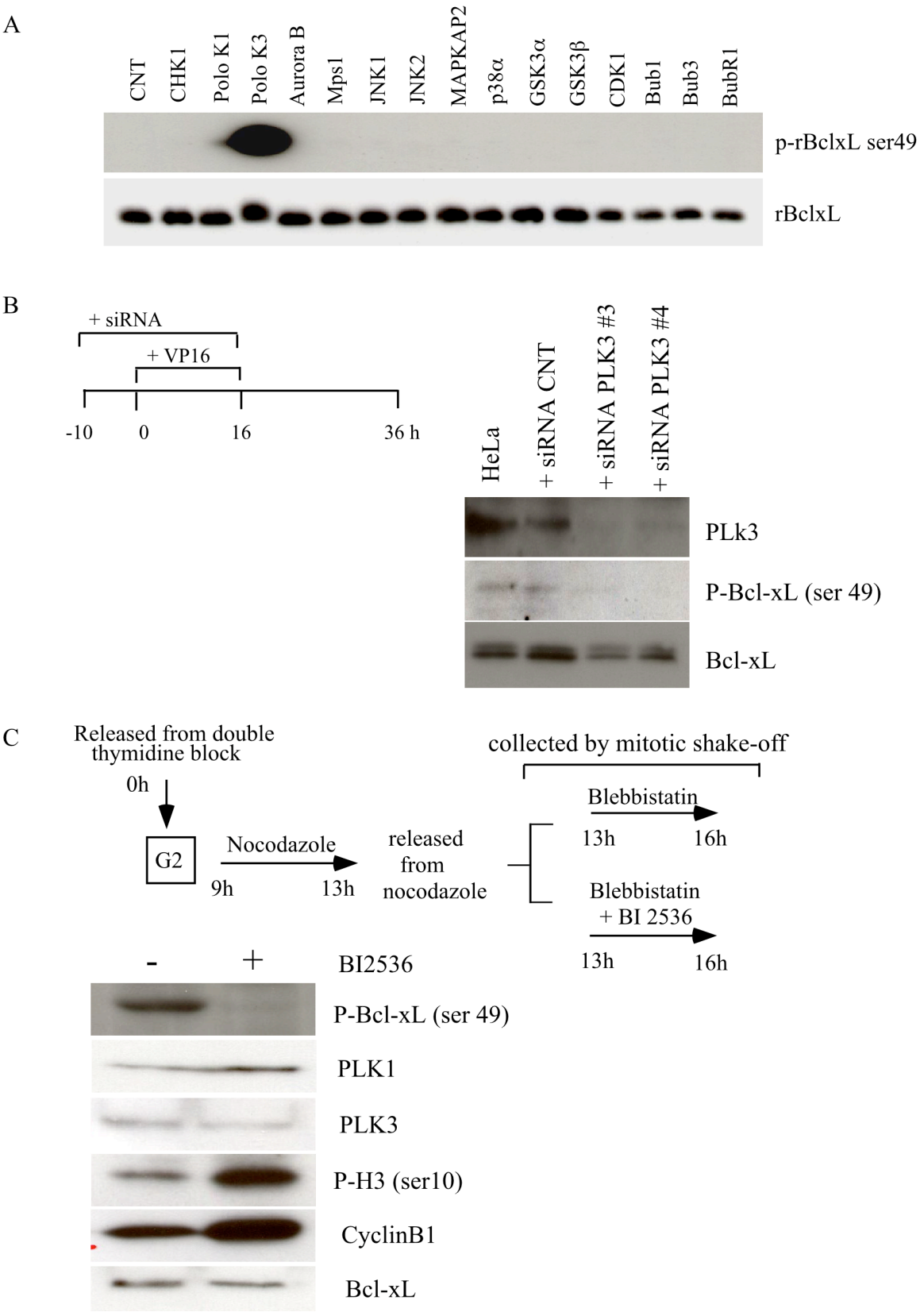
A
CNT
CHK1
Polo K1
Polo K3
Aurora B
Mps1
JNK1
JNK2
MAPKAP2
p38α
GSK3α
GSK3β
CDK1
Bub1
Bub3
BubR1
p-rBclxL ser49
rBclxL
B
+ siRNA
+ VP16
-10
0
16
36 h
HeLa
+ siRNA CNT
+ siRNA PLK3 #3
+ siRNA PLK3 #4
PLk3
P-Bcl-xL (ser 49)
Bcl-xL
C
Released from double thymidine block
0h
G2
Nocodazole
9h
13h
released from nocodazole
collected by mitotic shake-off
Blebbistatin
13h
16h
Blebbistatin + BI 2536
13h
16h
-
+
BI2536
P-Bcl-xL (ser 49)
PLK1
PLK3
P-H3 (ser10)
CyclinB1
Bcl-xL

Figure 4

Figure 4 PLK3 is involved in Bcl-xL(Ser49) phosphorylation. **A**) *In vitro* assays of a panel of purified and active protein kinases with recombinant human Bcl-xL(ΔTM) protein as substrate. All enzyme activities were tested on control substrates in Supplemental Figure S2, and validation by mass spectrometry appears in Supplemental Figure S3. Western blots are representative of 3 independent experiments. **B**) Effects of 2 specific siRNAs targeting PLK3 mRNA on the expression kinetics of phospho-Bcl-xL(Ser49), Bcl-xL and PLK3 in wt HeLa cells exposed to VP16. The design of these experiments is presented on the left. **C**) Effects of a PLK inhibitor (BI-2536, 0.1 μm) on phospho-Bcl-xL(Ser49), Bcl-xL, PLK1 and PLK3 expression in synchronized wt HeLa cells released from nocodazole in the presence of blebbistatin to obtain enriched telophase/cytokinesis. The design of these experiments is presented at the top. Western blots are representative of 2 independent experiments.

A)

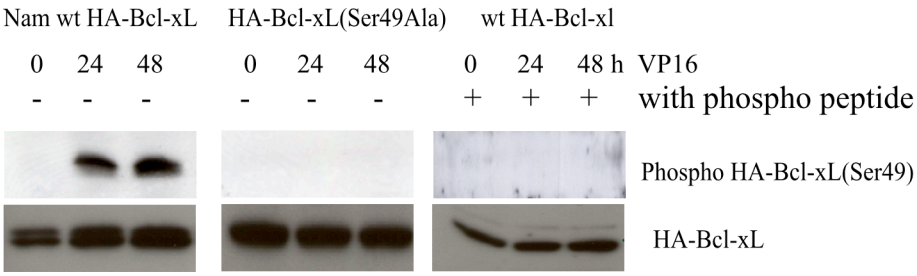

B)

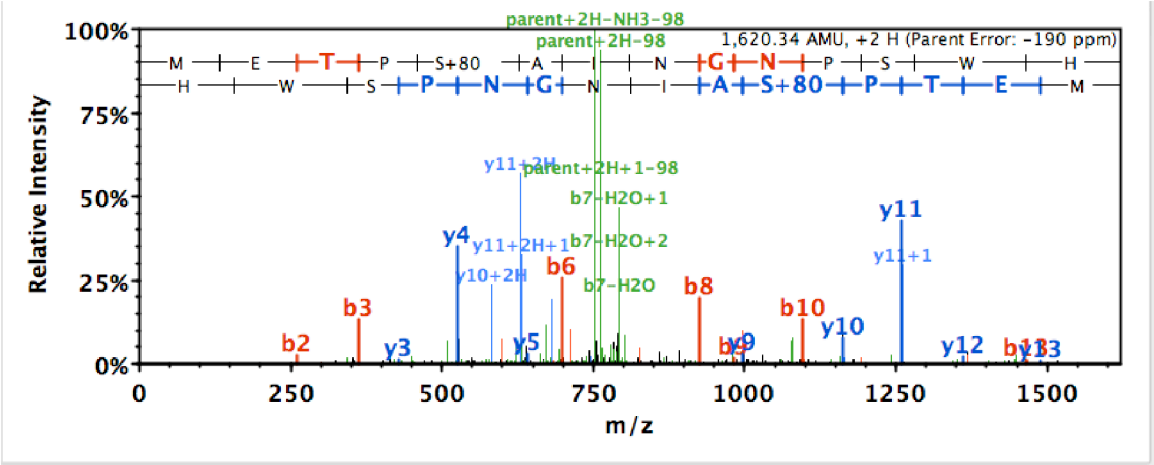

Supplemental Figure S1

Supplementary Figure S1

A) Specificity of the phospho-Bcl-xL(ser49) antibodies**.** Expression of phospho-HA-Bcl-xL(Ser49) in Namalwa cells expressing expressing wt HA-Bcl-xL and HA-Bcl-xL(Ser49Ala) mutant exposed to VP16 (10 μM for 30 min). HA-Bcl-xL expression is shown as control. In the right panels, antibodies were first incubated with excess phophorylated peptide (CTESEMETP(pS)AING) prior to Western blotting.

B) Tandem mass spectra of phospho(Ser49) analysed using Mascot (Matrix Science, London, UK; version Mascot). Mascot was searched with a fragment ion mass tolerance of 0.50 Da and a parent ion tolerance of 2.0 Da. Scaffold (version Scaffold_3_00_02, Proteome Software Inc., Portland, OR) was used to validate MS/MS based peptide and protein identifications. Peptide identifications were accepted if they could be established at greater than 95.0% probability. Validation of phosphate positions were conducted using Ascore. On that spectrum, Ascore score is of 42.65

SUPPLEMENTAL TABLE S1 Phase distribution *versus* labeling (number of cells) in synchronized human wt HeLa cells collected from 9 to 12 h after double thymidine block-release

Phospho-Bcl-xL (S49)	PROMETAPHASE	METAPHASE	ANAPHASE	TELOPHASE	CYOKINESIS	TOTAL
+ CENPA	28/28 (-)	12/12 (-)	10/10 (-)	12/12 (-)	18/18 (-)	80
+ PLK1	41/41 (-)	32/32 (-)	30/30 (-)	25/31 (-)	23/23 (-)	157
+ γ-Tubulin	20/28 (-)	23/23 (-)	13/13 (-)	10/16 (-)	12/15 (-)	95
+ Clip-170	30/30 (-)	22/22 (-)	19/19 (-)	10/14 (-)	18/21 (-)	106
+ Dynein	35/35 (-)	21/21 (-)	11/11 (-)	10/10 (+)	08/11 (+)	88
+ HEC1	36/36 (-)	25/25 (-)	09/09 (-)	09/13 (-)	12/15 (-)	98

Supplemental TABLE S2

ANTIBODIES	ID	Species	Source
Cdc2/CDK1	# PC25	rabbit pAb	Calbiochem
Cdc2/CDK1	clone 1/cdk1	mouse mAb	BD Biosciences
Plk1	clone 208G4	rabbit mAb	Cell Signaling
Plk3	clone B37-2	mouse mAb	BD Biosciences
Aurora A	clone 1G4	rabbit mAb	Cell Signaling
Aurora B	# 3094	rabbit mAb	Cell Signaling
MAPKAPK2	# 3042	rabbit pAB	Cell Signaling
MAPK14/SAPK p38α	clone L53F8	mouse mAb	Cell Signaling
MAPK8/ JNK1	clone G151-333	mouse mAb	BD Biosciences
MAPK9/ JNK2	# 4672	rabbit pAb	Cell Signaling
MPS1/TKK	# 3255	rabbit pAb	Cell Signaling
MPS1/TKK	clone BC032858	mouse mAb	Abcam
Bub1	clone 14H5	mouse mAb	Upstate/ Millipore
BubR1	# A300-386A	rabbit pAb	Bethyl
BubR1	# 4116	rabbit pAb	Cell Signaling
BubR1	clone9/BubR1	mouse mAb	BD Transduction
Bub3	clone31/Bub3	mouse mAb	BD Transduction
Bub3	# 3049	rabbit pAb	Cell Signaling
Mad2	# A300-300A	rabbit pAb	Bethyl Lab
Mad2	clone 48/Mad2	mouse mAb	BD Transduction
cdc20	clone 41/p55cdc	mouse mAb	BD Transduction
cdc20	# A301-179A	rabbit pAb	Bethyl Lab
cdc20	# A301-180A	rabbit pAb	Bethyl Lab
CENP-A	# 07-574	rabbit pAb	Upstate/Millipore
CENP-A	clone 3-19	mouse mAb	Assay Designs
Dynein	clone 74.1	mouse mAb	Millipore
HEC1	clone 9G3	mouse mAb	Abcam
EB1	clone 5/ EB1	mouse mAb	BD Transduction
Clip-170	custom	from Niels Galjart,	Rotterdam
Bcl-xL	clone 2H12	mouse mAb	BD Biosciences
Phospho-BclxL Ser49	custom	rabbit pAb	GenScript
HA tag	clone 12CA5	mouse mAb	Roche Applied Sci
HA tag	# A00168	goat pAb	GenScript
γ-tubulin	clone GTU88	mouse mAb	Abcam
α-tubulin	clone DM1A	mouse mAb	Sigma-Aldrich
β-tubulin	clone DM1B	mouse mAb	Calbiochem
β-Actin	clone 4C40	mouse mAb	Sigma
Phospho H3(ser10)	# 06-570	rabbit pAb	Upstate/Millipore
Phospho H3 ser10 Alexa 488	# 9708	rabbit pAb	Cell Signaling
Anti-Mouse IgG Alexa 488	# A11001	goat pAb	InVitroGen
Anti-Rabbit IgG Alexa 488	# A11008	goat pAb	InVitroGen
Anti-Mouse IgG Alexa 594	# A11005	goat pAb	InVitroGen
Anti-Rabbit IgG Alexa 594	#A11012	goat pAb	InVitroGen
Anti-Mouse IgG HP-linked	# NA931V	sheep pAb	GE Healthcare
Anti-Rabbit IgG HP-linked	# NA934V	donkey pAb	GE Healthcare
Normal Rabbit IgG	# sc-2027	rabbit IgG	Santa Cruz Biotech
Normal Mouse IgG	# sc-2025	mouse IgG	Santa Cruz Biotech

Supplemental Table S2

Supplemental TABLE S3

Recombinant Enzyme	Source	Control Substrate	Source	Buffer
CHK1	Sigma-Aldrich	RXRX(L/A)S((R/F)	Cell Signaling	A
MAPK14/SAPK p38α	Cell Signaling	ATF-2 (19-96)	Cell Signaling	B
MAPK8/ JNK1	Cell Signaling	c-Jun (1-89)	Cell Signaling	B+
MAPK9/ JNK2	Cell Sciences	c-Jun (1-89)	Cell Signaling	A
MAPKAPK2	Cell Signaling	KKKLNRTLSVA	AnaSpec	A+
PLK1	Cell Signaling	RISDELMDATFADQEAK	AnaSpec	A
PLK3	Cell Signaling	RISDELMDATFADQEAK	AnaSpec	A
Aurora A	Cell Signaling	RRSLLE	Cell Signaling	A
Aurora B	Cell Signaling	LRRLSLGLRRLSLGLRRL SLGLRRLSLG	AnaSpec	A
NEK2	Cell Signaling	RFRRSRRMI	AnaSpec	A
GSK3α	Cell Signaling	RRAAEELDSRAGSPQL	AnaSpec	A
GSK3β	Sigma-Aldrich	GPHRSTPESRAAV	AnaSpec	A+
Mps1	Cell Signaling	Myelin basic protein	Sigma-Aldrich	B
Immunprecipitated Enzyme				
CDC2/CDK1	Namalwa cells	Histone H1/ MBP	Sigma-Aldrich	B+
Bub1	Namalwa cells	Histone H1/MBP	Sigma-Aldrich	B+
BubR1	Namalwa cells	Histone H1/MBP	Sigma-Aldrich	B+
Bub3	Namalwa cells	Histone H1/ MBP	Sigma-Aldrich	B+

Buffer A (5x):	25 mM MOPS pH 7.2 25 mM $MgCl_2$ 12.5 mM β-glycerol-2-phosphate 0.5 mM Na_3VO_4 5 mm EGTA 2 mM EDTA 0.25 mM dithiothreitol 500 μM ATP* * 0.05 μCi/μl [^{32}P]-γATP
Buffer A+ (5x):	buffer A + 50 μg/ ml BSA

Buffer B (5x):	125 mM TRIS pH 7.2 50 mM $MgCl_2$ 25 mM β-glycerol-2-phosphate 0.5 mM Na_3VO_4 10 mM dithiothreitol 500 μM ATP* * 0.05 μCi/μl [^{32}P]-γATP
Buffer B+ (5x):	buffer B + 50 μg/ ml BSA

Supplemental Table S3. Listing of the protein kinase assays

6. Discussion

In these studies, we investigated the functional importance of phosphorylation events within Bcl-xL's unstructured flexible loop domain during G2 and the SAC as well as for cytokinesis and mitotic exit in a series of Bcl-xL phosphorylation mutants, including Thr41Ala, Ser43Ala, Thr47Ala, Ser49Ala, Ser56Ala, Ser62Ala and Thr115Ala. Our results demonstrate that Bcl-xL Ser49 and Ser62 undergo differential phosphorylation/dephosphorylation events during cell cycle progression, in association with the G2 checkpoint, the SAC, cytokinesis and mitotic exit.

6.1 Bcl-xL and its unstructured flexible loop domain

The unstructured Bcl-xL loop domain, which has various flexible and unstable conformations in space, first emerged from Bcl-xL's 3-dimensional structure [359]. Then, sequence homology alignment revealed that among all Bcl-2 family members, only Bcl-2 and Bcl-xL contain such a flexible loop domain [367]. It was postulated to be the target for post-translational modifications that would affect Bcl-xL function [367]. Studies with Bcl-xL loop domain deletion mutants indicated that this protein domain was not essential for the anti-apoptotic function of Bcl-xL against irradiation- and DNA topoisomerase I and II inhibitor-induced OMM permeabilization, cytochrome c release, caspase activation and apoptosis [20, 367, 368]. Liu et al. reported that the flexible loop domain was somehow involved in Bcl-xL's binding to Bim, and changed shape upon Bcl-xL-Bim interaction [462]. They also suggested that the engagement of Bim makes the Bcl-xL flexible loop domain more susceptible to proteolysis [462]. Other studies indicated that Bcl-xL(Ser62), located within the flexible loop domain, undergoes phosphorylation when cells are exposed to microtubule poisons [449, 451-453, 461, 463-466], a post-translational modification that paradoxically has been claimed to maintain or impair the anti-apoptotic effect of Bcl-xL [452, 465]. No experiments have yet directly addressed the effect of Bcl-xL(Ser62) phosphorylation on cell cycle progression and checkpoints. We are the first to uncover Bcl-xL(Ser49) phosphorylation. Indeed, our investigations of Bcl-xL(Ser49) represent the first observation that Bcl-xL undergoes cell cycle-dependent phosphorylation on Ser49.

Among all the phosphorylation mutants deployed in these studies, only Bcl-xL Ser49Ala and Ser62Ala showed phenotypic functional effects on the stability of the G2 checkpoint and the SAC and on the kinetics of cytokinesis and mitotic exit. With flow cytometry assays, we designed experimental protocols to screen the effects conferred by these mutants, monitoring the stability of VP16-induced G2 arrest and microtubule poisoning-induced SAC as well as the kinetics of cytokinesis and mitotic exit. Simultaneously, these screening assays also monitored the kinetics of cell death. They let us distinguish between the cell death and cell cycle functional effects of Bcl-xL phosphorylation mutants, and clearly revealed that the cell cycle effects of the Bcl-xL phosphorylation mutants Ser49Ala and Ser62Ala are separable from Bcl-xL's function in cell death. In synchronized and untreated cells and in drug-exposed cells, Bcl-xL is phosphorylated on Ser62 and Ser49 at various phases of the cell cycle, at diverse locations in cells, and binds differently to cell checkpoint components, indicating dissimilar functions of Bcl-xL Ser62 and Ser49 phosphorylation/dephosphorylation events during cell cycle progression and checkpoints.

Together, our studies reveal that the unstructured flexible loop domain, that is only present in Bcl-xL and Bcl-2 among all Bcl-2 family members [367], has an unique role in regulating Bcl-xL's functions on cell cycle progression and checkpoints. Bcl-xL post-translational modifications within its unstructured flexible loop domain, as postulated in 1997 by Chang at al. [367], are part of the complex signaling networks that control cell cycle progression and checkpoints. Our studies shed some light on the unstructured flexible loop domain mystery.

6.2 Bcl-xL phosphorylation and the cell cycle

6.2.1 Bcl-xL and the MAPK family

A few studies have mentioned the relationship between Bcl-xL and JNKs, normally activated at G2/M, in taxol-induced Bcl-xL phosphorylation at Ser62 and apoptosis [451, 460], whereas Kharbanda et al. suggested that JNKs were associated with Bcl-xL Thr47 and Thr115 phosphorylation in response to ionizing radiation [454]. These

investigations were conducted with pharmacological inhibitors but without RNA interference. In our studies, we deployed 3 different approaches, including *in vitro* kinase assays, pharmacological inhibitors and siRNA to dissect which kinases are involved in Bcl-xL(Ser62) phosphorylation during the G2 checkpoint and the SAC. Our experiments implicated both MAPK8/JNK1 and MAPK9/JNK2 in Bcl-xL(Ser62) phosphorylation during the G2 checkpoint, but only MAPK9/JNK2 activity was associated with the nucleolar localization of phospho-Bcl-xL(Ser62) during the G2 checkpoint. None of them was linked with Bcl-xL phosphorylation at the SAC. MAPK8/JNK1 and MAPK9/JNK2 are known to be strongly expressed during G2, accumulating in the nucleus, and playing a role in proper mitosis entry [467-469].

During the SAC, we observed that MAPK14/SAPKp38α phosphorylates Bcl-xL(Ser62). Our experiments were conducted on highly-enriched mitotic cell populations collected by mitotic shake-off, to eliminate and avoid contamination or unwanted effects of protein kinases involved in the G2 cell population. The importance of MAPK14/SAPKp38α during mitosis and the SAC has been well documented in previous studies [99, 470-477]. Interestingly, Yen and Yang reported that MAPK14/SAPKp38α signals CDC20 ubiquitination and proteolysis during the SAC and that it is also necessary for the formation of MAD2-bound CDC20 complex [475]. As we discerned that phospho-Bcl-xL(Ser62) binds to the BUBR1-MAD2-BUB3-CDC20- inhibitory complex, we are tempted to suggest that, in addition to the MAPK14/SAPKp38α effect on MAD-2-bound complex [475], MAPK14/SAPKp38α also influences the dynamics of BUBR1-bound complexes via Bcl-xL(Ser62) phosphorylation. MAPK14/SAPKp38α activity, through its direct activation of MAPKAPK2, is also required for proper spindle assembly at metaphase [476]. Consistently, MAPK14/SAPKp38α activity is involved in the timely, stable attachment of kinetochores to spindle microtubules, but not in mitotic process fidelity [477]. It is also suggested that MAPK14/SAPKp38α promotes checkpoint satisfaction; in the absence of MAPK14/SAPKp38α activity, the duration of mitosis is prolonged by about 40% in non-transformed human RPE-1, 80% in PtK2, and 25% in mouse cells [477]. This is a similar effect that we noted in cells expressing the phosphorylation mutant Bcl-xL(Ser62Ala), with prolonged duration of the SAC. Together, MAPK14/SAPKp38α activity was associated with checkpoint satisfaction [477]

and, in our studies, Bcl-xL(Ser62) phosphorylation was also linked with checkpoint satisfaction, facilitating metaphase-to-anaphase transition. MAPK14/SAPKp38α and phospho-Bcl-xL(Ser62) appear to work in the same direction for SAC resolution.

6.2.2 Bcl-xL and the polo kinase family

PLK1, a serine/threonine protein kinase highly regulated in time and space, is involved in multiple key events during G2/M transition and mitosis, playing roles in centrosome maturation, spindle assembly, chromosome segregation, cytokinesis and mitotic exit (reviewed in [136, 478]). Recently, in a series of *in vitro* experiments, Tamura et al. postulated that PLK1 could phosphorylate Bcl-xL at least on 13 residues, including Ser23, Ser28, Thr35, Ser43, Ser49, Ser56, Thr69, Ser72, Ser74, Thr109, Ser122 and Thr190, but not Ser62 [453]. They also suggested that Bcl-xL(Ser62) was phosphorylated after pironetin treatment by a JNK-related kinase, but not PLK1 [453]. This contradicts the results of our studies. In our experiments, we found that silencing PLK1 reduced the level of phospho-Bcl-xL(Ser62) at the G2 checkpoint induced by DNA damage, and in the early phase of mitosis, the latter investigation being performed on highly-enriched mitotic cells collected by mitotic shake-off without drug treatment. Because silencing PLK1 resulted mostly in cells arrested in G2, the mitotic shake-off protocol was essential to collect cells in early mitosis. Proper control included the monitoring of phospho-histone H3(Ser10) in these samples. In the experiments by Tamura et al., in cells treated with pironetin and siRNA targeting PLK1, no control of mitotic cells was included, suggesting that their preparations could be contaminated by a high level of G2 cells. Indeed, we did observe that both MAPK8/JNK1 and MAPK9/JNK2 were involved in Bcl-xL(Ser62) phosphorylation during DNA damage-induced G2 arrest. We did not monitor the effect of PLK1 on Bcl-xL(ser62) during normal synchronized and unperturbed cell cycle progression at G2. It is possible that PLK1-mediated phosphorylation of Bcl-xL during G2 only occurs during DNA damage.

The functions of PLK3, a PLK family member, are much less known (reviewed in [479]). In the interphase, PLK3 has been observed in centrosomes and nucleoli [307, 480]. During mitosis, it is found at spindle poles and midbody during cytokinesis [307, 481]. PLK3 activity increases rapidly after DNA damage in an ATM-dependent manner, and is

involved in G2 arrest by phosphorylating and inhibiting CDC25C phosphatase [145, 482-484]. Overexpression of PLK3's polo box domain-only, which acts as a dominant negative form of PLK3, causes mitotic arrest and cytokinesis defects [307, 481, 485]. Similarly, cells treated with siRNA targeting PLK3 presented incomplete cytokinesis and produced multinucleated cells [486]. In our *in vitro* kinase screening, PLK3 was the only protein kinase that strongly phosphorylated Bcl-xL in Ser49, experiments that were confirmed by mass spectrometry. siRNA targeting, during G2 arrest, confirmed that PLK3 is the key enzyme in Bcl-xL(Ser49) phosphorylation. This is in agreement with the known function of PLK3 as a negative regulator of G2/M transition, participating in the G2 checkpoint, by phosphorylating and inhibiting CDC25C phosphatase [145]. During cytokinesis, our results are not only correlative but also strongly indicative of PLK3's involvement, having demonstrated correlations between PLK3 expression and activity, failure to enter cytokinesis and to phosphorylate Bcl-xL at Ser49. Our study is the first to reveal that Bcl-xL is phosphorylated on Ser49 during cell cycle progression and cytokinesis.

6.2.3 Bcl-xL and CDK1(CDC2) kinase

Several contradictions arose between what we observed and a recent publication on Bcl-xL and CDK1(CDC2) [466]. The authors reported that cyclin B1/CDK1(CDC2) kinase is responsible for mitotic arrest-induced Bcl-xL/Bcl-2 phosphorylation. They used protein purification and mass spectrometry to identify the major vinblastine-induced phosphorylation site in Bcl-xL as Ser62, in the flexible loop domain between BH3 and BH4 domains. Then, they showed that vinblastine-induced Bcl-xL/Bcl-2 phosphorylation was inhibited in the presence of a CDK1(CDC2) inhibitor. With *in vitro* kinase assay, they also determined that recombinant CDK1(CDC2) could phosphorylate Bcl-xL(Ser62). In our *in vitro* kinase assays, active cyclin/CDK1(CDC2) obtained by immunoprecipitation was unable to phosphorylate Bcl-xL at Ser62, while active on other natural substrates, either histone H1 or basic myelin protein. In their experiments, Terrano et al. performed *in vitro* kinase assays for 5 hours [466]. In our studies, *in vitro* kinase assays were run for 30 minutes, a standard protocol employed regularly by investigators that probably reflects enzyme kinetics more adequately. Indeed, in cells,

cyclin B1/CDK1(CDC2) kinase activity is organized timely, its initial activation occurring only 20 to 25 minutes before mitosis onset [120, 121]. It is possible that Terrano et al. might have detected "star activity" or unspecific activity of their recombinant enzyme by conducting their kinase assays for 5 hours. Highly-sensitive controls with radioactive ^{32}P-ATP as phosphate donor were also deployed in our assays, and other kinases, including MAPK8/JNK1, MAPK9/JNK2 and PLK1, exerted a strong effect on Bcl-xL phosphorylation within the 30-minute assays, demonstrating much stronger affinity. A second conflict is that we routinely encountered recombinant Bcl-xL inhibition of cyclin B1/CDK1(CDC2) activity *in vitro* with 30-minute kinase assays [20]. In their experiments with CDK1(CDC2) inhibitor, no controls were added to indicate that the cells were actually in mitosis. Given the importance of CDK1(CDC2) for G2-to-mitosis transition, their cells were probably in G2. We believe that our experiments were conducted with more appropriate controls.

6.3 Phospho-Bcl-xL(Ser62) and (Ser49) location

6.3.1 Phospho-Bcl-xL(Ser49) and (Ser62) and centrosomes

Centrosomes play fundamental roles in organizing the interphase cytoskeleton and bipolar mitotic spindle. More recently, centrosomes were revealed as important organization centers that integrate cell cycle arrest and DNA repair signaling networks in response to genotoxic stress [487]. We found that a pool of phospho-Bcl-xL(Ser49) co-localizes with γ-tubulin at centrosomes after DNA damage in G2-arrested cells. In contrast, a pool of phospho-Bcl-xL(Ser62) segregates to centrosomes in early mitosis. Although not further exploited in our studies, these observations indicate a function of phospho-Bcl-xL(Ser49) and (Ser62) in centrosomes. One important aspect of centrosome biology is the control of cyclin B1/CDK1(CDC2) activity for entry into mitosis. Indeed, centrosomal activation of cyclin B1/CDCk1(CDC2) precedes its translocation to the nucleus, where the accumulation of active cyclin B1/CDK1(CDC2) complexes drives cells into mitosis [137]. The phosphatase CDC25B activates cyclin B1/CDK1(CDC2) complexes at centrosomes, and regulates centrosomal microtubule nucleation at G2/M

transition [488-490]. Consistent with these observations, Aurora A and PLK1 have also been localized at centrosomes [491, 492]. In the late G2 phase, Aurora A, first activated at centrosomes, is required for initial recruitment and activation of cyclin B1/CDK1(CDC2) at centrosomes, and entry into mitosis [492]. CHK1 has also been found to prevent the premature initiation of mitosis by inhibiting centrosome-associated cyclin B1/CDK1(CDC2) through CDC25B phosphatase at centrosomes [118, 493].

6.3.2 Phospho-Bcl-xL(Ser62) and nucleoli

The nucleolus, a central hub, coordinates the stress response. Although it was primarily associated with ribosome biogenesis, the nucleolus has now been shown to be multifunctional and also regulates cell-cycle progression as well as stress signaling, including DNA damage responses [494]. The nucleolus acts primarily by phased sequestration and the release of regulatory proteins, including the tumor suppressor p53, p19/ARF and Mdm2 proteins, CDC14 and PP1 phosphatases, DNA telomerase and the DNA helicases Wagner and Bloom [495]. CDK1(CDC2) as well as Bcl-xL and Bcl-2 have also been reported previously in nucleolar structures [20, 443, 496]. Phospho-Bcl-xL(Ser62) expression dramatically increases in nucleoli during the G2 checkpoint induced by DNA damage, whereas that of the Bcl-xL(Ser62Ala) mutant protein does not. Phospho-Bcl-xL(Ser62) co-locates and binds to CDK1(CDC2) in nucleoli. These results indicate that phospho-Bcl-xL(Ser62) could timely trap CDK1(CDC2) in nucleoli, thereby preventing the release and activation of a CDK1(CDC2) pool during G2 arrest.

6.3.3 Phospho-Bcl-xL(Ser62) and Cajal bodies

First identified in human neurons in 1903 by the Spanish neuro-cytologist Santiago Ramon, Cajal bodies have since been described in many other organisms and cell types [497]. They are primarily involved in distinct cellular pathways, including small ribonucleoprotein biogenesis as well as histone mRNA processing [498]. In addition, Cajal bodies are linked to the regulation of cell-cycle progression, and their number and composition vary throughout the cell cycle, disappearing, like other interphasic nuclear structures, at early mitosis with nuclear membranes [499]. They are also intimately linked with the nucleolus, and encompass dynamic trafficking and fusion with nucleolar

structures, although the regulation of these processes are not yet understood [495, 499, 500]. Phospho-Bcl-xL(Ser62) has been observed in Cajal bodies in interphasic cells in our studies, and further experiments, including fluorescence time-lapse microscopy imaging in living cells, will be required to further investigate the dynamic relationship and trafficking, if any, between thems and nucleoli during the G2 checkpoint.

6.3.4 Phospho-Bcl-xL(Ser49) and (Ser62) and microtubules

Dynein motor protein plays key roles at almost every step in mitotic spindle assembly and function, providing outward force to separate spindle poles during anaphase and cytokinesis [271, 272, 275, 501-510]. Both phospho-Bcl-xL(Ser49) and Ser(62) timely co-localize with dynein at different steps of mitosis. Given the large amount of dynein proteins along the spindle, it is unclear if any functional mechanisms couple phospho-Bcl-xL(Ser49) and Ser(62) with dynein motor activity. Additional experiments are required with other microtubule and spindle markers to dissect these interactions. Interestingly, the BH3-only protein Bim is well-known to interact with the dynein light chain LC8 and is thereby sequestered in microtubule-associated dynein motor complexes in cells [511-513]. Bim function at this location is clearly unknown. Considering the high affinity between Bcl-xL and Bim and the observations reported by Liu et al. that the flexible loop domain is somehow involved in Bcl-xL's binding to Bim [462], it would be of interest to further characterize Bcl-xL-Bim interaction at the level of dynein motor protein complexes during mitosis. It would be the first demonstration of an interaction between 2 Bcl-2 family members, anti- and pro-apoptotic proteins, with functions uncoupled from apoptosis.

6.4 Bcl-xL, cell survival and genomic stability

By default, anti-apoptotic proteins, such as Bcl-2 and Bcl-xL, maintain cell survival and normal cell homeostasis by inhibiting constitutively-expressed pro-apoptotic Bax and Bak proteins [332, 514-518]. Mice deficient in the Bcl-x gene manifests abnormal development and death of fetal erythroid progenitors and neuronal cells, with the animals dying around embryonic day 14 displaying severe defects in development [332]. In response to cancer radiotherapeutic and chemotherapeutic agents, anti-apoptotic protein like Bcl-

xL stands out among the most crucial regulators of apoptosis and promotes drug resistance and treatment failure [21-30]. During development and in response to various cellular stresses, eukaryotic cells must also inhibit anti-apoptotic proteins and activate pro-apoptotic proteins to eliminate unwanted cells and undergo apoptosis. This is achieved by BH3-only proteins. Subsets of these proteins, BH3-only enabler or sensitizing proteins, promote apoptosis by binding to and inhibiting pro-survival proteins, such as Bcl-2 and Bcl-xL, whereas BH3-only activator or activating proteins bind to and activate multidomain pro-apoptotic Bax and Bak proteins [363, 384]. The process eliminates unwanted and damaged cells and maintains genomic stability.

Apoptosis is a barrier to cancer development and, as a whole biological system, acts with tumor suppressive activities [78, 82]. However, dysregulation of apoptosis by means of anti-apoptotic protein overexpression showed oncogenic properties. Indeed, the Bcl-2 gene itself was first identified at the chromosomal breakpoint of t(14:18)-bearing B cell lymphomas, and found to act as a new class of oncogenes that function to prevent apoptosis and sustain cell survival instead of promoting cellular proliferation, and that synergize with classical oncogenes for tumor development [519-527]. More recent observations, that Bcl-2 and/or Bcl-xL modulate the Rad51-dependent homologous recombination pathway as well as non-homologous end-joining and DNA damage mismatch repair activities [48-51], are consistent with tumor suppressive activities.

Our studies show that Bcl-xL plays a role during the G2 checkpoint and the SAC, functions that appear independent of Bcl-xL known function on apoptosis. By stabilizing the G2 checkpoint after DNA damage, Bcl-xL could either allow more times for DNA repair and promote cell survival, or facilitate the establishment of premature senescence. These effects of Bcl-xL could have dramatic consequences on cell responses to radiotherapy and chemotherapy. During mitosis, by facilitating the progression of mitosis, acceleration of SAC resolution and mitotic exit, Bcl-xL could increase genomic instability in presence of unattached kinetochores. In addition, we also reported that silencing Bcl-xL expression leads nocodazole-exposed cells to tetraploidy and binucleation. These observations are consistent with the tumor suppressive activity of Bcl-xL, to maintain genomic stability. Our work is also "in line" with modern cell biology studies indicating, more and more, that gene expression is only the beginning.

Post-translation modifications, location and protein-protein interactions govern the various cellular functions of a given protein. Additional works will be required to clearly evaluate the consequences of Bcl-xL expression, phosphorylation and location on cell cycle progression and checkpoints, particularly in cell responses to radiotherapy and chemotherapy.

7. Conclusion

Our studies uncovered novel Bcl-xL functions during cell cycle progression and checkpoints. Major findings are summarized in Figure 12.

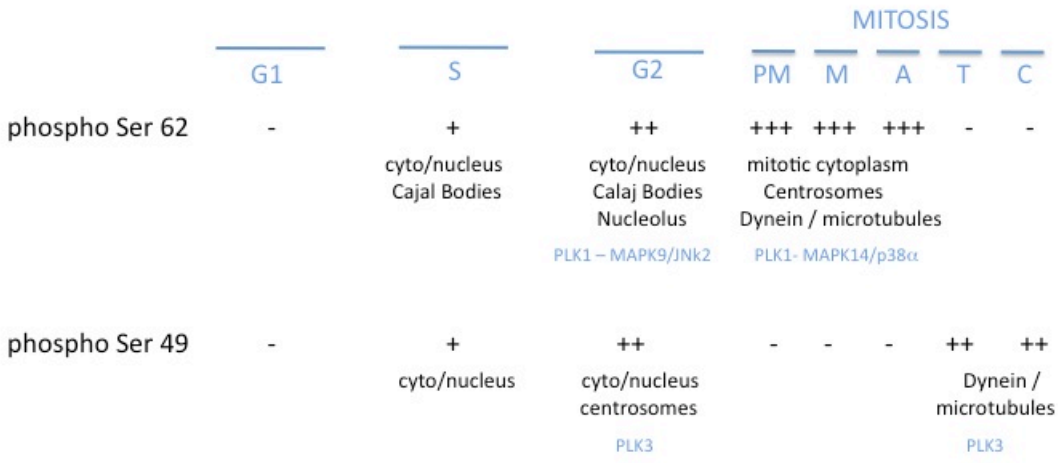

Figure 12. Schematic illustration of major findings in these studies

7.1 Major findings

The 1st appended manuscript reports that Bcl-xL undergoes Ser62 phosphorylation during the normal cell cycle and in DNA-damage-induced G2 arrest. PLK1 and MAPK9/JNK2 are responsible for Bcl-xL(Ser62) phosphorylation and progressive accumulation in nucleolar structures during the stabilization of DNA damage-induced G2 arrest. This function of phospho-Bcl-xL(Ser62) was clearly separable from Bcl-xL's known purpose in apoptosis, as the Bcl-xL(Ser62Ala) phosphorylation mutant retained its anti-apoptotic effect but lacked the G2-arrest

stabilization function. Phosphorylation of Bcl-xL(Ser62) is associated with its translocation into the nucleolus after DNA damage, where it will meet CDK1(CDC2). It is suggested that phospho-Bcl-xL(Ser62) participates in the G2 checkpoint by trapping CDK1(CDC2) in nucleolar structures.

The 2nd appended manuscript indicates that during the SAC, PLK1 and MAPK14/p38α mediate Bcl-xL(Ser62) phosphorylation, binding it to the inhibitory CDC20/MAD2/BUBR1/BUB3 complex in a way that accelerates SAC resolution. Silencing Bcl-xL expression also leads nocodazole-exposed cells to tetraploidy and binucleation, consistent with Bcl-xL function in genomic stability. Phospho-Bcl-xL(Ser62) also localizes in centrosomes with γ-tubulin and along the microtubule spindle with dynein motor protein, but its functions at these locations were not further addressed in this study. Again, phospho-Bcl-xL(Ser62) function in mitosis appears to be separable from Bcl-xL's known role in apoptosis.

The 3rd appended manuscript discloses a yet uncharacterized phosphorylation site within Bcl-xL. Bcl-xL(Ser49) is phosphorylated during normal cell cycle progression and checkpoints. Interfering with Bcl-xL(Ser49) phosphorylation destabilizes DNA damage-induced G2 arrest and slows entry into cytokinesis, but has no effect on the kinetics of VP16- and taxol-induced apoptosis. Our data indicate that PLK3 is involved in Bcl-xL(Ser49) phosphorylation at the G2 checkpoint and cytokinesis.

7.2 Future directions

These studies yield many future directions to further understand the role and functional importance of phospho-Bcl-xL(Ser49) and (Ser62) during cell cycle progression. Dynamic protein location and interaction with components of cell cycle checkpoints and microtubules during mitosis will be addressed by time-lapse fluorescence microscopy imaging in living cells and with Forster resonance energy transfer monitoring [385]. To achieve this goal, wt Bcl-xL, Bcl-xL(Ser49Ala), Bcl-xL(Ser49Asp), Bcl-xL(Ser62Ala), Bcl-xL(Ser62Asp) and the dual mutants Bcl-xL(Ser49Ala/Ser62Ala) and Bcl-xL(Ser49Asp/Ser62Asp) will be generated in a lentivirus expression system coupled with a fluorescence tag and expressed in cells. First, we will monitor their dynamic movement and location in synchronized cells and cells

exposed to DNA-damaging agents and microtubule poisons. To confirm interactions with CDK1(CDC2), BUBRI-MAD2-BUB3-CDC20 complex and dynein motor protein complex, these will be expressed with another fluorescent tag, and co-localization monitored by time-lapse fluorescence microscopy in living cells and with Forster resonance energy transfer, again in synchronized cells and cells exposed to DNA-damaging agents and microtubule poisons [385].

To further dissect Bcl-xL interaction with BUBR1-bound complexes, we will deploy a cell-free system recently described by Kulukian et al. to study the kinetics of formation of these complexes [262]. Briefly, in this cell-free system, kinetochore-mediated SAC signaling is reconstructed by adding sequentially, one by one, purified components of the SAC and then measuring the ubiquitin-ligase activity of APC/C-CDC20 on purified cyclin B1. By incorporating recombinant wt Bcl-xL, Bcl-xL(Ser49Ala), Bcl-xL(Ser49Asp), Bcl-xL(Ser62Ala), Bcl-xL(Ser62Asp) and the dual mutants Bcl-xL(Ser49Ala/Ser62Ala**)** and Bcl-xL**(**Ser49Asp/Ser62Asp) to this system, we will hopefully dissect the molecular interactions between Bcl-xL with MAD2- and BUBR1-bound complexes and their effects on APC/C-CDC20 activity.

Two approaches will be taken to further investigate the involvement of wt Bcl-xL and various mutants in genomic stability: BJ normal foreskin fibroblast cells, and *C. elegans,* an *in vivo* model [528]. BJ normal foreskin fibroblast cells have a reported normal diploid karyotype at population doubling 61 but an abnormal karyotype at population doubling 82 [529]. We will infect these cells with our constructs coding for wt Bcl-xL as well as all mutants and, in parallel, silence the expression of endogenous Bcl-xL protein to eliminate background. To do so, we will deploy a targeted sequence located in the 3'-end of the non-coding region of Bcl-xL mRNA, as described in the second manuscript. Infection will be evoked around doubling time 40. Then, at 5 doubling time intervals, we will analyze cell karyotypes. Our hypothesis is that cells expressing Bcl-xL(Ser62Ala) and (Ser49Ala) mutants will rapidly show abnormal karyotypes.

In *C. elegans*, we will use Ced 9 mutant animals and re-introduce wt Bcl-xL as well as all Bcl-xL mutants. We expect that all Bcl-xL constructs will reverse the Ced 9 mutant phenotypes as all Bcl-xL constructs, including the mutants, should retain their anti-apoptotic function. However, it is expected that the Bcl-xL(Ser62Ala) and

(Ser49Ala) mutants might confer some genomic instability in *C. elegans*. In the long-term, mice models could be developed as well.

Finally, postulating that Bcl-xL Ser49 and Ser62 are important for genomic stability, an *in silico* search could be performed to investigate if any sequencing already done on clinical tumor specimens could be informative for the presence of mutations within these residues. Alternately and/or in parallel, high-throughput sequencing of Bcl-xL could be undertaken on tumor tissue banks already existing in Canada. These investigations will indicate if Bcl-xL Ser49 and Ser62 mutations occur in human tumors and, eventually, correlation with treatment outcome could be addressed.

8. Bibliography

1. Evan GI, Brown L, Whyte M, Harrington E. Apoptosis and the cell cycle. Curr Opin Cell Biol 1995; 7:825-834.
2. Lundberg AS, Weinberg RA. Control of the cell cycle and apoptosis. Eur J Cancer 1999; 35:531-539.
3. Reed JC. Dysregulation of apoptosis in cancer. J Clin Oncol 1999; 17:2941-2953.
4. Jacotot E, Ferri KF, Kroemer G. Apoptosis and cell cycle: distinct checkpoints with overlapping upstream control. Pathol Biol (Paris) 2000; 48:271-279.
5. Evan GI, Vousden KH. Proliferation, cell cycle and apoptosis in cancer. Nature 2001; 411:342-348.
6. Hakem R, Mak TW. Animal models of tumor-suppressor genes. Annu Rev Genet 2001; 35:209-241.
7. Kaufmann SH. Induction of endonucleolytic DNA cleavage in human acute myelogenous leukemia cells by etoposide, camptothecin, and other cytotoxic anticancer drugs: a cautionary note. Cancer Res 1989; 49:5870-5878.
8. Barry MA, Behnke CA, Eastman A. Activation of programmed cell death (apoptosis) by cisplatin, other anticancer drugs, toxins and hyperthermia. Biochem Pharmacol 1990; 40:2353-2362.
9. Bertrand R, Sarang M, Jenkin J, Kerrigan D, Pommier Y. Differential induction of secondary DNA fragmentation by topoisomerase II inhibitors in human tumor cell lines with amplified c-myc expression. Cancer Res 1991; 51:6280-6285.
10. Lock RB, Ross WE. Inhibition of p34cdc2 kinase by etoposide or irradiation as a mechanism of G2 arrest in chinese hamster ovary cells. Cancer Res 1990; 50:3761-3766.
11. Bartek J, Lukas J. Mammalian G1- and S-phase checkpoints in response to DNA damage. Curr Opin Cell Biol 2001; 13:738-747.
12. Kastan MB, onyekwere O, Sidransky D, Vogelstein B, Craig RW. Participation of p53 protein in cellular response to DNA damage. Cancer Res 1991; 51:6304-6308.
13. Kastan MB, Kuerbitz SJ. Control of G1 arrest after DNA damage. Envir Health Perps 1993; 101(Suppl5):55-58.
14. Hartwell LH, Kastan MB. Cell cycle control and cancer. Science 1994; 266:1821-1828.
15. Kohn KW, Jackman J, O'Connor PM. Cell cycle control and cancer chemotherapy. J Cell Biochem 1994; 54:440-452.
16. Chang BD, Broude EV, Dokmanovic M, Zhu H, Ruth A, Xuan Y, Kandel ES, Lausch E, Christov K, Roninson IB. A senescence-like phenotype distinguishes tumor cells that undergo terminal proliferation arrest after exposure to anticancer agents. Cancer Res 1999; 59:3761-3767.

17. Campisi J. Cellular senescence as a tumor-suppressor mechanism. Trends Cell Biol 2001; 11:S27-31.
18. Schmitt CA, Lowe SW. Apoptosis and chemoresistance in transgenic cancer models. J Mol Med 2002; 80:137-146.
19. Johnstone RW, Ruefli AA, Lowe SW. Apoptosis. A link between cancer genetics and chemotherapy. Cell 2002; 108:153-164.
20. Schmitt E, Beauchemin M, Bertrand R. Nuclear co-localization and interaction between Bcl-xL and Cdk1(cdc2) during G2/M cell cycle checkpoint. Oncogene 2007; 26:5851-5865.
21. Reed JC. Bcl-2 family proteins: regulators of chemoresistance in cancer. Toxicol Lett 1995; 3:155-158.
22. Yang E, Korsmeyer SJ. Molecular thanatopsis: a discourse on the bcl2 family and cell death. Blood 1996; 88:386-401.
23. Reed JC. Bcl-2: prevention of apoptosis as a mechanism of drug resistance. Hematol Oncol Clin North Am 1995; 9:451-473.
24. Boise LH, Gottschalk AR, Quintans J, Thompson CB. Bcl-2 and Bcl-2-related proteins in apoptosis regulation. Curr Topics Microbiol Immunol 1995; 200:107-121.
25. Hickman JA. Apoptosis and chemotherapy resistance. Eur J Cancer 1996; 32A:921-926.
26. Reed JC. Bcl-2 family proteins: regulators of apoptosis and chemoresistance in hematologic malignancies. Semin Hematol 1997; 34:9-19.
27. Schmitt E, Sane AT, Steyeart A, Cimoli G, Bertrand R. The Bcl-xL and Bax control points: modulation of cancer chemotherapy-induced apoptosis and relation to TPCK-sensitive protease and caspase activation. Biochem Cell Biol 1997; 75:301-314.
28. Schmitt E, Cimoli G, Steyaert A, Bertrand R. Bcl-xL modulates apoptosis induced by anticancer drugs and delays DEVDase and DNA fragmentation-promoting activities. Exp Cell Res 1998; 240:107-121.
29. Schmitt E, Steyaert A, Cimoli G, Bertrand R. Bax-alpha promotes apoptosis induced by cancer chemotherapy and accelerates the activation of caspase 3-like cysteine proteases in p53 double mutant B lymphoma Namalwa cells. Cell Death Differ 1998; 5:506-516.
30. Cory S, Adams JM. The bcl2 family: regulators of the cellular life-or-death switch. Nat Rev Cancer 2002; 2:647-656.
31. Borner C. Diminished cell proliferation associated with the death-protective activity of Bcl-2. J Biol Chem 1996; 271:12695-12698.
32. Brady HJM, Gil-Gómez G, Kirberg J, Berns AJM. Bax-α perturbs T cell development and affects cell cycle entry of T cells. EMBO J 1996; 15:6991-7001.
33. Vairo G, Innes KM, Adams JM. Bcl-2 has a cell cycle inhibitory function separable from its enhancement of cell survival. Oncogene 1996; 13:1511-1519.

34. Mazel S, Burtrum D, Petrie HT. Regulation of cell division cycle progression by Bcl-2 expression: a potential mechanism for inhibition of programmed cell death. J Exp Med 1996; 183:2219-2226.

35. O'Reilly LA, Huang DCS, Strasser A. The death inhibitor Bcl-2 and its homologues influence control of cell cycle. EMBO J 1996; 15:6979-6990.

36. Linette GP, Li Y, Roth K, Korsmeyer SJ. Cross talk between cell death and cell cycle progression: Bcl-2 regulates Nfat-mediated activation. Proc Natl Acad Sci USA 1996; 93:9545-9552.

37. Huang DCS, Oreilly LA, Strasser A, Cory S. The anti-apoptosis function of Bcl-2 can be genetically separated from its inhibitory effect on cell cycle entry. EMBO J 1997; 16:4628-4638.

38. Knowlton K, Mancini M, Creason S, Morales C, Hockenbery D, Anderson BO. Bcl-2 slows in vitro breast cancer growth despite its antiapoptotic effect. J Surg Res 1998; 76:22-26.

39. Gillardon F, Moll I, Meyer M, Michaelidis TM. Alterations in cell death and cell cycle progression in the UV-irradiated epidermis of Bcl-2-deficient mice. Cell Death Differ 1999; 6:55-60.

40. Fujise K, Zhang D, Liu J, Yeh ET. Regulation of apoptosis and cell cycle progression by MCL1. Differential role of proliferating cell nuclear antigen. J Biol Chem 2000; 275:39458-39465.

41. Janumyan YM, Sansam CG, Chattopadhyay A, Cheng N, Soucie EL, Penn LZ, Andrews D, Knudson CM, Yang E. Bcl-xL/Bcl-2 coordinately regulates apoptosis, cell cycle arrest and cell cycle entry. EMBO J 2003; 22:5459-5470.

42. Jamil S, Sobouti R, Hojabrpour P, Raj M, Kast J, Duronio V. A proteolytic fragment of Mcl-1 exhibits nuclear localization and regulates cell growth via interaction with Cdk1. Biochem J 2005; 387:659-667.

43. Zinkel SS, Hurov KE, Ong C, Abtahi FM, Gross A, Korsmeyer SJ. A role for proapoptotic BID in the DNA-damage response. Cell 2005; 122:579-591.

44. Kamer I, Sarig R, Zaltsman Y, Niv H, Oberkovitz G, Regev L, Haimovich G, Lerenthal Y, Marcellus RC, Gross A. Proapoptotic Bid is an ATM effector in the DNA-damage response. Cell 2005; 122:593-603.

45. Jamil S, Mojtabavi S, Hojabrpour P, Cheah S, Duronio V. An essential role for MCL-1 in ATR-mediated CHK1 phosphorylation. Mol Biol Cell 2008; 19:3212-3220.

46. Janumyan Y, Cui Q, Yan L, Sansam CG, Vanlentin M, Yang E. G0 function of Bcl-2 and Bcl-xL requires Bax, Bak, and p27 phosphorylation by Mirk, revealing a novel role of Bax and Bak in quiescence regulation. J Biol Chem 2008; 283:34108-34120.

47. Komatsu K, Miyashita T, Hang H, Hopkins KM, Zheng W, Cuddeback S, Yamada M, Lieberman HB, Wang HG. Human homologue of S. pombe Rad9 interacts with Bcl-2/Bcl-x L and promotes apoptosis. Nat Cell Biol 2000; 2:1-6.

48. Saintigny Y, Dumay A, Lambert S, Lopez BS. A novel role for the Bcl-2 protein family: specific suppression of the RAD51 recombination pathway. EMBO J 2001; 20:2596-2607.

49. Wang Q, Gao F, May WS, Zhang Y, Flagg T, Deng X. Bcl-2 negatively regulates DNA double-strand-break repair through a nonhomologous end-joining pathway. Mol Cell 2008; 29:488-498.

50. Wiese C, Pierce AJ, Gauny SS, Jasin M, Kronenberg A. Gene conversion is strongly induced in human cells by double-strand breaks and is modulated by the expression of Bcl-x(L). Cancer Res 2002; 62:1279-1283.

51. Youn CK, Cho HJ, Kim SH, Kim HB, Kim MH, Chang IY, Lee JS, Chung MH, Hahm KS, You HJ. Bcl-2 expression suppresses mismatch repair activity through inhibition of E2F transcriptional activity. Nat Cell Biol 2005; 7:137-147.

52. Youle RJ, Strasser A. The Bcl-2 protein family: opposing activities that mediate cell death. Nat Rev Mol Cell Biol 2008; 9:47-59.

53. Hartwell LH, Kastan MB. Cell cycle control and cancer. Science 1994; 266:1821-1828.

54. Hunter T, Pines J. Cyclins and cancer. 2: Cyclin D and CDK inhibitors come of age. Cell 1994; 79:573-582.

55. Nigg EA. Cyclin-dependent protein kinases; key regulators of the eucaryotic cell cycle Bioessays 1995; 17:471-480.

56. Morgan DO. Principle of CDK regulation. Nature 1995; 374:131-134.

57. Chin PC, D'Mello SR. Brain chemotherapy from the bench to the clinic: targeting neuronal survival with small molecule inhibitors of apoptosis. Front Biosci 2005; 10:552-568.

58. Pardee AB. G1 events and regulation of cell proliferation. Science 1989; 246:603-608.

59. Blagosklonny MV, Pardee AB. The restriction point of the cell cycle. Cell Cycle 2002; 1:103-110.

60. Lopes M, Cotta-Ramusino C, Pellicioli A, Liberi G, Plevani P, Muzi-Falconi M, Newlon CS, Foiani M. The DNA replication checkpoint response stabilizes stalled replication forks. Nature 2001; 412:557-561.

61. Bartek J, Lukas C, Lukas J. Checking on DNA damage in S phase. Nat Rev Mol Cell Biol 2004; 5:792-804.

62. Machida YJ, Dutta A. Cellular checkpoint mechanisms monitoring proper initiation of DNA replication. J Biol Chem 2005; 280:6253-6256.

63. Schmitt CA. Cellular senescence and cancer treatment. Biochim Biophys Acta 2007; 1775:5-20.

64. Liu E, Lee AY, Chiba T, Olson E, Sun P, Wu X. The ATR-mediated S phase checkpoint prevents rereplication in mammalian cells when licensing control is disrupted. J Cell Biol 2007; 179:643-657.

65. Chan GK, Liu ST, Yen TJ. Kinetochore structure and function. Trends Cell Biol 2005; 15:589-598.

66. Musacchio A, Salmon ED. The spindle-assembly checkpoint in space and time. Nature Rev Mol Cell Biol 2007; 8:379-393.

67. Baker DJ, Dawlaty MM, Galardy P, van Deursen JM. Mitotic regulation of the anaphase-promoting complex. Cell Mol Life Sci 2007; 64:589-600.

68. Yu H. Cdc20: a WD40 activator for a cell cycle degradation machine. Mol Cell 2007; 27:3-16.

69. Cheeseman IM, Desai A. Molecular architecture of the kinetochore-microtubule interface. Nature Rev Mol Cell Biol 2008; 9:33-46.

70. Bolanos-Garcia VM, Blundell TL. BUB1 and BUBR1: multifaceted kinases of the cell cycle. Trends Biochem Sci 2011; 36:141-150.

71. D'Amours D, Amon A. At the interface between signaling and executing anaphase--Cdc14 and the FEAR network. Genes Dev 2004; 18:2581-2595.

72. Bosl WJ, Li R. Mitotic-exit control as an evolved complex system. Cell 2005; 121:325-333.

73. Torres-Rosell J, Machin F, Aragon L. Cdc14 and the temporal coordination between mitotic exit and chromosome segregation. Cell Cycle 2005; 4:109-112.

74. Piatti S, Venturetti M, Chiroli E, Fraschini R. The spindle position checkpoint in budding yeast: the motherly care of MEN. Cell Div 2006; 1:2.

75. Kapuy O, He E, Uhlmann F, Novak B. Mitotic exit in mammalian cells. Mol Syst Biol 2009; 5:324.

76. Hartwell L, Weinert T, Kadyk L, Garvik B. Cell Cycle Checkpoints, Genomic Integrity, and Cancer. Cold Spring Harbor Symposia on Quantitative Biology 1994; 59:259-263.

77. Kastan MB, Canman CE, Leonard CJ. p53, cell cycle control and apoptosis: implications for cancer. Cancer Metast Rev 1995; 14:3-15.

78. Hanahan D, Weinberg RA. The hallmarks of cancer. Cell 2000; 100:57-70.

79. Bharadwaj R, Yu H. The spindle checkpoint, aneuploidy, and cancer. Oncogene 2004; 23:2016-2027.

80. Pellman D. Cell biology: aneuploidy and cancer. Nature 2007; 446:38-39.

81. Suijkerbuijk SJ, Kops GJ. Preventing aneuploidy: the contribution of mitotic checkpoint proteins. Biochim Biophys Acta 2008; 1786:24-31.

82. Hanahan D, Weinberg RA. Hallmarks of cancer: the next generation. Cell 2011; 144:642-674.

83. Lohka MJ, Hayes MK, Maller JL. Purification of maturation-promoting factor, an intracellular regulator of early mitotic events. Proc Natl Acad Sci USA 1988; 85:3009-3013.

84. Labbe JC, Picard A, Peaucellier G, Cavadore JC, Nurse P, Doree M. Purification of MPF from starfish: identification as the H1 histone kinase p34cdc2 and a possible mechanism for its periodic activation. Cell 1989; 57:253-263.

85. Gautier J, Minshull J, Lohka M, Glotzer M, Hunt T, Maller JL. Cyclin is a component of maturation-promoting factor from Xenopus. Cell 1990; 60:487-494.

86. Matsuoka S, Huang M, Elledge SJ. Linkage of ATM to cell cycle regulation by the Chk2 protein kinase. Science 1998; 282:1893-1897.

87. Chaturvedi P, Eng WK, Zhu Y, Mattern MR, Mishra R, Hurle MR, Zhang X, Annan RS, Lu Q, Faucette LF, Scott GF, Li X, Carr SA, Johnson RK, Winkler JD, Zhou BB. Mammalian Chk2 is a downstream effector of the ATM-dependent DNA damage checkpoint pathway. Oncogene 1999; 18:4047-4054.

88. Tominaga K, Morisaki H, Kaneko Y, Fujimoto A, Tanaka T, Ohtsubo M, Hirai M, Okayama H, Ikeda K, Nakanishi M. Role of human Cds1 (Chk2) kinase in DNA damage checkpoint and its regulation by p53. J Biol Chem 1999; 274:31463-31467.

89. Martinho RG, Lindsay HD, Flaggs G, DeMaggio AJ, Hoekstra MF, Carr AM, Bentley NJ. Analysis of Rad3 and Chk1 protein kinases defines different checkpoint responses. EMBO J 1998; 17:7239-7249.

90. Guo Z, Kumagai A, Wang SX, Dunphy WG. Requirement for Atr in phosphorylation of Chk1 and cell cycle regulation in response to DNA replication blocks and UV-damaged DNA in Xenopus egg extracts. Genes Dev 2000; 14:2745-2756.

91. Liu Q, Guntuku S, Cui XS, Matsuoka S, Cortez D, Tamai K, Luo G, Carattini-Rivera S, DeMayo F, Bradley A, Donehower LA, Elledge SJ. Chk1 is an essential kinase that is regulated by Atr and required for the G(2)/M DNA damage checkpoint. Genes Dev 2000; 14:1448-1459.

92. Zhao H, Piwnica-Worms H. Atr-mediated checkpoint pathways regulate phosphorylation and activation of human Chk1. Mol Cell Biol 2001; 21:4129-4139.

93. Cliby WA, Lewis KA, Lilly KK, Kaufmann SH. S phase and G2 arrests induced by topoisomerase I poisons are dependent on ATR kinase function. J Biol Chem 2002; 277:1599-1606.

94. Bulavin DV, Higashimoto Y, Popoff IJ, Gaarde WA, Basrur V, Potapova O, Appella E, Fornace AJ. Initiation of a G2/M checkpoint after ultraviolet radiation requires p38 kinase. Nature 2001; 411:102-107.

95. Manke IA, Nguyen A, Lim D, Stewart MQ, Elia AE, Yaffe MB. MAPKAP kinase-2 is a cell cycle checkpoint kinase that regulates the G2/M transition and S phase progression in response to UV irradiation. Mol Cell 2005; 17:37-48.

96. Hirose Y, Katayama M, Stokoe D, Haas-Kogan DA, Berger MS, Pieper RO. The p38 mitogen-activated protein kinase pathway links the DNA mismatch repair system to the G2 checkpoint and to resistance to chemotherapeutic DNA-methylating agents. Mol Cell Biol 2003; 23:8306-8315.

97. Mikhailov A, Shinohara M, Rieder CL. Topoisomerase II and histone deacetylase inhibitors delay the G2/M transition by triggering the p38 MAPK checkpoint pathway. J Cell Biol 2004; 166:517-526.

98. Reinhardt HC, Aslanian AS, Lees JA, Yaffe MB. p53-deficient cells rely on ATM- and ATR-mediated checkpoint signaling through the p38MAPK/MK2 pathway for survival after DNA damage. Cancer Cell 2007; 11:175-189.

99. Cha H, Wang X, Li H, Fornace AJ, Jr. A functional role for p38 MAPK in modulating mitotic transit in the absence of stress. J Biol Chem 2007; 282:22984-22992.

100. Pines J, Hunter T. Isolation of a human cyclin cDNA: evidence for cyclin mRNA and protein regulation in the cell cycle and for interaction with p34cdc2. Cell 1989; 58:833-846.

101. Piaggio G, Farina A, Perrotti D, Manni I, Fuschi P, Sacchi A, Gaetano C. Structure and growth-dependent regulation of the human cyclin B1 promoter. Exp Cell Res 1995; 216:396-402.

102. Lock RB, Ross WE. Possible role for p34cdc2 kinase in etoposide-induced cell death of Chinese hamster ovary cells. Cancer Res 1990; 50:3767-3771.

103. Parker LL, Atherton-Fessler S, Lee MS, Ogg S, Falk JL, Swenson KI, Piwnica-Worms H. Cyclin promotes the tyrosine phosphorylation of p34cdc2 in a Wee1+ dependent manner. EMBO J 1991; 10:1255-1263.

104. Parker LL, Atherton-Fessler S, Piwnica-Worms H. p107wee1 is a dual-specificity kinase that phosphorylates p34cdc2 on tyrosine 15. Proc Natl Acad Sci USA 1992; 89:2917-2921.

105. Parker LL, Piwnica-Worms H. Inactivation of the p34cdc2-cyclin B complex by the human WEE1 tyrosine kinase. Science 1992; 257:1955-1957.

106. Atherton-Fessler S, Parker LL, Geahlen RL, Piwnica-Worms H. Mechanisms of p34cdc2 regulation. Mol Cell Biol 1993; 13:1675-1685.

107. McGowan CH, Russell P. Cell cycle regulation of human WEE1. EMBO J 1995; 14:2166-2175.

108. Mueller PR, Coleman TR, Kumagai A, Dunphy WG. Myt1: a membrane-associated inhibitory kinase that phosphorylates Cdc2 on both threonine-14 and tyrosine-15. Science 1995; 270:86-90.

109. Booher RN, Holman PS, Fattaey A. Human Myt1 is a cell cycle-regulated kinase that inhibits Cdc2 but not Cdk2 activity. J Biol Chem 1997; 272:22300-22306.

110. Liu F, Stanton JJ, Wu Z, Piwnica-Worms H. The human Myt1 kinase preferentially phosphorylates Cdc2 on threonine 14 and localizes to the endoplasmic reticulum and Golgi complex. Mol Cell Biol 1997; 17:571-583.

111. Lee J, Kumagai A, Dunphy WG. Positive regulation of Wee1 by Chk1 and 14-3-3 proteins. Mol Biol Cell 2001; 12:551-563.

112. Furnari B, Rhind N, Russell P. Cdc25 mitotic inducer targeted by Chk1 DNA damage checkpoint kinase. Science 1997; 277:1495-1497.

113. Sanchez Y, Wong C, Thoma RS, Richman R, Wu Z, Piwnica-Worms H, Elledge SJ. Conservation of the Chk1 checkpoint pathway in mammals: linkage of DNA damage to Cdk regulation through Cdc25. Science 1997; 277:1497-1501.

114. Peng CY, Graves PR, Thoma RS, Wu Z, Shaw AS, Piwnica-Worms H. Mitotic and G2 checkpoint control: regulation of 14-3-3 protein binding by phosphorylation of Cdc25C on serine-216. Science 1997; 277:1501-1505.

115. Zeng Y, Forbes KC, Wu Z, Moreno S, Piwnica-Worms H, Enoch T. Replication checkpoint requires phosphorylation of the phosphatase Cdc25 by Cds1 or Chk1. Nature 1998; 395:507-510.

116. Baldin V, Pelpel K, Cazales M, Cans C, Ducommun B. Nuclear localization of Cdc25B1 and serine 146 integrity are required for induction of mitosis. J Biol Chem 2002; 277:35176-35182.

117. Cazales M, Schmitt E, Montembault E, Dozier C, Prigent C, Ducommun B. CDC25B phosphorylation by Aurora-A occurs at the G2/M transition and is inhibited by DNA damage. Cell Cycle 2005; 4:1233-1238.

118. Schmitt E, Boutros R, Froment C, Monsarrat B, Ducommun B, Dozier C. CHK1 phosphorylates CDC25B during the cell cycle in the absence of DNA damage. J Cell Sci 2006; 119:4269-4275.

119. Matsuoka S, Ballif BA, Smogorzewska A, McDonald ER, 3rd, Hurov KE, Luo J, Bakalarski CE, Zhao Z, Solimini N, Lerenthal Y, Shiloh Y, Gygi SP, Elledge SJ. ATM and ATR substrate analysis reveals extensive protein networks responsive to DNA damage. Science 2007; 316:1160-1166.

120. Gavet O, Pines J. Progressive activation of CyclinB1-Cdk1 coordinates entry to mitosis. Dev Cell 2010; 18:533-543.

121. Gavet O, Pines J. Activation of cyclin B1-Cdk1 synchronizes events in the nucleus and the cytoplasm at mitosis. J Cell Biol 2010; 189:247-259.

122. Mailand N, Falck J, Lukas C, Syljuasen RG, Welcker M, Bartek J, Lukas J. Rapid destruction of human Cdc25A in response to DNA damage. Science 2000; 288:1425-1429.

123. Bernardi R, Liebermann DA, Hoffman B. Cdc25A stability is controlled by the ubiquitin-proteasome pathway during cell cycle progression and terminal differentiation. Oncogene 2000; 19:2447-2454.

124. Donzelli M, Squatrito M, Ganoth D, Hershko A, Pagano M, Draetta GF. Dual mode of degradation of Cdc25 A phosphatase. EMBO J 2002; 21:4875-4884.

125. Jin J, Shirogane T, Xu L, Nalepa G, Qin J, Elledge SJ, Harper JW. SCFbeta-TRCP links Chk1 signaling to degradation of the Cdc25A protein phosphatase. Genes Dev 2003; 17:3062-3074.

126. Busino L, Chiesa M, Draetta GF, Donzelli M. Cdc25A phosphatase: combinatorial phosphorylation, ubiquitylation and proteolysis. Oncogene 2004; 23:2050-2056.

127. Donzelli M, Busino L, Chiesa M, Ganoth D, Hershko A, Draetta GF. Hierarchical order of phosphorylation events commits Cdc25A to betaTrCP-dependent degradation. Cell Cycle 2004; 3:469-471.

128. Kanemori Y, Uto K, Sagata N. Beta-TrCP recognizes a previously undescribed nonphosphorylated destruction motif in Cdc25A and Cdc25B phosphatases. Proc Natl Acad Sci USA 2005; 102:6279-6284.

129. van Vugt MA, Smits VA, Klompmaker R, Medema RH. Inhibition of Polo-like kinase-1 by DNA damage occurs in an ATM- or ATR-dependent fashion. J Biol Chem 2001; 276:41656-41660.

130. Deming PB, Flores KG, Downes CS, Paules RS, Kaufmann WK. ATR enforces the topoisomerase II-dependent G2 checkpoint through inhibition of Plk1 kinase. J Biol Chem 2002; 277:36832-36838.

131. Smits VA, Klompmaker R, Arnaud L, Rijksen G, Nigg EA, Medema RH. Polo-like kinase-1 is a target of the DNA damage checkpoint. Nat Cell Biol 2000; 2:672-676.

132. Toyoshima-Morimoto F, Taniguchi E, Shinya N, Iwamatsu A, Nishida E. Polo-like kinase 1 phosphorylates cyclin B1 and targets it to the nucleus during prophase. Nature 2001; 410:215-220.

133. Yuan J, Eckerdt F, Bereiter-Hahn J, Kurunci-Csacsko E, Kaufmann M, Strebhardt K. Cooperative phosphorylation including the activity of polo-like kinase 1 regulates the subcellular localization of cyclin B1. Oncogene 2002; 21:8282-8292.

134. Tsvetkov L, Stern DF. Phosphorylation of Plk1 at S137 and T210 is inhibited in response to DNA damage. Cell Cycle 2005; 4:166-171.

135. Bartek J, Lukas J. DNA damage checkpoints: from initiation to recovery or adaptation. Curr Opin Cell Biol 2007.

136. Archambault V, Glover DM. Polo-like kinases: conservation and divergence in their functions and regulation. Nat Rev Mol Cell Biol 2009; 10:265-275.

137. Jackman M, Lindon C, Nigg EA, Pines J. Active cyclin B1-Cdk1 first appears on centrosomes in prophase. Nat Cell Biol 2003; 5:143-148.

138. Qian YW, Erikson E, Taieb FE, Maller JL. The polo-like kinase Plx1 is required for activation of the phosphatase Cdc25C and cyclin B-Cdc2 in Xenopus oocytes. Mol Biol Cell 2001; 12:1791-1799.

139. Toyoshima-Morimoto F, Taniguchi E, Nishida E. Plk1 promotes nuclear translocation of human Cdc25C during prophase. EMBO Rep 2002; 3:341-348.

140. van Vugt MA, Bras A, Medema RH. Polo-like kinase-1 controls recovery from a G2 DNA damage-induced arrest in mammalian cells. Mol Cell 2004; 15:799-811.

141. Mamely I, van Vugt MA, Smits VA, Semple JI, Lemmens B, Perrakis A, Medema RH, Freire R. Polo-like kinase-1 controls proteasome-dependent degradation of Claspin during checkpoint recovery. Curr Biol 2006; 16:1950-1955.

142. Macurek L, Lindqvist A, Lim D, Lampson MA, Klompmaker R, Freire R, Clouin C, Taylor SS, Yaffe MB, Medema RH. Polo-like kinase-1 is activated by aurora A to promote checkpoint recovery. Nature 2008; 455:119-123.

143. Fu Z, Malureanu L, Huang J, Wang W, Li H, van Deursen JM, Tindall DJ, Chen J. Plk1-dependent phosphorylation of FoxM1 regulates a transcriptional programme required for mitotic progression. Nat Cell Biol 2008; 10:1076-1082.

144. Ouyang B, Li W, Pan H, Meadows J, Hoffmann I, Dai W. The physical association and phosphorylation of Cdc25C protein phosphatase by Prk. Oncogene 1999; 18:6029-6036.

145. Xie S, Wu H, Wang Q, Cogswell JP, Husain I, Conn C, Stambrook P, Jhanwar-Uniyal M, Dai W. Plk3 functionally links DNA damage to cell cycle arrest and apoptosis at least in part via the p53 pathway. J Biol Chem 2001; 276:43305-43312.

146. Allday MJ, Inman GJ, Crawford DH, Farrell PJ. DNA damage in human B cells can induce apoptosis, proceeding from G1/S when p53 is transactivation competent and G2/M when it is transactivation defective. EMBO J 1995; 14:4994-5005.

147. Powell SN, DeFrank JS, Connell P, Eogan M, Preffer F, Dombkowski D, Tang W, Friend S. Differential sensitivity of p53(-) and p53(+) cells to caffeine-induced radiosensitization and override of G2 delay. Cancer Res 1995; 55:1643-1648.

148. Stewart N, Hicks GG, Paraskevas F, Mowat M. Evidence for a second cell cycle block at G2/M by p53. Oncogene 1995; 10:109-115.

149. Morgan SE, Kastan MB. p53 and ATM: cell cycle, cell death, and cancer. Adv Cancer Res 1997; 71:1-25.

150. Schmidt-Kastner PK, Jardine K, Cormier M, McBurney MW. Absence of p53-dependent cell cycle regulation in pluripotent mouse cell lines. Oncogene 1998; 16:3003-3011.

151. Ceraline J, Deplanque G, Duclos B, Limacher JM, Hajri A, Noel F, Orvain C, Frebourg T, Klein-Soyer C, Bergerat JP. Inactivation of p53 in normal human cells increases G2/M arrest and sensitivity to DNA-damaging agents. Int J Cancer 1998; 75:432-438.

152. Waterman MJF, Stavridi ES, Waterman JLF, Halazonetis TD. ATM-dependent activation of p53 involves dephosphorylation and association with 14-3-3 proteins. Nature Genet 1998; 19:175-178.

153. Schwartz D, Rotter V. p53-dependent cell cycle control: response to genotoxic stress. Semin Cancer Biol 1998; 8:325-336.

154. Wang XW, Zhan Q, Coursen JD, Khan MA, Kontny HU, Yu L, Hollander MC, O'Connor PM, Fornace AJ, Jr., Harris CC. GADD45 induction of a G2/M cell cycle checkpoint. Proc Natl Acad Sci USA 1999; 96:3706-3711.

155. Bache M, Dunst J, Wurl P, Frode D, Meye A, Schmidt H, Rath FW, Taubert H. G2/M checkpoint is p53-dependent and independent after irradiation in five human sarcoma cell lines. Anticancer Res 1999; 19:1827-1832.

156. Taylor WR, Stark GR. Regulation of the G2/M transition by p53. Oncogene 2001; 20:1803-1815.

157. Stark GR, Taylor WR. Analyzing the G2/M checkpoint. Methods Mol Biol 2004; 280:51-82.

158. Stark GR, Taylor WR. Control of the G2/M transition. Mol Biotechnol 2006; 32:227-248.

159. Schmitt E, Paquet C, Beauchemin M, Bertrand R. DNA-damage response network at the crossroads of cell-cycle checkpoints, cellular senescence and apoptosis. J Zhejiang Univ Sci B 2007; 8:377-397.

160. Slichenmyer WJ, Nelson WG, Slebos RJ, Kastan MB. Loss of a p53-associated G1 checkpoint does not decrease cell survival following DNA damage. Cancer Res 1993; 53:4164-4168.

161. Deng C, Zhang P, Harper JW, Elledge SJ, Leder P. Mice lacking p21CIP1/WAF1 undergo normal development, but are defective in G1 checkpoint control. Cell 1995; 82:675-684.

162. Bae I, Fan S, Bhatia K, Kohn KW, Fornace AJ, Jr., O'Connor PM. Relationships between G1 arrest and stability of the p53 and p21Cip1/Waf1 proteins following gamma-irradiation of human lymphoma cells. Cancer Res 1995; 55:2387-2393.

163. Dubspoterszman MC, Tocque B, Wasylyk B. Mdm2 transformation In the absence of p53 and abrogation of the p107 G1 cell-cycle arrest. Oncogene 1995; 11:2445-2449.

164. Waldman T, Kinzler KW, Vogelstein B. P21 is necessary for the p53-mediated G(1) arrest In human cancer cells. Cancer Res 1995; 55:5187-5190.

165. Delsal G, Murphy M, Ruaro EM, Lazarevic D, Levine AJ, Schneider C. Cyclin D1 and P21/Waf1 are both involved in p53 growth suppression. Oncogene 1996; 12:177-185.

166. O'Connor PM. Mammalian G1 and G2 phase checkpoints. Cancer Surv 1997; 29:151-182.

167. Bissonnette N, Hunting DJ. P21-induced cycle arrest in G(1) protects cells from apoptosis induced by Uv-irradiation or RNA polymerase II blockage. Oncogene 1998; 16:3461-3469.

168. Wang XW, Zhan Q, Coursen JD, Khan MA, Kontny HU, Yu L, Hollander MC, O'Connor PM, Fornace AJ, Jr., Harris CC. GADD45 induction of a G2/M cell cycle checkpoint. Proc Natl Acad Sci USA 1999; 96:3706-3711.

169. Aliouat-Denis CM, Dendouga N, Van den Wyngaert I, Goehlmann H, Steller U, van de Weyer I, Van Slycken N, Andries L, Kass S, Luyten W, Janicot M, Vialard JE. p53-independent regulation of p21Waf1/Cip1 expression and senescence by Chk2. Mol Cancer Res 2005; 3:627-634.

170. Rodriguez R, Meuth M. Chk1 and p21 cooperate to prevent apoptosis during DNA replication fork stress. Mol Biol Cell 2006; 17:402-412.

171. Jin L, Williamson A, Banerjee S, Philipp I, Rape M. Mechanism of ubiquitin-chain formation by the human anaphase-promoting complex. Cell 2008; 133:653-665.

172. Taylor SS, Scott MI, Holland AJ. The spindle checkpoint: a quality control mechanism which ensures accurate chromosome segregation. Chromosome Res 2004; 12:599-616.

173. Hartwell LH, Culotti J, Reid B. Genetic control of the cell-division cycle in yeast. I. Detection of mutants. Proc Natl Acad Sci USA 1970; 66:352-359.

174. Hartwell LH, Mortimer RK, Culotti J, Culotti M. Genetic control of the cell division cycle in yeast: V. Genetic analysis of cdc mutants. Genetics 1973; 74:267-286.

175. Weinstein J, Jacobsen FW, Hsu-Chen J, Wu T, Baum LG. A novel mammalian protein, p55CDC, present in dividing cells is associated with protein kinase activity and has homology to the Saccharomyces cerevisiae cell division cycle proteins Cdc20 and Cdc4. Mol Cell Biol 1994; 14:3350-3363.

176. Weinstein J. Cell cycle-regulated expression, phosphorylation, and degradation of p55Cdc. A mammalian homolog of CDC20/Fizzy/slp1. J Biol Chem 1997; 272:28501-28511.

177. Yamasaki L, Pagano M. Cell cycle, proteolysis and cancer. Curr Opin Cell Biol 2004; 16:623-628.

178. Nakayama KI, Nakayama K. Ubiquitin ligases: cell-cycle control and cancer. Nat Rev Cancer 2006; 6:369-381.

179. Reed SI. The ubiquitin-proteasome pathway in cell cycle control. Results Probl Cell Differ 2006; 42:147-181.

180. Shirayama M, Toth A, Galova M, Nasmyth K. APC(Cdc20) promotes exit from mitosis by destroying the anaphase inhibitor Pds1 and cyclin Clb5. Nature 1999; 402:203-207.

181. Zur A, Brandeis M. Securin degradation is mediated by fzy and fzr, and is required for complete chromatid separation but not for cytokinesis. EMBO J 2001; 20:792-801.

182. Zur A, Brandeis M. Timing of APC/C substrate degradation is determined by fzy/fzr specificity of destruction boxes. EMBO J 2002; 21:4500-4510.

183. Irniger S. Cyclin destruction in mitosis: a crucial task of Cdc20. FEBS Lett 2002; 532:7-11.

184. Yamano H, Gannon J, Mahbubani H, Hunt T. Cell cycle-regulated recognition of the destruction box of cyclin B by the APC/C in Xenopus egg extracts. Mol Cell 2004; 13:137-147.

185. Wasch R, Engelbert D. Anaphase-promoting complex-dependent proteolysis of cell cycle regulators and genomic instability of cancer cells. Oncogene 2005; 24:1-10.

186. Yamamoto TM, Iwabuchi M, Ohsumi K, Kishimoto T. APC/C-Cdc20-mediated degradation of cyclin B participates in CSF arrest in unfertilized Xenopus eggs. Dev Biol 2005; 279:345-355.

187. Zachariae W. Destruction with a box: substrate recognition by the anaphase-promoting complex. Mol Cell 2004; 13:2-3.

188. Fry AM, Yamano H. APC/C-mediated degradation in early mitosis: how to avoid spindle assembly checkpoint inhibition. Cell Cycle 2006; 5:1487-1491.

189. Lindon C. Control of mitotic exit and cytokinesis by the APC/C. Biochem Soc Trans 2008; 36:405-410.

190. Marangos P, Carroll J. Securin regulates entry into M-phase by modulating the stability of cyclin B. Nat Cell Biol 2008; 10:445-451.

191. Stemmann O, Zou H, Gerber SA, Gygi SP, Kirschner MW. Dual inhibition of sister chromatid separation at metaphase. Cell 2001; 107:715-726.

192. Wheatley SP, Hinchcliffe EH, Glotzer M, Hyman AA, Sluder G, Wang Y. CDK1 inactivation regulates anaphase spindle dynamics and cytokinesis in vivo. J Cell Biol 1997; 138:385-393.

193. Wolf F, Wandke C, Isenberg N, Geley S. Dose-dependent effects of stable cyclin B1 on progression through mitosis in human cells. EMBO J 2006; 25:2802-2813.

194. Wolf F, Sigl R, Geley S. The end of the beginning: cdk1 thresholds and exit from mitosis. Cell Cycle 2007; 6:1408-1411.

195. Ditchfield C, Johnson VL, Tighe A, Ellston R, Haworth C, Johnson T, Mortlock A, Keen N, Taylor SS. Aurora B couples chromosome alignment with anaphase by targeting BubR1, Mad2, and Cenp-E to kinetochores. J Cell Biol 2003; 161:267-280.

196. Johnson VL, Scott MI, Holt SV, Hussein D, Taylor SS. Bub1 is required for kinetochore localization of BubR1, Cenp-E, Cenp-F and Mad2, and chromosome congression. J Cell Sci 2004; 117:1577-1589.

197. Lou Y, Yao J, Zereshki A, Dou Z, Ahmed K, Wang H, Hu J, Wang Y, Yao X. NEK2A interacts with MAD1 and possibly functions as a novel integrator of the spindle checkpoint signaling. J Biol Chem 2004; 279:20049-20057.

198. Morrow CJ, Tighe A, Johnson VL, Scott MI, Ditchfield C, Taylor SS. Bub1 and aurora B cooperate to maintain BubR1-mediated inhibition of APC/CCdc20. J Cell Sci 2005; 118:3639-3652.

199. Zhao Y, Chen RH. Mps1 phosphorylation by MAP kinase is required for kinetochore localization of spindle-checkpoint proteins. Curr Biol 2006; 16:1764-1769.

200. Wong OK, Fang G. Cdk1 phosphorylation of BubR1 controls spindle checkpoint arrest and Plk1-mediated formation of the 3F3/2 epitope. J Cell Biol 2007; 179:611-617.

201. Chen Q, Zhang X, Jiang Q, Clarke PR, Zhang C. Cyclin B1 is localized to unattached kinetochores and contributes to efficient microtubule attachment and proper chromosome alignment during mitosis. Cell Res 2008; 18:268-280.

202. Abrieu A, Magnaghi-Jaulin L, Kahana JA, Peter M, Castro A, Vigneron S, Lorca T, Cleveland DW, Labbe JC. Mps1 is a kinetochore-associated kinase essential for the vertebrate mitotic checkpoint. Cell 2001; 106:83-93.

203. Kang J, Chen Y, Zhao Y, Yu H. Autophosphorylation-dependent activation of human Mps1 is required for the spindle checkpoint. Proc Natl Acad Sci USA 2007; 104:20232-20237.

204. Tighe A, Staples O, Taylor S. Mps1 kinase activity restrains anaphase during an unperturbed mitosis and targets Mad2 to kinetochores. J Cell Biol 2008; 181:893-901.

205. Hauf S. Mps1 checks up on chromosome attachment. Cell 2008; 132:181-182.
206. Jelluma N, Brenkman AB, van den Broek NJ, Cruijsen CW, van Osch MH, Lens SM, Medema RH, Kops GJ. Mps1 phosphorylates Borealin to control Aurora B activity and chromosome alignment. Cell 2008; 132:233-246.
207. Xu Q, Zhu S, Wang W, Zhang X, Old W, Ahn N, Liu X. Regulation of kinetochore recruitment of two essential mitotic spindle checkpoint proteins by Mps1 phosphorylation. Mol Biol Cell 2009; 20:10-20.
208. Zachos G, Black EJ, Walker M, Scott MT, Vagnarelli P, Earnshaw WC, Gillespie DA. Chk1 is required for spindle checkpoint function. Dev Cell 2007; 12:247-260.
209. Peddibhotla S, Lam MH, Gonzalez-Rimbau M, Rosen JM. The DNA-damage effector checkpoint kinase 1 is essential for chromosome segregation and cytokinesis. Proc Natl Acad Sci USA 2009.
210. Taylor SS, McKeon F. Kinetochore localization of murine Bub1 is required for normal mitotic timing and checkpoint response to spindle damage. Cell 1997; 89:727-735.
211. Adams RR, Carmena M, Earnshaw WC. Chromosomal passengers and the (aurora) ABCs of mitosis. Trends Cell Biol 2001; 11:49-54.
212. Schwab MS, Roberts BT, Gross SD, Tunquist BJ, Taieb FE, Lewellyn AL, Maller JL. Bub1 is activated by the protein kinase p90(Rsk) during Xenopus oocyte maturation. Curr Biol 2001; 11:141-150.
213. Chen RH. Phosphorylation and activation of Bub1 on unattached chromosomes facilitate the spindle checkpoint. EMBO J 2004; 23:3113-3121.
214. Qi W, Tang Z, Yu H. Phosphorylation- and polo-box-dependent binding of Plk1 to Bub1 is required for the kinetochore localization of Plk1. Mol Biol Cell 2006; 17:3705-3716.
215. Zhang X, Lan W, Ems-McClung SC, Stukenberg PT, Walczak CE. Aurora B phosphorylates multiple sites on mitotic centromere-associated kinesin to spatially and temporally regulate its function. Mol Biol Cell 2007; 18:3264-3276.
216. Famulski JK, Chan GK. Aurora B kinase-dependent recruitment of hZW10 and hROD to tensionless kinetochores. Curr Biol 2007; 17:2143-2149.
217. Monje-Casas F, Prabhu VR, Lee BH, Boselli M, Amon A. Kinetochore orientation during meiosis is controlled by Aurora B and the monopolin complex. Cell 2007; 128:477-490.
218. Mistry HB, Maccallum DE, Jackson RC, Chaplain MA, Davidson FA. Modeling the temporal evolution of the spindle assembly checkpoint and role of Aurora B kinase. Proc Natl Acad Sci USA 2008; 105:20215-20220.
219. Emanuele MJ, Lan W, Jwa M, Miller SA, Chan CS, Stukenberg PT. Aurora B kinase and protein phosphatase 1 have opposing roles in modulating kinetochore assembly. J Cell Biol 2008; 181:241-254.
220. Liu D, Lampson MA. Regulation of kinetochore-microtubule attachments by Aurora B kinase. Biochem Soc Trans 2009; 37:976-980.

221. Xu Z, Ogawa H, Vagnarelli P, Bergmann JH, Hudson DF, Ruchaud S, Fukagawa T, Earnshaw WC, Samejima K. INCENP-aurora B interactions modulate kinase activity and chromosome passenger complex localization. J Cell Biol 2009; 187:637-653.

222. Spankuch-Schmitt B, Bereiter-Hahn J, Kaufmann M, Strebhardt K. Effect of RNA silencing of Polo-like kinase-1 (PLK1) on apoptosis and spindle formation in human cancer cells. J Natl Cancer Inst 2002; 94:1863-1877.

223. Santamaria A, Neef R, Eberspacher U, Eis K, Husemann M, Mumberg D, Prechtl S, Schulze V, Siemeister G, Wortmann L, Barr FA, Nigg EA. Use of the novel Plk1 inhibitor ZK-thiazolidinone to elucidate functions of Plk1 in early and late stages of mitosis. Mol Biol Cell 2007; 18:4024-4036.

224. Lee KS, Oh DY, Kang YH, Park JE. Self-regulated mechanism of Plk1 localization to kinetochores: lessons from the Plk1-PBIP1 interaction. Cell Div 2008; 3:4.

225. Seki A, Coppinger JA, Du H, Jang CY, Yates JR, 3rd, Fang G. Plk1- and {beta}-TrCP-dependent degradation of Bora controls mitotic progression. J Cell Biol 2008; 181:65-78.

226. Seki A, Coppinger JA, Jang CY, Yates JR, Fang G. Bora and the kinase Aurora a cooperatively activate the kinase Plk1 and control mitotic entry. Science 2008; 320:1655-1658.

227. Margottin-Goguet F, Hsu JY, Loktev A, Hsieh HM, Reimann JD, Jackson PK. Prophase destruction of Emi1 by the SCF(betaTrCP/Slimb) ubiquitin ligase activates the anaphase promoting complex to allow progression beyond prometaphase. Dev Cell 2003; 4:813-826.

228. Miller JJ, Summers MK, Hansen DV, Nachury MV, Lehman NL, Loktev A, Jackson PK. Emi1 stably binds and inhibits the anaphase-promoting complex/cyclosome as a pseudosubstrate inhibitor. Genes Dev 2006; 20:2410-2420.

229. Reimann JD, Freed E, Hsu JY, Kramer ER, Peters JM, Jackson PK. Emi1 is a mitotic regulator that interacts with Cdc20 and inhibits the anaphase promoting complex. Cell 2001; 105:645-655.

230. Reimann JD, Gardner BE, Margottin-Goguet F, Jackson PK. Emi1 regulates the anaphase-promoting complex by a different mechanism than Mad2 proteins. Genes Dev 2001; 15:3278-3285.

231. Baumann C, Korner R, Hofmann K, Nigg EA. PICH, a centromere-associated SNF2 family ATPase, is regulated by Plk1 and required for the spindle checkpoint. Cell 2007; 128:101-114.

232. Hames RS, Wattam SL, Yamano H, Bacchieri R, Fry AM. APC/C-mediated destruction of the centrosomal kinase Nek2A occurs in early mitosis and depends upon a cyclin A-type D-box. EMBO J 2001; 20:7117-7127.

233. Lukas J, Lukas C, Bartek J. Mammalian cell cycle checkpoints: signalling pathways and their organization in space and time. DNA Repair (Amst) 2004; 3:997-1007.

234. Draviam VM, Stegmeier F, Nalepa G, Sowa ME, Chen J, Liang A, Hannon GJ, Sorger PK, Harper JW, Elledge SJ. A functional genomic screen identifies a role for TAO1 kinase in spindle-checkpoint signalling. Nat Cell Biol 2007; 9:556-564.

235. Zich J, Hardwick KG. Getting down to the phosphorylated 'nuts and bolts' of spindle checkpoint signalling. Trends Biochem Sci 2010; 35:18-27.

236. Liu T, Rohn JL, Picone R, Kunda P, Baum B. Tao-1 is a negative regulator of microtubule plus-end growth. J Cell Sci 2010; 123:2708-2716.

237. Tang Z, Shu H, Oncel D, Chen S, Yu H. Phosphorylation of Cdc20 by Bub1 provides a catalytic mechanism for APC/C inhibition by the spindle checkpoint. Mol Cell 2004; 16:387-397.

238. Vanoosthuyse V, Hardwick KG. Bub1 and the multilayered inhibition of Cdc20-APC/C in mitosis. Trends Cell Biol 2005; 15:231-233.

239. Kallio M, Weinstein J, Daum JR, Burke DJ, Gorbsky GJ. Mammalian p55CDC mediates association of the spindle checkpoint protein Mad2 with the cyclosome/anaphase-promoting complex, and is involved in regulating anaphase onset and late mitotic events. J Cell Biol 1998; 141:1393-1406.

240. Fang G, Yu H, Kirschner MW. The checkpoint protein MAD2 and the mitotic regulator CDC20 form a ternary complex with the anaphase-promoting complex to control anaphase initiation. Genes Dev 1998; 12:1871-1883.

241. Luo X, Tang Z, Xia G, Wassmann K, Matsumoto T, Rizo J, Yu H. The Mad2 spindle checkpoint protein has two distinct natively folded states. Nat Struct Mol Biol 2004; 11:338-345.

242. Luo X, Yu H. Purification and assay of Mad2: a two-state inhibitor of anaphase-promoting complex/cyclosome. Methods Enzymol 2005; 398:246-255.

243. Wassmann K, Liberal V, Benezra R. Mad2 phosphorylation regulates its association with Mad1 and the APC/C. EMBO J 2003; 22:797-806.

244. Mapelli M, Massimiliano L, Santaguida S, Musacchio A. The Mad2 conformational dimer: structure and implications for the spindle assembly checkpoint. Cell 2007; 131:730-743.

245. Yu H. Structural activation of Mad2 in the mitotic spindle checkpoint: the two-state Mad2 model versus the Mad2 template model. J Cell Biol 2006; 173:153-157.

246. Shah JV, Cleveland DW. Waiting for anaphase: Mad2 and the spindle assembly checkpoint. Cell 2000; 103:997-1000.

247. Sironi L, Mapelli M, Knapp S, De Antoni A, Jeang KT, Musacchio A. Crystal structure of the tetrameric Mad1-Mad2 core complex: implications of a 'safety belt' binding mechanism for the spindle checkpoint. EMBO J 2002; 21:2496-2506.

248. Howell BJ, Moree B, Farrar EM, Stewart S, Fang G, Salmon ED. Spindle checkpoint protein dynamics at kinetochores in living cells. Curr Biol 2004; 14:953-964.

249. De Antoni A, Pearson CG, Cimini D, Canman JC, Sala V, Nezi L, Mapelli M, Sironi L, Faretta M, Salmon ED, Musacchio A. The Mad1/Mad2 complex as a template for Mad2 activation in the spindle assembly checkpoint. Curr Biol 2005; 15:214-225.

250. Nezi L, Rancati G, De Antoni A, Pasqualato S, Piatti S, Musacchio A. Accumulation of Mad2-Cdc20 complex during spindle checkpoint activation requires binding of open and closed conformers of Mad2 in Saccharomyces cerevisiae. J Cell Biol 2006; 174:39-51.

251. Vink M, Simonetta M, Transidico P, Ferrari K, Mapelli M, De Antoni A, Massimiliano L, Ciliberto A, Faretta M, Salmon ED, Musacchio A. In vitro FRAP identifies the minimal requirements for Mad2 kinetochore dynamics. Curr Biol 2006; 16:755-766.

252. Simonetta M, Manzoni R, Mosca R, Mapelli M, Massimiliano L, Vink M, Novak B, Musacchio A, Ciliberto A. The influence of catalysis on mad2 activation dynamics. PLoS Biol 2009; 7:e10.

253. Wu H, Lan Z, Li W, Wu S, Weinstein J, Sakamoto KM, Dai W. p55CDC/hCDC20 is associated with BUBR1 and may be a downstream target of the spindle checkpoint kinase. Oncogene 2000; 19:4557-4562.

254. Tang Z, Bharadwaj R, Li B, Yu H. Mad2-independent inhibition of APCCdc20 by the mitotic checkpoint protein BubR1. Dev Cell 2001; 1:227-237.

255. Sudakin V, Chan GK, Yen TJ. Checkpoint inhibition of the APC/C in HeLa cells is mediated by a complex of BUBR1, BUB3, CDC20, and MAD2. J Cell Biol 2001; 154:925-936.

256. Fang G. Checkpoint protein BubR1 acts synergistically with Mad2 to inhibit anaphase-promoting complex. Mol Biol Cell 2002; 13:755-766.

257. Shannon KB, Canman JC, Salmon ED. Mad2 and BubR1 function in a single checkpoint pathway that responds to a loss of tension. Mol Biol Cell 2002; 13:3706-3719.

258. Dai W, Wang Q, Liu T, Swamy M, Fang Y, Xie S, Mahmood R, Yang YM, Xu M, Rao CV. Slippage of mitotic arrest and enhanced tumor development in mice with BubR1 haploinsufficiency. Cancer Res 2004; 64:440-445.

259. Yu H, Tang Z. Bub1 multitasking in mitosis. Cell Cycle 2005; 4:262-265.

260. Perera D, Tilston V, Hopwood JA, Barchi M, Boot-Handford RP, Taylor SS. Bub1 maintains centromeric cohesion by activation of the spindle checkpoint. Dev Cell 2007; 13:566-579.

261. Saitoh S, Kobayashi Y, Ogiyama Y, Takahashi K. Dual regulation of Mad2 localization on kinetochores by Bub1 and Dam1/DASH that ensure proper spindle interaction. Mol Biol Cell 2008; 19:3885-3897.

262. Kulukian A, Han JS, Cleveland DW. Unattached kinetochores catalyze production of an anaphase inhibitor that requires a Mad2 template to prime Cdc20 for BubR1 binding. Dev Cell 2009; 16:105-117.

263. King EM, van der Sar SJ, Hardwick KG. Mad3 KEN boxes mediate both Cdc20 and Mad3 turnover, and are critical for the spindle checkpoint. PLoS ONE 2007; 2:e342.

264. Pan J, Chen RH. Spindle checkpoint regulates Cdc20p stability in Saccharomyces cerevisiae. Genes Dev 2004; 18:1439-1451.

265. Reddy SK, Rape M, Margansky WA, Kirschner MW. Ubiquitination by the anaphase-promoting complex drives spindle checkpoint inactivation. Nature 2007; 446:921-925.

266. Nilsson J, Yekezare M, Minshull J, Pines J. The APC/C maintains the spindle assembly checkpoint by targeting Cdc20 for destruction. Nat Cell Biol 2008; 10:1411-1420.

267. Xia G, Luo X, Habu T, Rizo J, Matsumoto T, Yu H. Conformation-specific binding of p31(comet) antagonizes the function of Mad2 in the spindle checkpoint. EMBO J 2004; 23:3133-3143.

268. Yang M, Li B, Tomchick DR, Machius M, Rizo J, Yu H, Luo X. p31comet blocks Mad2 activation through structural mimicry. Cell 2007; 131:744-755.

269. Stegmeier F, Rape M, Draviam VM, Nalepa G, Sowa ME, Ang XL, McDonald ER, 3rd, Li MZ, Hannon GJ, Sorger PK, Kirschner MW, Harper JW, Elledge SJ. Anaphase initiation is regulated by antagonistic ubiquitination and deubiquitination activities. Nature 2007; 446:876-881.

270. Howell BJ, Hoffman DB, Fang G, Murray AW, Salmon ED. Visualization of Mad2 dynamics at kinetochores, along spindle fibers, and at spindle poles in living cells. J Cell Biol 2000; 150:1233-1250.

271. Howell BJ, McEwen BF, Canman JC, Hoffman DB, Farrar EM, Rieder CL, Salmon ED. Cytoplasmic dynein/dynactin drives kinetochore protein transport to the spindle poles and has a role in mitotic spindle checkpoint inactivation. J Cell Biol 2001; 155:1159-1172.

272. Hoffman DB, Pearson CG, Yen TJ, Howell BJ, Salmon ED. Microtubule-dependent changes in assembly of microtubule motor proteins and mitotic spindle checkpoint proteins at PtK1 kinetochores. Mol Biol Cell 2001; 12:1995-2009.

273. Holmfeldt P, Larsson N, Segerman B, Howell B, Morabito J, Cassimeris L, Gullberg M. The catastrophe-promoting activity of ectopic Op18/stathmin is required for disruption of mitotic spindles but not interphase microtubules. Mol Biol Cell 2001; 12:73-83.

274. Griffis ER, Stuurman N, Vale RD. Spindly, a novel protein essential for silencing the spindle assembly checkpoint, recruits dynein to the kinetochore. J Cell Biol 2007; 177:1005-1015.

275. Mische S, He Y, Ma L, Li M, Serr M, Hays TS. Dynein light intermediate chain: an essential subunit that contributes to spindle checkpoint inactivation. Mol Biol Cell 2008; 19:4918-4929.

276. Vanoosthuyse V, Hardwick KG. Overcoming inhibition in the spindle checkpoint. Genes Dev 2009; 23:2799-2805.

277. Vanoosthuyse V, Hardwick KG. A novel protein phosphatase 1-dependent spindle checkpoint silencing mechanism. Curr Biol 2009; 19:1176-1181.

278. Vanoosthuyse V, Meadows JC, van der Sar SJ, Millar JB, Hardwick KG. Bub3p facilitates spindle checkpoint silencing in fission yeast. Mol Biol Cell 2009; 20:5096-5105.

279. Pollard TD. Mechanics of cytokinesis in eukaryotes. Curr Opin Cell Biol 2010; 22:50-56.

280. Wasch R, Cross FR. APC-dependent proteolysis of the mitotic cyclin Clb2 is essential for mitotic exit. Nature 2002; 418:556-562.

281. Sullivan M, Morgan DO. Finishing mitosis, one step at a time. Nat Rev Mol Cell Biol 2007; 8:894-903.

282. Parry DH, Hickson GR, O'Farrell PH. Cyclin B destruction triggers changes in kinetochore behavior essential for successful anaphase. Curr Biol 2003; 13:647-653.

283. Visintin R, Prinz S, Amon A. CDC20 and CDH1: a family of substrate-specific activators of APC-dependent proteolysis. Science 1997; 278:460-463.

284. Kramer ER, Scheuringer N, Podtelejnikov AV, Mann M, Peters JM. Mitotic regulation of the APC activator proteins CDC20 and CDH1. Mol Biol Cell 2000; 11:1555-1569.

285. Pfleger CM, Lee E, Kirschner MW. Substrate recognition by the Cdc20 and Cdh1 components of the anaphase-promoting complex. Genes Dev 2001; 15:2396-2407.

286. Wan Y, Kirschner MW. Identification of multiple CDH1 homologues in vertebrates conferring different substrate specificities. Proc Natl Acad Sci USA 2001; 98:13066-13071.

287. Hagting A, Den Elzen N, Vodermaier HC, Waizenegger IC, Peters JM, Pines J. Human securin proteolysis is controlled by the spindle checkpoint and reveals when the APC/C switches from activation by Cdc20 to Cdh1. J Cell Biol 2002; 157:1125-1137.

288. Kraft C, Vodermaier HC, Maurer-Stroh S, Eisenhaber F, Peters JM. The WD40 propeller domain of Cdh1 functions as a destruction box receptor for APC/C substrates. Mol Cell 2005; 18:543-553.

289. Robbins JA, Cross FR. Regulated degradation of the APC coactivator Cdc20. Cell Div 2010; 5:23.

290. Raff JW, Jeffers K, Huang JY. The roles of Fzy/Cdc20 and Fzr/Cdh1 in regulating the destruction of cyclin B in space and time. J Cell Biol 2002; 157:1139-1149.

291. Floyd S, Pines J, Lindon C. APC/C Cdh1 targets aurora kinase to control reorganization of the mitotic spindle at anaphase. Curr Biol 2008; 18:1649-1658.

292. Gruneberg U, Neef R, Honda R, Nigg EA, Barr FA. Relocation of Aurora B from centromeres to the central spindle at the metaphase to anaphase transition requires MKlp2. J Cell Biol 2004; 166:167-172.

293. Garcia-Higuera I, Manchado E, Dubus P, Canamero M, Mendez J, Moreno S, Malumbres M. Genomic stability and tumour suppression by the APC/C cofactor Cdh1. Nat Cell Biol 2008; 10:802-811.

294. Taguchi S, Honda K, Sugiura K, Yamaguchi A, Furukawa K, Urano T. Degradation of human Aurora-A protein kinase is mediated by hCdh1. FEBS Lett 2002; 519:59-65.

295. Littlepage LE, Ruderman JV. Identification of a new APC/C recognition domain, the A box, which is required for the Cdh1-dependent destruction of the kinase Aurora-A during mitotic exit. Genes Dev 2002; 16:2274-2285.

296. Gergely F. Mitosis: Cdh1 clears the way for anaphase spindle assembly. Curr Biol 2008; 18:R1009-1012.

297. van Leuken R, Clijsters L, van Zon W, Lim D, Yao X, Wolthuis RM, Yaffe MB, Medema RH, van Vugt MA. Polo-like kinase-1 controls Aurora A destruction by activating APC/C-Cdh1. PLoS ONE 2009; 4:e5282.

298. Cui Y, Cheng X, Zhang C, Zhang Y, Li S, Wang C, Guadagno TM. Degradation of the human mitotic checkpoint kinase Mps1 is cell cycle-regulated by APC-cCdc20 and APC-cCdh1 ubiquitin ligases. J Biol Chem 2010; 285:32988-32998.

299. Hayes MJ, Kimata Y, Wattam SL, Lindon C, Mao G, Yamano H, Fry AM. Early mitotic degradation of Nek2A depends on Cdc20-independent interaction with the APC/C. Nat Cell Biol 2006; 8:607-614.

300. Nguyen HG, Chinnappan D, Urano T, Ravid K. Mechanism of Aurora-B degradation and its dependency on intact KEN and A-boxes: identification of an aneuploidy-promoting property. Mol Cell Biol 2005; 25:4977-4992.

301. Stewart S, Fang G. Destruction box-dependent degradation of aurora B is mediated by the anaphase-promoting complex/cyclosome and Cdh1. Cancer Res 2005; 65:8730-8735.

302. Qi W, Yu H. KEN-box-dependent degradation of the Bub1 spindle checkpoint kinase by the anaphase-promoting complex/cyclosome. J Biol Chem 2007; 282:3672-3679.

303. Li L, Zhou Y, Sun L, Xing G, Tian C, Sun J, Zhang L, He F. NuSAP is degraded by APC/C-Cdh1 and its overexpression results in mitotic arrest dependent of its microtubules' affinity. Cell Signal 2007; 19:2046-2055.

304. Seki A, Fang G. CKAP2 is a spindle-associated protein degraded by APC/C-Cdh1 during mitotic exit. J Biol Chem 2007; 282:15103-15113.

305. Stewart S, Fang G. Anaphase-promoting complex/cyclosome controls the stability of TPX2 during mitotic exit. Mol Cell Biol 2005; 25:10516-10527.

306. Lindon C, Pines J. Ordered proteolysis in anaphase inactivates Plk1 to contribute to proper mitotic exit in human cells. J Cell Biol 2004; 164:233-241.

307. Jiang N, Wang X, Jhanwar-Uniyal M, Darzynkiewicz Z, Dai W. Polo box domain of Plk3 functions as a centrosome localization signal, overexpression of which causes mitotic arrest, cytokinesis defects, and apoptosis. J Biol Chem 2006; 281:10577-10582.

308. Asiedu M, Wu D, Matsumura F, Wei Q. Phosphorylation of MyoGEF on Thr-574 by Plk1 promotes MyoGEF localization to the central spindle J Biol Chem 2008; 283:28392–28400.

309. Wolfe BA, Takaki T, Petronczki M, Glotzer M. Polo-like kinase 1 directs assembly of the HsCyk-4 RhoGAP/Ect2 RhoGEF complex to initiate cleavage furrow formation. PLoS Biol 2009:e1000110.

310. Piekny AJ, Glotzer M. Anillin is a scaffold protein that links RhoA, actin, and myosin during cytokinesis. Curr Biol 2008; 18:30-36.

311. Miller AL, Bement WM. Regulation of cytokinesis by Rho GTPase flux Nat Cell Biol 2009; 11:71-77.

312. Wan J, Xu H, Grunstein M. CDC14 of Saccharomyces cerevisiae. Cloning, sequence analysis, and transcription during the cell cycle. J Biol Chem 1992; 267:11274-11280.

313. Visintin R, Craig K, Hwang ES, Prinz S, Tyers M, Amon A. The phosphatase Cdc14 triggers mitotic exit by reversal of Cdk-dependent phosphorylation. Mol Cell 1998; 2:709-718.

314. Geymonat M, Jensen S, Johnston LH. Mitotic exit: the Cdc14 double cross. Curr Biol 2002; 12:R482-484.

315. Jensen S, Geymonat M, Johnston LH. Mitotic exit: delaying the end without FEAR. Curr Biol 2002; 12:R221-223.

316. Geil C, Schwab M, Seufert W. A nucleolus-localized activator of Cdc14 phosphatase supports rDNA segregation in Yeast mitosis. Curr Biol 2008; 18:1001-1005.

317. Clemente-Blanco A, Mayan-Santos M, Schneider DA, Machin F, Jarmuz A, Tschochner H, Aragon L. Cdc14 inhibits transcription by RNA polymerase I during anaphase. Nature 2009; 458:219-222.

318. Bloom J, Cristea IM, Procko AL, Lubkov V, Chait BT, Snyder M, Cross FR. Global analysis of CDC14 phosphatase reveals diverse roles in mitotic processes. J Biol Chem 2011; 286:5434-5445.

319. Manzoni R, Montani F, Visintin C, Caudron F, Ciliberto A, Visintin R. Oscillations in Cdc14 release and sequestration reveal a circuit underlying mitotic exit. J Cell Biol 2010; 190:209-222.

320. Mocciaro A, Schiebel E. Cdc14: a highly conserved family of phosphatases with non-conserved functions? J Cell Sci 2010; 123:2867-2876.

321. Oliferenko S, Balasubramanian MK. Cell cycle: The Flp side of Cdc14. Curr Biol 2001; 11:R872-874.

322. Trautmann S, McCollum D. Cell cycle: new functions for cdc14 family phosphatases. Curr Biol 2002; 12:R733-R735.

323. Stegmeier F, Amon A. Closing mitosis: the functions of the Cdc14 phosphatase and its regulation. Annu Rev Genet 2004; 38:203-232.

324. Tournebize R, Andersen SS, Verde F, Doree M, Karsenti E, Hyman AA. Distinct roles of PP1 and PP2A-like phosphatases in control of microtubule dynamics during mitosis. Embo J 1997; 16:5537-5549.

325. Bloecher A, Tatchell K. Dynamic localization of protein phosphatase type 1 in the mitotic cell cycle of Saccharomyces cerevisiae. J Cell Biol 2000; 149:125-140.

326. Queralt E, Lehane C, Novak B, Uhlmann F. Downregulation of PP2A(Cdc55) phosphatase by separase initiates mitotic exit in budding yeast. Cell 2006; 125:719-732.

327. Skoufias DA, Indorato RL, Lacroix F, Panopoulos A, Margolis RL. Mitosis persists in the absence of Cdk1 activity when proteolysis or protein phosphatase activity is suppressed. J Cell Biol 2007; 179:671-685.

328. De Wulf P, Montani F, Visintin R. Protein phosphatases take the mitotic stage. Curr Opin Cell Biol 2009; 21:806-815.

329. Wu JQ, Guo JY, Tang W, Yang CS, Freel CD, Chen C, Nairn AC, Kornbluth S. PP1-mediated dephosphorylation of phosphoproteins at mitotic exit is controlled by inhibitor-1 and PP1 phosphorylation. Nat Cell Biol 2009; 11:644-651.

330. Boise LH, Gonzalez-Garcia M, Postema CE, Ding L, Lindsten T, Turka LA, Mao X, Nunez G, Thompson CB. Bcl-x, a bcl-2-related gene that functions as a dominant regulator of apoptotic cell death. Cell 1993; 74:597-608.

331. Nunez G, Merino R, Grillot D, Gonzalez-Garcia M. Bcl-2 and Bcl-x: regulatory switches for lymphoid death and survival. . Immunology Today 1994; 15:582-588.

332. Motoyama N, Wang F, Roth KA, Sawa H, Nakayama K, Nakayama K, Negishi I, Senju S, Zhang Q, Fujii S, Loh DY. Massive cell death of immature hematopoietic cells and neurons in Bcl-x-deficient mice. Science 1995; 267:1506-1510.

333. Ma M, Pena J, Chang B, Margosian E, Davidson L, Alt F, Thompson C. Bclx regulates the survival of double-positive thymocytes. Proc Natl Acad Sci USA 1995; 92:4763-4767.

334. Minn AJ, Rudin CM, Boise LH, Thompson CB. Expression of bcl-xL can confer a multidrug resistance phenotype. Blood 1995; 86:1903-1910.

335. Schott AF, Apel IJ, Nunez G, Clarke MF. Bcl-X(L) protects cancer cells from p53-mediated apoptosis. Oncogene 1995; 11:1389-1394.

336. Park JR, Bernstein ID, Hockenbery DM. Primitive Human Hematopoietic Precursors Express Bcl-X But Not Bcl-2. Blood 1995; 86:868-876.

337. Schlaifer D, March M, Krajewski S, Laurent G, Pris J, Delsol G, Reed JC, Brousset P. High expression of the bcl-x gene in Reed-Sternberg cells of Hodgkin's disease. Blood 1995; 10:2671-2674.

338. Tuscano JM, Druey KM, Riva A, Pena J, Thompson CB, Kehrl JH. Bcl-X Rather Than Bcl-2 Mediates Cd40-Dependent Centrocyte Survival In the Germinal Center. Blood 1996; 88:1359-1364.

339. Michaud GY, Kamesaki H, Cossman J. Expression of Bcl-X in T cells. Leukemia Res 1996; 20:683-691.

340. Minn AJ, Velez P, Schendel SL, Liang H, Muchmore SW, Fesik SW, Fill M, Thompson CB. Bcl-xL forms an ion channel in synthetic lipid membranes. Nature 1997; 385:353-357.

341. Vander Heiden MG, Chandel NS, Williamson EK, Schumacker PT, Thompson CB. Bcl-X(L) regulates the membrane potential and volume homeostasis of mitochondria. Cell 1997; 91:627-637.

342. Olopade OI, Adeyanju MO, Safa AR, Hagos F, Mick R, Thompson CB, Recant WM. Overexpression of Bcl-X protein in primary breast cancer is associated with high tumor grade and nodal metastases. Cancer J 1997; 3:230-237.

343. Sanz C, Benito A, Silva M, Albella B, Richard C, Segovia JC, Insunza A, Bueren JA, Fernandezluna JL. The expression of Bcl-X is downregulated during differentiation of human hematopoietic progenitor cells along the granulocyte but not the monocyte/macrophage lineage. Blood 1997; 89:3199-3204.

344. Sattler M, Liang H, Nettesheim D, Meadows RP, Harlan JE, Eberstadt M, Yoon HS, Shuker SB, Chang BS, Minn AJ, Thompson CB, Fesik SW. Structure of Bcl-x(L)-Bak peptide complex: recognition between regulators of apoptosis. Science 1997; 275:983-986.

345. Parsadanian AS, Cheng Y, Kellerpeck CR, Holtzman DM, Snider WD. Bcl-X(L) is an antiapoptotic regulator for postnatal CNS neurons. J Neuros 1998; 18:1009-1019.

346. Pena JC, Rudin CM, Thompson CB. A Bcl-x(L) transgene promotes malignant conversion of chemically initiated skin papillomas. Cancer Res 1998; 58:2111-2116.

347. Okada S, Zhang H, Hatano M, Tokuhisa T. A physiologic role of Bcl-X(L) induced in activated macrophages. J Immunol 1998; 160:2590-2596.

348. Taylor JK, Zhang QQ, Monia BP, Marcusson EG, Dean NM. Inhibition of Bcl-xL expression sensitizes normal human keratinocytes and epithelial cells to apoptotic stimuli. Oncogene 1999; 18:4495-4504.

349. Minn AJ, Kettlun CS, Liang H, Kelekar A, Vander Heiden MG, Chang BS, Fesik SW, Fill M, Thompson CB. Bcl-x(L) regulates apoptosis by heterodimerization-dependent and -independent mechanisms. EMBO J 1999; 18:632-643.

350. Motoyama N, Kimura T, Takahashi T, Watanabe T, Nakano T. Bcl-x prevents apoptotic cell death of both primitive and definitive erythrocytes at the end of maturation. J Exp Med 1999; 189:1691-1698.

351. Roth KA, Kuan C, Haydar TF, D'Sa-Eipper C, Shindler KS, Zheng TS, Kuida K, Flavell RA, Rakic P. Epistatic and independent functions of Caspase-3 and Bcl-X(L) in developmental programmed cell death. Proc Natl Acad Sci USA 2000; 97:466-471.

352. Simoes-Wust AP, Olie RA, Gautschi O, Leech SH, Haner R, Hall J, Fabbro D, Stahel RA, Zangemeister-Wittke U. Bcl-xl antisense treatment induces apoptosis in breast carcinoma cells. Int J Cancer 2000; 87:582-590.

353. Wang S. Targeting Bcl-xL enhances the cytotoxicity of chemotherapeutics. Cancer Biol Ther 2008; 7:61-62.

354. Noble CG, Dong JM, Manser E, Song H. Bcl-xL and UVRAG cause a monomer-dimer switch in Beclin1. J Biol Chem 2008; 283:26274-26282.

355. Krajewski S, Bodrug S, Krajewska M, Shabaik A, Gascoyne R, Berean K, Reed JC. Immunohistochemical analysis of Mcl-1 protein in human tissues. Differential regulation of Mcl-1 and Bcl-2 protein production suggests a unique role for Mcl-1 in control of programmed cell death in vivo. American J Pathol 1995; 146:1309-1319.

356. Krajewski S, Krajewska M, Ehrmann J, Sikorska M, Lach B, Chatten J, Reed JC. Immunohistochemical analysis of Bcl-2, Bcl-X, Mcl-1, and Bax in tumors of central and peripheral nervous system origin. American J Pathol 1997; 150:805-814.

357. Paquet C, Schmitt E, Beauchemin M, Bertrand R. Activation of multidomain and BH3-only pro-apoptotic Bcl-2 family members in p53-defective cells. Apoptosis 2004; 9:815-831.

358. Danial NN. BCL-2 family proteins: critical checkpoints of apoptotic cell death. Clin Cancer Res 2007; 13:7254-7263.

359. Muchmore SW, Sattler M, Liang H, Meadows RP, Harlan JE, Yoon HS, Nettesheim D, Chang BS, Thompson CB, Wong SL, Ng SC, Fesik SW. X-ray and NMR structure of human Bcl-xL, an inhibitor of programmed cell death. Nature 1996; 381:335-341.

360. Diaz JL, Oltersdorf T, Horne W, McConnell M, Wilson G, Weeks S, Garcia T, Fritz LC. A common binding site mediates heterodimerization and homodimerization of Bcl-2 family members. J Biol Chem 1997; 272:11350-11355.

361. Sedlak TW, Oltvai ZN, Yang E, Wang K, Boise LH, Thompson CB, Korsmeyer SJ. Multiple Bcl-2 family members demonstrate selective dimerizations with Bax. Proc Natl Acad Sci USA 1995; 92:7834-7838.

362. Cheng EH-YA, Wei MC, Weiler S, Flavell RA, Mak TW, Lindsten T, Korsmeyer SJ. Bcl-2, bcl-x(l) sequester BH3 domain-only molecules preventing bax- and bak-mediated mitochondrial apoptosis. Mol Cell 2001; 8:705-711.

363. Letai A, Bassik M, Walensky L, Sorcinelli M, Weiler S, Korsmeyer S. Distinct BH3 domains either sensitize or activate mitochondrial apoptosis, serving as prototype cancer therapeutics. Cancer Cell 2002; 2:183-192.

364. Kuwana T, Bouchier-Hayes L, Chipuk JE, Bonzon C, Sullivan BA, Green DR, Newmeyer DD. BH3 domains of BH3-only proteins differentially regulate Bax-mediated mitochondrial membrane permeabilization both directly and indirectly. Mol Cell 2005; 17:525-535.

365. Certo M, Del Gaizo Moore V, Nishino M, Wei G, Korsmeyer S, Armstrong SA, Letai A. Mitochondria primed by death signals determine cellular addiction to antiapoptotic BCL-2 family members. Cancer Cell 2006; 9:351-365.

366. Willis SN, Fletcher JI, Kaufmann T, van Delft MF, Chen L, Czabotar PE, Ierino H, Lee EF, Fairlie WD, Bouillet P, Strasser A, Kluck RM, Adams JM, Huang DC. Apoptosis initiated when BH3 ligands engage multiple Bcl-2 homologs, not Bax or Bak. Science 2007; 315:856-859.

367. Chang BS, Minn AJ, Muchmore SW, Fesik SW, Thompson CB. Identification of a novel regulatory domain in Bcl-X(L) and Bcl-2. EMBO J 1997; 16:968-977.

368. Burri SH, Kim CN, Fang GF, Chang BS, Perkins C, Harris W, Davis LW, Thompson CB, Bhalla KN. 'Loop' domain deletional mutant of Bcl-xL is as effective as p29Bcl-xL in inhibiting radiation-induced cytosolic accumulation of cytochrome C (cyt c), caspase-3 activity, and apoptosis. Int J Radiat Oncol Biol Phys 1999; 43:423-430.

369. Schmitt E, Sane AT, Bertrand R. Activation and role of caspases in chemotherapy-induced apoptosis. Drug Resist Updates 1999; 2:21-29.

370. Paquet C, Bertrand R. Unique and multi-domain Bcl-2 family members: Post-translation modification and apoptosis regulation. In: Gayathri A. ed. Recent Research Developments in Biophysics and Biochemistry. Research Signpost Publisher: Trivandrum 2003:291-325.

371. Adams JM, Cory S. The Bcl-2 apoptotic switch in cancer development and therapy. Oncogene 2007; 26:1324-1337.

372. Liu X, Kim CN, Yang J, Wang X. Induction of apoptotic program in cell-free extracts: requirement for dATP and cytochrome c. Cell 1996; 86:147-157.

373. Kluck RM, Bossywetzel E, Green DR, Newmeyer DD. The release of cytochrome C from mitochondria: a primary site for Bcl-2 regulation of apoptosis. Science 1997; 275:1132-1136.

374. Li P, Nijhawan D, Budihardjo I, Srinivasula SM, Ahmad M, Alnemri ES, Wang X. Cytochrome c and dATP-dependent formation of Apaf-1/caspase-9 complex initiates an apoptotic protease cascade. Cell 1997; 91:479-489.

375. Hakem R, Hakem A, Duncan GS, Henderson JT, Woo M, Soengas MS, Elia A, Delapompa JL, Kagi D, Khoo W, Potter J, Yoshida R, Kaufman SA, Lowe SW, Penninger JM, Mak TW. Differential requirement for caspase 9 in apoptotic pathways in vivo. Cell 1998; 94:339-352.

376. Li H, Kolluri SK, Gu J, Dawson MI, Cao X, Hobbs PD, Lin B, Chen G, Lu J, Lin F, Xie Z, Fontana JA, Reed JC, Zhang X. Cytochrome c release and apoptosis induced by mitochondrial targeting of nuclear orphan receptor TR3. Science 2000; 289:1159-1164.

377. Goldstein JC, Waterhouse NJ, Juin P, Evan GI, Green DR. The coordinate release of cytochrome c during apoptosis is rapid, complete and kinetically invariant. Nat Cell Biol 2000; 2:156-162.

378. Cain K, Bratton SB, Langlais C, Walker G, Brown DG, Sun XM, Cohen GM. Apaf-1 oligomerizes into biologically active ~700-kDa and inactive ~1.4- MDa apoptosome complexes. J Biol Chem 2000; 275:6067-6070.

379. Hausmann G, O'Reilly LA, van Driel R, Beaumont JG, Strasser A, Adams JM, Huang DC. Pro-apoptotic apoptosis protease-activating factor 1 (Apaf-1) has a

cytoplasmic localization distinct from Bcl-2 or Bcl-x(L). J Cell Biol 2000; 149:623-634.

380. Adams JM, Cory S. Apoptosomes: engines for caspase activation. Curr Opin Cell Biol 2002; 14:715-720.

381. Pop C, Timmer J, Sperandio S, Salvesen GS. The apoptosome activates caspase-9 by dimerization. Mol Cell 2006; 22:269-275.

382. Schafer ZT, Kornbluth S. The apoptosome: physiological, developmental, and pathological modes of regulation. Dev Cell 2006; 10:549-561.

383. Shi Y. Mechanical aspects of apoptosome assembly. Curr Opin Cell Biol 2006.

384. Chittenden T. BH3 domains: intracellular death-ligands critical for initiating apoptosis. Cancer Cell 2002; 2:165-166.

385. Lovell JF, Billen LP, Bindner S, Shamas-Din A, Fradin C, Leber B, D.W. A. Membrane binding by tBid initiates an ordered series of events culminating in membrane permeabilization by Bax. Cell 2008; 135:10-74-1084.

386. Kim H, Tu H-C, Ren D, Takeuchi O, Jeffers JR, Zambetti GP, Hsieh JJ-D, Cheng EH-Y. Stepwise activation of Bax and Bak by tBid, Bim and Puma initiates mitochondrial apoptosis. Mol Cell 2009; 36:487-499.

387. Dewson G, Kluck RM. Mechanisms by which Bak and Bax permeabilise mitochondria during apoptosis. J Cell Sci 2009; 122:2801-2808.

388. Gavathiotis E, Reyna DE, Davis ML, Bird GH, Walensky LD. BH3-triggered structural reorganization drives the activation of proapoptotic Bax. Mol Cell 2010; 40:481-492.

389. Zoratti M, Szabo I. The mitochondrial permeability transition. Biochim Biophys Acta 1995; 1241:139-176.

390. Shimizu S, Narita M, Tsujimoto Y. Bcl-2 family proteins regulate the release of apoptogenic cytochrome c by the mitochondrial channel VDAC. Nature 1999; 399:483-487.

391. Harris MH, Thompson CB. The role of the Bcl-2 family in the regulation of outer mitochondrial membrane permeability. Cell Death Differ 2000; 7:1182-1191.

392. Shimizu S, Konishi A, Kodama T, Tsujimoto Y. BH4 domain of antiapoptotic bcl-2 family members closes voltage-dependent anion channel and inhibits apoptotic mitochondrial changes and cell death. Proc Natl Acad Sci USA 2000; 97:3100-3105.

393. Shimizu S, Shinohara Y, Tsujimoto Y. Bax and bcl-xL independently regulate apoptotic changes of yeast mitochondria that require VDAC but not adenine nucleotide translocator. Oncogene 2000; 19:4309-4318.

394. Kroemer G, Reed JC. Mitochondrial control of cell death. Nature Med 2000; 6:513-519.

395. Zamzami N, Kroemer G. The mitochondrion in apoptosis: how Pandora's box opens. Nat Rev Mol Cell Biol 2001; 2:67-71.

396. Pavlov EV, Priault M, Pietkiewicz D, Cheng EH, Antonsson B, Manon S, Korsmeyer SJ, Mannella CA, Kinnally KW. A novel, high conductance channel

of mitochondria linked to apoptosis in mammalian cells and Bax expression in yeast. J Cell Biol 2001; 155:725-732.

397. Kroemer G, Galluzzi L, Brenner C. Mitochondrial membrane permeabilization in cell death. Physiol Rev 2007; 87:99-163.

398. Qian S, Wang W, Yang L, Huang HW. Structure of transmembrane pore induced by Bax-derived peptide: Evidence for lipidic pores. Proc Natl Acad Sci USA 2008.

399. Yamaguchi R, Lartigue L, Perkins G, Scott RT, Dixit A, Kushnareva Y, Kuwana T, Ellisman MH, Newmeyer DD. Opa1-mediated cristae opening is Bax/Bak and BH3 dependent, required for apoptosis, and independent of Bak oligomerization. Mol Cell 2008; 31:557-569.

400. Tait SW, Green DR. Mitochondria and cell death: outer membrane permeabilization and beyond. Nat Rev Mol Cell Biol 2010; 11:621-632.

401. Lowe SW, Ruley HE, Jacks T, Housman DE. p53-dependent apoptosis modulates the cytotoxicity of anticancer agents. Cell 1993; 74:957-967.

402. Miyashita T, Krajewski S, Krajewska M, Wang HG, Lin HK, Liebermann DA, Hoffman B, Reed JC. Tumor suppressor p53 is a regulator of bcl-2 and bax gene expression in vitro and in vivo. Oncogene 1994; 9:1799-1805.

403. Miyashita T, Reed JC. Tumor suppressor p53 is a direct transcriptional activator of the human bax gene. Cell 1995; 80:293-299.

404. Sax JK, Fei P, Murphy ME, Bernhard E, Korsmeyer SJ, El-Deiry WS. BID regulation by p53 contributes to chemosensitivity. Nature Cell Biol 2002; 4:842-849.

405. Nakano K, Vousden KH. Puma, a novel proapoptotic gene, is induced by p53. Mol Cell 2001; 7:683-694.

406. Yu J, Wang Z, Kinzler KW, Vogelstein B, Zhang L. PUMA mediates the apoptotic response to p53 in colorectal cancer cells. Proc Natl Acad Sci USA 2003; 100:1931-1936.

407. Oda E, Ohki R, Murasawa H, Nemoto J, Shibue T, Yamashita T, Tokino T, Taniguchi T, Tanaka N. Noxa, a BH3-only member of the bcl-2 family and candidate mediator of p53-induced apoptosis. Science 2000; 288:1053-1058.

408. Villunger A, Michalak EM, Coultas L, Mullauer F, Bock G, Ausserlechner MJ, Adams JM, Strasser A. p53- and drug-induced apoptotic responses mediated by BH3-only proteins Puma and Noxa. Science 2003; 302:1036-1038.

409. Chipuk JE, Kuwana T, Bouchier-Hayes L, Droin NM, Newmeyer DD, Schuler M, Green DR. Direct activation of Bax by p53 mediates mitochondrial membrane permeabilization and apoptosis. Science 2004; 303:1010-1014.

410. Leu JIJ, Dumont P, Hafey M, Murphy ME, George DL. Mitochondrial p53 activates Bak and causes disruption of a Bak-Mcl1 complex. Nat Cell Biol 2004; 6:443-450.

411. Perfettini JL, Kroemer RT, Kroemer G. Fatal liaisons of p53 with bax and Bak. Nat Cell Biol 2004; 6:386-387.

412. Chipuk JE, Bouchier-Hayes L, Kuwana T, Newmeyer DD, Green DR. Puma couples the nuclear and cytoplasmic proapoptotic function of p53. Science 2005; 309:1732-1735.

413. Bertrand R, Solary E, Jenkins J, Pommier Y. Apoptosis and its modulation in human promyelocytic HL-60 cells treated with DNA topoisomerase I and II inhibitors. Exp Cell Res 1993; 207:388-397.

414. Strasser A, Harris AW, Jacks T, Cory S. DNA damage can induce apoptosis in proliferating lymphoid cells via p53-independent mechanisms inhibitable by Bcl-2 Cell 1994; 79:329-339.

415. Malcomson RDG, Oren M, Wyllie AH, Harrison DJ. P53-independent death and p53-induced protection against apoptosis in fibroblasts treated with chemotherapeutic drugs. Br J Cancer 1995; 72:952-957.

416. Gupta M, Fan SJ, Zhan QM, Kohn KW, Oconnor PM, Pommier Y. Inactivation of p53 increases the cytotoxicity of camptothecin in human colon HCT116 and breast MCF-7 cancer cells. Clin Cancer Res 1997; 3:1653-1660.

417. Slichenmyer WJ, Nelson WG, Slebos RJ, Kastan MB. Loss of a p53-associated G1 checkpoint does not decrease cell survival following DNA damage. Cancer Res 1993; 53:4164-4168.

418. Woods CM, Zhu J, McQueney PA, Bollag D, Lazarides E. Taxol-induced mitotic block triggers rapid onset of a p53-independent apoptotic pathway. Mol Med 1995; 1:506-526.

419. Thomas A, Elrouby S, Reed JC, Krajewski S, Silber R, Potmesil M, Newcomb EW. Drug-induced apoptosis in B-cell chronic lymphocytic leukemia: relationship between p53 gene mutation and Bcl-2/Bax proteins in drug resistance. Oncogene 1996; 12:1055-1062.

420. Wahl AF, Donaldson KL, Fairchild C, Lee FYF, Foster SA, Demers GW, Galloway DA. Loss of normal p53 function confers sensitization to taxol by increasing G2/M arrest and apoptosis. Nature Med 1996; 2:72-79.

421. Shimizu T, Pommier Y. Camptothecin-induced apoptosis in p53-null human leukemia Hl60 cells and their isolated nuclei - Effects of the protease inhibitors z-VAD-fmk and dichloroisocoumarin suggest an involvement of both caspases and serine proteases. Leukemia 1997; 11:1238-1244.

422. Zamble DB, Jacks T, Lippard SJ. P53-dependent and -independent responses to cisplatin in mouse testicular teratocarcinoma cells. Proc Natl Acad Sci USA 1998; 95:6163-6168.

423. Kaufmann SH, Earnshaw WC. Induction of apoptosis by cancer chemotherapy. Exp Cell Res 2000; 256:42-49.

424. Degenhardt K, Chen G, Lindsten T, White E. Bax and Bak mediate p53-independent suppression of tumorigenesis. Cancer Cell 2002; 2:193-201.

425. Fleischer A, Rebollo A. Induction of p53-independent apoptosis by the BH3-only protein ITM2Bs. FEBS Lett 2004; 557:283-287.

426. Qin JZ, Stennett L, Bacon P, Bodner B, Hendrix MJ, Seftor RE, Seftor EA, Margaryan NV, Pollock PM, Curtis A, Trent JM, Bennett F, Miele L, Nickoloff BJ. p53-independent NOXA induction overcomes apoptotic resistance of malignant melanomas. Mol Cancer Ther 2004; 3:895-902.

427. Jullig M, Zhang WV, Ferreira A, Stott NS. MG132 induced apoptosis is associated with p53-independent induction of pro-apoptotic Noxa and transcriptional activity of beta-catenin. Apoptosis 2006; 11:627-641.

428. Yu J, Zhang L. PUMA, a potent killer with or without p53. Oncogene 2008; 27 Suppl 1:S71-83.

429. Armstrong JL, Veal GJ, Redfern CP, Lovat PE. Role of Noxa in p53-independent fenretinide-induced apoptosis of neuroectodermal tumours. Apoptosis 2007; 12:613-622.

430. Nip J, Strom DK, Fee BE, Zambetti G, Cleveland JL, Hiebert SW. E2F-1 cooperates with Topoisomerase Ii inhibition and DNA damage to selectively augment p53-independent apoptosis. Mol Cell Biol 1997; 17:1049-1056.

431. Jost CA, Marin MC, Kaelin WG. p73 is a human p53-related protein that can induce apoptosis. Nature 1997; 389:191-194.

432. Yang AN, Kaghad M, Wang YM, Gillett E, Fleming MD, Dotsch V, Andrews NC, Caput D, McKeon F. P63, a p53 homolog at 3q27-29, encodes multiple products with transactivating, death-inducing, and dominant-negative activities. Mol Cell 1998; 2:305-316.

433. Yuan ZM, Shioya H, Ishiko T, Sun X, Gu J, Huang YY, Lu H, Kharbanda S, Weichselbaum R, Kufe D. p73 is regulated by tyrosine kinase c-Abl in the apoptotic response to DNA damage. Nature 1999; 399:814-817.

434. Agami R, Blandino G, Oren M, Shaul Y. Interaction of c-Abl and p73 alpha and their collaboration to induce apoptosis. Nature 1999; 399:809-813.

435. Irwin M, Marin MC, Phillips AC, Seelan RS, Smith DI, Liu W, Flores ER, Tsai KY, Jacks T, Vousden KH, Kaelin WG, Jr. Role for the p53 homologue p73 in E2F-1-induced apoptosis. Nature 2000; 407:645-648.

436. Stiewe T, Putzer BM. Role of the p53-homologue p73 in E2F1-induced apoptosis. Nat Genet 2000; 26:464-469.

437. Flores ER, Tsai KY, Crowley D, Sengupta S, Yang A, McKeon F, Jacks T. p63 and p73 are required for p53-dependent apoptosis in response to DNA damage. Nature 2002; 416:560-564.

438. Sunters A, Fernandez de Mattos S, Stahl M, Brosens JJ, Zoumpoulidou G, Saunders CA, Coffer PJ, Medema RH, Coombes RC, Lam EW. FoxO3a transcriptional regulation of Bim controls apoptosis in paclitaxel-treated breast cancer cell lines. J Biol Chem 2003; 278:49795-49805.

439. Urist M, Tanaka T, Poyurovsky MV, Prives C. p73 induction after DNA damage is regulated by checkpoint kinases Chk1 and Chk2. Genes Dev 2004; 18:3041-3054.

440. Urbich C, Knau A, Fichtlscherer S, Walter DH, Bruhl T, Potente M, Hofmann WK, de Vos S, Zeiher AM, Dimmeler S. FOXO-dependent expression of the proapoptotic protein Bim: pivotal role for apoptosis signaling in endothelial progenitor cells. Faseb J 2005.

441. You H, Pellegrini M, Tsuchihara K, Yamamoto K, Hacker G, Erlacher M, Villunger A, Mak TW. FOXO3a-dependent regulation of Puma in response to cytokine/growth factor withdrawal. J Exp Med 2006.

442. Tsai WB, Chung YM, Takahashi Y, Xu Z, Hu MC. Functional interaction between FOXO3a and ATM regulates DNA damage response. Nat Cell Biol 2008; 10:460-467.

443. Barboule N, Truchet I, Valette A. Localization of phosphorylated forms of Bcl-2 in mitosis: co-localization with Ki-67 and nucleolin in nuclear structures and on mitotic chromosomes. Cell Cycle 2005; 4:590-596.

444. Kozopas KM, Yang T, Buchan HL, Zhou P, Craig RW. Mcl-1, a gene expressed in programmed myeloid cell differentiation, has sequence similarity to Bcl-2. Proc Natl Acad Sci USA 1993; 90:3516-3520.

445. Craig RW. Mcl1 provides a window on the role of the Bcl2 family in cell proliferation, differentiation and tumorigenesis. Leukemia 2002; 16:444-454.

446. Haldar S, Jena N, Croce CM. Inactivation of Bcl-2 by phosphorylation. Proc Natl Acad Sci USA 1995; 92:4507-4511.

447. Haldar S, Chintapalli J, Croce CM. Taxol induces Bcl-2 phosphorylation and death of prostate cancer cells. Cancer Res 1996; 56:1253-1255.

448. Blagosklonny MV, Giannakakou P, Eldeiry WS, Kingston DGI, Higgs PI, Neckers L, Fojo T. Raf-1/Bcl-2 phosphorylation: a step from microtubule damage to cell death. Cancer Res 1997; 57:130-135.

449. Poruchynsky MS, Wang EE, Rudin CM, Blagosklonny MV, Fojo T. Bcl-X(L) is phosphorylated in malignant cells following microtubule disruption. Cancer Res 1998; 58:3331-3338.

450. Domina AM, Vrana JA, Gregory MA, Hann SR, Craig RW. MCL1 is phosphorylated in the PEST region and stabilized upon ERK activation in viable cells, and at additional sites with cytotoxic okadaic acid or taxol. Oncogene 2004; 23:5301-5315.

451. Basu A, Haldar S. Identification of a novel Bcl-xL phosphorylation site regulating the sensitivity of taxol- or 2-methoxyestradiol-induced apoptosis. FEBS Lett 2003; 538:41-47.

452. Du L, Lyle CS, Chambers TC. Characterization of vinblastine-induced Bcl-xL and Bcl-2 phosphorylation: evidence for a novel protein kinase and a coordinated phosphorylation/dephosphorylation cycle associated with apoptosis induction. Oncogene 2005; 24:107-117.

453. Tamura Y, Simizu S, Muroi M, Takagi S, Kawatani M, Watanabe N, Osada H. Polo-like kinase 1 phosphorylates and regulates Bcl-x(L) during pironetin-induced apoptosis. Oncogene 2009; 28:107-116.

454. Kharbanda S, Saxena S, Yoshida K, Pandey P, Kaneki M, Wang Q, Cheng K, Chen YN, Campbell A, Sudha T, Yuan ZM, Narula J, Weichselbaum R, Nalin C, Kufe D. Translocation of SAPK/JNK to mitochondria and interaction with Bcl-x(L) in response to DNA damage. J Biol Chem 2000; 275:322-327.

455. Blagosklonny MV, Schulte T, Nguyen P, Trepel J, Neckers LM. Taxol-induced apoptosis and phosphorylation of Bcl-2 protein involves c-Raf-1 and represents a novel c-Raf-1 signal transduction pathway. Cancer Res 1996; 56:1851-1854.

456. Ruvolo PP, Deng XM, Carr BH, May WS. A functional role for mitochondrial protein kinase C-alpha in Bcl-2 phosphorylation and suppression of apoptosis. J Biol Chem 1998; 273:25436-25442.

457. Srivastava RK, Srivastava AR, Korsmeyer SJ, Nesterova M, Chochung YS, Longo DL. Involvement of microtubules in the regulation of Bcl-2 phosphorylation and apoptosis through cyclic AMP-dependent protein kinase. Mol Cell Biol 1998; 18:3509-3517.

458. Maundrell K, Antonsson B, Magnenat E, Camps M, Muda M, Chabert C, Gillieron C, Boschert U, Vialknecht E, Martinou JC, Arkinstall S. Bcl-2 undergoes phosphorylation by C-Jun N-terminal kinase stress-activated protein kinases in the presence of the constitutively active GTP-binding protein Rac1. J Biol Chem 1997; 272:25238-25242.

459. Yamamoto K, Ichijo H, Korsmeyer SJ. Bcl-2 is phosphorylated and inactivated by an ASK1/Jun N-terminal protein kinase pathway normally activated at G(2)/M. Mol Cell Biol 1999; 19:8469-8478.

460. Fan M, Goodwin M, Vu T, Brantley-Finley C, Gaarde WA, Chambers TC. Vinblastine-induced phosphorylation of Bcl-2 and Bcl-XL is mediated by JNK and occurs in parallel with inactivation of the Raf-1/MEK/ERK cascade. J Biol Chem 2000; 275:29980-29985.

461. Fan M, Du C, Stone AA, Gilbert KM, Chambers TC. Modulation of mitogen-activated protein kinases and phosphorylation of Bcl-2 by vinblastine represent persistent forms of normal fluctuations at G2-M. Cancer Res 2000; 60:6403-6407.

462. Liu X, Dai S, Zhu Y, Marrack P, Kappler JW. The structure of a Bcl-xL/Bim fragment complex: implications for Bim function. Immunity 2003; 19:341-352.

463. Fang GF, Chang BS, Kim CN, Perkins C, Thompson CB, Bhalla KN. Loop domain is necessary for taxol-induced mobility shift and phosphorylation of Bcl-2 as well as for inhibiting taxol-induced cytosolic accumulation of cytochrome c and apoptosis. Cancer Res 1998; 58:3202-3208.

464. Johnson AL, Bridgham JT, Jensen T. Bcl-x(Long) protein expression and phosphorylation in granulosa cells. Endocrinology 1999; 140:4521-4529.

465. Upreti M, Galitovskaya EN, Chu R, Tackett AJ, Terrano DT, Granell S, Chambers TC. Identification of the major phosphorylation site in Bcl-xL induced by microtubule inhibitors and analysis of its functional significance. J Biol Chem 2008; 283:35517-35525.

466. Terrano DT, Upreti M, Chambers TC. Cyclin-dependent kinase 1-mediated Bcl-xL/Bcl-2 phosphorylation acts as a functional link coupling mitotic arrest and apoptosis. Mol Cell Biol 2010; 30:640-656.

467. MacCorkle RA, Tan TH. Inhibition of JNK2 disrupts anaphase and produces aneuploidy in mammalian cells. J Biol Chem 2004; 279:40112-40121.

468. Oktay K, Buyuk E, Oktem O, Oktay M, Giancotti FG. The c-Jun N-terminal kinase JNK functions upstream of Aurora B to promote entry into mitosis. Cell Cycle 2008; 7:533-541.

469. Gutierrez GJ, Tsuji T, Chen M, Jiang W, Ronai ZA. Interplay between Cdh1 and JNK activity during the cell cycle. Nat Cell Biol 2010; 12:686-695.

470. Takenaka K, Moriguchi T, Nishida E. Activation of the protein kinase p38 in the spindle assembly checkpoint and mitotic arrest. Science 1998; 280:599-602.

471. Kurata S. Selective activation of p38 MAPK cascade and mitotic arrest caused by low level oxidative stress. J Biol Chem 2000; 275:23413-23416.

472. Chao JI, Yang JL. Opposite roles of ERK and p38 mitogen-activated protein kinases in cadmium-induced genotoxicity and mitotic arrest. Chem Res Toxicol 2001; 14:1193-1202.

473. Campos CB, Bedard PA, Linden R. Activation of p38 mitogen-activated protein kinase during normal mitosis in the developing retina. Neuroscience 2002; 112:583-591.

474. Fan L, Yang X, Du J, Marshall M, Blanchard K, Ye X. A novel role of p38 alpha MAPK in mitotic progression independent of its kinase activity. Cell Cycle 2005; 4:1616-1624.

475. Yen AH, Yang JL. Cdc20 proteolysis requires p38 MAPK signaling and Cdh1-independent APC/C ubiquitination during spindle assembly checkpoint activation by cadmium. J Cell Physiol 2010; 223:327-334.

476. Yuan J, Xu BZ, Qi ST, Tong JS, Wei L, Li M, Ouyang YC, Hou Y, Schatten H, Sun QY. MAPK-activated protein kinase 2 is required for mouse meiotic spindle assembly and kinetochore-microtubule attachment. PLoS ONE 2010; 5:e11247.

477. Lee K, Kenny AE, Rieder CL. P38 mitogen-activated protein kinase activity is required during mitosis for timely satisfaction of the mitotic checkpoint but not for the fidelity of chromosome segregation. Mol Biol Cell 2010; 21:2150-2160.

478. Takaki T, Trenz K, Costanzo V, Petronczki M. Polo-like kinase 1 reaches beyond mitosis-cytokinesis, DNA damage response, and development. Curr Opin Cell Biol 2008; 20:650-660.

479. Strebhardt K. Multifaceted polo-like kinases: drug targets and antitargets for cancer therapy. Nat Rev Drug Discov 2010; 9:643-660.

480. Zimmerman WC, Erikson RL. Polo-like kinase 3 is required for entry into S phase. Proc Natl Acad Sci USA 2007; 104:1847-1852.

481. Wang Q, Xie S, Chen J, Fukasawa K, Naik U, Traganos F, Darzynkiewicz Z, Jhanwar-Uniyal M, Dai W. Cell cycle arrest and apoptosis induced by human

Polo-like kinase 3 is mediated through perturbation of microtubule integrity. Mol Cell Biol 2002; 22:3450-3459.

482. Bahassi EM, Conn CW, Myer DL, Hennigan RF, McGowan CH, Sanchez Y, Stambrook PJ. Mammalian Polo-like kinase 3 (Plk3) is a multifunctional protein involved in stress response pathways. Oncogene 2002; 21:6633-6640.

483. Myer DL, Bahassi el M, Stambrook PJ. The Plk3-Cdc25 circuit. Oncogene 2005; 24:299-305.

484. Bahassi EM, Myer DL, McKenney RJ, Hennigan RF, Stambrook PJ. Priming phosphorylation of Chk2 by polo-like kinase 3 (Plk3) mediates its full activation by ATM and a downstream checkpoint in response to DNA damage. Mutat Res 2006; 596:166-176.

485. Conn CW, Hennigan RF, Dai W, Sanchez Y, Stambrook PJ. Incomplete cytokinesis and induction of apoptosis by overexpression of the mammalian polo-like kinase, Plk3. Cancer Res 2000; 60:6826-6831.

486. Naik MU, Naik UP. Calcium- and integrin-binding protein 1 regulates microtubule organization and centrosome segregation through polo like kinase 3 during cell cycle progression. Int J Biochem Cell Biol 2011; 43:120-129.

487. Loffler H, Lukas J, Bartek J, Kramer A. Structure meets function--centrosomes, genome maintenance and the DNA damage response. Exp Cell Res 2006; 312:2633-2640.

488. Gabrielli BG, De Souza CP, Tonks ID, Clark JM, Hayward NK, Ellem KA. Cytoplasmic accumulation of cdc25B phosphatase in mitosis triggers centrosomal microtubule nucleation in HeLa cells. J Cell Sci 1996; 109:1081-1093.

489. Lammer C, Wagerer S, Saffrich R, Mertens D, Ansorge W, Hoffmann I. The cdc25B phosphatase is essential for the G2/M phase transition in human cells. J Cell Sci 1998; 111:2445-2453.

490. Lindqvist A, Kallstrom H, Lundgren A, Barsoum E, Rosenthal CK. Cdc25B cooperates with Cdc25A to induce mitosis but has a unique role in activating cyclin B1-Cdk1 at the centrosome. J Cell Biol 2005; 171:35-45.

491. Golsteyn RM, Mundt KE, Fry AM, Nigg EA. Cell cycle regulation of the activity and subcellular localization of Plk1, a human protein kinase implicated in mitotic spindle function. J Cell Biol 1995; 129:1617-1628.

492. Hirota T, Kunitoku N, Sasayama T, Marumoto T, Zhang D, Nitta M, Hatakeyama K, Saya H. Aurora-A and an interacting activator, the LIM protein Ajuba, are required for mitotic commitment in human cells. Cell 2003; 114:585-598.

493. Kramer A, Mailand N, Lukas C, Syljuasen RG, Wilkinson CJ, Nigg EA, Bartek J, Lukas J. Centrosome-associated Chk1 prevents premature activation of cyclin-B-Cdk1 kinase. Nat Cell Biol 2004; 6:884-891.

494. Boisvert FM, van Koningsbruggen S, Navascues J, Lamond AI. The multifunctional nucleolus. Nat Rev Mol Cell Biol 2007; 8:574-585.

495. Boulon S, Westman BJ, Hutten S, Boisvert FM, Lamond AI. The Nucleolus under Stress. Mol Cell 2010; 40:216-227.

496. Migone F, Deinnocentes P, Smith BF, Bird RC. Alterations in CDK1 expression and nuclear/nucleolar localization following induction in a spontaneous canine mammary cancer model. J Cell Biochem 2006; 98:504-518.

497. Matera AG, Shpargel KB. Pumping RNA: nuclear bodybuilding along the RNP pipeline. Curr Opin Cell Biol 2006; 18:317-324.

498. Cioce M, Lamond AI. Cajal bodies: a long history of discovery. Annu Rev Cell Dev Biol 2005; 21:105-131.

499. Dellaire G, Bazett-Jones DP. Beyond repair foci: subnuclear domains and the cellular response to DNA damage. Cell Cycle 2007; 6:1864-1872.

500. Gall JG. Cajal bodies: the first 100 years. Annu Rev Cell Dev Biol 2000; 16:273-300.

501. Tulu US, Fagerstrom C, Ferenz NP, Wadsworth P. Molecular requirements for kinetochore-associated microtubule formation in mammalian cells. Curr Biol 2006; 16:536-541.

502. Varma D, Monzo P, Stehman SA, Vallee RB. Direct role of dynein motor in stable kinetochore-microtubule attachment, orientation, and alignment. J Cell Biol 2008; 182:1045-1054.

503. Woodruff JB, Drubin DG, Barnes G. Dynein-driven mitotic spindle positioning restricted to anaphase by She1p inhibition of dynactin recruitment. Mol Biol Cell 2009; 20:3003-3011.

504. Ma L, Tsai MY, Wang S, Lu B, Chen R, Iii JR, Zhu X, Zheng Y. Requirement for Nudel and dynein for assembly of the lamin B spindle matrix. Nat Cell Biol 2009; 11:247-256.

505. Chan YW, Fava LL, Uldschmid A, Schmitz MH, Gerlich DW, Nigg EA, Santamaria A. Mitotic control of kinetochore-associated dynein and spindle orientation by human Spindly. J Cell Biol 2009; 185:859-874.

506. Sivaram MV, Wadzinski TL, Redick SD, Manna T, Doxsey SJ. Dynein light intermediate chain 1 is required for progress through the spindle assembly checkpoint. EMBO J 2009; 28: 902-914.

507. Bader JR, Vaughan KT. Dynein at the kinetochore: Timing, Interactions and Functions. Semin Cell Dev Biol 2010; 21:269-275.

508. Li H, Liu XS, Yang X, Song B, Wang Y, Liu X. Polo-like kinase 1 phosphorylation of p150Glued facilitates nuclear envelope breakdown during prophase. Proc Natl Acad Sci U S A 2010; 107:14633-14638.

509. Roca MG, Kuo HC, Lichius A, Freitag M, Read ND. Nuclear dynamics, mitosis and the cytoskeleton during the early stages of colony initiation in Neurospora crassa. Eukaryot Cell 2010; 9:1171-1183.

510. Rome P, Montembault E, Franck N, Pascal A, Glover DM, Giet R. Aurora A contributes to p150(glued) phosphorylation and function during mitosis. J Cell Biol 2010; 189:651-659.

511. Puthalakath H, Huang DCS, O'Reilly LA, King SM, Strasser A. The proapoptotic activity of the Bcl-2 family member Bim is regulated by interaction with the dynein motor complex. Mol Cell 1999; 3:287-296.

512. Pinon JD, Labi V, Egle A, Villunger A. Bim and Bmf in tissue homeostasis and malignant disease. Oncogene 2008; 27 Suppl 1:S41-52.

513. Strasser A, Puthalakath H, Bouillet P, Huang DC, O'Connor L, O'Reilly LA, Cullen L, Cory S, Adams JM. The role of Bim, a proapoptotic BH3-only member of the Bcl-2 family in cell-death control. Ann N Y Acad Sci 2000; 917:541-548.

514. Veis DJ, Sorenson CM, Shutter JR, Korsmeyer SJ. Bcl-2-deficient mice demonstrate fulminant lymphoid apoptosis, polycystic kidneys, and hypopigmented hair. Cell 1993; 75:229-240.

515. Chao DT, Linette GP, Boise LH, White LS, Thompson CB, Korsmeyer SJ. Bcl-XL and Bcl-2 repress a common pathway of cell death. J Exp Med 1995; 182:821-828.

516. Korsmeyer SJ. Regulators of cell death. Trends Genet 1995; 11:101-105.

517. Chao DT, Korsmeyer SJ. Bcl-2 family: regulators of cell death. Annu Rev Immunol 1998; 16:395-419.

518. Schorr K, Li M, Bar-Peled U, Lewis A, Heredia A, Lewis B, Knudson CM, Korsmeyer SJ, Jager R, Weiher H, Furth PA. Gain of Bcl-2 is more potent than bax loss in regulating mammary epithelial cell survival in vivo. Cancer Res 1999; 59:2541-2545.

519. Tsujiimoto Y, Finger LR, Yunis J, Nowell PC, Croce CM. Cloning of the chromosome breakpoint of neoplastic B cells with the t(14:18) chromosome translocation. Science 1984; 226:1097-1099.

520. Clarke ML, Smith SD, Sklar J. Cloning and structural analysis of cDNAs for bcl-2 and a hybrid bcl-2/immunoglobulin transcript resulting from the t(14;18) translocation. Cell 1986; 47:19-28.

521. Vaux DL, Cory S, Adams JM. Bcl-2 gene promotes haemopoietic cell survival and cooperates with c-myc to immortalize pre-B cells. Nature 1988; 355:440-442.

522. Hockenbery D, Nunez G, Milliman C, Schreiber RD, Korsmeyer SJ. Bcl-2 is an inner mitochondrial membrane protein that blocks programmed cell death. Nature 1990; 348:334-336.

523. Hockenbery DM. The bcl-2 oncogene and apoptosis. Semin Immunol 1992; 4:413-420.

524. Bissonnette RP, Echeverri F, Mahboubi A, Green DR. Apoptotic cell death induced by c-myc is inhibited by bcl-2. Nature 1992; 359:552-554.

525. Juin P, Hunt A, Littlewood T, Griffiths B, Swigart LB, Korsmeyer S, Evan G. c-Myc functionally cooperates with Bax to induce apoptosis. Mol Cell Biol 2002; 22:6158-6169.

526. Korsmeyer SJ. Bcl-2 initiates a new category of oncogenes: regulators of cell death. Blood 1992; 80:879-886.

527. Rinkenberger JL, Korsmeyer SJ. Errors of homeostasis and deregulated apoptosis. Cur Opin Gene Dev 1997; 7:589-596.

528. Hengartner MO, Ellis RE, Horvitz HR. Caenorhabditis elegans gene ced-9 protects cells from programmed cell death. Nature 1992; 356:494-496.

529. Morales CP, Holt SE, Ouellette M, Kaur KJ, Yan Y, Wilson KS, White MA, Wright WE, Shay JW. Absence of cancer-associated changes in human fibroblasts immortalized with telomerase. Nat Genet 1999; 21:115-118.